

MODELING OF PLASMID DYNAMICS
AND PERSISTENCE IN A COMMUNITY OF HOSTS

by

SÓNIA CRISTINA SANTOS MARTINS

A thesis submitted to the University of Birmingham

for the degree of

DOCTOR OF PHILOSOPHY

Centre for Systems Biology
School of Biosciences
College of Life and
Environmental Sciences
University of Birmingham
September 2012

UNIVERSITY OF
BIRMINGHAM

University of Birmingham Research Archive

e-theses repository

This unpublished thesis/dissertation is copyright of the author and/or third parties. The intellectual property rights of the author or third parties in respect of this work are as defined by The Copyright Designs and Patents Act 1988 or as modified by any successor legislation.

Any use made of information contained in this thesis/dissertation must be in accordance with that legislation and must be properly acknowledged. Further distribution or reproduction in any format is prohibited without the permission of the copyright holder.

ABSTRACT

Some bacterial plasmids have a narrow (*NHR*) while others have a broad host-range (*BHR*), facilitating the propagation of antibiotic resistance genes through natural communities. An extended host-range should mean less adaptation to any particular host and this should result on average, in a greater fitness burden for its hosts. Thus, what are the advantages of having a broad host-range?

The dynamics of transfer of BHR plasmids competing with faster growing NHR-plasmid bearing cells in two-species assemblages in chemostats and biofilms was analysed using mathematical models. In chemostats a costly NHR plasmid that can survive in a single species population could not survive in a two-species assemblage. Adding a BHR competitor helps the NHR plasmid to survive and coexistence of both plasmids becomes possible if the plasmids are incompatible. In two-species biofilms the BHR plasmid is the better competitor despite the higher costs, whereas NHR spreading is severely hindered by biofilm patchiness. Experimentally, mating experiments and growth curves showed a strong dependency of plasmids transfer frequency and fitness burden on species background.

Overall, this work demonstrates how competition, differences in host-range and compatibility relationships between plasmids can enhance the chances of plasmid persistence in two-species assemblages.

“Essentially, all models are wrong but some are useful ”

George E. Box & Norman R. Draper, 1987

ACKNOWLEDGEMENTS

Five years ago I joined the PhD program in Computational Biology (PDBC) hosted by the Gulbenkian Institute for Science for what turned out to be the longest and more challenging professional project so far.

I want to start by thanking the PDBC direction and in particular Jorge Carneiro for believing in my abilities and giving me the opportunity to pursue a PhD project in a field of my choice. I also thank you Manuela Cordeiro for always being available to help sorting out any bureaucratic details.

I would also like to acknowledge the financial support received from the Foundation for Science and Technology (FCT), Siemens SA Portugal and Fundação Calouste Gulbenkian, which sponsored my enrolment in PDBC, financed my PhD project and allowed my participation in national and international conferences.

I thank you my main supervisor, Dr Jan-Ulrich Kreft for welcoming me in his group, for his guidance and teaching (and perseverance), for the exhausting and living discussions, for his negative and positive feedback, all of which have contributed to build up my critical spirit. I would also like to thank you Professor Chris Thomas, my co-supervisor, for taking time in sharing his vast and detailed knowledge on plasmid biology and advice on experimental design, for listening to and discussing my project ideas.

Most of my time at the University of Birmingham was spent in the Centre for Systems Biology surrounded by open-minded and creative people with whom I have shared many laughs but also deep scientific discussions. In particular, I would like to thank you my fellow PhD students Dorota, Bhima, Chinmay, Olga, Rafik, Ralf and Rob and our past post-doc Susanne for their sincere friendship and support. I also want to thank you Claudia, Francis, Hansong, Pedro, Roshini and Sudha for their friendship and for fulfilling my free time with high quality humour and organizing outstanding social and musical events!

Many thanks must also go to all the members of the T101 Lab in the School of Biosciences, which welcomed me in their lab meetings, helped finding space to set up my lab bench and introduced me to all the central services routines. I also thank you the members of Professor Chris Thomas' group for the help with the strain and plasmid collections.

I would also like to thank you my past students, namely Hayley Gibbins and Zuha Khan, for the fulfilling experience of teaching basic plasmid biology and microbiology techniques and witnessing their evolution towards autonomous undergraduate researchers.

I also want to thank you my fellow colleagues from the PDBC 2007 edition, namely Afonso, Assunção, Bruno, Hugo F., Hugo M., Paula, Ricardo, Rodrigo, Susana and Zé, for making the first year of PDBC such a lively time and for their companionship throughout the tough project assignments.

I heartily thank you my parents and grandparents for their life lessons, for their relentless support and unconditional love, for their encouragement to pursuit my dreams wherever they might take me, and for taking care of my financial needs during the writing up period of my PhD thesis.

Finally, I want to thank you my beloved boyfriend, Nuno, for his relentless support to all my endeavours, for listening, and for always finding the best in me. Thank you for taking the risk of coming to UK to work and live with me, for making it a memorable year and lighting up my soul in my weakest moments.

Obrigado!

CONTENTS

List of Figures	1
List of Tables	7
List of Abbreviations and Symbols	10
Chapter 1: Introduction	13
1.1. Plasmid Biology	14
1.1.1. Plasmid structure and transfer	16
1.1.2. Replication and copy number control	20
1.1.3. Incompatibility groups	22
1.2. Plasmid maintenance	25
1.2.1. Partition and resolution systems	25
1.2.2. Post-segregational systems	26
1.3. Plasmid host-range	29
1.3.1. Narrow and broad host-ranges plasmids	29
1.3.2. Evolution of host-range	30
1.4. Conjugative Transfer of Plasmids	36
1.4.1. Monitoring plasmid transfer	36
1.4.2. Factors affecting plasmid transfer and establishment	37
1.4.3. Plasmid transfer in chemostats and biofilms	39
1.5. Mathematical Modeling of Plasmid Dynamics	42
1.5.1. Modeling plasmid dynamics in chemostats	42
1.5.2. Modeling plasmid dynamics in structured communities	53
1.5.2.1. Biofilms and biofilm modeling	53
1.5.2.2. Models of plasmid transfer	68
1.6. Objectives	73
Chapter 2: Model Development	75

2.1.	Chemostat	76
2.1.1.	ODE models	76
2.1.2.	Individual-based chemostat model	83
2.1.3.	Individual-based chemostat model of plasmid transfer	87
2.2.	Biofilm	93
2.2.1.	Individual-based biofilm model of plasmid transfer	93
Chapter 3: Modeling Plasmid Dynamics In A Chemostat		104
3.1.	Introduction	105
3.2.	Results	108
3.2.1.	Minimum transfer rate for survival	109
3.2.2.	Transfer of a NHR plasmid in a two-species assemblage	115
3.2.3.	Compatible plasmids	117
3.2.3.1.	Effect of host-range	117
3.2.3.2.	Effect of fitness cost	122
3.2.3.3.	Effect of transfer rate	125
3.2.3.4.	Effect of loss rate	127
	Summary for compatible plasmids	129
3.2.4.	Incompatible plasmids	130
3.2.4.1.	Effect of host-range	130
3.2.4.2.	Effect of fitness cost	137
3.2.4.3.	Effect of transfer rate	139
3.2.4.4.	Effect of loss rate	142
	Summary for incompatible plasmids	148
3.2.5.	The role of stochasticity	149
3.3.	Discussion	156
Chapter 4: Modeling Plasmid Dynamics In A Biofilm		164
4.1.	Introduction	165
4.2.	Results	170

4.2.1. Biofilm structures	171
4.2.2. Transfer of a NHR in a two-species assemblage	177
4.2.3. Compatible plasmids	182
4.2.3.1. Effect of host-range	182
4.2.3.2. Effect of fitness cost and transfer probability in mixed biofilms	185
4.2.3.3. Effect of patchiness	190
Summary for compatible plasmids	195
4.2.4. Incompatible plasmids	196
4.2.4.1. Effect of host-range	196
4.2.4.2. Effect of fitness cost and transfer probability in mixed biofilms	199
4.2.4.3. Effect of patchiness	201
Summary for incompatible plasmids	206
4.3. Discussion	207

Chapter 5: Fitness Cost And Transfer Frequency Of Rk2 And R387 In <i>E. coli</i> , <i>P. aeruginosa</i> And <i>P. putida</i>	
	212
5.1. Introduction	213
5.2. Materials and methods	216
5.2.1. Strains and plasmids	216
5.2.2. Growth curves	218
5.2.3. Membrane filter matings	219
5.2.4. Propagation in two-species assemblages	222
5.2.5. Materials	223
5.3. Results	224
5.3.1. Relative fitness	224
5.3.2. Transfer frequency	228
5.3.3. Transfer dynamics in a two-species assemblage	233
5.4. Discussion	236

Chapter 6: General Discussion	244
Chapter 7: Conclusions and future prospects	252
References	256

Appendix

Lardon, LA, Merkey, BV, Martins, S, Dotsch, A, Picioreanu, C, Kreft, J-U, and Smets, BF. (2011) Idynamics: Next-Generation Individual-Based Modeling of Biofilms. **Environ Microbiol**, 13: 2416-34.

List of Figures

Chapter One

- Figure 1.1. The mosaic structure of plasmids 19
- Figure 1.2. Segregation of incompatible plasmids 24
- Figure 1.3. Schematic representation of host-range evolution and mechanisms involved in its expansion towards a BHR or contraction towards a NHR. 34
- Figure 1.4. Bar plot showing the number of candidate evolutionary hosts for each plasmid. 35
- Figure 1.5. Schematic view of a chemostat. 44
- Figure 1.6. Graph of the Monod equation (1) fit to the observed data. 45
- Figure 1.7. Population growth and transfer dynamics of plasmid F in (A) exponentially growing cultures, (B) at stationary phase and (C) in steady-state chemostat cultures. 48
- Figure 1.8. Four compartments typically defined in a biofilm system: bulk liquid, boundary layer, biofilm and substratum. 55
- Figure 1.9. BacSim IbM structure. 60
- Figure 1.10 The computational domain in iDynoMiCS including the support as an external boundary. 65
- Figure 1.11 Example biofilm structures from 3D simulations (with-cost case). 67

Chapter Two

- Figure 2.1. ODE model of the population dynamics of two conjugative plasmids with different host-ranges in a two-species assemblage. 82
- Figure 2.2: Comparison of simulations of the stochastic chemostat model using iDynoMiCS (3 replicates) with simulations of the deterministic ODE model 86
- Figure 2.3. One time step in iDynoMiCS biofilm model of plasmid dynamics. 102

Chapter Three

- Figure 3.1. Frequency of plasmid-bearing (P^+) cells at steady-state for increasing transfer rates for plasmids with different fitness costs in a single species population. 111
- Figure 3.2. Dynamics of plasmid invasion for a plasmid with a 21% fitness cost, for increasing transfer rates in a single species population. 113
- Figure 3.3. Dynamics of plasmid invasion of a costly NHR plasmid and a NHR conferring zero cost in a two-species assemblage. 116
- Figure 3.4. Effect of different transfer rates for the BHR plasmid, on the dynamics of invasion of two compatible plasmids in single and two-species assemblages. 119
- Figure 3.5. Effect of host-range for different fitness costs for the BHR plasmid, on the dynamics of two compatible plasmids invasion in single and two-species assemblages. 121
- Figure 3.6. Effect of varying the fitness cost of compatible NHR and BHR plasmids competing in a two-species assemblage, on their frequency in steady state. 124

- Figure 3.7. Effect of varying the transfer rate of compatible NHR and BHR plasmids competing in a two-species assemblage, on their frequency in steady state. 126

- Figure 3.8 Effect of varying the loss rate of compatible NHR and BHR plasmids competing in a two-species assemblage, on their frequency in steady state. 128

- Figure 3.9. Effect of host-range for different transfer rates for the NHR plasmid, on the dynamics of two incompatible plasmids invading single and two-species assemblages. 133

- Figure 3.10. Effect of host-range for different transfer rates for the NHR plasmid, on the dynamics of two incompatible plasmids invading single and two-species assemblages. 134

- Figure 3.11. Effect of host-range for different fitness costs for the BHR plasmid, on the dynamics of two incompatible plasmids invading single and two-species assemblages. 136

- Figure 3.12. Effect of varying the fitness cost of incompatible NHR and BHR plasmids competing in a two-species assemblage, on their frequency in steady state. 138

- Figure 3.13. Effect of varying the transfer rate of NHR and BHR incompatible plasmids competing in a two-species assemblage, on their frequency in steady state. 141

- Figure 3.14. Effect of varying the loss rate of incompatible NHR and BHR plasmids competing in a two-species assemblage, on their frequency in steady state. 143

- Figure 3.15. Effect of varying the loss rate of incompatible NHR and BHR plasmids competing in a two-species assemblage, on their frequency in steady state (numerical results obtained after > 300 days simulated time). 145

- Figure 3.16. Effect of transfer rate of the BHR plasmid (panel A) and fitness cost of the BHR plasmid (panel B) on the frequency at steady-state of BHR and NHR plasmids in two species assemblages. 147

- Figure 3.17. Effect of varying the transfer of NHR and BHR compatible plasmids on their transfer dynamics in a two-species assemblage. 151

- Figure 3.18. Effect of different transfer rates for the BHR plasmid on the dynamics of two incompatible plasmids invading a two-species assemblage. 153

- Figure 3.19. Effect of stochasticity on the dynamics of two incompatible plasmids invading a two-species assemblage. 154

Chapter Four

- Figure 4.1. 2D representation of biofilm thickness (X) and solute concentration gradient (g L^{-1}) over the length of the biofilm (Y) at steady state after 8 days of growth. 174

- Figure 4.2. Dynamics of transfer of a NHR plasmid and a BHR plasmid in a two-species mixed biofilm illustrated for different time-points. 175

- Figure 4.3. Dynamics of transfer of a NHR plasmid and a BHR plasmid in a two-species patchy biofilm illustrated for different time-points. 176

- Figure 4.4. Effect of varying the transfer probability on the dynamics of plasmid invasion of a NHR plasmid in a two-species biofilm assemblage for the different biofilm structures. 178

- Figure 4.5. Dynamics of transfer of a NHR plasmid in a two-species patchy biofilm illustrated for different time-points. 179

- Figure 4.6. Effect of host-range for decreasing values of the transfer probability for the BHR plasmid on the dynamics of two compatible plasmids invasion in single and two-species mixed biofilms. 184

- Figure 4.7. Effect of fitness cost and transfer probability on the total frequency of compatible BHR and NHR plasmids transferring in a two-species mixed biofilm for 100 days. 187

- Figure 4.8. Effect of an increased fitness cost on the frequency of plasmids with different host-ranges when competing with each other. 188

- Figure 4.9. Effect of decreasing the transfer probability on the frequency of plasmids with different host-ranges when competing with each other. 189

- Figure 4.10. A typical replicate simulation of the dynamics of transfer of two compatible NHR and BHR plasmids in two-species biofilms. Effect of an increased fitness cost on the frequency of each plasmid in different biofilm structures. 193

- Figure 4.11. Effect of transfer probability on the total frequency of compatible BHR and NHR plasmids transferring in a mixed and a patchy biofilm for 100 days. 194

- Figure 4.12. Effect of host-range for decreasing values of the transfer probability for the BHR plasmid on the dynamics of invasion of two incompatible plasmids in single and two-species mixed biofilms. 197

- Figure 4.13. Effect of fitness cost and transfer probability on the total frequency of incompatible BHR and NHR plasmids transferring in a two-species mixed biofilm for 100 days. 200

- Figure 4.14. Effect of fitness cost on the total frequency of incompatible BHR and NHR plasmids transferring in a mixed and a patchy biofilm for 100 days. 203

- Figure 4.15. Effect of transfer probability on the total frequency of BHR and NHR incompatible plasmids transferring in a mixed and a patchy biofilm for 100 days. 204

- Figure 4.16. Transfer of incompatible NHR and BHR plasmids in mixed and patchy biofilms over time. 205

Chapter Five

- Figure 5.1. Transfer rate of RK2 among *Pseudomonas* and *Escherichia* species for 30 minutes on LB agar plates at three different temperatures. 230

- Figure 5.2. Transfer dynamics of RK2 in *E. coli* populations in LB agar plates at two different temperatures: scenario A, 37°C and scenario B, 26°C. 232

- Figure 5.3. Transfer dynamics of RK2 or R387 in two-species assemblages in LB agar plates at 37°C for 24 hours. 234

List of Tables

Chapter One

- Algorithm 1.1 Pseudo-code describing one global timestep iteration of the individual-based simulator iDynoMiCS 66
- Table 1.1 iDynoMiCS HGT parameters 72

Chapter Two

- Table 2.1 Description of the variables used in the different models 81
- Table 2.2 Comparison of HGT parameters for the ODE model and lbM 91
- Table 2.3 Growth and system parameters (ODE chemostat) 91
- Table 2.4 iDynoMiCS chemostat system parameters 92
- Table 2.5 System parameters (iDynoMiCS biofilm) 103
- Table 2.6 Growth parameters (iDynoMiCS biofilm) 103
- Table 2.7 HGT parameters 104

Chapter Three

- Table 3.1 Growth and system parameters 110
- Table 3.2 Plasmid-related parameters 115
- Table 3.3 Frequency of plasmid-bearing cells (T_N^B) and recipients (R_N) at steady state obtained with the ODE and the lbM models for different transfer rates. 115

Chapter Four

- Table 4.1 Effect of varying the transfer probability (p) or the fitness cost (α) on the frequency of the NHR plasmid transferring in two-species biofilms. 182

Chapter Five

- Table 5.1 List of plasmids and strains used in the present work. 217
- Table 5.2 Summary of antibiotics used to select for donors, transconjugants and recipients in the mating experiments performed between the different strains. 220
- Table 5.3 List of antibiotics used for selecting donors, transconjugants and recipients in the two-species scenario for R387 and RK2 plasmids. 222
- Table 5.4 List of antibiotics and suppliers 223
- Table 5.5 Summary of growth rates and doubling time for the bacterial strains chosen for this study, carrying either RK2 or R387 plasmid or no plasmid, under different growth conditions. Three replicates were used to calculate the mean and the corresponding standard deviation. 226
- Table 5.6 Summary of Kruskal-Wallis test results for the effect of each main factor on the observed growth rates. 227
- Table 5.7 Summary of t-test results for the relative fitness of strains carrying either RK2 or R387 plasmids. 227
- Table 5.8 Summary of the transfer frequency (T/D) for RK2 and R387 plasmids in different hosts. 228

- Table 5.9 Summary of Kruskal-Wallis test results for the effect of each main factor on the observed transfer frequencies. 229

List of Abbreviations and Symbols

BacSim	individual-based Bacterial colony growth Simulator
BHR	Broad Host Range
CA	Cellular Automata
COD	Chemical Oxygen Demand
Crb	Carbenicillin
FACS	Fluorescence Activated Cell Sorter
Fin	Fertility inhibition
Gent	Gentamycin
HGT	Horizontal Gene Transfer
HR	Host Range
IbM	Individual-based Model
iDynaMiCS	individual-based Dynamics of Microbial Communities Simulator
Inc	Incompatibility group
Km	Kanamycin
LB	Luria Broth
MGE	Mobile Genetic Elements
MPF-complex	Mating Pair Formation complex
mrs	multimer resolution system
Nal	Nalidixic acid
NHR	Narrow Host Range
ODE	Ordinary Differential Equation
PBS	Phosphate Buffer Saline
PSK	Post-segregational killing system
SCLM	Scanning Confocal Microscopy
Str	Streptomycin
Tc	Tetracycline

Symbol	Description
--------	-------------

R_N	Recipient cell of species N
R_B	Recipient cell of species B
T_N^N	Transconjugant cell of species N carrying a NHR plasmid
T_N^B	Transconjugant cell of species N carrying a BHR plasmid
$T_N^{B,N}$	Transconjugant cell of species N carrying both BHR and NHR plasmids
T_B^B	Transconjugant cell of species B carrying a BHR plasmid
$T_{B,N}^B$	Sum of transconjugant cells of species B and N that carry a BHR plasmid
μ_{\max}	Maximum rate of growth on substrate S
X	Biomass
S	Substrate
S^B	Substrate concentration in the bulk compartment
S_R	Substrate concentration in the reservoir (chemostat)
Y	Biomass yield for growth on substrate S
K_S	Substrate concentration for half-max growth rate
ρ_X	Biomass density
r_d	Division radius
r_m	Death radius
ω	Dilution rate
t_s	Time spent between each iteration
ϵ	Conversion factor (mass to cell numbers)
c	Coefficient of encounters by collision
l	Side length of 3D domain
Symbol	Description

p_{dil}	Probability of an agent being lost from the chemostat due to stochastic dilution
N_{screen}	Number of agents that is screened to attempt the transfer or reception of a plasmid by a cell during one time step in the chemostat
N_{total}	Total number of agents in the chemostat
D_S	S (substrate) diffusion coefficient
l_{BL}	Boundary layer thickness
k_{det}	Erosion strength coefficient
σ_R	Specific area
r	Resolution of 2D domain
v_s	Conjugal pilus scan speed
d_p	Pilus reach distance
p_i	Transfer proficiency (probability of success)
γ	Transfer rate
p_{lossi}	Probability of segregative loss of plasmid during cell division
τ	Loss rate
$t_{recipient}$	Maturation period following initial plasmid receipt
t_{donor}	Recovery period following plasmid transfer
α_i	Plasmid burden

Chapter 1

Introduction

INTRODUCTION

In this chapter, the literature review is divided into five main topics each covering different aspects of plasmid biology and mathematical modeling of the transfer and persistence of plasmids in different environments. It starts with the description of plasmid structure, replication and classification. Following, plasmid maintenance mechanisms and the host-range of plasmids are surveyed. The factors affecting the conjugative transfer of plasmids in various natural environments and in laboratory setups are reviewed in section 1.4. Finally, in a section dedicated to mathematical modeling of horizontal gene transfer, the first models of plasmid transfer in bacterial populations growing in chemostats are revisited and the latest developments in modeling plasmid transfer in structured bacterial assemblages are critically analysed.

1.1. Plasmid Biology

Plasmids are non-essential linear or circular double stranded DNA molecules, which are able to replicate autonomously and in a controlled way within the host. Lederberg and Tatum discovered plasmids in 1946 when they noticed that phenotypic traits carried by mutant strains of the gut bacterium *Escherichia coli* K-12 could be horizontally transmitted (Lederberg and Tatum, 1946b; Lederberg and Tatum, 1946a). For their discovery the two researchers were awarded the Nobel Prize in Physiology or Medicine in 1958. This extra-chromosomal DNA element was

first named Fertility factor as an analogy to the process of sexual reproduction in eukaryotes.

Some plasmids have the ability to transfer horizontally among Bacteria and Archae (Smillie et al., 2010; Solar et al., 2010). Horizontal gene transfer (HGT) can also proceed via transformation (introduction or uptake of extracellular genetic material through pores in the bacterial cell wall) or transduction (bacterial DNA becomes integrated into a phage particle and is transferred from one bacterium to another by a bacteriophage) (Thomas and Nielsen, 2005). Genome sequencing has shown that frequent acquisition of genetic material from phylogenetically distant bacteria and even other organisms such as eukaryotes, has occurred extensively throughout evolution (Koonin et al., 2001; Jain et al., 2003). Mobile genetic elements (MGE) such as bacteriophages, transposons and plasmids are the agents carrying out HGT. They are the vectors involved in the spread of many important bacterial properties such as antibiotic resistance, virulence and biodegradation of recalcitrant compounds (Elsas and Bailey, 2002). MGE have been identified in various natural habitats such as soils, sewage and activated sludge (Davison, 1999; Heuer et al., 2012b) where resistance genes often found on conjugative plasmids can proliferate and increase antibiotic resistance among microorganisms (Tamminen et al., 2012).

The current escalation of antibiotic resistance combined with the slow rate at which new and effective chemical drugs are discovered represents a real threat to Human and animal health. Thus, it is important to know how these MGE are transferred and maintained in between the various environmental ecosystems.

1.1.1. Plasmid structure and transfer

The size of natural occurring plasmids can range from few hundreds of base pairs to more than 5 megabases (Casse et al., 1979). The structure of plasmids is mosaic: the essential functions (e.g. replication, maintenance or transfer) and accessory functions (those contributing to a particular phenotype on the host cell) are organized in different blocks of genes - operons - readily identifiable from sequence analysis. In Figure 1 a schematic representation of the structure of a plasmid is depicted. The absolute minimum requirement for a plasmid to exist is its ability to replicate and the genetic sequences required for plasmid replication are clustered in a small region called the replicon. Basic replicons consist of an origin of replication (*ori*), *cop*/*inc* genes involved in the control of the initiation and replication and *rep* genes encoding Rep proteins required for replication and often participating in its control. The accessory genes associated with resistance to antibiotics or pathogenicity are often found in transposons and integron elements, and can contribute to the propagation of the plasmid in the bacterial host (Heuer et al., 2012a).

The process of gene exchange mediated by self-transmissible plasmids is termed conjugation and requires close proximity between the donor and the recipient bacterium, which can be attained by production of a filamentous surface appendage called the sex pilus (Thomas, 2000). The transfer of DNA via bacterial conjugation obeys a series of steps starting with the expression of the transfer genes *tra* encoded in the plasmid. These gene products are then used to assemble the pilus and the type IV secretion apparatus (the supramolecular protein complex spanning the cell envelope involved in the transfer of single-stranded DNA from the donor to the recipient). The recipient cells must be recognized by the donor cell probably via

interactions between the pilus tip and the surface components on the recipient cell. This screening prevents the self-mating between two donor cells carrying the same sex pilus type and it has been attributed to plasmid-encoded entry exclusion systems (Garcillan-Barcia and de la Cruz, 2008). In Gram-positive systems, physical contact is triggered by peptide pheromones that induce the synthesis of surface aggregation substances leading to mating aggregates being formed between donors and recipient cells (Thomas, 2000). The initiation complex for the conjugative transfer involves a specific DNA-protein structure, the relaxosome, placed at the transfer origin *oriT* of the plasmid. At this point the DNA is nicked and a single strand DNA is transferred into the recipient cell via rolling circle replication where elongation and transfer of the leading strand is accompanied by the displacement of the parental strand (Lanka and Wilkins, 1995). Thus, transfer is a replicative process in which a new plasmid copy is created in the recipient cell.

Triggering of conjugative transfer is tightly regulated by plasmid-encoded effectors, as to minimize the metabolic burden on the host. The plasmids belonging to the IncP1 group have evolved a complex but efficient regulatory system involving both global regulators (e.g. KorA and KorB are repressors of genes involved in plasmid replication, transfer and stable maintenance, and TrbA is a repressor of genes for the conjugative apparatus, *tra* and *trb*) and local autoregulatory circuits. The down-regulation of the transfer genes is initiated once the bacterium has a functional conjugative apparatus (Zatyka and Thomas, 1998). Unlike IncP1 plasmids, the F-like transfer system is controlled by the fertility inhibition system (FinOP system) which constitutively expresses a plasmid-specific antisense RNA (FinP) and a polypeptide (FinO) which together repress the translation of *traJ* mRNA.

If TraJ protein is not expressed the genes necessary for plasmid transfer are not transcribed. Thus, within a population, carrying an F-like plasmid (except the F itself which is a derepressed mutant), only few bacteria will actually be transfer proficient (Zatyka and Thomas, 1998).

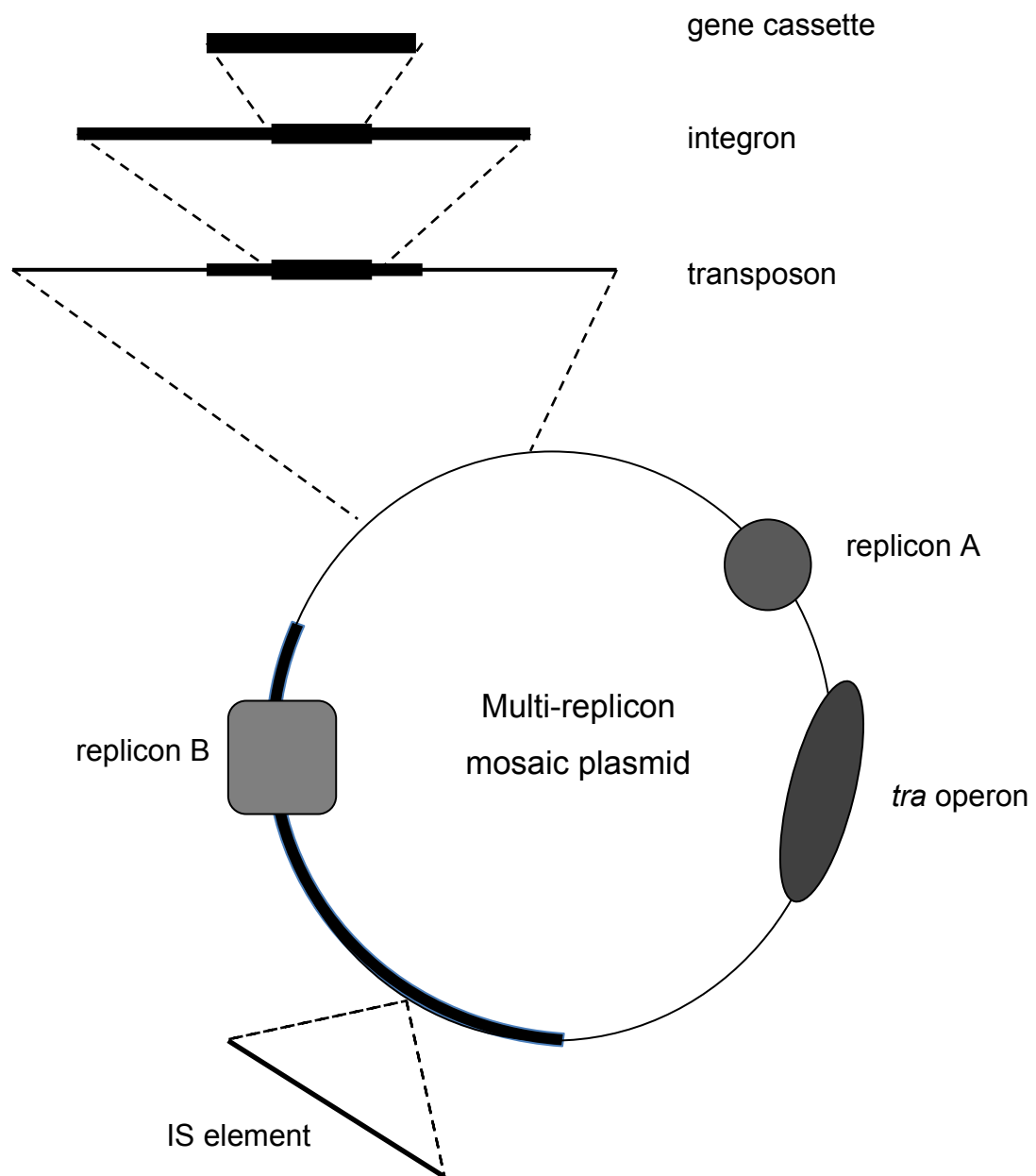


Figure 1.1. The mosaic structure of plasmids (adapted from Thomas, 2000)

1.1.2. Replication and copy number control

From the studies on plasmid replicons it appears there are a limited number of replication strategies. The principal difference resides in the strategy to load and assemble the replisome complex at the origin of replication (Thomas, 2000; del Solar et al., 1998).

One option is to use a primary transcript or a set of repeated A+T rich binding sites (iterons) located in the origin where a Rep protein can bind and unwind the region forming the replication bubble. This type of replication is equivalent to the chromosome replication where following the unwinding of DNA a primase is recruited to initiate the leading strand synthesis, a process that produces a DNA structure resembling the letter θ from the Greek alphabet and thus has been named theta replication. This strategy has been described for plasmids isolated from Gram-negative bacteria, such as ColE1, F or RK2/RP4 (Thomas, 2000).

The alternative strategy consists in a single strand nick on the DNA introduced by a Rep protein and the generation of a 3'-OH end, which is used as a primer for the leading strand synthesis. Elongation is then accomplished by the host proteins accompanied by the displacement of the parental strand [+], which overall involves a rolling-circle mechanism. This is the route that many small multicopy plasmids isolated from Gram-positive bacteria adopt in order to replicate (Novick, 1989).

In order to maintain an average number of plasmid copies within a given host under certain growth conditions, the plasmid has evolved efficient replication control

mechanisms to avoid either being lost by segregation or becoming an unsupportable metabolic burden for the host. All plasmids studied so far control their copy number at the replication initiation step by means of a negative feedback loop (Thomas, 2000). The regulators that carry out this control are themselves encoded in the replicon region and they are usually one of two types: small trans-acting counter-transcript RNAs whose target is a complementary region of the RNA primer required for initiation of replication; or iterons where the Rep proteins can bind and self-regulate their expression levels (Thomas, 2000).

The cost associated with carrying a plasmid is mostly attributed to the exploitation of the machinery of the host cell for replication, regulation and transfer of the plasmid. In general, the cost seems to increase with copy number and length of the plasmid (Smith and Bidochka, 1998; Corchero and Villaverde, 1998). In the limit, a rise in plasmid copy number resulting in increased metabolic burden for the host can lead to cell death (Velmurugan et al., 2003). Nevertheless, plasmids with copy numbers in the order of 200 have been observed in natural populations (Projan et al., 1987; Acebo et al., 1996). Watve et al. (2010) investigated the stably existence of low copy number plasmids despite the possibility of copy-up "cheater" mutants arising and outcompeting the wild-type low copy plasmids. Using a multilevel selection mathematical model they showed that sociobiological interactions among different types of plasmids allowed the coexistence of plasmids with varied copy numbers. Specifically, the high fitness cost of high copy plasmid mutants will allow the wild-type low copy number plasmid to proliferate after initial invasion by the former, leading to a rock-paper-scissor like dynamics where above a fitness threshold the intra-host selection is overcompensated by inter-host selection. Among

the interesting model predictions is the coexistence of low copy transferrable plasmids and high copy number non-transferrable plasmids. Overall, their conclusions underlie the importance of the interaction between the two types of cheating (high copy number and ability to transfer) in the maintenance of plasmid diversity at the copy number and transfer proficiency levels.

1.1.3. *Incompatibility Groups*

Plasmid classification became important at the end of the 1950's following the discovery of R plasmids (plasmids carrying virulence factors or antibiotic-resistant genes) and their wide distribution (Datta and Hedges, 1972; Datta and Hedges, 1972; Smith et al., 1975). Datta (1979) introduced a formal scheme of classification based on incompatibility in 1979. This system of classification relies on differences in the replication control of different replicons. The replicon, as defined in section 1.1.1, is a small region in the plasmid where all the genes required for plasmid replication and its control are clustered. It consists of an origin of replication (*oriV* or *ori*), *cop/inc* genes involved in the control of the initiation of replication and *rep* genes whose products are required for replication and also participate in its control (Thomas, 2000). Incompatibility usually arises when two plasmids employ the same mechanism to control their replication or partitioning, which leads to unbalanced number of plasmid copies for each incompatible plasmid (Projan and Novick, 1984). Represented in Figure 1.2 is a sequence of events that can lead to a generation of daughter cells harbouring only one type of plasmid, despite their precursor originally

carrying two incompatible plasmids. Changes in the relative number of copies of each plasmid make it impossible for both plasmids to be stably propagated within the same cell line.

The observation that conjugative transfer of the F plasmid was severely impaired when recipient cells already carried the same F factor led to the recognition of another "incompatibility" phenomenon: entry exclusion (Watanabe, 1963; Watanabe, 1967; Novick, 1969). The entry exclusion constitutes a physical barrier to the transfer of DNA between cells carrying isogenic or closely related sex factors and it seems to be present in most conjugative plasmids studied to date (Garcillan-Barcia and de la Cruz, 2008). It effectively prevents the entry of an incompatible plasmid into the host cell, which could lead to the elimination of the pre-existing plasmid. Most conjugative elements carry one gene coding for an inner membrane protein which when expressed in the recipient cell blocks DNA transfer within stable mating pairs. Another type of exclusion consists in the interference with the initial attachment of a donor bacterium to a potential recipient.

Technical difficulties in distinguishing entry exclusion systems from replication incompatibility or the presence of more than one replicon in a plasmid represent confounding factors for the establishment of a reliable system of classification.

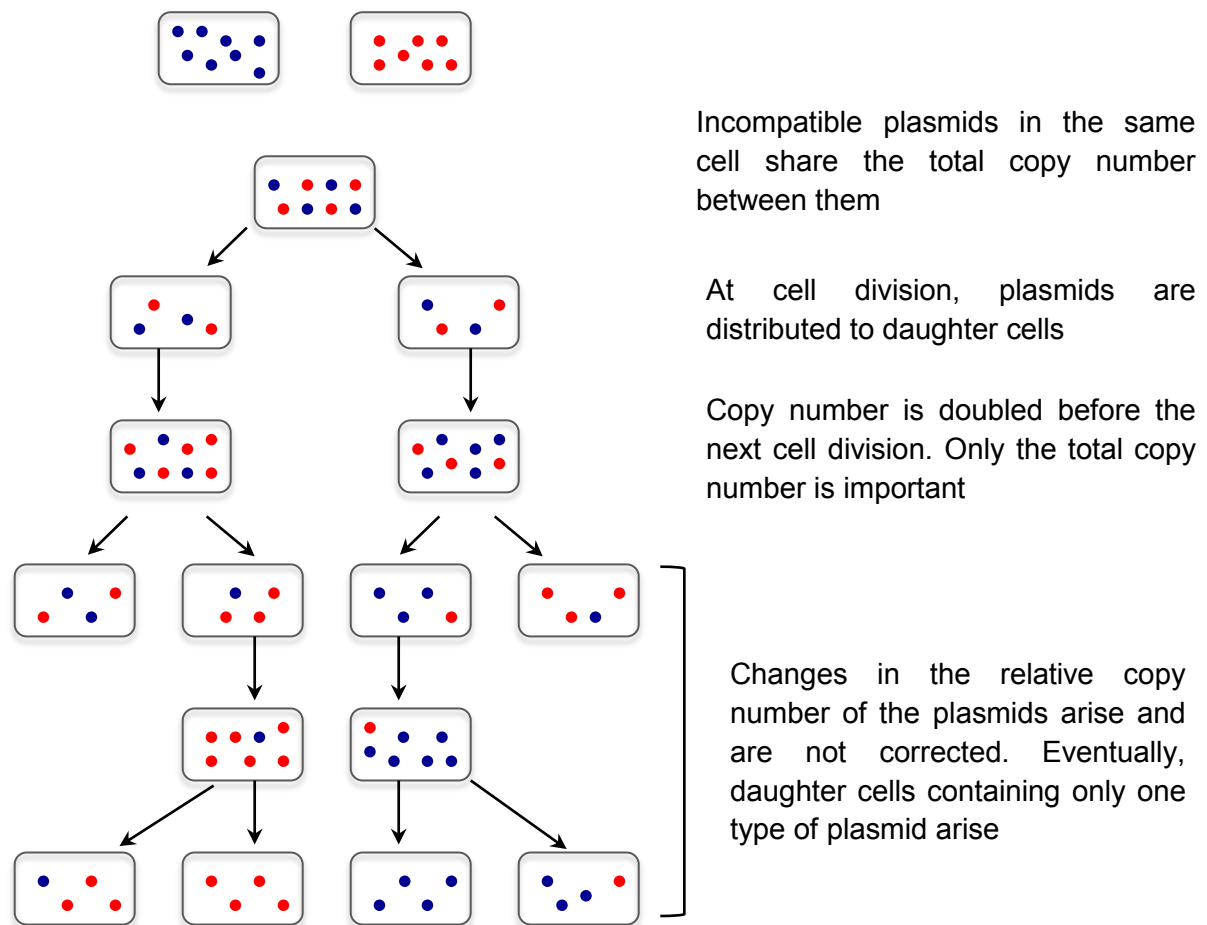


Figure 1.2. Segregation of incompatible plasmids (adapted from Thomas and Summers, 2008).

1.2. Plasmid Maintenance

Successful plasmid transfer and maintenance depends on various factors related both to the host and to the plasmid but also on the host-plasmid interaction. Carrying a plasmid may represent an excessive burden to the host due to additional DNA replication and protein production needed for plasmid maintenance and transfer. The only benefit to the host is if this extra-chromosomal piece of DNA encodes for advantageous genetic traits in a particular environment. It is thus not surprising to find a few but very efficient mechanisms that ensure the stable maintenance of plasmids, preventing their loss upon cell division. These plasmid maintenance systems include active partitioning systems and multimer resolution systems (mrs), post-segregational killing systems (PSK) and plasmid-encoded restriction-modification systems (Thomas, 2000).

1.2.1. Partitioning and Resolution Systems

The tight regulation of the number of origins of plasmid replication has a direct impact on the number of plasmid copies during cell growth, which in turn determines the probability that one daughter cell will become plasmid free during cell division. In the case of high copy number plasmids, such as ColE1 (average copy number between 10 to 30), the distribution of the plasmids between two descendent cells at cell division is a random process (Thomas, 2000). During homologous recombination, identical copies of a plasmid can form high order oligomers decreasing the number of

independent molecules available for segregation. Site-specific recombination systems ensure that plasmid multimers that have arisen during replication or recombination will be resolved and converted into free monomers and subject to random distribution into the daughter cells.

The probability of loss would be higher for low-copy number plasmids if they were to follow a random distribution. The ParA/*res* system of the IncP-1 plasmid RK2, a low copy number (5 to 8 copies) plasmid able to stably propagate in a wide range of gram-negative bacteria, is an example of an integrated plasmid resolution system and an active partitioning system (Adamczyk and Jagura-Burdzy, 2003). The active partitioning mechanism employed by various low-copy number plasmids is very similar to the process of bacterial chromosome segregation to daughter cells (Yamaichi et al., 2000). Three main components drive the partitioning process: two *trans*-acting factors, namely ParA and ParB and a *cis*-acting centromere-like site where the nucleoprotein complex is assembled. They are encoded by a single operon located in the *par* locus of the plasmid and their function is to actively and evenly distribute the plasmid copies to each daughter cell at cell division.

1.2.2. *Post-segregational Killing Systems*

Another strategy to improve stable inheritance is to produce a long-lived toxin and the corresponding short-lived antitoxin. When such a system is encoded by a plasmid, the plasmid-free cells will be killed by the toxin activity, which explains the observed decrease in frequency of plasmid-free cells in a growing bacterial culture

(Brendler et al., 2004). Post-segregation killing systems and active partitioning systems are usually found in low-copy plasmids, as is the case for plasmids belonging to the IncP-1 α group (although IncP-1 β plasmids rely only on active partitioning) (Adamczyk and Jagura-Burdzy, 2003). The PSK system of RK2 encompasses the *parDE* operon and codes for a proteic PSK system of two proteins, ParD whose N-terminus has been found to possess both DNA binding properties used to auto-regulate its expression and anti-toxic activity to inhibit ParE toxicity (Roberts et al., 1993). Another example is the *hok/sok* PSK system encoded by the plasmid R1 of *Escherichia coli*. In this case the *hok* gene encodes a toxic protein involved in the depolarization of the cell membrane and the *sok* gene encodes an antisense mRNA transcript which blocks *hok*'s mRNA translation (Thisted et al., 1995). An alternative PSK system is the one based on restriction modification modules carrying pairs of genes encoding a restriction endonuclease and their cognate modification enzymes. Restriction modification systems have been found both in prokaryotes and Archae but not in eukaryotes (Nolling et al., 1992).

The effect of killing plasmid-free daughter cells has been taken to contribute significantly to ensure plasmid vertical stability, however PSK does not directly increase neither the likelihood of plasmid inheritance nor the number of plasmid-bearing cells (Mongold, 1992). Cooper and Heinemann (2000) experimentally tested this "stability" hypothesis by performing competition experiments between bacteria carrying either *psk*⁺ or *psk*⁻ plasmids. They found that *psk*⁺ plasmids were only benefitted if cell death is accompanied by elimination of a competing *psk*⁻ plasmid. Thus, widespread of PSK systems among conjugative plasmids may have evolved

as a consequence of plasmid-plasmid competition and not because of a well-protected host-plasmid relationship.

1.3. Plasmid Host-Range

The host-range of a plasmid is the range of species and/or genera in which it can replicate. This needs to be experimentally assessed for each plasmid, as stability of a plasmid in different bacterial species can vary considerably (De Gelder et al., 2007). It is plausible that the range of species into which a plasmid can transfer is larger than the range in which it can replicate and be vertically inherited (Guiney et al., 1984; Thomas and Smith, 1987).

1.3.1. Narrow and Broad host range plasmids

Some plasmids can only replicate within few species of one genus (narrow host-range - NHR) while others have a host range spanning many genera (broad host-range - BHR) (Guiney, 1982; Mazodier and Davies, 1991). The terms NHR and BHR do not represent two discrete classes of plasmids, but are used as qualitative indicators instead (del Solar et al., 1996; Suzuki et al., 2010). Generally, conjugative plasmids belonging to the Incompatibility groups IncP, IncN, and IncW have been designated as having a broad host-range, whereas plasmids from IncF, IncH and IncI groups are considered to have a narrow host-range (Datta and Hedges, 1972; Mazodier and Davies, 1991). Mobilizable plasmids belonging to IncQ incompatibility group also display a broad host-range (Meyer, 2009; Hoffmann et al., 1998). Broad host-range plasmids have been widely used in molecular genetics and their potential applications keep increasing (Lale et al., 2011; Smorawska et al., 2012).

Although plasmids are characterized by their ability to replicate autonomously, their replication is not completely independent of host factors. Critical stages upon transfer into a new host include the increase in copy number, which may not be permitted in some hosts, and the adequate expression of plasmid-encoded replication regulatory systems, which in turn may be affected by the degree of plasmid DNA supercoiling in its new host. Therefore, strategies that promote the independence from host replication factors (e.g. DNA Polymerase I) and a versatile communication between plasmid- and host-specific proteins involved in the initiation of replication will broaden the spectrum of hosts in which a plasmid can survive (del Solar et al., 1996). One way of achieving this would be for a plasmid to acquire different replicons, which would increase the probability of efficient replication in several hosts. This is the case for the BHR pGSH5000 plasmid, which carries two functional replicons (pCU-1 and F-like replicons) active in different hosts (da Silva-Tatley and Steyn, 1993). However, there are also examples of NHR plasmids such as the F plasmid that often contain multiple replicons (Bergquist et al., 1986).

1.3.2. Evolution of host-range

In Figure 1.3, a schematic representation of how host-range can evolve in opposite directions is depicted. NHR plasmids are usually found in a limited range of species where they have been kept for long enough time that the burden imposed on the host is very small. Indeed, various reports have shown that when a plasmid is maintained in the same host for numerous generations, a decrease in fitness cost for the host

occurs. Dahlberg and Chao, (2003) found evidence for amelioration of the cost of carriage as a result of plasmid-host co-evolution. Increased bacterial fitness following co-evolution of R1 plasmid in *E. coli* K12 after 420 generations has also been reported (Dionisio et al., 2005). In order to investigate the ability of pB10 to adapt to unfavorable hosts, De Gelder et al., (2008) conducted evolution experiments where two hosts (*S. maltophilia* P21 and *P. putida* H2) in which the plasmid is highly unstable were used. After 500 generations in host P21, plasmid stability was improved and a decreased cost in its ancestral host was also observed, resulting in host-range expansion. DNA sequence analysis of the evolved plasmids revealed only one genetic change, a single mutation in the prepilin protein, TrbC, involved in pilus assembly which could lead to higher transfer frequencies thus contributing for plasmid maintenance in the population by countering segregational loss. This study also showed that regular switching between hosts in the course of the evolution experiments could slightly hinder plasmid adaptation. Specialization of a plasmid has also been described, where the plasmid effectively loses the ability to replicate in a species where it was previously found to be stably inherited (Sota et al., 2010), revealing a trade-off between improved stability in a new host and the ability to replicate in the former host.

Conjugative transfer of a plasmid is, nevertheless, a replicative process and thus prone to DNA replicative errors despite the high fidelity of Polymerase I. Kunz and Glickman (1983), measured the accuracy of replication and transfer of a *lacI* gene on an F plasmid and found a 300-fold increase in the rate of base substitution during conjugation when compared to vegetative replication. These results were independent of *recA*-dependent processes. Other reports have also showed that

replicative transfer increases reversion of mutations on genes carried by plasmids (Peters et al., 1996; Christensen et al., 1985). Thus, frequent rounds of conjugational transfer into new hosts could, in principle, accelerate expansion of host-range by generating a larger pool of mutations from which adaptation and ability to replicate in a new host could follow (Figure 1.3).

Despite the increased fitness cost that BHR plasmids represent to their hosts, they are frequently over-represented in stressed environments (Smalla et al., 2006), which suggests that their ability to transfer between and replicate within many different hosts might be sufficiently advantageous in natural environments. A mathematical analysis carried out by Bergstrom et al. (2000) addresses the question of how plasmids manage to persist over evolutionary time when empirical studies suggest that plasmids are not transferred at rates high enough to be maintained as genetic parasites. Assuming that beneficial genes carried by plasmids can move to the host chromosome, the authors conclude that plasmids can only be maintained in pure populations if these undergo frequent selective sweeps or if they have the ability to shuttle genes across species boundaries. The latter condition is satisfied by plasmids with a broad-host range.

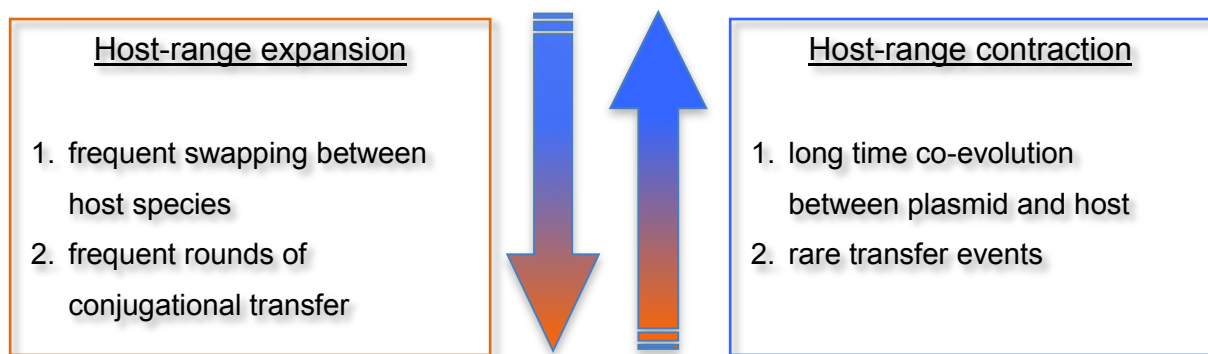
Recently, Suzuki et al. (2010), developed a method to infer the evolutionary host range of a plasmid based on their genomic signatures. The authors define the evolutionary host-range of a plasmid as the entire range of hosts in which a plasmid has replicated at some point during the course of its evolutionary path. It has been found that the nucleotide composition, or genomic signature of plasmids, is usually similar to their host's chromosome, which suggests that plasmids tend to acquire the host's genomic signature over time (Campbell et al., 1999; Suzuki et al., 2008). A list

of 55 plasmid sequences from six incompatibility groups and 817 bacterial chromosomes were used to calculate the genomic signature of the DNA sequences. They found that both at the class and at the order taxonomic levels, plasmids from IncP group showed the broader candidate evolutionary hosts, which included three proteobacterial subgroups (see Figure 1.4). Figure 1.4 also shows that all plasmids from the other incompatibility group IncF had been assigned candidate evolutionary hosts belonging only to *Gammaproteobacteria*. Their results are consistent with experimental observations of IncP plasmids transferring and replicating in bacterial hosts from the three classes within the phylum *Proteobacterium*, as well as for the IncF and IncI plasmids, which are known for their limited host range to members of the *Enterobacteriales* order. This study opens a new research tool to study the host-range of plasmids, which will become more accurate when more plasmid and prokaryote chromosome DNA sequences become available. Knowledge of plasmids host-range and their evolutionary history is very important given that these are keyplayers in the dissemination of antibiotic resistance worldwide (Levy and Marshall, 2004).

Host-range

Narrow host-range (NHR):

1. replicates and transfers within few species of a genus
2. long term association of plasmid and host leads to improved stability and decrease in burden



Broad host-range (BHR):

1. replicates and transfers in many genera
2. not enough time for co-evolution may result in increased fitness cost for the host

Figure 1.3. Schematic representation of host-range evolution and mechanisms involved in its expansion towards a BHR or contraction towards a NHR.

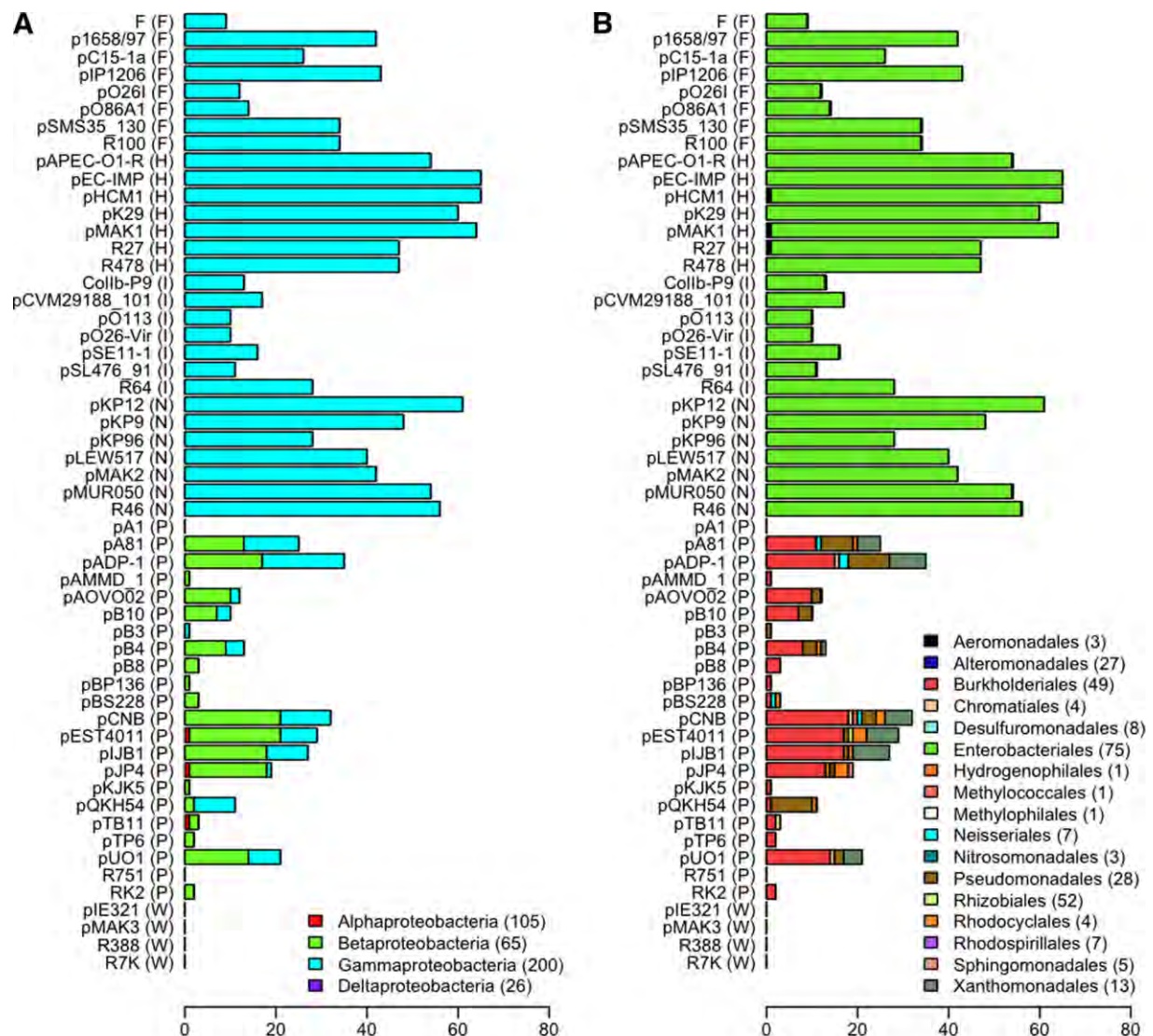


Figure 1.4. Bar plot showing the number of candidate evolutionary hosts for each plasmid. Different colors represent different taxonomic groups at the level of class (A) and order (B). The number of strains belonging to each taxon is given in parentheses. Each character (F, H, I, N, P and W) denotes the incompatibility group to which each plasmid belongs (taken from Suzuki et al., 2010).

1.4. Conjugative Transfer of Plasmids

1.4.1. Monitoring plasmid transfer

Conjugative plasmid transfer has been investigated since the 50's but despite the considerable amount of molecular data available, the precise biochemical mechanisms that regulate conjugative transfer and how environmental and host-dependent factors modulate gene transfer remain to be determined (Thomas and Nielsen, 2005; Sorensen et al., 2005).

Direct experimental study of horizontal gene transfer has been undertaken using methods that rely on culturing of transconjugant cells and more recently with the reporter-gene approach. The latter is a powerful molecular technique that makes use of different fluorescent biomarkers (Larrainzar et al., 2005) to monitor over time plasmid transfer events *in situ* by means of scanning confocal laser microscopy (SCLM) (Haagensen et al., 2002; Babic et al., 2008; Babic et al., 2011). Flow cytometry recently became a high-throughput method to quantify plasmid transfer frequencies as it allows quick detection of recombinant cells expressing a fluorescent protein (Bahl et al., 2004). Plasmid transfer efficiency has been defined as the ratio between the number of transconjugants and donors (T/D) and although this does not allow the direct comparison of the rate of transfer of different plasmids or in different environments that is what can be extracted from most studies (Sorensen et al., 2005).

Conjugative transfer is generally regarded as a unidirectional flow of genes from plasmid-containing donor cells to plasmid-free recipient cells. Yet, the

phenomenon of retrotransfer, i.e., a conjugational biparental event leading to the capture of new genetic traits (chromosomal or plasmid-borne) by the original host of a conjugative plasmid, has been reported to occur at high frequencies among various plasmids belonging to the IncP1, IncN, IncF and IncW groups (Beaudoin et al., 1998; Szpirer et al., 1999; Timmerly et al., 2009). This process can significantly contribute to the evolution and adaptation of microbial communities by promoting new combinations of genes.

1.4.2. Factors affecting plasmid transfer and establishment

The kinetics of conjugal plasmid transfer is influenced by many factors such as the types of organisms involved (Sota and Top, 2008) or the physiological state of the donor (Muela et al., 1994; Smets et al., 1993). Using the conjugative TOL plasmid, Pinedo and Smets, 2005 analyzed the effect of restriction proficiency, toxicant stress and cell density ratios on the overall rate of plasmid transfer between *P. putida* and *P. aeruginosa*. They found that the recipient's restriction system was the principal barrier to efficient plasmid transfer, which was only slightly attenuated by preliminary exposure of the recipient cells to chemical toxicants.

The genetic background of the donor and/or recipient cell can greatly influence the stability of a plasmid in the bacterial population. For example, although IncP-1 plasmids generally exhibit a broad host-range among Gram-negative bacteria their persistence in the absence of selective pressure is in part determined by strain-specific factors (Sota and Top, 2008). A similar finding was described by Dionisio et

al. (2002), where they refer to the existence of “amplifier cells” that can speed up R1 plasmid transfer in a heterogeneous population of enterobacterial species.

Not only does the host’s genetic background influence the replication process of a plasmid but also its ability to transfer into new hosts. This has been reported for the BHR IncP-1 β plasmid pB10 where its conjugative transfer into an activated sludge microbial community was strongly dependent on the type of donor used (Gelder et al., 2005). De Gelder et al. (2007) used this same plasmid to compare its stability among different hosts where the plasmid is known to be able to replicate, namely *Alpha*-, *Beta*- and *Gammaproteobacteria*. The fact that a plasmid is able to replicate in a given host does not imply its long-term stable maintenance in host’s progeny in the absence of selective pressure. Their work shows a large variation in the stability of pB10 in the different hosts: in some strains it was lost after only 80 generations whereas in others, persistence was observed for about 800 generations. This result correlates with the observed high variation in cost for the same plasmid in the different hosts.

1.4.3. *Plasmid transfer in chemostats and biofilms*

Conjugative transfer efficiency in bulk environments (either in water or soil) is usually very low (T/D lower than 10^{-5}) when compared to hot spots of bacterial metabolic activity and HGT found in the rhizosphere or other biofilm-related environments (T/D ratios greater than 10^{-3}) (Sorensen et al., 2005). The sex pili of F-like plasmids are long (up to 20 μm) and flexible, features that may be responsible for its high transfer efficiency in liquid culture (Clarke et al., 2008; Andrup and Anderson, 1999). In contrast, IncP plasmids group produce very rigid pili (e.g. RK2), appropriate for surface-bound matings (Bradley, 1980).

Biofilms are often considered to be hot spots for conjugation to take place and there have been a number of reports showing that the process of conjugation contributes significantly to biofilm development and further stabilization of its structure (Molin and Tolker-nielsen, 2003). A study carried out by Ghigo (2001) using the derepressed F-plasmid, demonstrates how the pilus-mediated network maintains the biofilm structure while expression of other adhesion factors contributes to its stickiness. In another study, May and Okabe (2008), found that the natural F-plasmid stimulates biofilm development and maturation by modulating the expression of two key players in this process: colanic acid and curli. Also, Reisner et al. (2006) observed that the ability of *E. coli* to promote biofilm formation was enhanced by conjugative transmission of natural plasmids carried by the *E. coli* isolates.

The higher efficiency of plasmid transfer in biofilms is expected because of the relative spatial stability of bacteria in biofilms that should favour conjugation. A report on R1 plasmid transfer between two marine strains has shown an increased

transfer frequency among the cells forming biofilms on the glass beads in a reactor when compared to their counterparts in the aqueous phase (Angles et al., 1993). Another study using *in situ* quantitative analysis to monitor conjugation events instead of the traditional plating method also reveals higher transfer rates of an RK2 plasmid derivative in a defined biofilm community independent of nutrient concentration in the medium (Hausner and Wuertz, 1999). This is in agreement with the fact that these plasmids produce short and rigid pili presumably optimized for mating on surfaces.

The direct comparison between suspended and sessile mating pairs of *E. coli* reported in the study by Licht et al. (1999), revealed differences in the rate at which transconjugants were formed between the biofilm and the chemostat system. In the biofilm, transconjugant cells appeared very rapidly but only initially, during a short period of time, which resulted in a small fraction (1-10%) of the population carrying the plasmid. Whereas in the chemostat at high cell densities, the effective mixing of the cells resulted in gradual appearance of transconjugant cells until virtually all the recipients had received a plasmid. The observation that only some of the recipient cells in a biofilm were able to receive the introduced plasmid was also reported for the establishment of the TOL plasmid in a multispecies biofilm (Christensen et al., 1998). In this case, the authors observed low transfer rates and thus the establishment of the TOL plasmid in the community was predominantly achieved by vertical transmission among the transconjugant cells or by rapid growth of the incoming donor cells. Here the transconjugant cells were preferentially located on the top of already pre-established microcolonies of potential recipient cells. The absence of further conjugal transfer of the plasmid from the colony surface to the

deeper layers of the microbial biofilm was attributed to a steep gradient of metabolic activity from the surface to the inner parts of the colonies. However, Hausner and Wuertz (1999) and Ehlers and Bouwer (1999) did not observe any dependency of plasmid transfer rates on nutrient concentrations. Yet Fox et al. (2008) using a combined approach of laboratory experiments and mathematical models found that invasion of an *E. coli* plasmid-free population, grown as colonies on agar plates, by the pB10 plasmid was more pronounced with increasing concentrations of glucose.

It is clear that plasmid invasion and establishment in a biofilm population depends on various factors such as the host metabolic state, the spatial arrangement of the donor and recipient cells or even the type of pili expressed by a particular plasmid (e.g. flexible or rigid pili). The observation of increased plasmid transfer rates under stressed conditions (Mc Mahon et al., 2007) puts forward another important factor to take into account when studying horizontal gene transfer: the role of the environment. Furthermore, there seems to be a dependency of the results on the experimental laboratory setup chosen to study plasmid transfer in structured communities, namely the physical conditions experienced by the cells may not be the same whether they grow as colonies on agar plates or in biofilm flow chambers or even in glass beads of a bioreactor.

1.5. Mathematical Modeling of Plasmid Dynamics

1.5.1. *Modeling plasmid dynamics in chemostats*

Chemostats

A chemostat is a bioreactor in which microorganisms can be grown under steady state conditions. The chemostat setup is composed of a nutrient reservoir connected to the growth chamber (reactor), which is continuously stirred in order to maintain a perfect mixing of all the material within the reaction vessel, as depicted in Figure 1.5. The constant inflow of fresh nutrients and outflow of the bulk liquid keeps the volume within the reactor constant (Novick and Szilard, 1950; James, 1961). Establishment of steady state will be achieved when no changes in the biomass and substrate concentration in the reactor are observed. At this point, microbial growth is balanced by dilution while substrate inflow is balanced by dilution and consumption due to growth. The dependence of growth on substrate consumption observed in the chemostat reactor is described by the Monod model, as illustrated in Figure 1.6. Each microorganism has a maximum specific growth rate, μ_{\max} , when growing on a particular substrate, which corresponds to the maximum rate of growth when that substrate is not limiting. Substrate affinity is expressed in terms of parameter K_s , which corresponds to the substrate concentration of half of the maximal specific growth rate. Thus, the chemostat has allowed investigators to study the physiological growth parameters of different microorganisms growing in various substrates. Other environmental parameters can be varied in a controlled manner,

such as temperature or pH, and their effect on growth kinetics evaluated (Herbert et al., 1956).

Chemostat mathematical models rely on the key assumption that mixing is perfect and hence, that the system is uniform in space. Other assumptions underlying modeling of microbial growth in chemostats include: microbes will not adapt physiologically and thus their kinetic parameters will remain constant, growth on the chemostat wall does not occur and all the individuals in a population are identical. Chemostats allow the production of high quantities of microbial biomass, which has been used, for example, in the production of antibiotics or therapeutic proteins, production of ethanol from sugar fermentation by bacteria or the production of fermented food such as cheese.

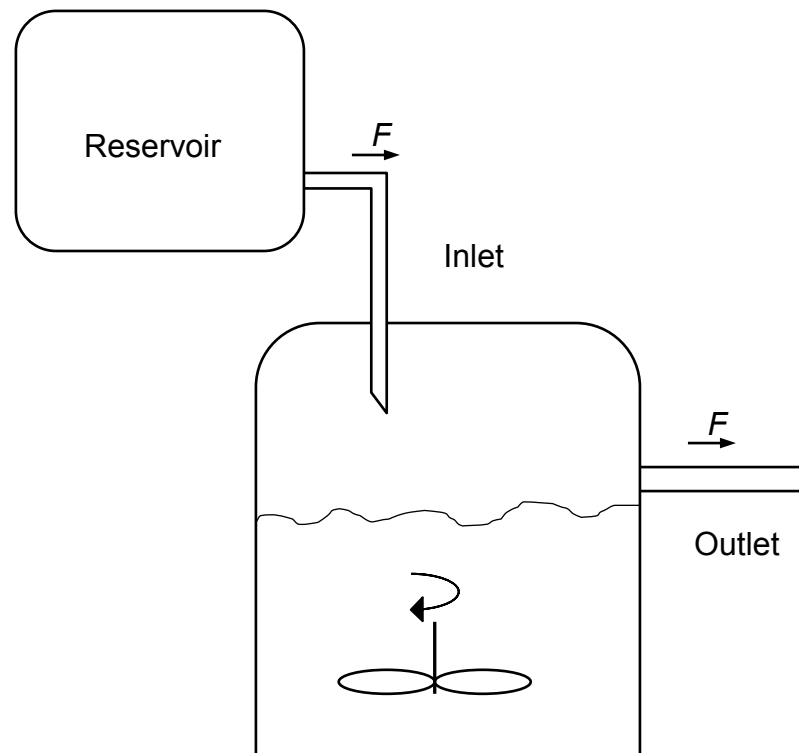
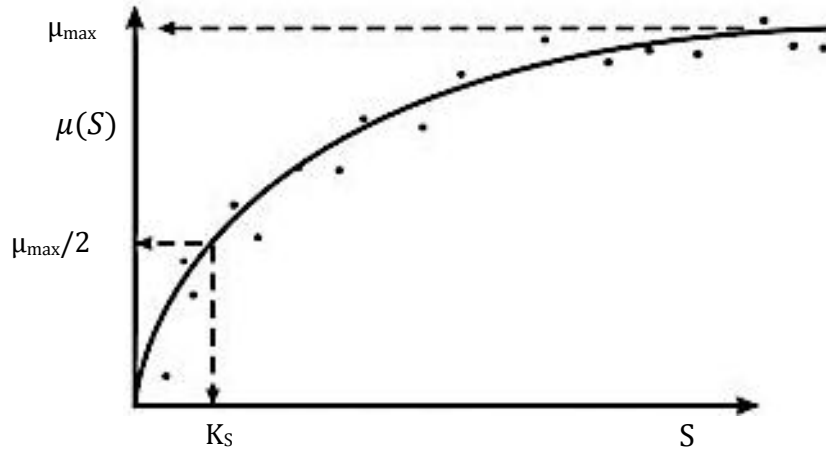


Figure 1.5. Schematic view of a chemostat. The ideal chemostat is characterized by continuous flowthrough and perfect mixing of material in the reaction vessel of volume V . Substrate is stored in the reservoir at concentration S_0 and a constant flow from the reservoir (inlet) into the vessel replenishes the chemostat with substrate S . The volume is kept constant by removing bulk liquid (containing bacteria, substrate and metabolites) from the reactor at the same rate F . This leads to dilution of all contents in the chemostat of dilution rate D , determined as F/V (adapted from Kreft, 2009).



$$(Eq. 1.1) \quad \mu(S) = \mu_{max} \left(\frac{S}{S + K_S} \right)$$

$$(Eq. 1.2) \quad \frac{dX}{dt} = \mu(S)X - \omega X$$

$$(Eq. 1.3) \quad \frac{dS}{dt} = -Y^{-1} \mu(S) X + \omega(S_0 - S)$$

Figure 1.6. Graph of the Monod equation (Eq. 1.1) fit to the observed data. The Monod function describes the dependence of specific growth rate, $\mu(S)$, on the substrate concentration, S . K_S is the substrate concentration at which half the maximal specific growth rate, μ_{max} is reached, Y is the yield coefficient (grams of biomass formed per gram of substrate consumed), ω is the dilution rate, and S_0 is the substrate concentration in the feed. Equations 1.2 and 1.3 describe the rate of change in biomass and substrate utilization, respectively.

Plasmid dynamics in chemostat models

Well-mixed liquid cultures (such as chemostats or batch cultures) have been the preferred systems to model plasmid dynamics in bacteria. Levin and co-workers began modeling of plasmid dynamics in the 1970's following the mass-action approach to population dynamics pioneered by Lotka and Volterra in the 1920's (Lotka, 1920, Volterra, 1926). They used first-order kinetics to express the proportionality between the overall transfer rate and plasmid-free and plasmid-bearing cell densities (Stewart and Levin, 1977). Using populations of *E. coli* K12 with F or R1 plasmids they estimated the parameters of the model by fitting of the mass-action model to the observed transfer kinetics to those predicted by this mass-action model (Levin et al., 1979). The main assumptions are that: (1) mating occurs at random with a frequency that is jointly proportional to the densities of plasmid-free and plasmid-bearing cells, (2) there is no significant delay between the time a transconjugant receives the plasmid and the time when it can begin to transmit it, (3) the original donors and the transconjugants transfer the plasmid at the same rate, and (4) all bacterial clones grow at the same rate. The model can be written as:

$$\begin{aligned}\mu(S) &= \mu_{max} \frac{S}{K_s + S} \\ \frac{dS}{dt} &= -\mu(S)(T + R) \frac{1}{Y} + \omega(S_0 - S) \\ \frac{dR}{dt} &= -\gamma RT + R(\mu(S) - \omega) + \tau T \\ \frac{dT}{dt} &= \gamma RT + T(\mu(S)(1 - \alpha) - \omega) - \tau T\end{aligned}$$

Eqs. 1.4

where μ_{max} is the maximum growth rate of that strain growing on substrate S , K_s is the Monod constant, ω the dilution rate, S_0 is the limiting substrate concentration in the reservoir, γ is the conjugational transfer rate constant, τ the segregational loss rate and α the burden on the growth rate of a plasmid-bearing bacteria. R and T represent changes in the recipients and transconjugants cells, respectively. Figure 1.7 illustrates the results obtained by Levin et al. (1979) by fitting the mass-action model of plasmid transfer to experimental data using *E. coli* K12 strains and the permanently derepressed plasmid F. In this work the authors assumed the contribution of segregational loss to be negligible as well as any differences in growth fitness between plasmid-bearing cells and plasmid-free cells. They compared the kinetics of plasmid transfer in bacterial populations in exponential growth (Figure 1.7A), lag phase (Figure 1.7B) and in steady-state chemostats (Figure 1.7C), and found that the model could fit the observed data reasonably well for bacterial populations growing at constant rate in either exponentially growing cultures or at equilibrium in chemostats. They also confirmed the model prediction that the magnitude of the transfer rate constant for these plasmids is insensitive to donor-recipient ratios. The transfer rate constant γ , implicitly incorporates information regarding the intrinsic transfer properties of the bacteria as well as the conditions in which the bacteria interact. The model can reasonably simulate plasmid transfer dynamics in well-mixed systems because they assume the complete absence of spatial dependence, random encounters between plasmid-bearing and plasmid-free cells, and the rates of change depending only on the bulk properties of the system.

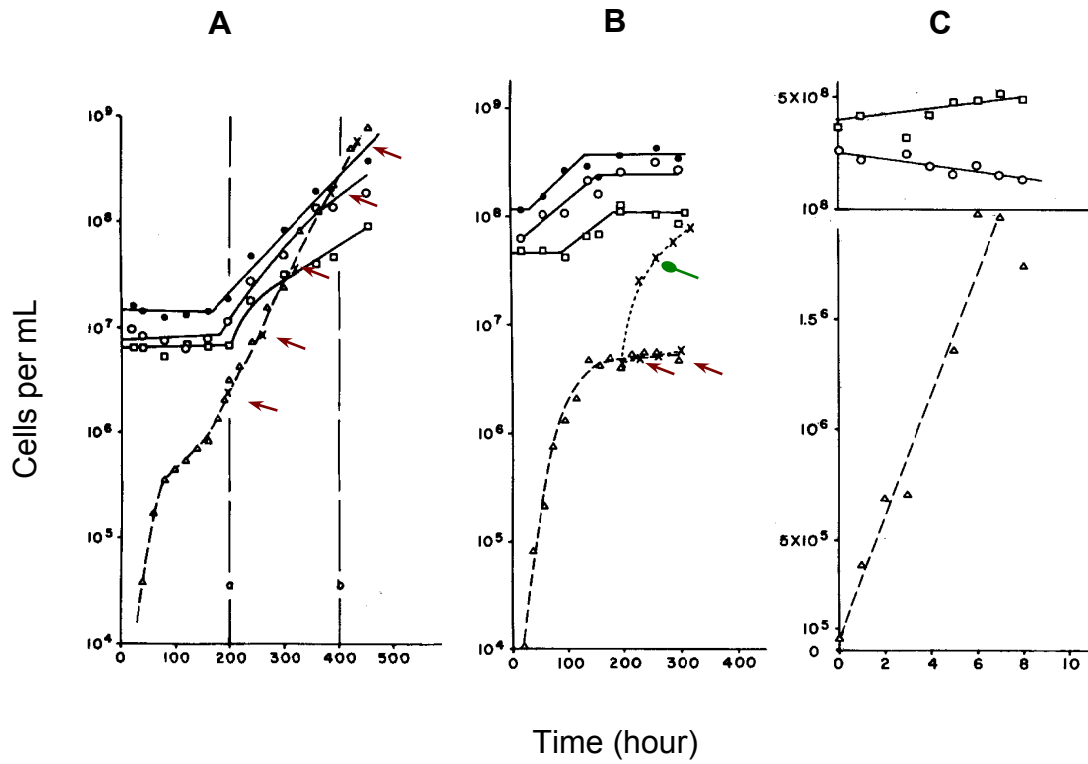


Figure 1.7. Population growth and transfer dynamics of plasmid F in (A) exponentially growing cultures, (B) at stationary phase and (C) in steady-state chemostat cultures. \circ donors, \square recipients, \triangle transconjugants; \times represent theoretical transconjugant trajectories indicated by the \rightarrow arrow, whilst the \longrightarrow arrow indicates the predicted theoretical trajectory for γ estimated for the plasmid in exponential phase. Estimated γ ($\text{mL cell}^{-1} \text{h}^{-1}$): (A) $\gamma = 1.55 \times 10^{-9}$, (B) $\gamma = 1.5 \times 10^{-11}$, (C) $\gamma = 3.26 \times 10^{-12}$ (adapted from Figures 1, 3 and 4 from Levin et al., 1979).

Thus, the apparent fit of the experimental data to the mass-action model does not provide evidence for the validity of the assumptions behind this model.

Numerical and analytical analysis of the model allowed the authors to investigate the role of segregational loss, conjugative transfer and fitness cost on the establishment and maintenance of plasmids in pure microbial populations. The fundamental idea that these models uncovered is the relationship between the transfer rate and the rate of loss and plasmid burden, i.e., for a plasmid to persist in a population the rate at which it is transmitted must overcome the combined effects of loss and fitness cost. Hence, the minimum transfer rate required for plasmid maintenance in bacterial populations is given by:

$$\gamma_{min} = \frac{\alpha\omega + \tau}{X^*}$$

Eq. 1.5

where X^* is the population density at steady state in chemostat cultures. In another theoretical study, Levin and Stewart (1980) investigated the necessary conditions for the existence of nonconjugative mobilizable plasmids in bacterial populations and found that although existence conditions exist, they are very stringent which suggests that it is very unlikely that such plasmids would become established and maintained in the absence of any direct selection favoring their carriage.

Freter et al. (1983), carried out experiments on plasmid transfer among *E. coli* strains *in vivo*, using gnotobiotic mice carrying a synthetic indigenous microflora, and *in vitro* in anaerobic chemostat cultures inoculated with intestinal microflora of the mouse. They used mass-action models to estimate transfer rates for various plasmids and found that these were of the same order of magnitude in both experimental setups, thus transfer was not impaired in the normal intestine. They

followed the transfer dynamics for more than 60 days and found that coexistence of both plasmid-bearing and plasmid-free cells was possible at least over short times. Lundquist and Levin, (1986) extended the study of plasmid transfer dynamics to wild-type naturally occurring plasmids and performed laboratory experiments using *E. coli* K12 growing in chemostats to ascertain if the plasmids could invade and persist in these bacterial populations. They found that although some plasmids failed to increase in frequency when introduced at low frequencies, two of them rapidly increased in frequency and plasmid-bearing bacteria become more abundant than plasmid-free ones. Through model development the authors concluded that although the plasmids were repressed for conjugative pili synthesis, differences between the transfer rates of newly formed transconjugants and repressed transconjugants could explain the observed experimental patterns and the persistence of the plasmid for at least 6 days.

van der Hoeven (1984) examined the possibility of coexistence of two or more incompatible plasmids in a bacterial population growing in a chemostat. From this mathematical study she concluded that coexistence of these plasmids is only possible if they follow different survival strategies, one having a high transfer rate and high fitness cost and the other with a low conjugative transfer rate and low burden for its host. Haft et al. (2009) have recently confirmed this prediction. Although the authors were primarily interested in the evolutionary advantages of plasmids carrying fertility inhibition systems, their results indicate the existence of a trade-off between transfer rate and host fitness. Competition between two incompatible plasmids that followed different survival strategies as those suggested by van der Hoeven (1984), favoured the evolution of plasmids with reduced cost for its bacterial host. This

observation indicated a competitive advantage in reducing horizontal transmission and allowing increased host replication and hence persistence of the plasmid through vertical transmission. Turner et al. (1998) had also described the existence of a trade-off between horizontal and vertical modes of transmission for plasmids due to increased fitness costs for higher transfer rates; through serial transfer experiments, the authors showed that when conjugation rate increased, the cost of plasmid carriage increased relative to the ancestral plasmid and vice versa. However, the model prediction that recipient density would determine the balance between horizontal and vertical transmission was not supported by experimental results. Zhong et al. (2010) have undertaken further refinement of the mass-action model for studying plasmid transfer dynamics by accounting for processes such as cell-cell attachment, DNA transfer and detachment dynamics. Decomposition of the process of plasmid transfer made it possible to account for other environmental effects, such as mixing. Using a combination of experiments and mathematical modeling the authors showed that plasmid transfer is maximal at low to moderate shaking speeds.

However, in spatially structured communities the assumptions used in mass-action models do not hold anymore. Indeed, there have been several experimental studies that demonstrate the failure of mass-action models to explain and predict the dynamics of plasmid transfer in spatially structured setups. In particular, neither the dependence of plasmid transfer efficiency on the initial donor to recipient ratio in filter matings (Simonsen, 1990) nor the dependence of the final transconjugant densities at stationary phase on increasing initial densities of donors and recipient cells (Pinedo and Smets, 2005) is captured by the mass-action models. Licht et al. (1999) also compared plasmid transfer dynamics in the intestine of streptomycin-treated

mice with the kinetics expected of a mixed-liquid system such as a chemostat, and found these to be quite different. In particular, they found that kinetics of plasmid transfer in the mouse intestine and in biofilm flow chambers to be quite similar in that transfer of the plasmid occurred at high rates following introduction of donors, after which no transfer was observed and after 8 days recipients still represented a large fraction of the biofilm population. In contrast, in the chemostat transfer proceeded at a constant rate until all recipients carried the plasmid. Meanwhile the effect of spatial structure both on microbial interactions and substrate gradients as well the role of mass transport phenomena have been recognized (Durrett and Levin, 1994; Wei and Krone, 2005) and a new set of modeling approaches for the analysis of plasmid transfer dynamics in structured communities has started to emerge (Lagido et al., 2003; Krone et al., 2007; Ponciano et al., 2007; Gregory et al., 2008; Merkey et al., 2011).

1.5.2. Modeling plasmid dynamics in structured communities

1.5.2.1. Biofilms and biofilm modeling

Prokaryotes represent the greatest diversity of life on our planet. It is predicted that most bacteria live in biofilm communities rather than planktonic free-living cells (Costerton et al., 1995). The first scientific description of a biofilm goes back to 1936 (Zobell and Anderson, 1936) and in the 1970's their ubiquity was recognized (Marshall, 1976; Costerton et al., 1978). The word biofilm implies a thin film made up of living material, i.e, microorganisms attaching and growing on a surface. A biofilm is composed of layers of microorganisms embedded in an adhesive matrix (EPS, exopolymeric substance), synthesized by the microbes themselves, which is constituted by exopolysaccharide, proteins and DNA. The spatial arrangement of cells, EPS and voids depends on the type of microorganism and on the growth conditions (Lawrence et al., 1991; Parsek and Tolker-Nielsen, 2008).

One apparent advantage of living inside a biofilm seems to be their inherent tolerance to various antimicrobial compounds targeting growing cells. Recent observations have shown the existence of two distinct subpopulations in a *Pseudomonas aeruginosa* biofilm differing in respect to their metabolic state (Pamp et al., 2008). As a consequence, antibiotics such as tetracycline or ciprofloxacin only kill the subset of the population that is metabolically active enabling biofilm recovery from the metabolically inactive subpopulation that survived the treatment (Pamp et al., 2008). The ability of bacteria to attach to surfaces and to form biofilms can become an important competitive advantage over bacteria growing in suspension.

Bacteria in a biofilm are protected from washout and they only have to grow fast enough to replace biomass losses due to detachment forces (Picioreanu et al., 2001). Some biofilms are good and have been used to treat wastewater or in the degradation of contaminants from the soil or groundwater (Nicolella et al., 2000; Wilderer et al., 2004). Other biofilms are bad, as they represent a major threat to human health for example in dental hygiene or infectious diseases (e.g. cystic fibrosis) (Paju and Scannapieco, 2007; Burmolle et al., 2010). Another frequent problem is the growth of biofilms in drinking-water distribution systems as biofilm development cannot be prevented and they are often difficult to remove (Wanner et al., 2006).

Studies on naturally occurring biofilms, either *in situ* or in bioreactors, have only shed light on the microbial population composition and their global response to ill defined environmental conditions. In order to better understand the structure of biofilms and the physiology of microbes living in biofilms, it is necessary to monitor biofilm development under laboratory-controlled conditions using simple and defined microbial communities and employment of advanced microscopy methods (Tolker-Nielsen and Molin, 2000; Pamp et al., 2009). The biofilm structure can be complex, characterized by layers of cells, exopolymeric material and extracellular spaces. The architecture of biofilms is not restricted to mushroom or finger-like structures interspaced with a labyrinthic network of channels, and very dense and flat biofilms are also found. The heterogeneity in biofilm structures is a result of the substrate gradients that develop inside the biofilm as a consequence of growing attached to a surface. A biofilm system can be divided into four main compartments, as depicted in Figure 1.8. The bulk liquid lying over the biofilm, the biofilm, the substratum where

microorganisms attach and grow, and the boundary layer constitute the basis for model development of biofilm growth and its emergent structure. The bulk-liquid compartment is very large when compared with the biofilm, and it is the source of nutrients utilized by the microorganisms in the biofilm. The mass-transfer boundary layer is the region above the biofilm surface where the fluid flow and convection are so slow that solutes are only transported by diffusion, e.g. from the bulk liquid as the source into the biofilm as the sink. The substratum is the solid inert surface on which the biofilm grows.

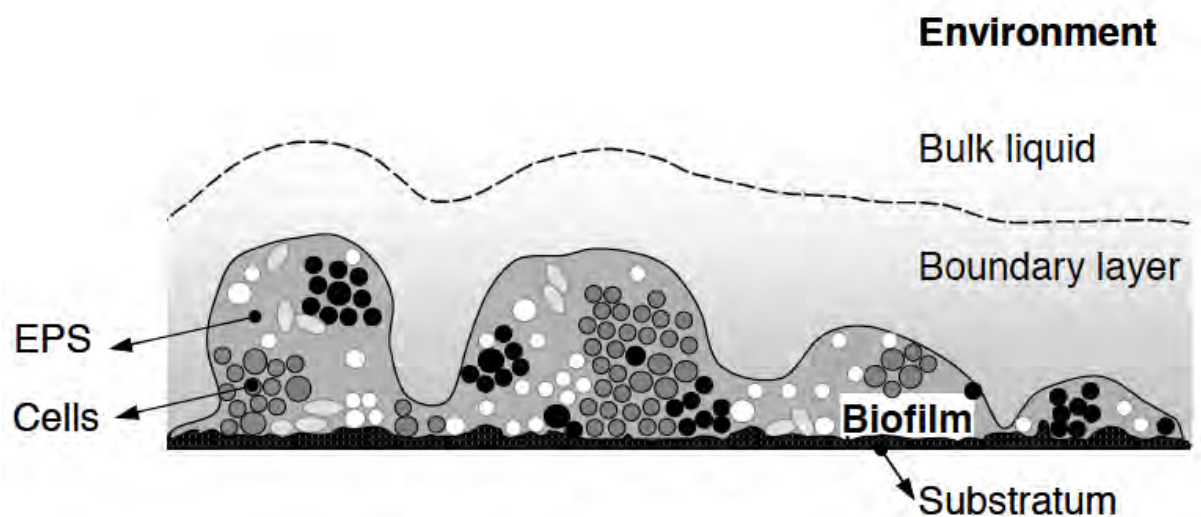


Figure 1.8 Four compartments typically defined in a biofilm system: bulk liquid, boundary layer, biofilm and substratum. (taken from Wanner et al., 2006)

Mathematical modeling of biofilm structures has contributed to the understanding of both physical and biological processes occurring in these peculiar communities. Modeling of biofilms started in the 1970"s focusing on substrate flux from the bulk liquid into the biofilm (Williamson and PL, 1976; Rittmann and McCarty, 1980; Rittmann and McCarty, 1981). Their primary goal was to describe mass flux into the biofilm and concentration profiles within the biofilm of one rate-limiting substrate. Subsequent models were able to incorporate a non-uniform biomass distribution in which complex structures could be modeled, and several substrates (Kissel et al., 1984; Wanner and Gujer, 1984; Rittmann and Manem, 1992). Since the 1990"s, new mathematical models have been developed in order to capture the two- and three-dimensional biofilm spatial structure motivated by observations made with newly available tools for observing biofilms in experimental systems, such as fluorescent proteins that allow visualization of microcolonies growing in multispecies biofilm structures under the confocal microscope. Thus, a huge diversity of approaches to biofilm modeling is available, ranging from analytical versus numerical, deterministic versus stochastic, continuum versus discrete, and hybrid continuum/discrete models (Wimpenny and Colasanti, 1997; Picioreanu et al., 1998b; Picioreanu et al., 1998a; Picioreanu et al., 2001; Picioreanu et al., 2004; Kreft et al., 1998; Kreft et al., 2001; Eberl et al., 2001; Pizarro et al., 2001; Lapidou and Rittmann, 2004; Xavier et al., 2004; Xavier et al., 2005b).

Among the models with discrete biomass there are two main types of approaches: the grid-based cellular automata (CA) and the particle-based models, where the particles are not constrained to move on a grid. Individual-based models

(IbMs) differ from the previous ones in that the discrete biomass blocks are allowed to have individuality and thus represent a higher level of complexity in modeling.

A definition of individual-based models is given in Grimm, (1999), as follows: “IbMs are simulation models that treat individuals as unique and discrete entities which have at least one property in addition to age that changes during the life cycle”. Individual-based modeling (IbM) has become widely used in describing complex systems constituted of autonomous entities such as those found in ecosystems and social networks. IbMs represent an alternative to the traditional population-level approach (aka continuum models), which deals with macroscopic variables (e.g. population biomass) and assumes averaged values to characterize the behavior of the individuals (e.g. average population growth rate), thus not taking into account local interactions or individual variability. In contrast, IbM are discrete models that by defining a set of rules, the variables that characterize each individual are calculated at each time step and then the state of the whole system is an emergent property. IbM follows a bottom-up approach useful to evaluate the impact of individual diversity on the emergent collective behavior of the population. They were first employed for the description of single microorganisms by Kreft et al. (1998) who developed the BacSim framework motivated primarily by the need to incorporate a physiological characterization of individual cells. A multi-substrate, multi-species version of BacSim was then developed in order to study nitrifying biofilms (Kreft et al., 2001) and the effect of EPS on the structure of these biofilms was also investigated (Kreft and Wimpenny, 2001). As depicted in Figure 1.9, in individual-based models of microorganisms there are two principal types of entities, the world and the agents, which interact. The *world* describes the environment in which the simulation takes

place, namely its geometry, the behavior at the boundaries as well as the transport of the nutrients by diffusion or other mass transport processes by means of partial differential equations. The *agents* are the “live” entities carrying out some sort of activity (this can include rules for the interaction with other agents or some differential equations describing the dependence of their growth rate on local nutrient concentrations). A review on the application of IbM in microbiology can be found in Hellweger and Bucci (2009).

An integrative approach to microbial systems requires the description of the system-level population dynamics by understanding its emergence from the underlying individual traits and interactions. CA models and IbMs both follow a bottom-up approach and are spatially explicit, i.e, space and spatial interactions are directly represented and thus information on their localization and distance between neighbors can be retrieved (Kreft, 2009). Yet, in IbMs individual members of a population are allowed to be in a different state from the other individuals of the same species. This is an important feature as it allows a range of approaches for modeling intracellular dynamics, such as metabolic pathways or networks of gene regulation or signal transduction. Moreover, CA models work on a spatial grid of “cells” (lattice cells) instead of carrying out the defined rules with the individuals and allowing them to continuously move all over the grids.

Since their introduction to modeling of microorganisms, IbMs have been used to model biofilm growth, biomass spreading and biomass detachment and their behavior in engineered systems for wastewater treatment. Their application to the study of microbial interactions and how these contribute to the emergence of biofilm structures was a natural path to explore as they offer the possibility to have multiple

solute species, biofilm biomass discretization into particulate species (e.g. EPS) and one or more bacterial species. Thus, IbMs have become an important modeling tool to study the evolution of cooperation in biofilms (Kreft, 2004; Xavier & Foster, 2007) or other social behavior (Nadell et al., 2009; Foster & Xavier, 2007; Mitri et al., 2011; Bucci et al., 2012) and also to investigate the process of how quorum sensing works in these structured communities (Nadell et al. 2008).

iDynoMiCS - individual-based Dynamics of Microbial Communities

A new platform dedicated to individual-based modeling of microbial communities has been put forward: iDynoMiCs (Lardon et al., 2011). This software was the result of a joint effort to merge the best features of previous programs, namely BacSim (Kreft et al., 1998) and Framework (Xavier et al., 2005b), and is meant to improve accessibility to non-programmers and to provide a backbone for future developments proposed by any interested contributor. It is written in Java and is thus platform (Windows, MacOS, Linux) independent.

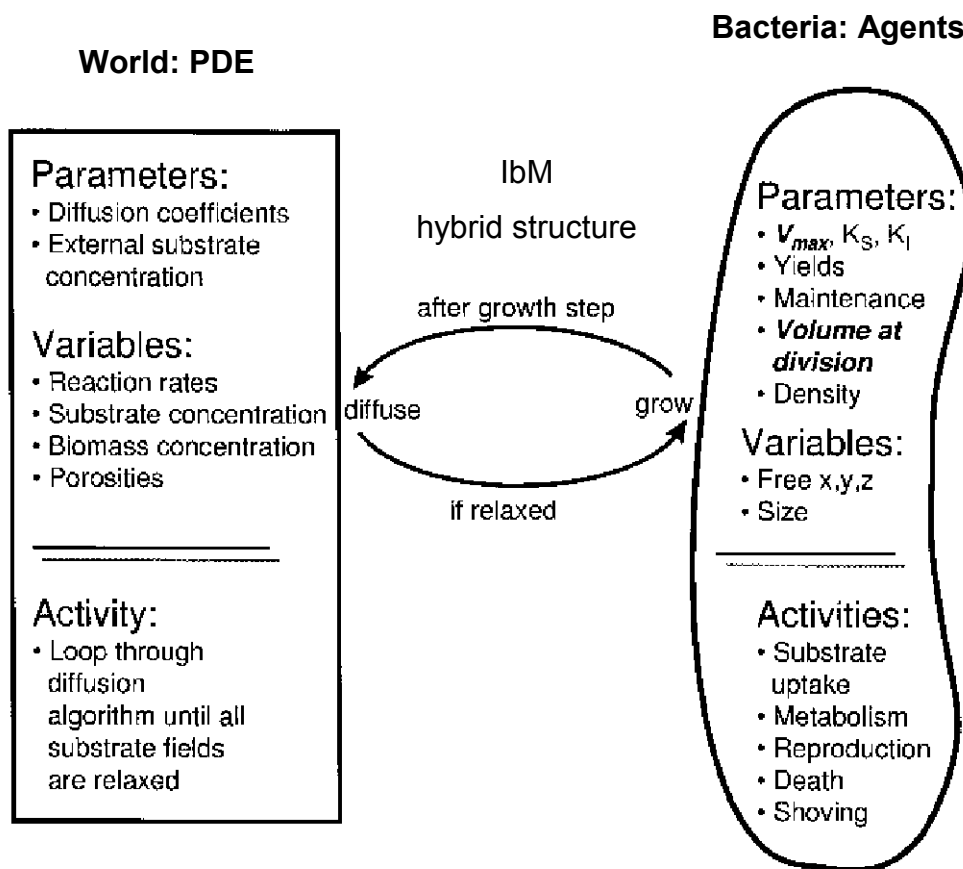


Figure 1.9. Individual-based model (IbM) structure. The program flows by alternating between diffusion (World) and growth (Bacteria) steps. PDE: partial differential equations. (adapted from Kreft et al., 2001)

The main components are the agents, the solutes, the reactions and the world. The agent is the fundamental unit in iDynoMiCS, it represents the individual microbe characterized by state variables including: location, size, density, relative composition (active biomass, inert biomass, EPS), species type, catalysed reactions and associated rate and stoichiometric coefficients, and genealogy. Particulate EPS is also modeled as a discrete entity produced by microbes through an excretion process and characterized by their species of origin, position, size and density. Individual agents interact directly mechanically through shoving in the competition for space and are represented by incompressible (hard) spheres (in 3D simulations) or cylinders (in 2D simulations). Solutes are the dissolved components that diffuse through water from/to the bulk compartment and are consumed and/or produced by the agents. The different time scales (Picioreanu et al., 2001) of bacterial growth and cell division (around one hour) and solute diffusion and uptake (around one minute) justify the assumption that solute fields are in pseudo-steady state with respect to biomass growth. Thus, at each time step, bacterial distribution is considered to be fixed when computing the concentration distribution, while the solute fields remain in pseudo-steady state when computing the new bacterial sizes and positions. The reactions are individual-based, i.e., each individual will have its own set of active reactions and different type of kinetics can be implemented. The world encompasses the properties of the computational domain, the bulk compartment and erosion forces. The computational domain, schematically represented in Figure 1.10, is an evenly spaced rectilinear grid described by its dimensionality (2D or 3D), its size (in the order of hundreds of micrometers), its geometry and the behavior at its boundaries. Several regions can be defined within the computational domain: the

support is the inert surface to which agents can attach, the biofilm matrix constituted by microbial cells embedded in a viscous medium (EPS) is represented in Region I; the bulk compartment (Region III) represents the larger liquid volume in which the biofilm is immersed and is treated as a well-mixed compartment (source of nutrients) and thus the solute concentrations are uniform. They are either assumed to be constant or determined by the reactions occurring in the biofilms and inflow and outflow; and Region II is a transfer boundary layer of liquid above the biofilm in which all the resistance to mass transport of dissolved components outside the biofilm is modelled. It can be viewed as a series of layers of liquid through which the solutes diffuse into or out of the biofilm compartment. In the biofilm compartment the main dynamics of the system that have to be modeled are: the cellular growth, spreading and detachment (including the production of EPS), the diffusion of substrates and their conversion by cells into products and biomass. Biomass erosion due to shear forces at the biofilm surface, is modeled implicitly, making the detachment speed at the biofilm interface a function of squared biofilm height for example (Xavier et al., 2005a). The detached bacteria are then removed from the computational domain, thus ceasing their existence. Algorithm 1.1 describes a single global timestep in iDynoMiCS, in which the dynamics of the solute concentration fields, the bulk compartment and the agents are applied independently, although the dynamics of each depend on the current state of the others. The source of stochasticity in iDynoMiCS comes from a range of processes related to growth of the agents: (i) the initial agent locations are randomly chosen within a particular rectangular region, unless the user specifies a list of agents with initial positions; (ii) the initial agent masses are randomly chosen around an average value, unless specified directly by

the user; (iii) the cell division threshold volume is chosen randomly around an average division size; (iv) the cell death threshold volume is chosen randomly around an average death size; (v) upon cell division, daughter cell sizes are chosen stochastically around equally sized daughter cells; (vi) also upon cell division, daughter cells are positioned with zero overlap and equidistant from the mother cell's centre, but are oriented in a random direction; (vii) EPS excretion in the form of new particles occurs in a randomly chosen direction; and (viii) the order in which agents are updated during a single global timestep is made random during each step.

iDynoMiCS can also be used to simulate bacteria growth and their interactions in an unstructured environment, such as a chemostat. In this case the spatial properties of agents and solutes is ignored, and thus solute concentrations do not vary spatially in the domain and their concentration corresponds to the balance between the processes of inflow, outflow and consumption due to bacterial growth. The dilution rate is used to calculate the fraction of agents to be removed stochastically from the system during the current time step. A more detailed description about iDynoMiCS design concepts and functionality can be found in Lardon et al., 2011), which is part of this thesis and included in the Appendix section.

In order to illustrate the value of uncoupling individual agents from their species' metabolism, a case study addressing a metabolic switch between aerobic respiration and nitrification was investigated using iDynoMiCS. A heterotroph population growing in an idealized wastewater treatment environment is modeled. There are three heterotrophic species (named as Lag-1, Lag-3, Lag-5) that have identical growth kinetics but differ in the induction lag times (1, 3 or 5 hours) leading to the activation of their denitrification pathways when the oxygen levels reaches low

concentrations. When the oxygen concentration increases (e.g., due to oxygen pulses into the system) the bacteria switch back to aerobic growth. It is assumed that a faster switching response demands a higher induction cost (and thus a reduction in growth rate). The switch between the two forms of metabolism is triggered by the local oxygen concentrations, affecting the metabolism of individual bacteria as the "switching threshold" is reached. Figure 1.11 shows example 3D biofilm structures obtained from simulations where oxygen was introduced in the bulk compartment every 4 hours. It was found that for the case where switching is costly, there is an optimal induction lag time for each pulse frequency because of the trade-off between costs and response time: the less frequently the environment changes, the longer the optimal response time will be. As a control for effect of spatial structure, the same case study was simulated in the individual-based chemostat, where coexistence of the different strategies is not found and the optimal strategy replaces all the others. In contrast, in the biofilm, the optimal strategy does not replace the others and a higher biodiversity is observed, at least in the short-term. Thus, this study exemplifies how iDynoMiCS can be used to investigate the impact of fluctuations in environmental conditions on microbial interactions, such as competition between different species growing in biofilms.

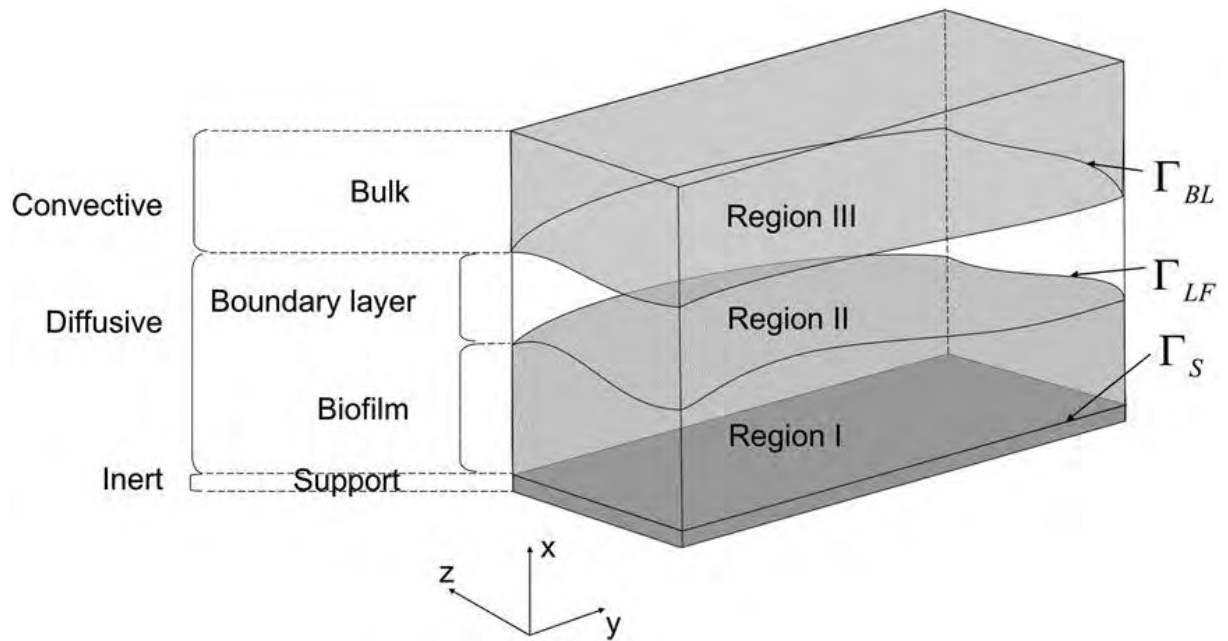


Figure 1.10 The computational domain including the support as an external boundary. Region I represents the biofilm, Region II the diffusion boundary layer and Region III the well-mixed bulk compartment. Γ : boundary conditions. While the choice of the orientation of the axes x , y and z is not conventional, it preserves the existence and location of x and y axes when reducing the model from 3D to 2D (taken from Lardon et al., 2011).

Algorithm 1.1 Pseudo-code describing one global timestep iteration of the individual-based simulator iDynoMiCS (taken from Lardon et al., 2011).

1 Solve solute mass balances in the computational domain for the given agent distribution and bulk solute concentrations; this sets the solute concentration fields

2 Update bulk concentrations based on new solute concentration fields

3 While agent timestep < global timestep

- a. Perform any actions specific to a particular species or agent type
- b. Compute growth, decay and division or death of agents to update agent size and mass, and add or remove agents if needed
- c. Compute pressure field and apply pressure-driven movements to agents
- d. Apply shoving and spring relaxation to update agent locations

4 Apply detachment of agents by erosion and remove disconnected parts of the biofilm

5 Update global timestep

When a chemostat is being simulated, step 1 is simplified due to the spatial homogeneity but the time resolution is increased, steps 2, 3c, and 3d are skipped, and step 4 is replaced by stochastic agent dilution.

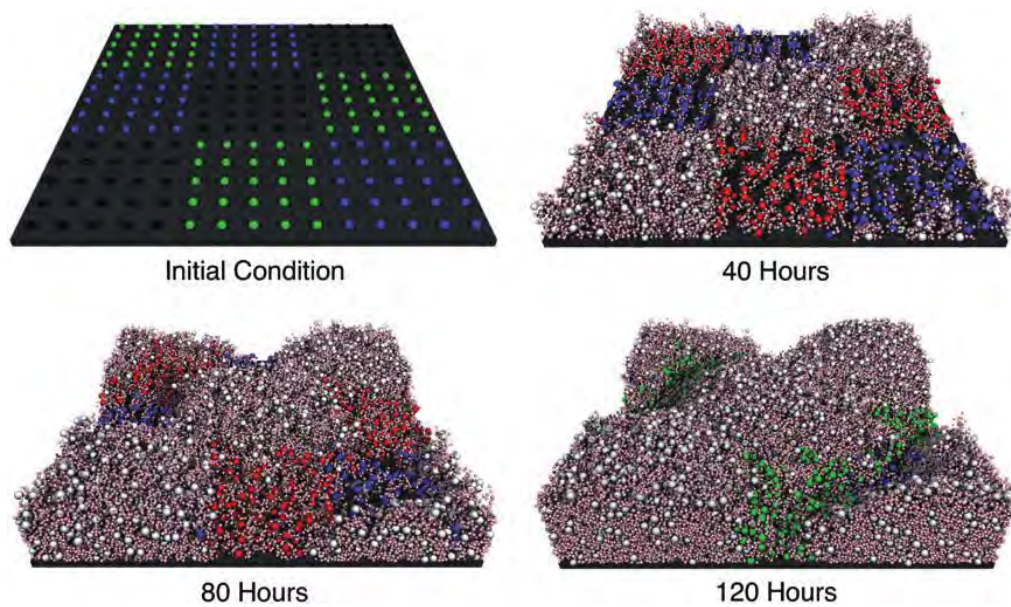


Figure 1.11 Example biofilm structures from 3D simulations (with-cost case). Time evolution of a biofilm growing under anoxic conditions with oxygen pulses occurring every 4 h. Agent colours are black/white for Lag-1, red/green for Lag-3, yellow/blue for Lag-5, and pink for EPS. The faster-switching species tend to outgrow the other species in spite of the cost for being a faster switcher (taken from Lardon et al., 2011).

1.5.2.2. Models of plasmid transfer

The complex spatial structure created by microbial growth on surfaces influences substrate gradients which in turn affect growth rates causing the spatial distribution of the cells to be modified again. Conjugative gene transfer adds another degree of complexity to this system since a side effect of this process is its impact on the structural organization of the microbial cells and *vice versa* (Ghigo, 2001). Moreover, depending on the fitness cost that the plasmid represents for the host, plasmid carriage will influence the host growth rate (De Gelder et al., 2007).

Lagido et al., (2003) constructed a mathematical model for plasmid transfer between bacteria growing in colonies on agar plates. The model assumes that bacteria are randomly placed on a planar surface according to the Poisson distribution. The radius, r , of a colony increases exponentially, and as colonies of donors and recipients grow they will touch each other when their centres are less than $2r$ apart. When colonies of donors and recipients meet, all recipients become transconjugants, after which they can behave as donors without further delay. The parameters needed by the model, such as surface area available for colonization, initial colony radius, specific growth rate, colony radial specific growth rate, maximum number of cells sustained by the system and the initial numbers of donors and recipients were measured experimentally and used to perform the computer simulation experiments. The final numbers of donors, recipients and transconjugants calculated with the model were compared to those obtained in filter mating experiments using strains of *P. fluorescens* and the plasmid RK2. The model predictions followed the experimental trends, but conjugation was overestimated.

The authors suggest that overestimation might be explained by the assumption of instantaneous conjugation or the fact that not all the cells within a colony can participate in conjugation. Indeed, there have been studies with plasmids in liquid matings that describe minimum periods of time for a plasmid to be transferred and also a period of recovery time of 5-30 min for the donors following conjugation before they can transfer a plasmid again and a delay in transfer of 40-80 min from newly formed transconjugants (Andrup et al., 1998; Andrup and Andersen, 1999 Cullum et al., 1978b).

Recent work by Krone et al. (2007), demonstrates how the introduction of a spatial component into an interactive particle lattice model (falls in the category of a discrete-space continuous-time stochastic CA model) can improve the description of the plasmid-host dynamic interactions. Using this approach they built a model that correctly simulates the observed patterns of plasmid spread and persistence in colonies. This model is built on a 2D square lattice (of size up to 1000 x1000) with periodic boundaries and with cells located at the lattice points. Each site in the lattice can be empty or contain a single unit of nutrient or/and up to two cells. The cell size is considered to be 1 or 2 μm and intercellular distances also in the order of a micrometer and with hundreds of lattice points per side of the grid the viewing window is 1 to 2 millimeters per side. Then division of a cell will take place if within its neighborhood (considered to be 9 sites) there is at least one unit of nutrient available. Conjugation events will not deplete nutrients although their rates may depend on local nutrient concentrations. The probability that during cell division a plasmid is lost in one of the daughter cells is represented by a probability for segregative loss. Repression of conjugative pilus synthesis is also considered and

thus upon plasmid reception the cells are assumed to be transitorily derepressed and to have a higher conjugation rate that will return to its basal value after a certain amount of time. With this simple set of rules the authors were able to simulate the observed rates of plasmid loss and conjugative transfer in bacterial colonies grown on agar plates. The development of the shape of the colonies over time in terms of transconjugants localization was another feature captured by the model. An extension of this model to a pseudo three-dimensional set up where they use the same lattice grid as before but now they distinguish cells located at the “top” or “bottom” level of the layer, was also capable of reproducing the observed dependence of IncP-1 plasmid infection and their abundance on spatial structure and nutrient availability (Fox et al., 2008). However in both cases their model relies on parameters from empirical studies on spatial patterns and therefore much of the information is fed into the model rather than being an emergent property of the simulation. In addition, the spatial scale chosen by the authors corresponds to clusters of cells and not individual cells.

Merkey et al. (2011) started modeling conjugal transfer of plasmids in biofilms, using iDynoMiCS, by introducing a third type of agent to represent plasmids, which can only exist in a bacterial agent. In their model they account for the recovery time upon plasmid transfer, i.e., the time that donors need to recover following conjugation before they can donate again; and maturation time, i.e., the time that a newly formed transconjugant will need before it can transfer the plasmid. For that they defined lag time parameters $t_{exchange}$ and $t_{reception}$ that are characteristic of a given plasmid for its donor or transconjugant cell, respectively. The length of the pilus (d_n) is used to define a spherical neighbourhood around the donor cell. Bacteria in the

neighbourhood are potential recipients, they will be screened and if a bacterium does not contain the plasmid, it will be infected with a probability p . There are a maximum number of candidates that a bacterium can screen in a given period of time, which is given by v_s , the scan speed. Thus, neighbours are picked at random to enter a round of conjugation until the maximum number of bacteria that can be screened is obtained. Following a successful transfer the donor agent will enter a recovery period of length t_{donor} before it can enter a new round of conjugation. Similarly, a recipient bacterium enters a maturation phase of length $t_{recipient}$ before it becomes a donor cell. A bacterium already carrying a plasmid cannot be infected. Upon cell division, a plasmid-bearing bacterium can lose its plasmid with a probability p_{loss} . Plasmid burden is modelled as a decrease in specific growth rate $\mu(S)$ by an absolute cost, b_p :

$$\mu(S) = (\mu(S) - b_p)X$$

Eq 1.6

where X stands for the bacterium's biomass. HGT parameters used in the model are listed in Table 1.1.

The authors hypothesized that the limited plasmid invasion observed in biofilms is caused by a dependence of conjugation on the growth rate of the donor cell. They conducted a sensitivity analysis of the various parameters involved in the transfer dynamics of a plasmid and found that timing (such as lag times, transfer proficiency and scan speed) and spatial reach (EPS yield, pilus length) parameters are more important for successful plasmid invasion than the recipient's growth rate or the probability of a plasmid being lost upon cell division. They have, thus identified one factor that can limit plasmid invasion in biofilms and the new IbM, iDynoMiCS,

can be used to test various hypothesis on the spread and maintenance of plasmids in biofilms but also chemostats.

Table 1.1 iDynoMiCS HGT parameters (adapted from Table 1 in Merkey et al., 2011).

Parameter	Parameter description	Units
v_s	Conjugal pilus scan speed	h^{-1}
d_p	Pilus reach distance	μm
p	Transfer proficiency (probability of success)	-
$t_{recipient}$	Maturation period following initial plasmid receipt	h
t_{donor}	Recovery period following plasmid transfer	h
p_{loss}	Probability of segregative loss during cell division	-
b_p	Plasmid maintenance rate	h^{-1}

1.6. Objectives

BHR plasmids are frequently found in diverse natural bacterial communities, such as those found in wastewater treatment (Bahl et al., 2009) or *Pseudomonas* related infections (Markowitz et al., 1978). Their ability to transfer into different species might come at the disadvantage of higher fitness costs of plasmid carriage for the infected host, due to poorer plasmid-host co-evolution. In contrast, NHR plasmids are expected to confer a smaller burden to their host because long-term co-evolution has been shown to ameliorate the fitness cost imposed by a plasmid on its host.

Competition between plasmids with different host-ranges and its consequences on plasmid invasion and persistence is thus the focus of this thesis. One of the goals of this work is to determine whether costly BHR plasmids can compete with faster growing NHR-plasmid bearing cells in two-species assemblages. The levels of competition encompass the indirect competition between plasmids via competition between the hosts, and direct competition between incompatible plasmids for plasmid-free cells. Since a plasmid can only exist inside a cell, the burden that a plasmid exerts on the host indirectly affects the fitness of the plasmid itself because vertical transmission (through host growth) contributes to plasmid's persistence.

The development of mathematical models, both deterministic (ODE's) and stochastic (individual-based) of plasmid transfer in two-species assemblages growing in chemostats or biofilms, constituted the initial step. The main aims for the modeling analysis were: (i) assess the impact of plasmid-related parameters such as transfer rate, fitness cost and loss rate on the persistence and coexistence of plasmids with

different host-ranges; (ii) evaluate the effect of compatible and incompatible relationships between the BHR and NHR plasmids on their competitiveness; (iii) test the hypothesis that BHR plasmids are more competitive than NHR plasmids in spatially structured bacterial assemblages; and (iv) compare the competitiveness of NHR and BHR plasmids in chemostats and biofilms.

Experimentally, the main goal was to explore an experimental framework that would allow study of the transfer dynamics of plasmids with different host-ranges in a microbial assemblage composed of two different species growing on filters on top of agar plates. More specifically, the aim was to investigate the effect of patchiness on the dissemination of a plasmid and how the transfer efficiency of a NHR plasmid is affected by the presence of a non-suitable recipient (i.e., a host it cannot infect). The two plasmids differing in their host-ranges and belonging to different incompatibility groups, namely the broad host-range RK2 and the narrow host-range R387 plasmids, were also used in filter mating experiments and to perform growth curves in batch cultures in order to determine: (i) plasmid transfer frequency; (ii) fitness burden imposed on various laboratory strains; and (iii) the effect of different temperatures on plasmid transfer efficiency and growth of plasmid-bearing hosts.

Chapter 2

Model Development

MODEL DEVELOPMENT

The models describe the transfer of two plasmids with different host ranges, a *NHR* (narrow host-range) and a *BHR* (broad host-range), in a microbial assemblage composed of two bacterial species, *N* and *B*. The rules are simple: the *NHR* can only infect species *N*, while the *BHR* plasmid can infect both species, *N* and *B*, which are equal otherwise. Regarding the relationship between the different plasmids, two scenarios are considered: compatible and incompatible plasmids. In the compatible case the two plasmids can co-exist in the same host, whereas in the incompatible case the second plasmid cannot enter a host already carrying the other plasmid.

2.1. Chemostat

To simulate the chemostat environment, both a continuum deterministic ODE (mass-action) and a discrete, stochastic (individual-based) version of the model were built in order to evaluate the effect of random events.

2.1.1. ODE chemostat model of plasmid dynamics

In the classical mass-action models developed by Levin and co-workers in the 1970's that describe the dynamics of transfer of a plasmid in a bacterial population, the main assumptions are (Levin et al., 1979): the rate of appearance of transconjugants (*T*) is proportional to the densities of donors (*D*) and recipients (*R*), and the constant of proportionality is given by the plasmid transfer rate γ ; the plasmid is lost at a rate τ , and it imposes a fitness burden on its host of α . Donors and transconjugants transfer

the plasmid at the same rate and are thus indistinguishable. The total density of plasmid-bearing hosts is then represented as T . The dilution rate is given by ω , and μ is the specific growth rate for the bacterial species growing on a limiting substrate according to the Monod equation (Monod, 1949). The model of one plasmid in a bacterial population is described by the following set of equations:

Model 1: One plasmid, One species

$$\mu(S) = \mu_{max} \frac{S}{K_s + S}$$

$$\frac{dS}{dt} = -\mu(S)(T + R) \frac{1}{Y} + \omega(S_0 - S)$$

$$\frac{dR}{dt} = -\gamma RT + R(\mu(S) - \omega) + \tau T$$

$$\frac{dT}{dt} = \gamma RT + T(\mu(S)(1 - \alpha) - \omega) - \tau T$$

This model was extended to the case of two plasmids with different host-ranges in a two-species bacterial assemblage. As mentioned before, the NHR plasmid can only infect species N , whereas the BHR plasmid can transfer into both species, N and B . The two bacterial species have identical growth kinetic parameters listed in Table 2.3, and are only distinguishable by their susceptibility to infection by the different plasmids. Each species can be in one of two states: recipient or transconjugant/donor if it carries any plasmid. Thus, χ_j^i describes the current state (χ) of species j and the plasmids i it carries, if any. The set of equations describing the competition between the two plasmids and their hosts in the compatible and incompatible scenarios are described below. As before, for model simplification

donors are assumed to behave in the same way as transconjugants. Therefore, there is no need for separate equations describing the dynamics of donors.

Model 2 - Two compatible plasmids, species N

$$\mu(S) = \mu_{max} \frac{S}{K_s + S}$$

$$\frac{dS}{dt} = -\mu(S)(T_N^N + T_N^B + T_N^{B,N} + R) \frac{1}{Y} + \omega(S_0 - S)$$

$$\frac{dR}{dt} = -\gamma_N R(T_N^N + T_N^{B,N}) - \gamma_B R(T_N^B + T_N^{B,N}) + R(\mu(S) - \omega) + \tau_N T_N^N + \tau_B T_N^B$$

$$\frac{dT_N^N}{dt} = \gamma_N R(T_N^N + T_N^{B,N}) - \gamma_B T_N^N(T_N^B + T_N^{B,N}) + T_N^N(\mu(S)(1 - \alpha_N) - \omega) - \tau_N T_N^N + \tau_B T_N^{B,N}$$

$$\frac{dT_N^B}{dt} = \gamma_B R(T_N^B + T_N^{B,N}) - \gamma_N T_N^B(T_N^N + T_N^{B,N}) + T_N^B(\mu(S)(1 - \alpha_B) - \omega) - \tau_B T_N^B + \tau_N T_N^{B,N}$$

$$\begin{aligned} \frac{dT_N^{B,N}}{dt} = & \gamma_N T_N^B(T_N^N + T_N^{B,N}) + \gamma_B T_N^N(T_N^B + T_N^{B,N}) + T_N^{B,N}(\mu(S)(1 - (\alpha_B + \alpha_N) - \omega) \\ & - T_N^{B,N}(\tau_N + \tau_B) \end{aligned}$$

Model 3 - Two incompatible plasmids, species N

$$\mu(S) = \mu_{max} \frac{S}{K_s + S}$$

$$\frac{dS}{dt} = -\mu(S)(T_N^N + T_N^B + R) \frac{1}{Y} + \omega(S_0 - S)$$

$$\frac{dR}{dt} = -\gamma_N R T_N^N - \gamma_B R T_N^B + R(\mu(S) - \omega) + \tau_N T_N^N + \tau_B T_N^B$$

$$\frac{dT_N^N}{dt} = \gamma_N R T_N^N + T_N^N(\mu(S)(1 - \alpha_N) - \omega) - \tau_N T_N^N$$

$$\frac{dT_N^B}{dt} = \gamma_B R T_N^B + T_N^B(\mu(S)(1 - \alpha_B) - \omega) - \tau_B T_N^B$$

Model 4 - Two compatible plasmids, species N and B

$$\mu(S) = \mu_{max} \frac{S}{K_s + S}$$

$$\frac{dS}{dt} = -\mu(S)(T_N^N + T_N^B + T_N^{B,N} + T_B^B + R_N + R_B) \frac{1}{Y} + \omega(S_0 - S)$$

$$\frac{dR_N}{dt} = -\gamma_N R_N(T_N^N + T_N^{B,N}) - \gamma_B R_N(T_B^B + T_N^B + T_N^{B,N}) + R_N(\mu(S) - \omega) + \tau_N T_N^N + \tau_B T_N^B$$

$$\frac{dR_B}{dt} = -\gamma_B R_B(T_B^B + T_N^B + T_N^{B,N}) + R_b(\mu(S) - \omega) + \tau_B T_B^B$$

$$\begin{aligned} \frac{dT_N^N}{dt} = & \gamma_N R_N(T_N^N + T_N^{B,N}) - \gamma_B T_N^N(T_B^B + T_N^B + T_N^{B,N}) + T_N^N(\mu(S)(1 - \alpha_N) - \omega) + \tau_B T_N^{B,N} \\ & - \tau_N T_N^N \end{aligned}$$

$$\begin{aligned} \frac{dT_N^B}{dt} = & \gamma_B R_N(T_B^B + T_N^B + T_N^{B,N}) - \gamma_N T_N^B(T_N^N + T_N^{B,N}) + T_N^B(\mu(S)(1 - \alpha_B) - \omega) - \tau_B T_N^B \\ & + \tau_N T_N^{B,N} \end{aligned}$$

$$\frac{dT_B^B}{dt} = \gamma_B R_B(T_B^B + T_N^B + T_N^{B,N}) + T_B^B(\mu(S)(1 - \alpha_B) - \omega) - \tau_B T_B^B$$

$$\begin{aligned}\frac{dT_N^{B,N}}{dt} = & \gamma_B T_N^N (T_B^B + T_N^B + T_N^{B,N}) + \gamma_N T_N^B (T_N^N + T_N^{B,N}) + T_N^{B,N} (\mu(S)(1 - (\alpha_B + \alpha_N) - \omega) \\ & - T_N^{B,N} (\tau_N + \tau_B))\end{aligned}$$

Model 5 - Two incompatible plasmids, species *N* and *B*

$$\mu(S) = \mu_{max} \frac{S}{K_S + S}$$

$$\frac{dS}{dt} = -\mu(S)(T_N^N + T_N^B + T_B^B + R_N + R_B) \frac{1}{Y} + \omega(S_0 - S)$$

$$\frac{dR_N}{dt} = -\gamma_N R_N T_N^N - \gamma_B R_N (T_N^B + T_B^B) + R_N (\mu(S) - \omega) + \tau_N T_N^N + \tau_B T_N^B$$

$$\frac{dR_B}{dt} = -\gamma_B R_B (T_N^B + T_B^B) + R_B (\mu(S) - \omega) + \tau_B T_B^B$$

$$\frac{dT_N^N}{dt} = \gamma_N R_N T_N^N + T_N^N (\mu(S)(1 - \alpha_N) - \omega) - \tau_N T_N^N$$

$$\frac{dT_N^B}{dt} = \gamma_B R_N (T_N^B + T_B^B) + T_N^B (\mu(S)(1 - \alpha_B) - \omega) - \tau_B T_N^B$$

$$\frac{dT_B^B}{dt} = \gamma_B R_B (T_B^B + T_N^B) + T_B^B (\mu(S)(1 - \alpha_B) - \omega) - \tau_B T_B^B$$

A schematic view of the transfer dynamics of two plasmids transferring in a two-species assemblage is depicted in Figure 2.1. Description of each variable can be found in Table 2.1. Growth and system parameters can be found in Table 2.3.

Numerical analysis of the different models was carried out using MATLAB student edition version 7.12. The solver chosen was ode23s, which can handle stiff problems, e.g., chemostat models. Problems are stiff if the dynamics occurs on

different timescales, i.e, slow and fast processes. In the chemostat, substrate dynamics are fast, while plasmid transfer and growth are slower, and plasmid loss is even slower.

Table 2.1 Description of the variables used in the different models

Variable ($\mu\text{g mL}^{-1}$)	Definition
R_N	Recipient cell of species N
R_B	Recipient cell of species B
T_N^N	Transconjugant cell of species N carrying a NHR plasmid
T_N^B	Transconjugant cell of species N carrying a BHR plasmid
$T_N^{B,N}$	Transconjugant cell of species N carrying both BHR and NHR plasmids
T_B^B	Transconjugant cell of species B carrying a BHR plasmid
$T_{B,N}^B$	Sum of transconjugant cells of species B and N that carry a BHR plasmid

Transconjugants are the result of the infection of plasmid-free recipients or division of plasmid containing cells. Donor cells are considered to behave in the same way as transconjugants

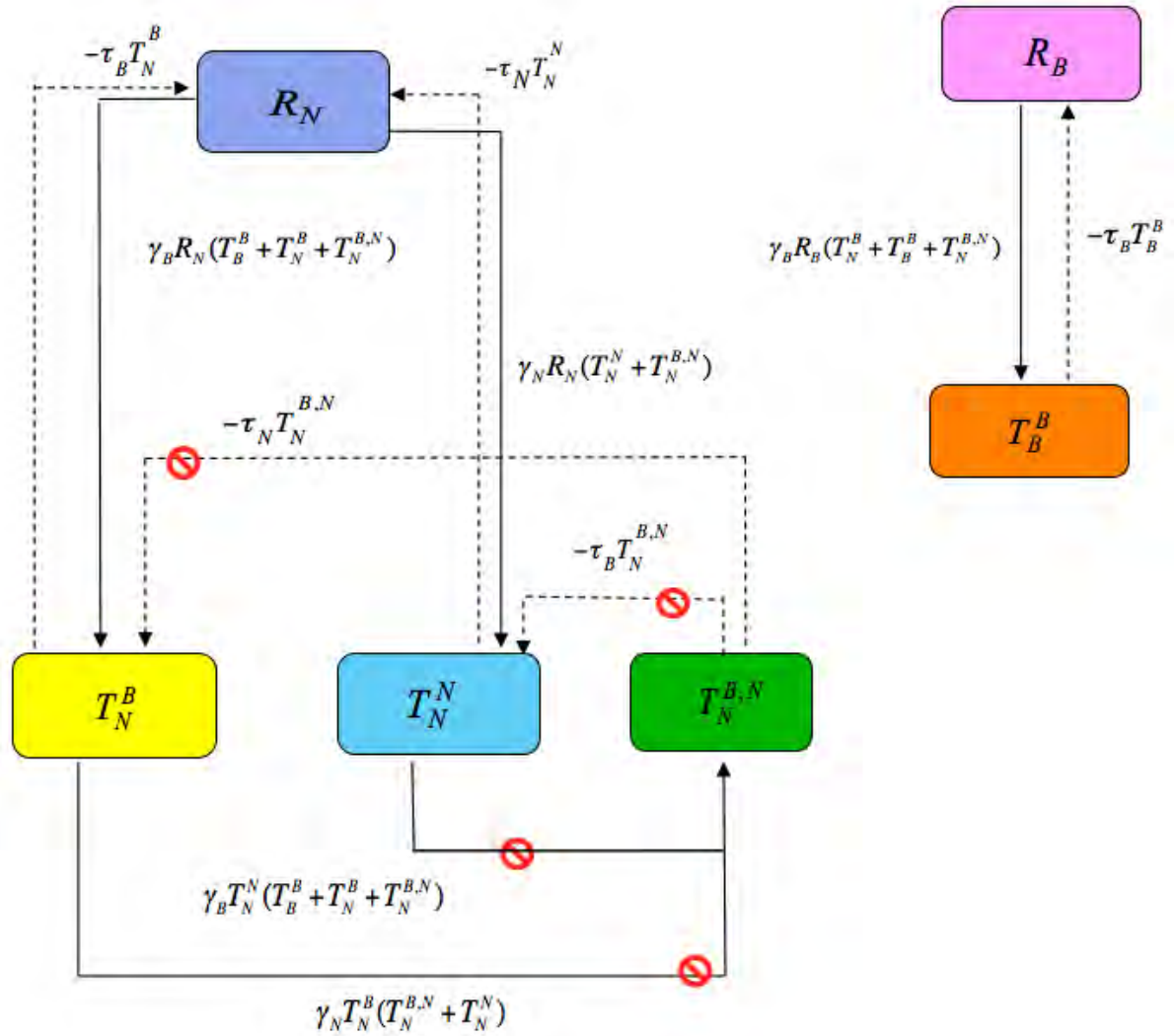



Figure 2.1 ODE model of the population dynamics of two conjugative plasmids with different host-ranges in a two-species assemblage. The symbol  represents the absence of the correspondent reaction in the scenario where the two plasmids are incompatible. Variables and parameters are described in Tables 2.1 and 2.3, respectively.

2.1.2. Individual-based chemostat model

In order to evaluate the effect of stochasticity on the competition between different bacterial species growing in a chemostat, an individual-based chemostat model was developed using the iDynoMiCS platform. This chemostat version of iDynoMiCS is also used as a reference case without spatial structure to evaluate the effect of spatial structure characteristic of biofilms. In the chemostat mode, some of the steps in each iteration of the algorithm (see Algorithm 1.1, section 1.5.2.1) are skipped for efficiency, namely the stages of spatial positioning of agents, computation of the pressure field and pressure-driven movements, and shoving and biomass detachment. In a chemostat, the medium is assumed to be uniformly mixed, and hence all agents „see“ the same concentration for all solutes. The concentrations of the solutes are governed by the processes of dilution (inflow and outflow at the same rate) and bacterial growth.

The dilution rate is used to calculate the fraction of agents to be removed stochastically from the system during the current time step. The dilution of agents is a stochastic process, in which all the individuals have the same probability of being washed out. The probability of an agent being lost from the chemostat due to dilution, p_{dil} , takes into account the dilution rate ω , the time step t_s and is given by:

$$p_{dil} = \omega t_s$$

Eq. 2.1

Because the chemostat equations are typically stiff ODEs, the diffusion-reaction problem is solved using a modified Rosenbrock pair formula based on partial

derivatives (Shampine 1982; Shampine and Reichelt 1997). The method is very dependent on an accurate Jacobian matrix (which is calculated analytically), and in this method the function is evaluated twice, yielding an intermediate solution estimate F1, which is used to obtain the solution for the next time-step, F2. If the calculated error is smaller than a given tolerance, then the step is considered successful and the predicted F2 solution will be used as the initial state for the next step; otherwise, the solver time step is decreased according to the standard rule used in numerical integration for initial value problems (Gear, 1971), and the step is carried out once more.

2.1.2.1. Validation of the IbM chemostat against the ODE model

In order to test the individual-based chemostat, microbial growth was simulated using a two-species assemblage composed of COD (chemical oxygen demand)-oxidising heterotrophs and ammonia-oxidising autotrophs, based on the BM3 benchmark problem (Rittman et al., 2004). For simplicity, the maintenance and inactivation reactions were ignored in these tests, and a lower influent COD concentration was used (3 mg COD/L rather than 30 mg COD/L). The corresponding deterministic model was simulated and analysed using Matlab (Ordinary Differential Equation solver ode23s), and the deterministic solution obtained this way was compared with the stochastic solution from iDynoMiCS. Solutions from the two simulation methods were compared in the solute and biomass concentrations predicted by each. In all simulations, the dilution rate was 0.02 h^{-1} , and the timestep 1 hour. For these conditions, the relative error of steady state variables was <2% for solutes, < 1% for

heterotrophs, and <15% for autotrophs. The higher discrepancy for the autotrophs is due to there being fewer individuals (usually only 1) compared to the heterotrophs (which usually number in the thousands); when the number of individuals is small, any variation (such as that due to stochastic dilution) is amplified for the population as a whole. The errors are lower when the time-step is reduced (e.g., autotroph error dropped to 9% when using a timestep of 0.5 hour rather than 1 hour), or when the system size is increased to closer approximate the continuous nature of the ODE solution (data not shown); these results indicate that the models' results converge as expected. For stochastic dilution in small systems (few cells; small volumes), any variation in the number of agents to be removed for each species can lead to discrepancies with the deterministic solution (as was the case in the chemostat model verification). Whether these differences will lead to divergent results will depend on the feedbacks in the system. In the present test case, results converged to the deterministic steady state solution despite strong initial differences due to the stochastic initialization of the IbM. Comparison of the time series of the stochastic iDynoMiCS runs (3 independent runs) with the deterministic model illustrates rapid convergence of the simulation results as the simulations progress toward the steady state, even after starting with quite different initial biomass values due to the stochastic initialization of the IbM (see Figure 2.2).

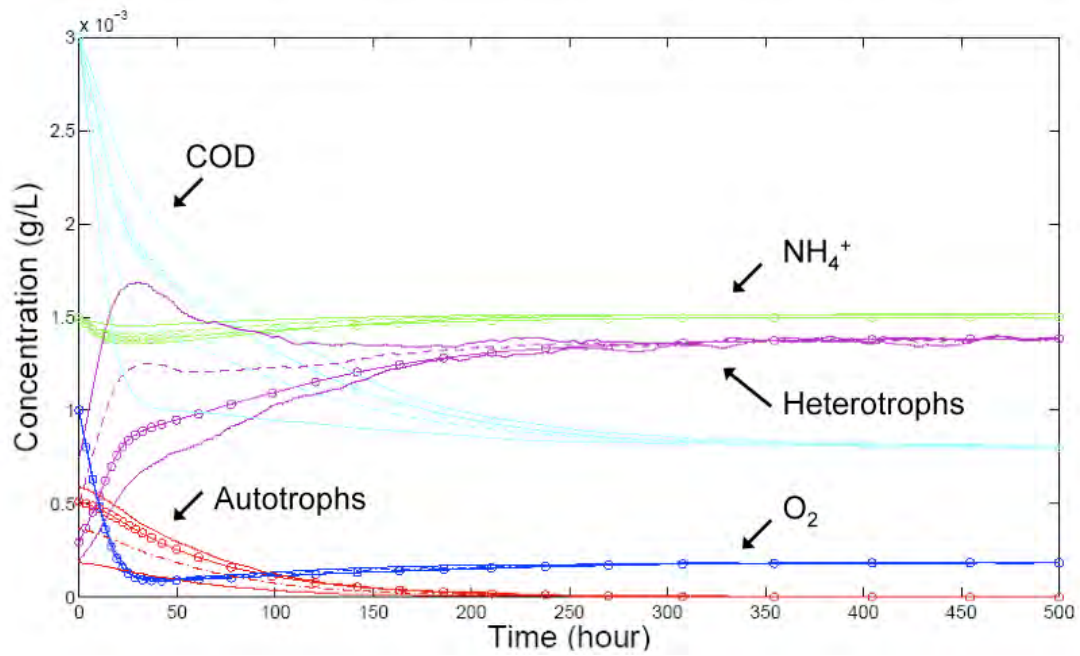


Figure 2.2: Comparison of simulations of the stochastic chemostat model using iDynaMiCS (3 replicates) with simulations of the deterministic ODE model ($\bullet\text{---}\bullet$) using the ODE solver ode23s of Matlab (adapted from Lardon et al., 2011).

2.1.3. *Individual-based chemostat model of plasmid dynamics*

The Individual-based chemostat feature of iDynoMiCS (Lardon et al., 2011) was used to model the transfer of plasmids with different host-ranges in a two-species assemblage. In iDynoMiCS individual organisms are agents that are modeled as discrete entities that can differ in their properties such as biomass or metabolic behavior. They can carry out different activities, e.g. growth and plasmid conjugation, within discrete time-steps. The individual-based nature of the model provides a framework where different individuals of the same bacterial species can be in different states, e.g., with or without a plasmid(s).

Implementation of the plasmid transfer model in the individual-based chemostat follows the assumptions of the mass-action models described in the previous section, but the interactions at the individual level require probabilistic parameters. In the individual-based chemostat model we split the coefficient of transfer, γ , into two components: c , the coefficient of encounters by collision, i.e., the number of individuals with which an individual can interact within one time step; and p , the probability of a plasmid being transferred (i.e., a new copy being created in the recipient cell) as a result of a collision. The product cp is then equivalent to γ , and by keeping c constant, p can be varied in order to test different transfer rates. The individuals can only exist in one of two states: recipient (plasmid-free cell) or transconjugant (plasmid-bearing cell). The fitness burden, α , of carrying a plasmid is reflected by a decrease in the growth rate of the host but leaving the rate of substrate consumption unaffected by this change in growth rate. Upon cell division the

probability of the plasmid being lost is given by p_{loss} . A comparison between the parameters used in the ODE model and in the lbM can be found in Table 2.2.

The simple case of one plasmid spreading in a bacterial population was used as a test case to verify the implementation of the plasmid transfer model in the stochastic chemostat against the numerical solution of the deterministic ODE model in Matlab. Because in the deterministic model the bacterial mass of the population is a continuous variable, the parameters that govern plasmid transfer are calculated in units of mass as opposed to number of individuals in the lbM. In order to convert the plasmid transfer rates and bacterial densities between the two models, the average mass of a cell of *E. coli* in the individual-based model $\varepsilon = 1.25 \times 10^{-7} \mu\text{g cell}^{-1}$ was used as a conversion factor. Growth and system parameters that are common to both ODE model and lbM are listed in Table 2.3.

In the lbM model, during a time step, every individual will screen a randomized fraction of the assemblage regardless of whether or not they contain any plasmids and then attempt to transfer or receive a plasmid, according to the probabilities of transfer, if and only if both of these conditions are met:

- a) the recipient cell is within the host-range of the plasmid
- b) the recipient does not already contain an incompatible plasmid or a plasmid of the same type

The number of agents that will be screened is given by the product between the coefficient of collision and the density of cells in the system at that moment:

$$N_{screen} = c \frac{N_{total}}{l^3}$$

Eq. 2.2

where l stands for side length of the cubic 3D domain in iDynoMiCS that is used to calculate the volume being simulated, l^3 ; and N_{total} is the total number of agents in the system.

The minimum transfer rate is the starting point for the analysis of the competition between the NHR and BHR plasmids in a two-species assemblage in two different scenarios, compatible and incompatible. In the incompatible scenario, an individual already carrying a plasmid cannot be infected with a different plasmid. In the compatible scenario, the burden imposed on a host carrying both plasmids corresponds to the sum of the individual burdens. In neither case will a second plasmid of the same type be transferred into the host (if it were, it would have no effect).

Simulations of the two plasmids invading one-species populations and two-species assemblages were performed by allowing the recipient population to reach steady state (3 generations) and then introducing donors for each plasmid at low frequency (8-10%). All the simulations were carried out for 200 days (> 600 generations). The time step used was 1 hour and the simulated volume was 2.7 μL containing roughly 6000-7000 agents at steady state, which translates into a population density of approximately 2×10^6 cells mL^{-1} . The coefficient of collision, c , was chosen to be 2×10^{-5} such that on average 45 agents were screened by each individual during each time step, which can be calculated from Eq. 2.2 to give $c = 2 \times 10^{-5}$. IbM system parameters are listed in Table 2.4. Agents have a biomass density of 290 g dry mass L^{-1} and when their radius reaches 0.53 μm the spherical cells divide into two daughter cells. Typically, 3 to 8 replicates were performed depending on how much variation was found among the replicates.

Table 2.2 Comparison of HGT parameters for the ODE model and IbM. The index i denotes which plasmid the parameter relates to.

Parameters	ODE model	IbM
Transfer	γ_i (mL $\mu\text{g}^{-1} \text{h}^{-1}$): coefficient of transfer rate	cp (mL $\text{cell}^{-1} \text{h}^{-1}$): c is the coefficient of collision, p is the probability of transfer
Loss	τ_i (h^{-1}): rate of loss of plasmid i	p_{lossi} : probability of loss upon each cell division
Fitness cost	α_i : burden conferred by plasmid	
Host-range	Defines the species that can host a given plasmid	

Table 2.3 Growth and system parameters

Parameter	Description	Value (units)
μ_{\max}	Maximum specific growth rate	$0.7 \text{ h}^{-1} \text{ (1)}$
K_s	Monod Constant	$0.25 \mu\text{g mL}^{-1} \text{ (1)}$
S_R	Substrate concentration in the reservoir	$0.5 \mu\text{g mL}^{-1} \text{ (A)}$
Y	Biomass yield for growth on substrate S	$0.66 \text{ g COD-X/g COD-S} \text{ (1)}$
ω	Dilution rate	$0.1 \text{ h}^{-1} \text{ (A)}$
ε	Conversion factor (mass to cell numbers)	$1.25 \times 10^{-7} \mu\text{g cell}^{-1}$

⁽¹⁾ Levin et al., 1977, Chao et al., 1977

S - substrate is glucose, COD - chemical oxygen demand

^(A) Assumed

Table 2.4. lbM chemostat system parameters

Parameter	Description	Value (units)
S^B	Substrate concentration in the chemostat reservoir	$0.2 \text{ mg L}^{-1} \text{ }^{(A)}$
t_s	Time spent between each iteration	$1 \text{ h }^{(A)}$
c	Coefficient of encounters by collision	$2 \times 10^{-5} \text{ mL cell}^{-1} \text{ h}^{-1}$
l	Side length of 3D domain	$1.4 \times 10^3 \text{ } \mu\text{m }^{(A)}$
t_s	Time spent between each iteration	$1 \text{ h }^{(A)}$
r_d	Division radius	$0.53 \text{ } \mu\text{m }^{(A)}$
r_m	Death radius	$0.29 \text{ } \mu\text{m }^{(A)}$

^(A) Assumed

2.2. Biofilm

2.2.1. Individual-based biofilm model of plasmid transfer

The platform chosen to develop an lbM that can simulate the transfer of plasmids with different host ranges in a two-species assemblage is iDynoMiCS (Lardon et al., 2011). The HGT model by Merkey et al. (2011), which is described in section 1.5.2.2 of Chapter One was extended in order to incorporate two or more different types of plasmids that can transfer in a two-species assemblage. The description of the model follows the Overview, Design concepts and Details (ODD) standard proposed by Grimm et al. (2006) to facilitate the evaluation and comparison of lbMs. Only the HGT-related processes are described in this section; further information about other processes and components in iDynoMiCS can be found in section 1.5.2.1 of Chapter One and in Lardon et al. (2011) included in the Appendix section of this thesis.

Purpose

The purpose of this model is to simulate the dynamics of different conjugal plasmids in planktonic (individual-based chemostat model of plasmid dynamics as described in section 2.1.2) and surface-based bacterial communities such as biofilms. Specifically, the aim of this model is to test the hypothesis that BHR plasmids are more competitive than NHR plasmids in two-species assemblages.

State variables and scales

There are two types of agents in this model: the bacterial cell and the plasmid. The bacterial agent is characterized by the following state variables: location, size, density, relative composition (in this case active biomass only), species type, catalysed reactions and associated coefficients (μ_{\max} , K_s and Yield), and genealogy. Two bacterial species are considered, named as species *N* and species *B*. Plasmid agents do not take up space and their existence is limited to being contained by a bacterial agent. For model simplification, it is assumed that no EPS is produced, and thus there are no EPS agents in the current model.

The simulations were carried out using a 2D computational domain where the biofilm domain has dimensions of 260 μm and a resolution of 4 μm , in which all agents and their activities are simulated. Within the computational domain, solutes are represented by concentration fields that vary in space and time due to mass transport dynamics and the reactions by which they are affected. The solute concentration in the bulk compartment was kept fixed. Physical interaction of the bulk liquid volume with the biofilm structure in the form of shear or erosion forces lead to the detachment of microbes from the biofilm, and the parameter controlling this process is k_{det} . All system parameters are listed in Table 2.5.

Process overview and scheduling

An overview of the algorithm for one global time-step is depicted in Figure 2.3.

Design concepts

The ecological concepts that are important in the design and implementation of the HGT model are described below.

Emergence

The dynamics of plasmid spread in the biofilm are an emergent property of the model and are a result of individual behaviour.

Fitness

Fitness of an agent depends on an agent's growth properties and competition

Prediction

This model can be used to make global predictions (but not of individual behaviour) of plasmid spread if the underlying processes and parameters are well characterized. In the present work, the assumptions made and the parameters used are not aimed at modeling a specific bacterial assemblage and thus, only qualitative trends are discussed.

Sensing

Plasmid-bearing agents search the neighbourhood for possible recipients to engage in conjugal transfer of the plasmid. They will only transfer the plasmid to a host that does not carry the same type of plasmid or if the host carries a compatible plasmid.

Interaction

Neighbouring agents interact in competition for nutrients and space. During a round of conjugation, the agents will interact in order to determine if a suitable recipient has been found to which a plasmid can be donated. These interactions are governed by parameters described in the section *Conjugal transfer of plasmids*.

Stochasticity

The source of stochasticity includes a range of processes related to growth of the agents, namely: (i) the initial agent locations are randomly chosen within a particular rectangular region, (ii) the initial agent masses are randomly chosen around an average value, unless specified directly by the user, (iii) the cell division threshold volume is chosen randomly around an average division size, (iv) the cell death threshold volume is chosen randomly around an average death size, (v) upon cell division, daughter cell sizes are chosen stochastically around equally sized daughter cells, (vi) also upon cell division, daughter cells are positioned with zero overlap and equidistant from the mother cell's centre, but are oriented in a random direction, and (viii) the order in which agents are updated during a single global timestep is made random during each step.

Other sources of stochasticity are related to the random search for a potential recipient in the neighbourhood, the probability of transferring the plasmid (p) and the probability of losing the plasmid upon cell division (p_{loss}).

Collectives

The biofilm as a whole is the only collective entity explicitly tracked, and this is done in order to delineate the biofilm surface and liquid subregions within the computational domain.

Observation

The model saves information about each agent, solute concentration fields and bulk compartment concentrations every 4 hours.

Initialization

Solute concentrations in the bulk compartment are specified in a parameter file and remained constant in all simulations. Two-species biofilm structures were obtained by randomly placing bacterial agents in the biofilm domain. The mixed biofilm structure was obtained by randomly positioning 4500 agents of each species within the biofilm domain during initialization. The patchy biofilm was obtained by random placement of 50 agents of each species throughout the length (260 μm) of the computational domain and left to grow into a mature biofilm. The mature biofilm structures were then initialized with one or two agents carrying a different plasmid.

Input

The inputs to the model include system, growth and HGT-related parameters listed in Tables 2.5, 2.6 and 2.7.

Conjugal transfer of plasmids

As mentioned before, this HGT model is an extension to the work developed by Merkey et al. (2011), a description of which can be found in section 1.5.2.2 of Chapter One. A plasmid-bearing agent uses its pili to randomly search the neighbourhood for potential recipients within the reach of the pili determined by d_p . Conjugative pili of Gram-negative bacteria consist of flexible tube-like structures such as the F pilus encoded by *E. coli* F plasmid (narrow host-range) and can measure between 2 and 20 μm in length (Lawley et al., 2003). In contrast, pili of the broad host-range RP4 (IncP group) plasmid is less than 1 μm in length (Eisenbrandt et al., 2000; Kalkum et al., 2004). In this work, it is assumed that both competing plasmids have a pilus with the same length, $d_p = 2\mu\text{m}$.

In order to model the transfer of two plasmids with different host-ranges, two plasmid's parameters were introduced: *host-range* and the *compatibility* markers. The *host-range* marker allows the identification of a suitable recipient, i.e., one where the plasmid can replicate and maintain itself according to its host-range definitions. The *compatibility* marker determines whether two different plasmids can coexist in the same bacterium or not, i.e., whether they are compatible or incompatible (same mode of replication). Successful transfer of the plasmid depends on the matching between its markers, i.e., both the name of the species to which the candidate recipient belongs and the name of the plasmid to be transferred match. In order to capture the prevalence of entry exclusion systems that are frequently found in many plasmids (Garcillan-Barcia and de la Cruz, 2008), a bacterium containing one type of plasmid cannot be infected with another plasmid of the same kind.

After finding a suitable recipient, the probability of transferring the plasmid is given by p , a parameter that captures any uncertainties in transfer success. There is

a maximum number of candidates that a bacterium can screen in a given period of time, which is given by v_s , the scan speed. This parameter describes the time needed for pilus extension and retraction and it has been measured experimentally for the F plasmid in *E. coli* by Clarke et al., (2008). The authors found that an *E. coli* carrying a F plasmid extends a pilus at a rate of 40 nm s^{-1} and retracts it at 16 nm s^{-1} , which gives a total of approximately 7 rounds of extension/retraction per hour. For all the simulations it was assumed that $v_s = 5 \text{ h}^{-1}$. In this model the lag times following receipt or transfer of the plasmid are zero, and thus the conjugation event is instantaneous and attempts to conjugate will continue until the maximum number of recipients to screen is achieved (see Figure 2.3).

In order to model the burden conferred by the plasmid, Merkey et al. (2011) included a maintenance reaction associated with the carriage of the plasmid, which reflects the consumption of cellular resources due to plasmid's replication, regulation and transfer processes. In the present work, the cost of carrying a plasmid has been modeled in a different way; a *fitness cost function* which models the decrease in the growth rate of a bacterium carrying a plasmid as a function of the time that the plasmid has co-evolved with its host is introduced. This function has the form of an exponential decay:

$$\alpha(t) = \alpha_0 e^{-\lambda t} - b$$

Eq. 2.3

where α_0 stands for the initial fitness cost of the plasmid upon entering a new host, λ is the parameter governing the rate at which the fitness cost ($\alpha(t)$) decreases during co-evolution of plasmid and host, t is time in hours and b is the basal or minimum cost that a plasmid imposes on its host after a long period of co-evolution. This

function was chosen because it can model the observed attenuation in plasmid carriage cost due to the co-evolution between the plasmid and its host (Dahlberg & Chao, 2003), which tends to decrease monotonically converging to a minimal cost (*b*). This type of implementation could be useful in testing hypothesis about the effects of selective pressures or competitive factors on the amelioration of plasmid burden. Nevertheless, all simulations carried out in this thesis have $\lambda = b = 0$, and thus the cost of the plasmid is fixed and does not vary with time. The effect on the growth of a plasmid-bearing agent is relative to its specific growth rate:

$$\mu(S) = [\mu(S) (1 - \alpha)]$$

Eq. 2.4

where X is the active biomass of the bacterium cell.

In order to simplify the system and decrease the number of confounding factors affecting plasmid dynamics, in the present work there are no EPS particles and transfer probability is independent of the growth status of the cell.

The data was analyzed using MATLAB® (2011a) routines to calculate overall frequencies of each plasmid in the microbial assemblage from 3 replicates.

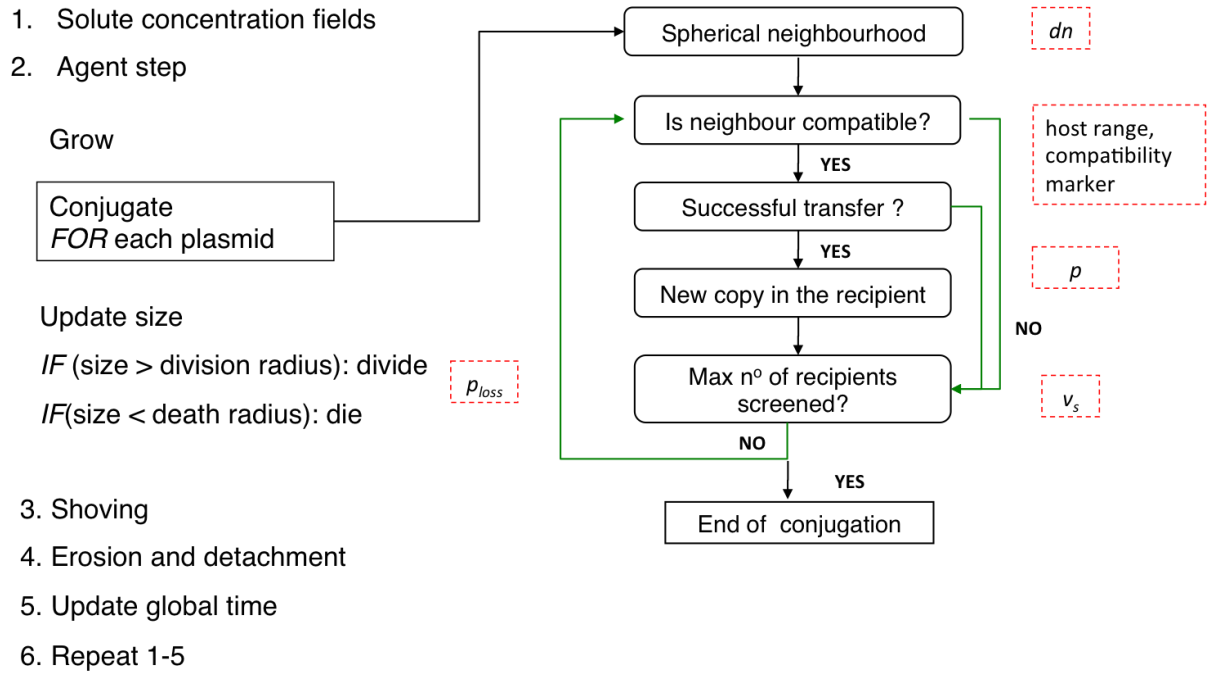


Figure 2.3 One time step in iDynoMiCS biofilm model of plasmid dynamics. During the agent step if the bacterium carries a plasmid, for each plasmid the length of the pilus (d_n) is used to define a spherical neighborhood, which contains potential recipients for the plasmid attempting to transfer. Each neighbor is then screened for compatibility with the host-range marker of the plasmid and for the compatibility marker of the plasmid it may carry. The transfer is successful if the random number generated is lower than the probability of transfer (p). Once the maximum number of recipients screened (v_s) the conjugation process is terminated.

Table 2.5. System related parameters

Parameter	Description	Value (units)
D_S	S diffusion coefficient	$10 \text{ mm}^2 \text{ day}^{-1} \text{ }^{(1)}$
S^B	Substrate concentration in the bulk compartment	$0.2 \text{ mg L}^{-1} \text{ }^{(A)}$
h_{BL}	Boundary layer thickness	$0.008 \text{ mm }^{(A)}$
k_{det}	Erosion strength coefficient	$7 \times 10^{-9} (\text{mm h})^{-1} \text{ }^{(A)}$
ω	Dilution rate	0.1 h^{-1}
σ_R	Specific area	$80 \text{ m}^2 \text{ m}^{-3} \text{ }^{(1)}$
t_s	Time spent between each iteration	$1 \text{ h }^{(A)}$
r	Resolution of 2D domain	$4 \text{ } \mu\text{m }^{(A)}$

⁽¹⁾ Wanner et al., 2006^(A) Assumed**Table 2.6.** Growth parameters

Parameter	Description	Value (Units)
μ_{\max}	Maximum rate of growth on substrate S	$0.7 \text{ h}^{-1} \text{ }^{(1)}$
Y	Biomass yield for growth on substrate S	$0.66 \text{ g COD-X/ g COD-S }^{(1)}$
K_S	S concentration for half-max growth rate	$2.54 \times 10^{-4} \text{ g L}^{-1} \text{ }^{(1)}$
ρ_X	Biomass density	$290 \text{ g COD L}^{-1} \text{ }^{(A)}$
r_d	Division radius	$0.8 \text{ } \mu\text{m }^{(A)}$
r_m	Death radius	$0.2 \text{ } \mu\text{m }^{(A)}$

⁽¹⁾ Levin et al., 1977, Chao et al., 1977^(A) Assumed

Table 2.7 HGT parameters

Parameter	Parameter description	Value (units)
v_s	Conjugal pilus scan speed	5 h^{-1} ⁽¹⁾
d_p	Pilus reach distance	$2 \text{ }\mu\text{m}$ ⁽²⁾
p_i	Transfer proficiency (probability of success)	$[0.001, 1]$ # successes / # trials
$t_{recipient}$	Maturation period following initial plasmid receipt	0 h ^(A)
t_{donor}	Recovery period following plasmid transfer	0 h ^(A)
p_{lossi}	Probability of segregative loss during cell division	10^{-4} per cell division ^(A)
α_i	Plasmid burden	$[0, 0.5]$ ^(A)
Host range	Defines the species by which the plasmid can be hosted	Name of a species
Compatibility	Defines the plasmids with which the plasmid can coexist in the same host	Name of a plasmid

⁽¹⁾ Clarke et al., 2008⁽²⁾ Lawley et al., 2003^(A) Assumed

Chapter 3

Modeling plasmid dynamics in a chemostat

MODELING PLASMID DYNAMICS IN A CHEMOSTAT

3.1. Introduction

Plasmids are autonomous self-replicating widespread genetic elements in bacterial communities. Their role together with other mobile genetic elements, in shaping bacterial adaptation and evolution has been recognized and used to explain evolutionary relationships between distant species (Ochman et al., 2000; Koonin et al., 2001).

Despite the vast knowledge on the molecular mechanisms of replication, stable inheritance and transfer, our understanding of the relationships between plasmids and bacterial populations is still scarce. In particular, we need an ecological and evolutionary framework to investigate how the phenotypic traits conferred by plasmids have contributed to their dissemination and evolution as autonomous genetic elements and if plasmids can persist parasitically in bacterial communities during periods where direct selection for the traits that benefit their bacterial hosts is absent. An approach involving simple experimental and theoretical systems is a good starting point. Indeed, since the late 1970's Levin and others have developed mathematical mass action models of plasmid transfer in bacterial populations capable of describing the plasmid transfer dynamics in *E. coli* populations growing in continuous cultures (chemostats) (Stewart and Levin, 1977; Levin et al., 1979; Levin and Stewart, 1980; Freter et al., 1983; Lundquist and Levin, 1986; Simonsen, 1991; Bergstrom et al., 2000). The plasmid of choice to perform these experiments was plasmid R1 and its mutant, R1d_{rd}19, which is de-repressed for transfer. The model analysis combined with the experimental data showed that

plasmids will be maintained in bacterial populations if their conjugal transfer rate is high enough to overcome their loss through segregation and selection against the burden they imposed on the host. Given the knowledge on the transfer rates of plasmids between *E. coli* strains isolated from natural populations, it was concluded that these were too low for plasmids to persist as parasites solely by infectious transfer (Gordon, 1992). Nevertheless, there are examples of wild plasmids that could invade and increase in frequency in chemostat cultures of *E. coli* K12 in the absence of selection, and could thus be maintained by infectious transfer alone (Lundquist and Levin, 1986). However, in all these studies, both theoretical models and experiments have been carried out using the simplest scenario: one plasmid transferring in a single species population.

In the present work a single-species population mass action model was extended to a two-species assemblage where one or two plasmids can transfer. Moreover, the conditions under which plasmids with different host-ranges can co-exist in two-species assemblages have been investigated. The recognition that broad host-range (BHR) plasmids are widespread throughout diverse environments (Smalla and Sobecky, 2002; Smalla et al., 2006; Moura et al., 2010; Heuer et al., 2012a) and their important role in antibiotic resistance dissemination (Novais et al., 2006), led to the hypothesis that BHR plasmids are more successful in two-species assemblages than narrow host-range (NHR) plasmids, despite higher fitness costs. An extended host-range of the plasmid means more frequent swapping of hosts and therefore less time to adapt to the new host which may lead to a greater fitness burden on average (De Gelder et al., 2008).

Thus, what is the basis of the apparent success of BHR plasmids in microbial communities? What are the most important factors contributing to the establishment of plasmids with different host-ranges? Can they persist in the absence of direct selection? These are some of the questions that are addressed in this chapter. Furthermore, the competition between compatible and incompatible NHR and BHR plasmids was examined. For each scenario, a series of parameter range variations was carried out for the three main processes affecting plasmid survival: fitness cost, transfer and segregational loss. The role of random events on the outcome of our competition simulations using an individual-based chemostat model is also investigated. The results of this study suggest that competition between plasmids can enhance the chances of survival of a NHR plasmid in two-species assemblages under a reasonable range of parameter values.

3.2. Results

The results presented here are organized in five sections: section 1 introduces the relationship between transfer rate and fitness cost and demonstrates how the lbM plasmid transfer model can reproduce the results obtained with the ODE model; section 2 addresses the conditions for the survival of a NHR plasmid in two-species assemblages; and finally the last three sections cover the two different scenarios of compatible or incompatible plasmids competing in two-species assemblages, and the effect of stochasticity on the outcome of competition, which was found to be a relevant factor for the biological interpretation of the system.

Throughout the mathematical analysis presented in the sections below, the fitness cost ranged from 0% to 50%. The transfer rate varied between 0 and 2.5×10^{-8} mL cell⁻¹ h⁻¹ and the loss rate between 0 and 0.1 h⁻¹. The model simulates a hypothetical assemblage composed of two species, *B* and *N*, which have the same growth parameters for the sake of simplicity since the main goal is to investigate competition of plasmids, not their hosts. This allows one to focus on the effect of plasmid-related parameters on the competitiveness of different plasmids spreading in two-species assemblages. The growth parameters were the same for both species and were kept constant throughout the simulations. Growth parameters can be found in Table 3.1. All the results are the product of simulated invasion experiments where the initial frequency of plasmid-bearing cells in the microbial assemblage is between 5 and 10% and simulations lasted for at least 200 days. Thus, the results obtained with the ODE model are the outcome of numerical simulations.

Table 3.1 Growth and system parameters

Parameter	Description	Value (units)
μ_{\max}	Maximum specific growth rate	$0.7 \text{ h}^{-1} \text{ }^{(1)}$
K_s	Monod Constant	$0.25 \text{ } \mu\text{g mL}^{-1} \text{ }^{(1)}$
S_R	Substrate concentration in the reservoir	$0.5 \text{ } \mu\text{g mL}^{-1} \text{ }^{(A)}$
Y_s	Biomass yield for growth on substrate S	$0.66 \text{ g COD-X/g COD-S }^{(1)}$
ω	Dilution rate	$0.1 \text{ h}^{-1} \text{ }^{(A)}$

⁽¹⁾ Levin et al., 1977, Chao et al., 1977, ^(A) Assumed
S - substrate is glucose

3.2.1. Minimum transfer rate for survival

The minimum transfer rate γ_{\min} required for the survival of a plasmid in a single species population growing in a chemostat can be derived from the classical mass-action model developed by Levin and co-workers in the 1970's (see Model development chapter section 2.1.1, Model 1). For a given population density (X^*) at steady state, dilution rate (ω), burden (α) and rate of loss (τ), the minimum transfer rate for a plasmid to survive in a single-species population is given by (Levin et al., 1979):

$$\gamma_{\min} = \frac{\alpha\omega + \tau}{X^*}$$

Eq. 3.1

From equation 3.1 it can be deduced that an increased fitness cost requires a higher transfer rate for a plasmid to persist in a bacterial population. In this study, experimentally measured fitness costs conferred by two plasmids in *E. coli*, the narrow host-range R1 and the broad host-range RK2, were used as a reference for

varying the fitness cost parameter. The NHR plasmid conferred a 6% reduction in growth and the BHR plasmid 21% (Dahlberg and Chao, 2003). The loss rate for both plasmids was 10^{-4} h^{-1} , and for this set of parameters the calculated minimum transfer rate for the NHR ($\alpha_{\text{NHR}} = 6\%$) and BHR ($\alpha_{\text{NHR}} = 21\%$) plasmids to survive in a single species population was 2.5×10^{-9} and $8.7 \times 10^{-9} \text{ mL cell}^{-1} \text{ h}^{-1}$, respectively, assuming that the total population density in steady state X^* does not change. This would be the case when the plasmid has no effect on substrate affinity and growth yield. Given the present set of parameters the population density is $X^* = 2.4 \times 10^6 \text{ cells mL}^{-1}$. A different steady state between plasmid-free and plasmid-bearing hosts is achieved for different transfer rates. As the transfer rate is increased, a higher proportion of plasmid-bearing cells can be found in steady state. Above a certain transfer rate there will be no detectable change in the total fraction of plasmid-bearing cells. This value represents a saturation level where the maximum frequency of plasmid-bearing cells for the specified parameters has been reached, i.e. more than 99% of the cells carry the plasmid. Figure 3.1 shows how the frequency of the plasmid-bearing cells (P^+) at steady state changes with increasing transfer rate for plasmids with different fitness costs. The graph shows a linear dependence between the frequency of P^+ cells and transfer rate, where the plasmid with a higher cost has the smaller slope. Thus, to achieve the same plasmid-frequency in a population of hosts, the plasmid with a higher cost needs a much higher transfer rate than a plasmid with a smaller cost. This result is independent of the initial frequency of plasmid-bearing cells.

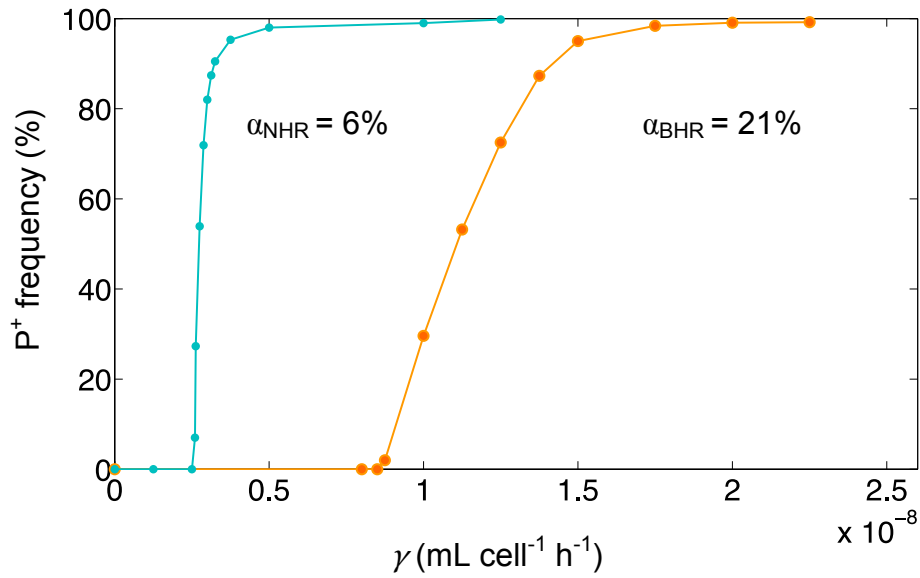


Figure 3.1: Frequency of plasmid-bearing (P^+) cells at steady-state for increasing transfer rates for plasmids with different fitness costs in a single species population. Results obtained with the deterministic model of one plasmid in one species population, long after the steady state has been reached (4800 hours), compare Figure 3.2. Parameters: $\tau = 10^{-4} \text{ h}^{-1}$, $\omega = 0.1 \text{ h}^{-1}$.

In the individual-based model (IbM) the combined effect of a small transfer rate and low initial frequency of donors can sometimes lead to failure of plasmid invasion and extinction of the plasmid. This is due to the stochastic nature of the dynamics where each individual cell has the same chance of being washed out. Thus, the plasmid can become extinct if the last plasmid-bearing cell in the system is lost. This feature will be investigated further in the results section 3.2.5. Nevertheless, the minimum transfer rate for a plasmid to invade and persist in a population of plasmid-free hosts in the individual-based model (cp) is lower than the one calculated with the mass-action model equation 3.1, see Table 3.2. Plasmid-related parameters used in the ODE model and in the IbM chemostat can be found in Table 3.2. The discrepancy in the minimum transfer rate between the IbM and the ODE models might be explained by the size structure of the population in the IbM model. In the IbM, the transfer process involves discrete cells regardless of their size, and because conversion between γ and cp was based on mean cell size, differences in the number of cells being simulated in the IbM and the total biomass in the mass-action model can lead to different values for the minimum transfer rate. Figure 3.2 compares plasmid invasion dynamics in the IbM model with the mass-action model for different values of the transfer rate. Notice that higher transfer rates are needed in the deterministic model to achieve levels of plasmid frequency similar to the IbM model. Steady state values for the plasmid frequencies in the ODE model and in the IbM chemostat are summarized in Table 3.3.

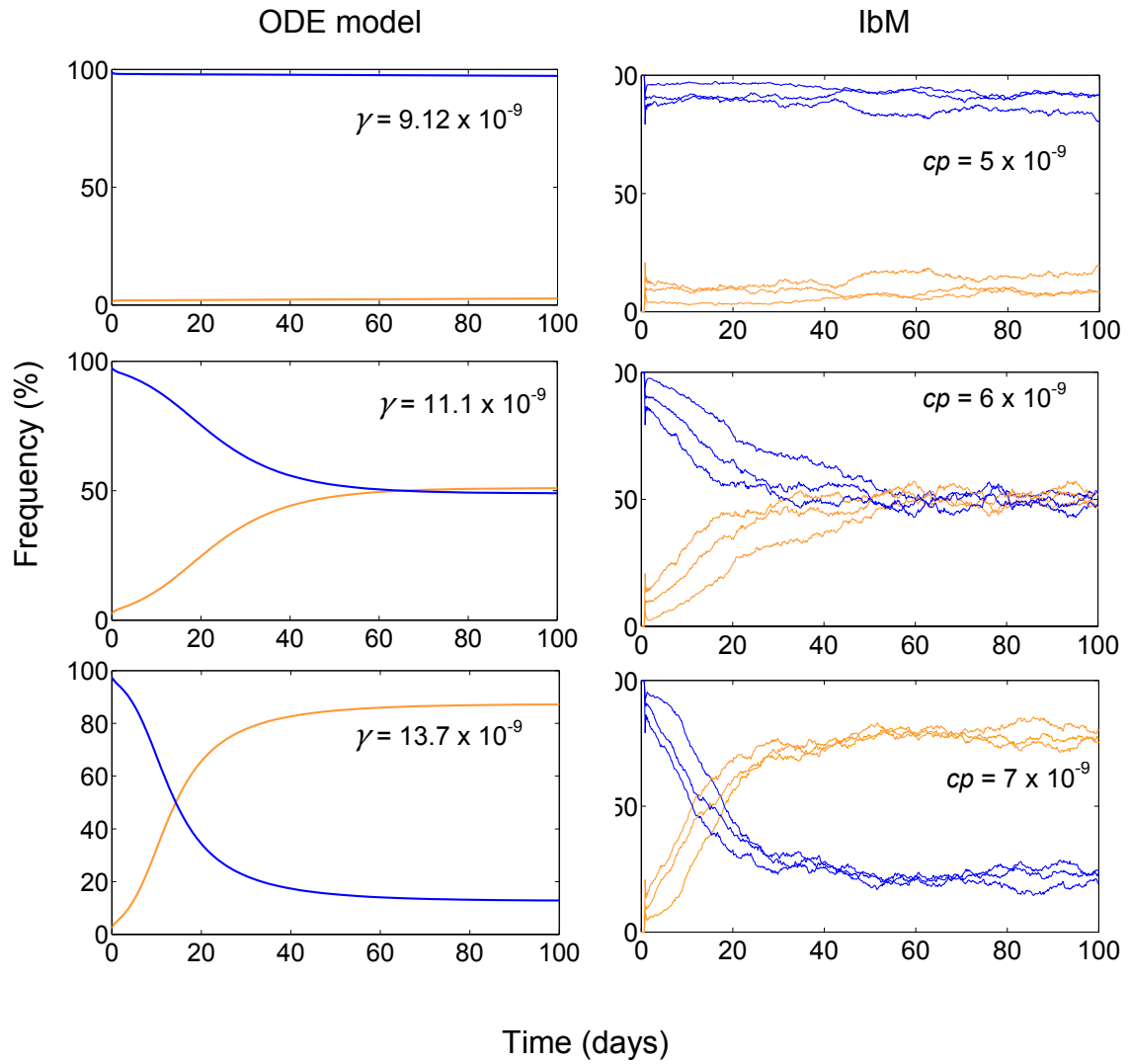


Figure 3.2: Dynamics of plasmid invasion for a plasmid with a 21% fitness cost, for increasing transfer rates in a single species population. Results obtained with the ODE (left panels) and the IbM (right panels) models. Output from three replicates is shown for the IbM model. Legend: — R_N , — T_N^B

Table 3.2 Plasmid-related parameters and results

Parameter	NHR	BHR
α_i	0.06	0.21
τ	10^{-4}	10^{-4}
Host-range	N	N,B
Results	NHR	BHR
$\gamma_{min} (mL\ cell^{-1} h^{-1})$	2.5×10^{-9}	8.8×10^{-9}
$cp_{min} (mL\ cell^{-1} h^{-1})$	$[1.4, 1.6] \times 10^{-9}$	$[5.0, 6.0] \times 10^{-9}$

Table 3.3 Frequency of plasmid-bearing cells (T_N^B) and recipients (R_N) at steady state obtained with the ODE and the IbM models for different transfer rates. Parameters are: $\tau = 10^{-4} h^{-1}$, $\omega = 0.1 h^{-1}$, $\alpha = 21\%$.

ODE model			IbM ^a		
$\gamma (mL\ cell^{-1} h^{-1})$ $\times 10^{-9}$	T_N^B	R_N	$cp (mL\ cell^{-1} h^{-1})$ $\times 10^{-9}$	$T_N^B \pm SD$	$R_N \pm SD$
9.12	10.0 %	90 %	5.0	$17.2 \pm 1.5 \%$	$82.8 \pm 1.5 \%$
11.1	51.0 %	49.0 %	6.0	$49.6 \pm 2.3 \%$	$50.4 \pm 2.3 \%$
13.7	87.3 %	12.7 %	7.0	$81.0 \pm 4.8 \%$	$19.0 \pm 4.8 \%$
17.5	98.4 %	1.6 %	8.0	$98.0 \pm 1.4 \%$	$2.0 \pm 1.4 \%$

^a Average of three replicates

3.2.2. *Transfer of a NHR plasmid in a two-species assemblage*

In this scenario the microbial assemblage is now composed of two species, N and B , and the NHR plasmid can only infect and replicate in cells of species N . Figure 3.3 compares the dynamics of invasion of a NHR plasmid with and without cost in a two-species assemblage using the lbM chemostat and the ODE model.

The costly NHR plasmid is quickly washed out from the chemostat as its host fails to compete against the faster-growing plasmid-free cells of species B . This observation holds as long as the plasmid confers a burden on its host even if very large transfer rate coefficients are more than sufficient to maintain the same plasmid in the single species case. In contrast, a NHR plasmid that does not confer any cost on its host is able to invade the two-species microbial assemblage and successfully maintain itself in competition with the plasmid-free hosts of species B .

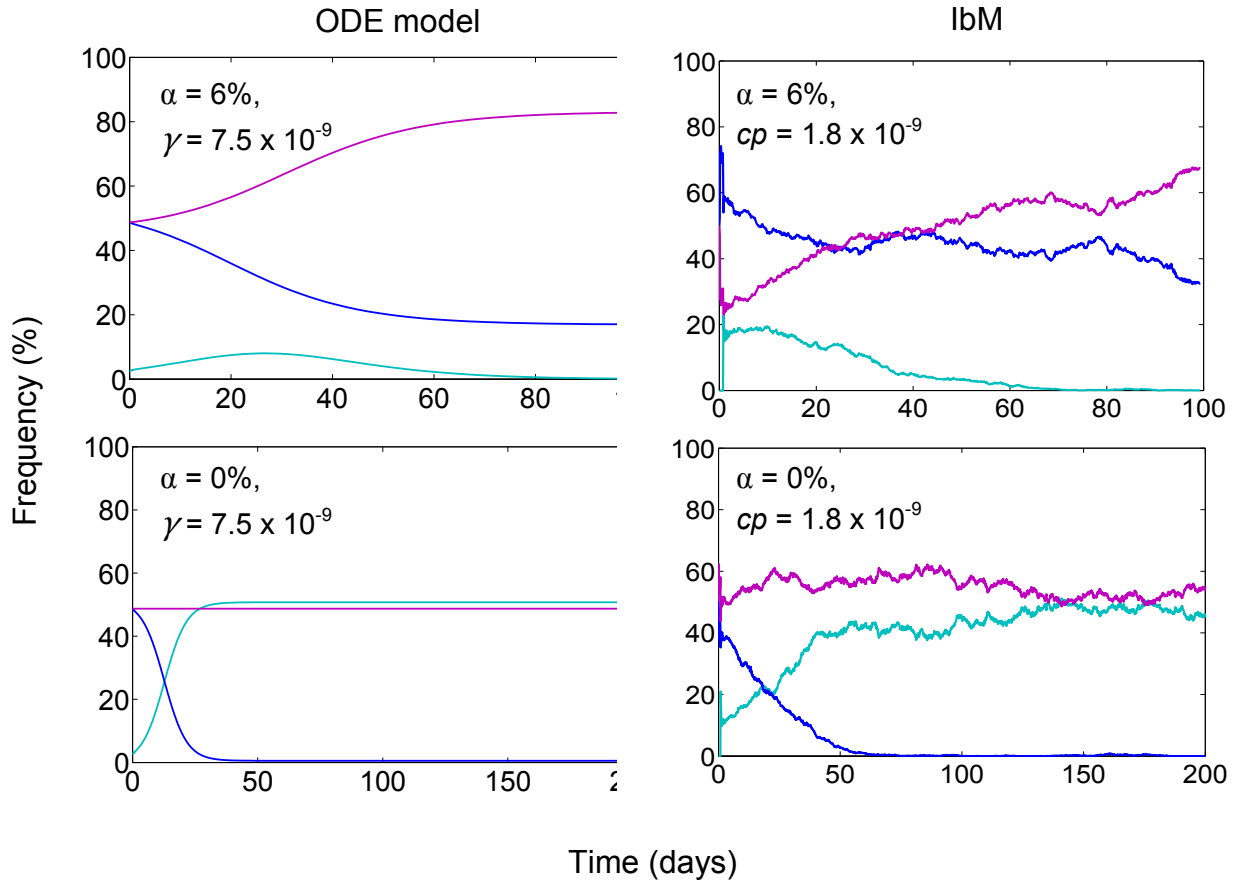


Figure 3.3: Dynamics of plasmid invasion of a costly NHR plasmid and a NHR conferring zero cost in a two-species assemblage. Results obtained with the ODE (left panel) and the IbM (right panel) models. Note that both recipients have equal fitness without plasmid, or if the plasmid causes no burden. Legend: R_N (blue), R_B (magenta), T_N^N (cyan)

T_N^N

3.2.3. Compatible plasmids

In this scenario, two compatible plasmids with different host-ranges compete for suitable hosts in a two-species assemblage. The plasmids belong to different incompatibility groups and thus they can co-exist in the same host.

The mathematical analysis presented herein was carried out using the ODE model. The steady state frequencies of NHR plasmid-bearing cells (T_N^N), BHR plasmid-bearing cells (T_N^B and T_B^B), dual plasmid-bearing cells ($T_N^{B,N}$), plasmid-free recipients of both species N and B (R_N, R_B) at steady state were calculated for different set of parameters in order to evaluate the effect of host-range, fitness cost, transfer rate and loss rate on the competitiveness of each plasmid. When one parameter was varied, all the other parameters were kept constant for both plasmids. The analysis is split into four subsections, each covering a different plasmid-related parameter.

3.2.3.1. Effect of host range

In order to evaluate the effect of a broader host-range on the competitiveness of a plasmid, we compared the dynamics of two competing plasmids in a single-species population (N) and in a two-species assemblage (N and B). The strategy consisted of keeping the plasmid-related parameters equal for both plasmids except the parameter being varied. Figures 3.4 and 3.5 illustrate how a broader host-range can be advantageous for a plasmid transferring in a two-species assemblage and the effect of varying either cost or transfer rate on its overall competitiveness.

In Figure 3.4 the cost for both plasmids was set to zero in order to have the NHR plasmid competing in the two-species assemblage, while varying the transfer rate of the BHR plasmid. Recall that a costly NHR plasmid cannot survive in a two-species assemblage alone nor in the presence of a compatible BHR plasmid. The transfer rate of the BHR plasmid is varied within the range for which survival of a costless plasmid in a single species population is expected.

In the single species (N) population an increase in the BHR transfer rate leads to the proliferation of hosts carrying both plasmids ($T_N^{B,N}$). When both plasmids have the same parameter values, their individual frequencies are the same. An increase in $T_N^{B,N}$ hosts is also observed for the two-species assemblage, although now the BHR plasmid-bearing hosts ($T_{N,B}^B$) are the most abundant. This is because of the broader-host range of the BHR plasmid, which can also proliferate among recipients of species B .

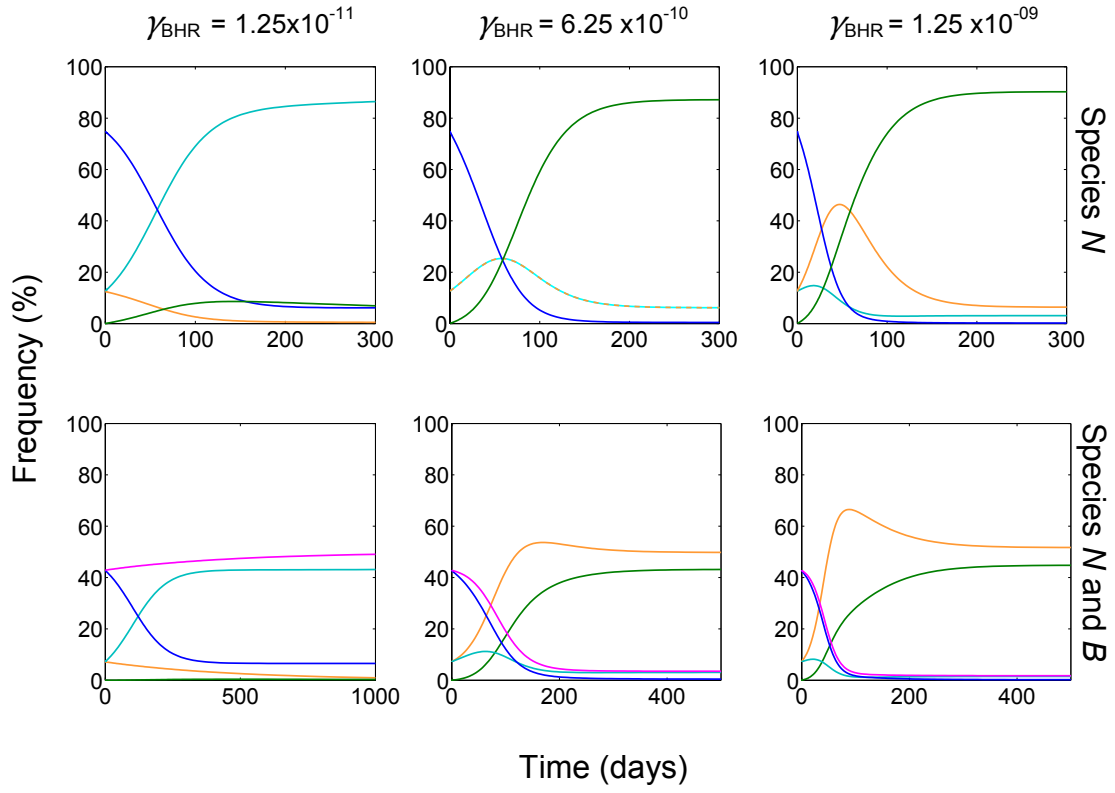


Figure 3.4: Effect of different transfer rates for the BHR plasmid, on the dynamics of invasion of two compatible plasmids in single and two-species assemblages. Notice that $T_{N,B}^B$ is the sum of hosts carrying only the BHR plasmid, i.e., T_N^B and T_B^B . Parameters are $\alpha_{\text{NHR}} = \alpha_{\text{BHR}} = 0\%$, $\tau_{\text{NHR}} = \tau_{\text{BHR}} = 10^{-4} \text{ h}^{-1}$, and $\gamma_{\text{NHR}} = 6.25 \times 10^{-10} \text{ mL cell}^{-1} \text{ h}^{-1}$. Legend: — R_N — R_B — T_N^N — $T_{N,B}^B$ — $T_N^{B,N}$

In Figure 3.5 fitness cost of the BHR plasmid was varied between 2% and 12%; ranging from a low but positive burden to a fitness cost that is too high for the plasmid to survive, given the combination of the transfer rate and loss rate parameter values chosen for this set of simulations. In the single species population, an increase in cost results in a decrease in $T_{N,B}^B$ and $T_N^{B,N}$ hosts, while at the same time T_N^N rises benefitting from a less competitive and more costly BHR plasmid. As expected, when the parameters for both plasmids are the same, their individual frequencies are the same. In contrast, in the two-species assemblage, a costly compatible NHR plasmid cannot survive, and survival of the BHR plasmid depends only on its own parameters. Notice that for $\alpha_{\text{BHR}} \leq 8\%$, the BHR plasmid will now survive in the two-species assemblage but not in the single-species population when competing against a less costly NHR plasmid as host-range is then the same.

Thus, a broader host-range can save a plasmid from extinction when competing with a compatible NHR plasmid with a lower burden.

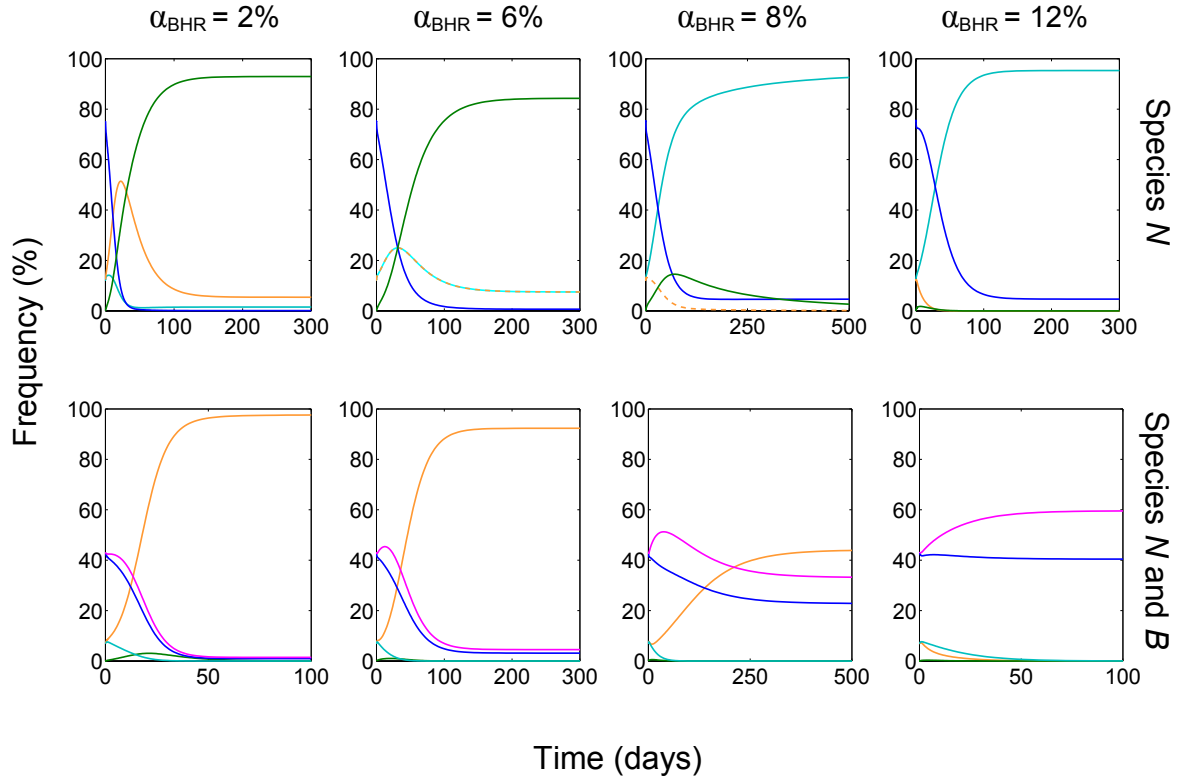


Figure 3.5 Effect of host-range for different fitness costs for the BHR plasmid, on the dynamics of two compatible plasmids invasion in single and two-species assemblages. Notice that $T_{N,B}^B$ is the sum of hosts carrying only the BHR plasmid, i.e., T_N^B and T_B^B . Parameters are $\gamma_{NHR} = \gamma_{BHR} = 3.75 \times 10^{-9} \text{ mL cell}^{-1} \text{ h}^{-1}$, $\tau_{NHR} = \tau_{BHR} = 10^{-4} \text{ h}^{-1}$, and $\alpha_{NHR} = 6\%$. Legend: — R_N — R_B — T_N^N — $T_{N,B}^B$ — $T_N^{B,N}$

3.2.3.2. Effect of fitness cost

The fitness cost for each plasmid was varied between 0 and 50 %, and the results are presented in Figure 3.6. From the figure, there are a number of observations that can be made. The NHR plasmid can only survive if it does not confer any cost. The NHR plasmid can either be found alone, in T_N^N hosts, or together with its competitor in $T_N^{B,N}$ hosts. For lower costs (0 and 6%) of the BHR plasmid, the NHR can only be found in $T_N^{B,N}$ hosts. However, for higher fitness costs of the BHR plasmid (21% and 50%), T_N^N hosts increase in frequency profiting from a decrease in T_B^B and T_N^B hosts. For the BHR plasmid, an increase in its fitness cost leads to a reduction in its final frequency in the microbial assemblage. Another feature is the prevalence of the BHR plasmid in hosts of species B , T_B^B . This is due to the initial rapid infection of recipients of species N by NHR and BHR plasmids resulting in dual-plasmid carrying hosts, $T_N^{B,N}$, which grow very slowly (the fitness costs of both plasmids add up) and are quickly washed out. This process leads to the extinction of the NHR plasmid when the plasmid confers a burden to its host.

The frequency of T_N^B increases with higher costs for the NHR plasmid. This is because the higher the NHR cost, the quicker the T_N^N hosts will be outcompeted resulting in a lower infection of R_N hosts, which are then readily available for the BHR plasmid to infect. Given the high transfer rate chosen for both plasmids, the abundance of free recipients is scarce throughout the presented analysis, except when the plasmid costs reach very high values (50%). R_N hosts are always less abundant than R_B since both plasmids can infect recipients from species N . The combined effect of high transfer rates and high fitness costs can lead to a dramatic

alteration in the microbial assemblage composition after the plasmids are washed out. For lower transfer rates the qualitative results are the same, except that the change in the final frequency of free-recipients of each species changes less dramatically (not shown).

Overall, a costly NHR plasmid cannot survive in a two-species assemblage in the presence or absence of a competitor BHR plasmid. An increase in the fitness cost of the BHR plasmid renders it less competitive.

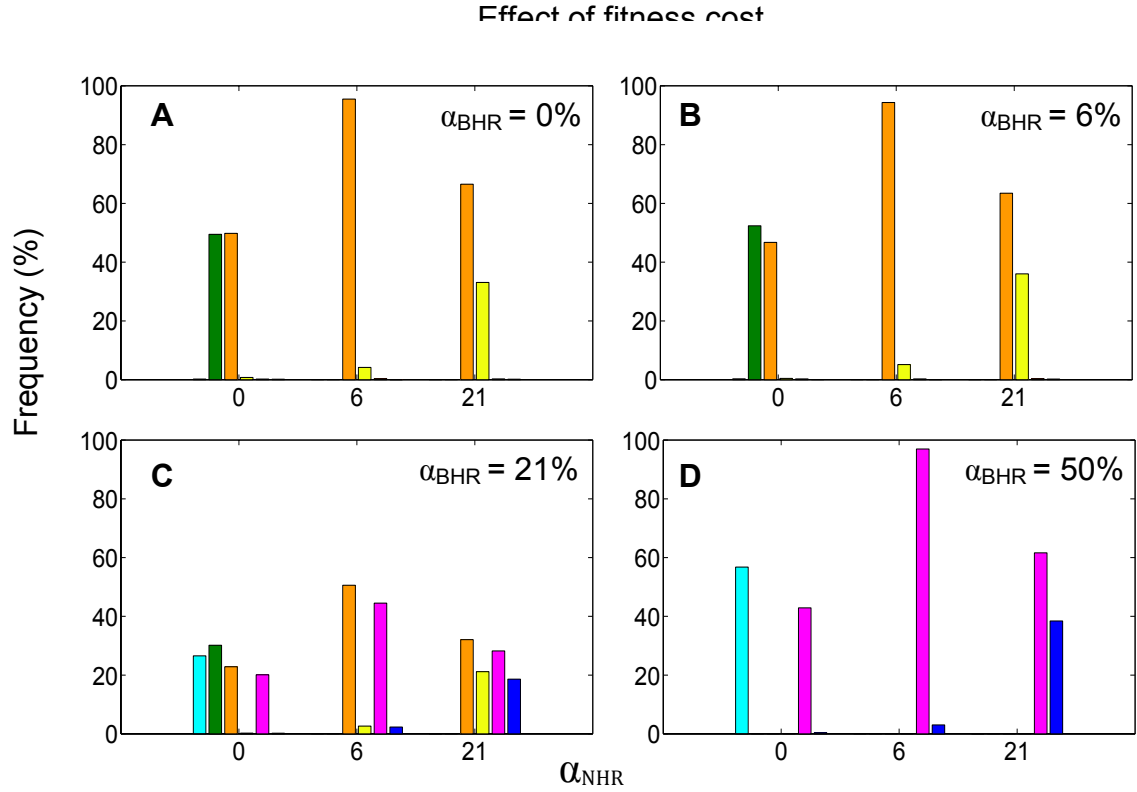


Figure 3.6 Effect of varying the fitness cost of compatible NHR and BHR plasmids competing in a two-species assemblage, on their frequency in steady state (numerical results obtained after > 300 days simulated time). The fitness cost of the NHR plasmid is represented on the X-axis, while the burden conferred by the BHR plasmid is kept constant in each panel. Parameters are $\gamma_{\text{NHR}} = \gamma_{\text{BHR}} = 1.13 \times 10^{-8} \text{ mL cell}^{-1} \text{ h}^{-1}$, $\tau_{\text{NHR}} = \tau_{\text{BHR}} = 10^{-4} \text{ h}^{-1}$. Legend: T_N^N (cyan), $T_N^{B,N}$ (green), T_B^B (orange), T_N^B (yellow), R_B (magenta), R_N (blue).

3.2.3.3. Effect of transfer rate

The effect of varying the transfer rate of each plasmid on their competitiveness was analyzed and the results are presented in Figure 3.7. The fitness cost for both plasmids was kept at 0% in order to ensure the presence of the NHR plasmid in the two-species assemblage. In the absence of a fitness burden, both plasmids can coexist under a wide range of transfer rates except if their transfer rate is zero. The NHR plasmid is only found in $T_N^{B,N}$ hosts whereas the BHR plasmid is split between $T_N^{B,N}$ and T_B^B hosts. Another consequence of having costless plasmids with reduced loss rates spreading in the microbial assemblage is the low abundance of plasmid free recipients, regardless of low transfer rates. For positive fitness costs the NHR plasmid does not survive and the frequency of the BHR plasmid in the microbial assemblage becomes dependent on the same relationship between transfer rate and fitness cost as the one observed for the single plasmid spreading in a single species population since the BHR plasmid does not distinguish species.

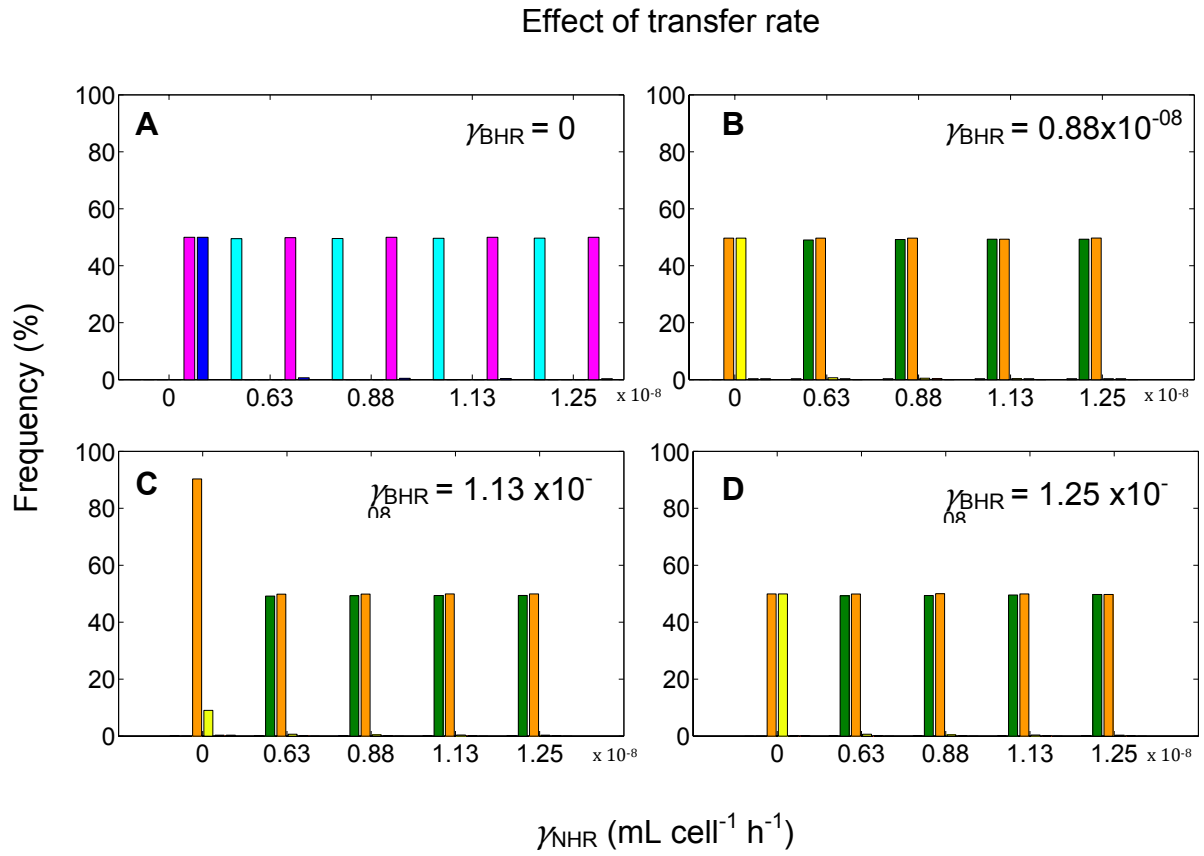


Figure 3.7. Effect of varying the transfer rate of compatible NHR and BHR plasmids competing in a two-species assemblage, on their frequency in steady state (numerical results obtained after > 300 days simulated time). The transfer rate for the NHR plasmid is represented by the X-axis, while the BHR transfer rate was kept constant in each subplot. The loss rate of the NHR plasmid is represented in the X-axis and the BHR loss rate was kept constant in each subplot. Parameters are $\alpha_{\text{NHR}} = \alpha_{\text{BHR}} = 0\%$, $\tau_{\text{NHR}} = \tau_{\text{BHR}} = 10^{-4} \text{ h}^{-1}$. Legend: T_N^N $T_N^{B,N}$ T_B^B T_N^B R_B R_N

3.2.3.4. Effect of loss rate

The effect of varying the loss rate of each plasmid on their ability to survive in a two-species assemblage was investigated and the results are presented in Figure 3.8. Again, the fitness cost was zero for both plasmids to guarantee that the NHR plasmid was not washed out due to another factor besides the loss rate. The two competing plasmids can coexist over a wide range of loss rates. Very low loss rates for both plasmids considerably reduce the abundance of plasmid-free recipients in the two-species assemblage, while promoting the proliferation of $T_N^{B,N}$ hosts. An increase in τ_{BHR} supports the existence of T_N^N hosts, whereas a rise in τ_{NHR} leads to an increase of T_N^B hosts. As BHR segregational loss increases, there are fewer BHR carrying hosts to infect the NHR carrying hosts, thus allowing a higher percentage of T_N^N hosts to exist. The opposite happens when the loss rate of the NHR plasmid increases, leading to an increase of hosts of species N carrying the BHR plasmid, T_N^B . For intermediate loss rates a higher diversity in hosts composition is observed. Very high loss rates, for which the value of the transfer rate is not sufficient to rescue the plasmid from washout, lead to the extinction of one or both plasmids.

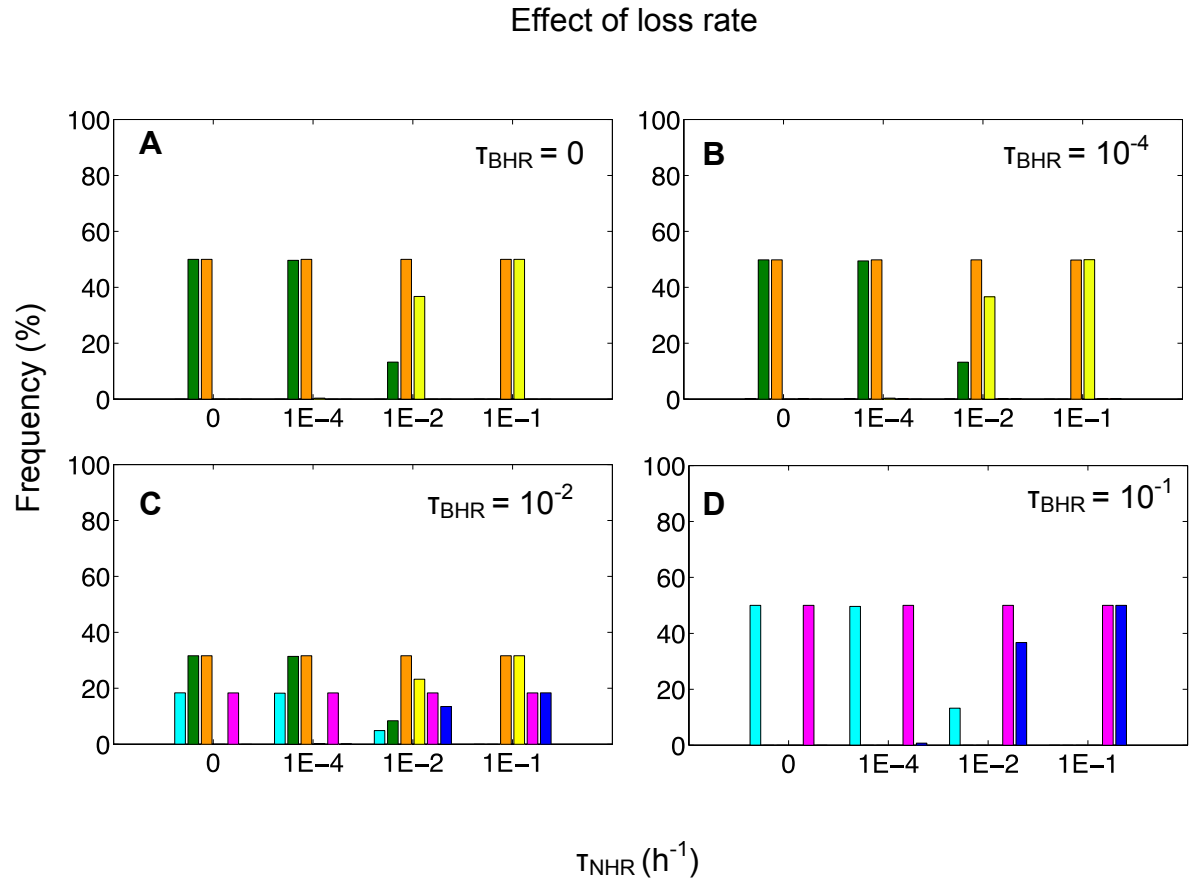


Figure 3.8: Effect of varying the loss rate of compatible NHR and BHR plasmids competing in a two-species assemblage, on their frequency in steady state (numerical results obtained after > 300 days simulation time). Parameters are $\alpha_{NHR} = \alpha_{BHR} = 0\%$, $\gamma_{NHR} = \gamma_{BHR} = 1.13 \times 10^{-8} \text{ mL cell}^{-1} \text{ h}^{-1}$ for both plasmids. Legend: T_N^N (cyan), $T_N^{B,N}$ (green), T_B^B (orange), T_N^B (yellow), R_B (magenta), R_N (blue).

Summary for *Compatible Plasmids*

- A costly plasmid with a broader, both species, host-range can survive in two-species assemblages and successfully compete with faster growing costless NHR plasmid-bearing hosts;
- A NHR plasmid can only coexist with a compatible BHR plasmid in two-species assemblages if its cost is zero;
- Competing compatible plasmids with high transfer rates and zero burden promote an increase in dual-plasmid carrying hosts, $T_N^{B,N}$;
- High loss rates lead to an increase of the number of co-existing types of hosts in the two-species assemblage: single plasmid, dual-plasmid bearing cells and plasmid-free recipients.

3.2.4. Incompatible plasmids

In this scenario, two incompatible plasmids with different host-ranges compete for suitable hosts in a two-species assemblage. The plasmids belong to the same incompatibility group and 100% exclusion between the two is assumed. Consequently a host will never simultaneously harbor both plasmids.

The mathematical analysis presented herein was carried out using the ODE model. The frequencies of NHR plasmid-bearing cells (T_N^N), BHR plasmid-bearing cells (T_N^B and T_B^B), and plasmid-free recipients of both species N and B (R_N, R_B) at steady state were calculated for different set of parameters in order to evaluate the effect of host-range, fitness cost, transfer rate and loss rate on the competitiveness of each plasmid.

The analysis is split into four subsections, each covering the variation of a different plasmid-related parameter. The effect of varying each parameter at a time, on the competitiveness of the two incompatible plasmids is analyzed. When one parameter was varied, all the other parameters were kept constant for both plasmids.

3.2.4.1. Effect of host range

The effect of a broader host-range on the interaction of incompatible plasmids was evaluated by comparing the propagation of two plasmids competing in a single species (N) population and in two-species (N, B) assemblages.

Figures 3.9 and 3.10 illustrate the transfer dynamics of incompatible NHR and BHR plasmids spreading in a single-species population and in a two-species assemblage

for different transfer rates of the NHR plasmid. In both figures the fitness costs were kept at $\alpha_{\text{NHR}} = 6\%$ and $\alpha_{\text{BHR}} = 21\%$. The difference between the two figures is then the transfer rate of the BHR plasmid, $\gamma_{\text{BHR}} = 1 \times 10^{-8} \text{ mL cell}^{-1} \text{ h}^{-1}$ in Figure 3.9 and $\gamma_{\text{BHR}} = 2.5 \times 10^{-8} \text{ mL cell}^{-1} \text{ h}^{-1}$ in Figure 3.10. Notice that $T_{N,B}^B$ is the sum of hosts carrying only the BHR plasmid, i.e., T_N^B and T_B^B .

In Figure 3.9, in the single-species (N) scenario the two plasmids cannot coexist, and the plasmid with the lower cost outcompetes the plasmid with higher costs, except when the NHR plasmid does not transfer (first row, first column). An increase in the transfer rate of the NHR plasmid increases its ability to outcompete the BHR plasmid when its host-range is of no advantage. In the two-species assemblage, the BHR plasmid is now more competitive and it can outcompete the less costly NHR plasmid, whereas in the single-species population it could not. The NHR plasmid is outcompeted by the BHR plasmid even if the transfer rate of the NHR plasmid is higher than that of the BHR plasmid, highlighting the advantage of having a broader host-range. However, when the transfer rate of the BHR plasmid is increased by 2.5 fold, coexistence of both plasmids in single species populations and in two-species assemblages becomes possible (Figure 3.10). In Figure 3.10, in the single species scenario, the two plasmids can now coexist by following different survival strategies, one with a higher transfer rate and high fitness cost (BHR) and the other with a lower transfer rate and a smaller cost (NHR). Notice, however, that coexistence was observed only for high ratios of $\gamma_{\text{BHR}} / \gamma_{\text{NHR}}$. As the γ_{NHR} is increased, the costly BHR plasmid can no longer compete with the less costly NHR plasmid. In contrast, in the two-species assemblage, coexistence of both plasmids is observed regardless of the transfer rate of the NHR plasmid. Furthermore, the final

frequency of the NHR plasmid in the two-species assemblage is not altered by an increase in its transfer rate. Coexistence is observed even if the transfer rate of the NHR plasmid is higher than that of the BHR plasmid (not shown). Thus, for higher transfer rates of the BHR, in two-species assemblages, plasmid coexistence of the two plasmids is possible and the frequency of the NHR plasmid is increased. Also, the difference in fitness cost and higher transfer rates generate damped oscillations in the system: a rise in $T_{N,B}^B$ is accompanied by a fall in plasmid-free recipients, R_{tot} and the decrease in $T_{N,B}^B$ is closely followed by an increase in T_N^N hosts until each variable stabilizes at their steady state value. This pattern is only observed when the fitness cost of the BHR plasmid is higher than the NHR plasmid and the transfer rate of the BHR plasmid is sufficiently high (Figure 3.10 and 3.11).

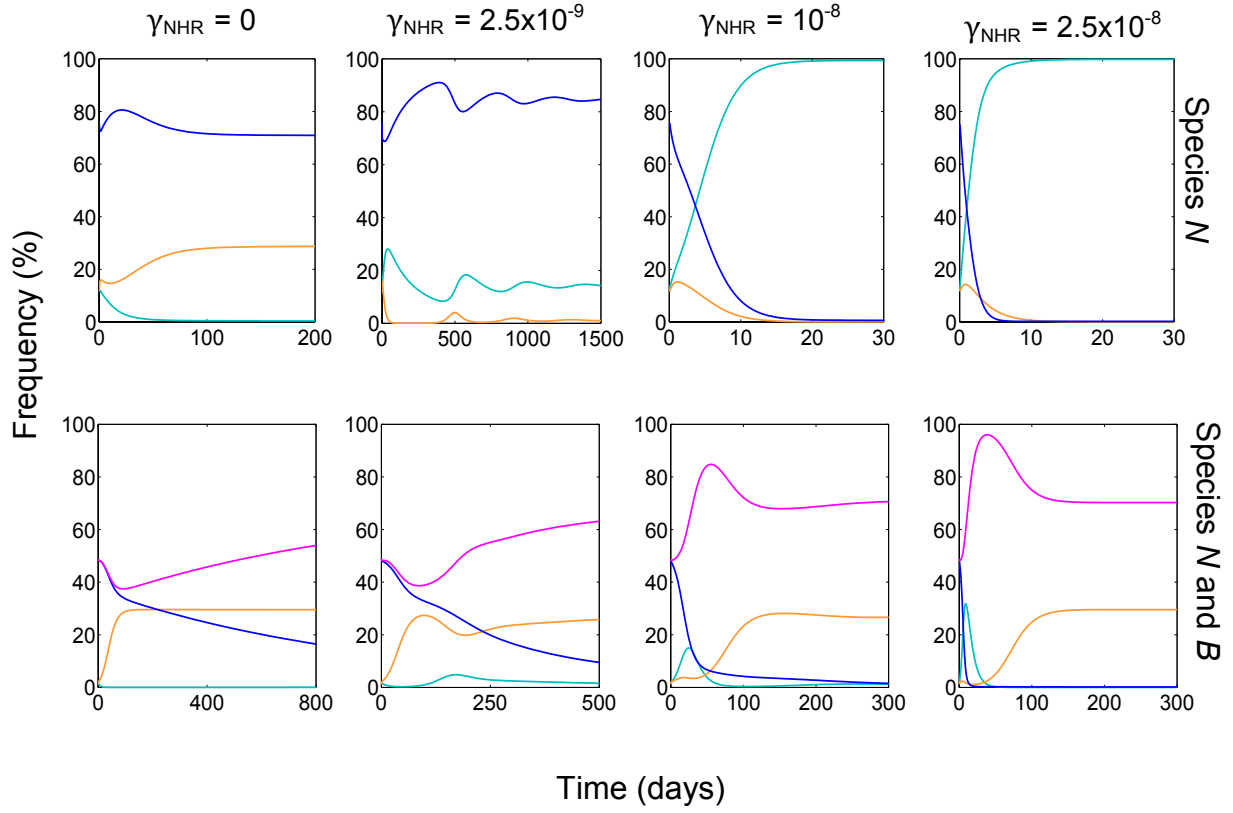


Figure 3.9 Effect of host-range for different transfer rates for the NHR plasmid, on the dynamics of two incompatible plasmids invading single and two-species assemblages. Parameters: $\alpha_{NHR} = 6\%$, $\alpha_{BHR} = 21\%$, $\tau_{NHR} = \tau_{BHR} = 10^{-4} \text{ h}^{-1}$, and $\gamma_{BHR} = 10^{-8} \text{ mL cell}^{-1} \text{ h}^{-1}$. See the next figure for higher BHR transfer rate (Figure 3.10).

Legend: — R_N — R_B — T_N^N — T_N^B

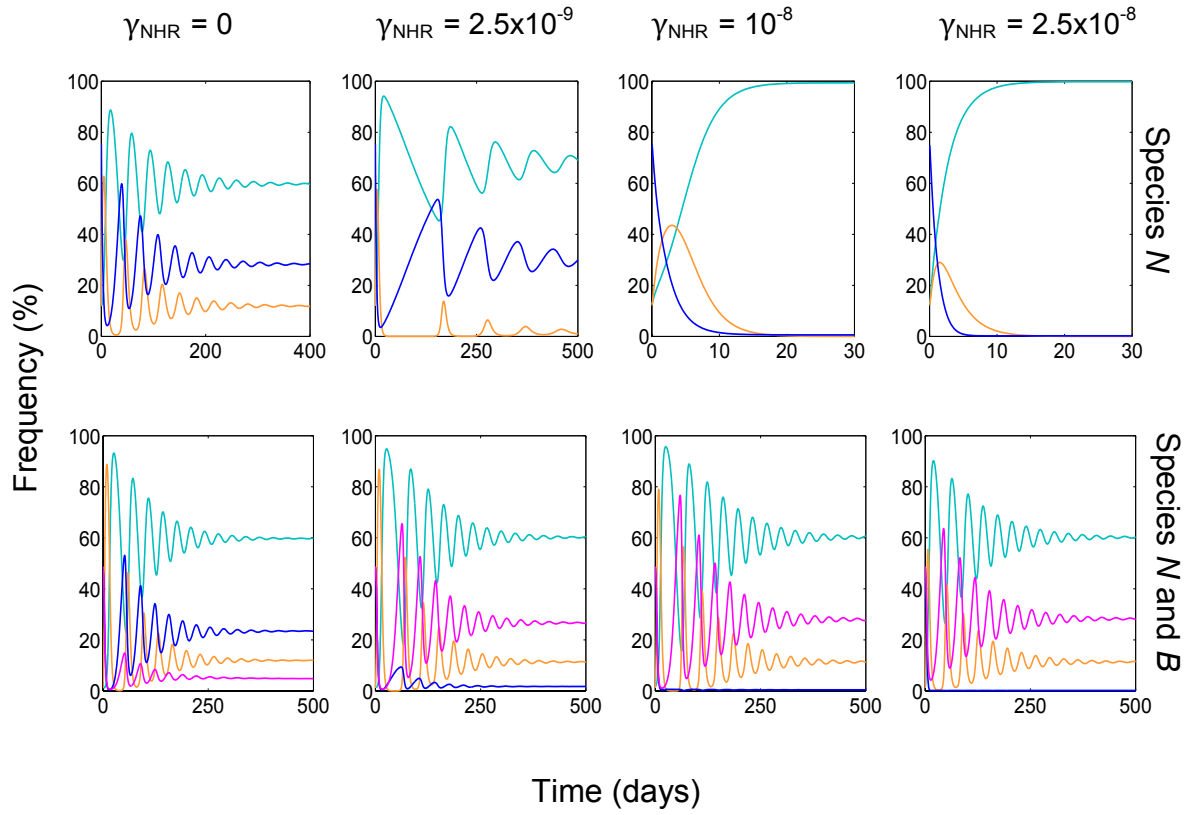


Figure 3.10 Effect of host-range for different transfer rates for the NHR plasmid, on the dynamics of two incompatible plasmids invading single and two-species assemblages. Parameters $\alpha_{\text{NHR}} = 6\%$, $\alpha_{\text{BHR}} = 21\%$, $\tau_{\text{NHR}} = \tau_{\text{BHR}} = 1 \times 10^{-4} \text{ h}^{-1}$, and $\gamma_{\text{BHR}} = 2.5 \times 10^{-8} \text{ mL cell}^{-1} \text{ h}^{-1}$. See previous figure for a lower BHR transfer rate (Figure 3.9). Legend: — R_N — R_B — T_N^N — $T_{N,B}^B$

In Figure 3.11 the fitness cost of the BHR plasmid was varied while keeping $\alpha_{\text{NHR}} = 6\%$ and the transfer rate for both plasmids at $2.5 \times 10^{-8} \text{ mL cell}^{-1} \text{ h}^{-1}$. In the single species population an increase in the fitness cost leads to extinction of the plasmid. Coexistence is only observed if both plasmids have the same cost (first row, second panel, for $\alpha = 6\%$). In the two-species assemblage, the BHR plasmid will win the competition for lower or equal fitness costs of the NHR plasmid (second row, first and second panels) due to its ability to infect recipients of species B , which the NHR plasmid cannot. Then, when the NHR plasmid has a fitness cost advantage over the BHR plasmid, coexistence of both plasmids is possible with the NHR plasmid being the most abundant plasmid in the two-species assemblage (second row, third and fourth panels). Once again, the phase shift of the oscillations is the same as before: a peak in $T_{N,B}^B$, followed by an increase in T_N^N when $T_{N,B}^B$ is starting to decline. Overall, the oscillatory behavior arises for sufficiently high transfer rates when the fitness costs of the competing plasmids are positive and different.

The comparison between Figure 3.10 and Figure 3.11 points to a determinant role of transfer rate and fitness cost on the outcome of competition between plasmids with different host-ranges, which is addressed in the next sections.

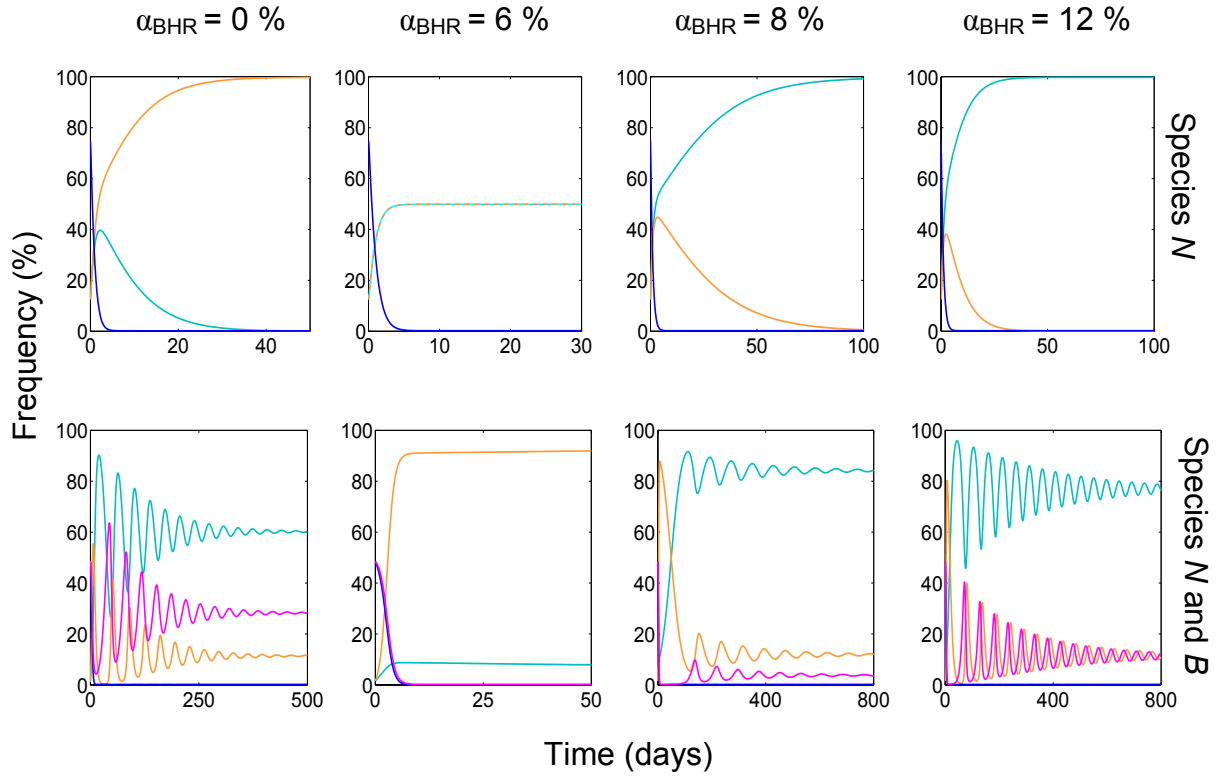


Figure 3.11: Effect of host-range for different fitness costs for the BHR plasmid, on the dynamics of two incompatible plasmids invading single and two-species assemblages. Parameters $\alpha_{\text{NHR}} = 6\%$, $\tau_{\text{NHR}} = \tau_{\text{BHR}} = 10^{-4} \text{ h}^{-1}$, and $\gamma_{\text{BHR}} = \gamma_{\text{NHR}} = 2.5 \times 10^{-8} \text{ mL cell}^{-1} \text{ h}^{-1}$. Legend: — R_N — R_B — T_N^N — $T_{N,B}^B$

3.2.4.2. Effect of fitness cost

Figure 3.12 presents the results for the variation of the fitness cost parameter on the competitiveness of each plasmid. The overall observation is that the NHR plasmid can only survive in the presence of a more costly BHR plasmid. Moreover, there seems to be an intermediate BHR fitness cost for which the NHR frequency in the two-species assemblage is highest. The success of the BHR in the assemblage also depends on the burden conferred by the NHR plasmid: the lower the cost of its competitor, the more difficult it is for the BHR to prosper. Due to the high transfer rate of the plasmids, a big part of the assemblage will be carrying either one plasmid or the other in most of the scenarios presented here. But for lower transfer rates, the steady state between plasmid-bearing hosts and plasmid-free hosts will be in favor of the latter (not shown). Nevertheless, in the examples presented in Figure 3.12 the frequency of R_B increases when the fitness cost of the BHR plasmid becomes higher. R_N can only thrive when the costs for both plasmids are high as a consequence of the plasmid-bearing species being less competitive. The frequency of T_N^B hosts is also dependent on the fitness cost of the NHR plasmid, since plasmid-free hosts of species N will only become available for BHR plasmids when the NHR plasmid is more costly. Consequently, the T_N^B host can only proliferate when the fitness cost of BHR is equal or lower than that of the NHR plasmid. Increasing the fitness cost of a plasmid leads to a decline on its frequency in the two-species assemblage. Generally, the fate of each plasmid was dependent on each other's burden.

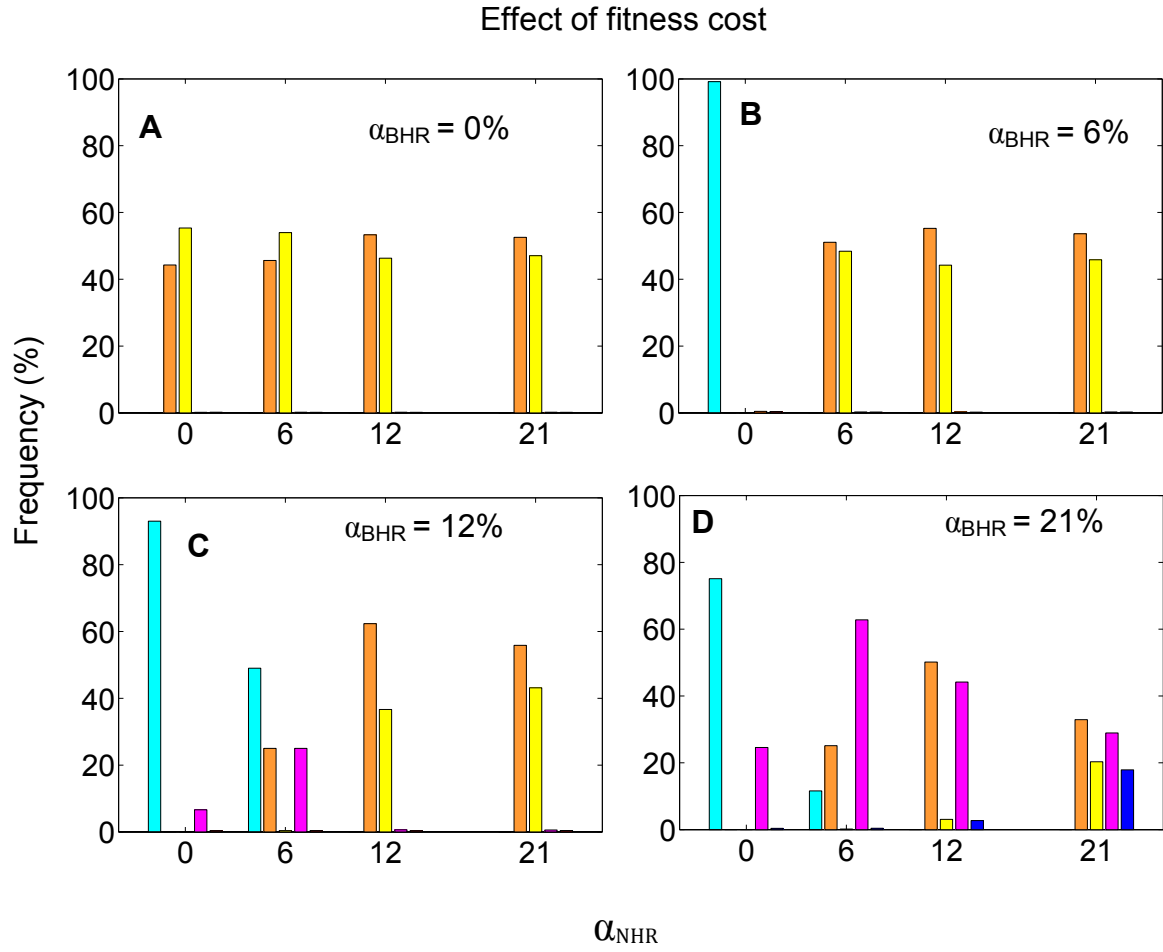


Figure 3.12: Effect of varying the fitness cost of incompatible NHR and BHR plasmids competing in a two-species assemblage, on their frequency in steady state (numerical results obtained after > 300 days simulated time). The X-axis represents the NHR burden, while the BHR cost is kept constant in each panel. Parameters are $\gamma_{NHR} = \gamma_{BHR} = 1.13 \times 10^{-8} \text{ mL cell}^{-1} \text{ h}^{-1}$ and $\tau_{NHR} = \tau_{BHR} = 10^{-4} \text{ h}^{-1}$.

Legend: T_N^N T_B^B T_N^B R_B R_N

3.2.4.3. Effect of transfer rate

Figure 3.13 comprises the results for varying the transfer rate of each plasmid. In this case, different costs were assigned to the different plasmids: 6% for the NHR and 12% for the BHR. This option is based on the previous observation that the NHR plasmid can only survive in the presence of a more costly BHR plasmid, and thus the choice of parameters suits the goal of analysing the effect of varying the transfer rate when both plasmids can otherwise co-exist. Nevertheless, analysis for different transfer rates with the costs set to zero was carried out and the only plasmid that was able to maintain itself in the assemblage was the BHR plasmid, confirming our previous result that a conjugative NHR plasmid cannot survive in the assemblage in the presence of a costless BHR plasmid, unless its competitor does not transfer ($\gamma_{\text{BHR}} = 0.0$) (not shown).

The results presented in Figure 3.13 show a surprising outcome: the NHR plasmid can survive in the two-species assemblage even if its transfer rate is zero, provided that it is competing against a more costly competitor. Not only can the NHR plasmid survive without transfer, its frequency in the two-species assemblage rises when the transfer rate of the BHR competitor plasmid is increased. At the same time, the BHR plasmid frequency declines when its transfer rate is too high. On the other hand, both NHR and BHR plasmid frequencies are not affected by an increase in NHR transfer rate, indicating that the transfer rate of its competitor is more important in controlling the persistence of the NHR plasmid. The frequencies of R_B and T_B^B are coupled; this is because as the NHR plasmid cannot infect recipients of species B , the steady state between the T_B^B and R_B is independent of T_N^N and R_N .

hosts. This trend can also be seen in the previous analysis of the fitness cost, where an increase in T_B^B hosts was linked with a proportional decrease in R_B , and vice-versa. A related observation is the very low frequency or total absence of T_N^B hosts, i.e, hosts of species N carrying the BHR plasmid. Even at low transfer rates for the NHR plasmid, the T_N^B host is not able to compete with the faster growing T_N^N hosts. This is because exclusion is assumed to be 100% and thus as long as the BHR plasmid has a higher fitness cost, the NHR plasmid will always win the competition for the recipients of species N .

Effect of transfer rate

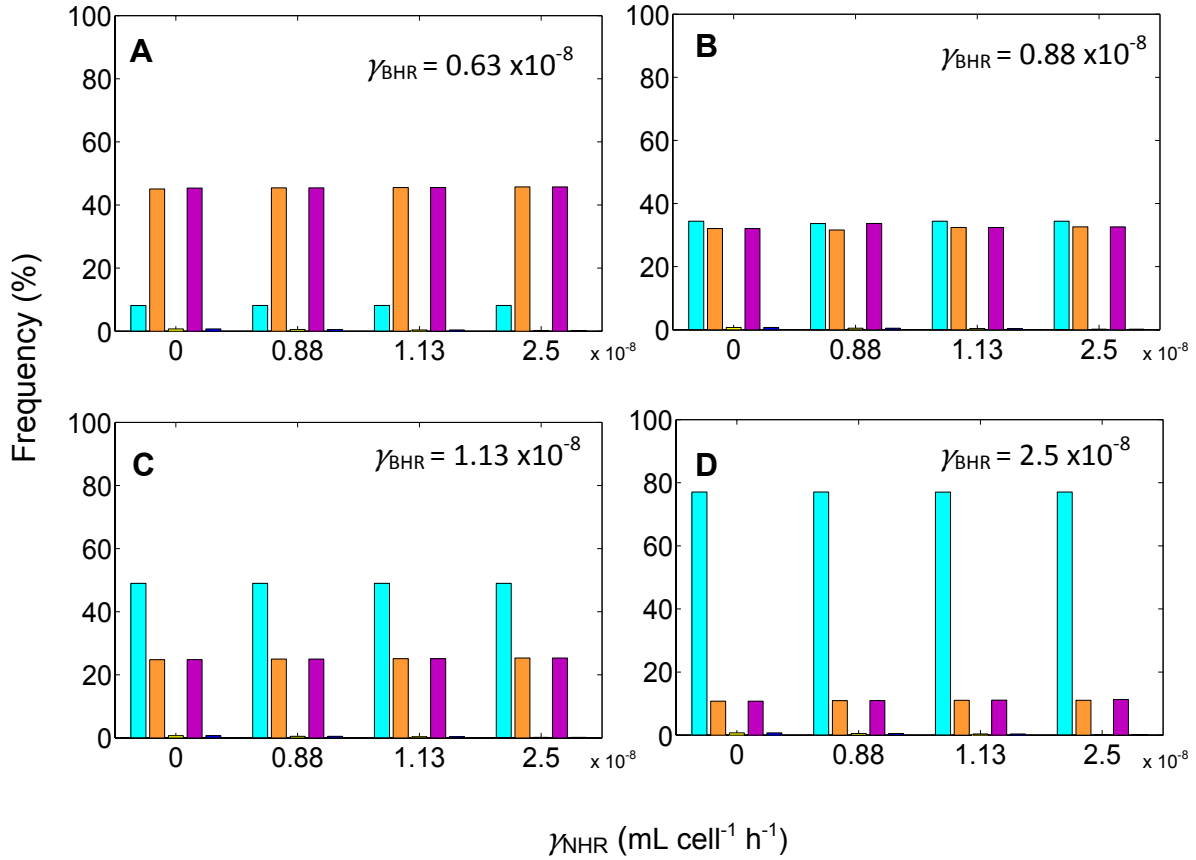


Figure 3.13: Effect of varying the transfer rate of NHR and BHR incompatible plasmids competing in a two-species assemblage, on their frequency in steady state (numerical results obtained after > 5 years simulated time). The X-axis represents the transfer rate of the NHR plasmid, while the transfer rate of the BHR plasmid is kept constant in each panel. Parameters are $\alpha_{\text{NHR}} = 6\%$, $\alpha_{\text{BHR}} = 12\%$ and $\tau_{\text{NHR}} = \tau_{\text{BHR}} = 10^{-4} \text{ h}^{-1}$. Legend: T_N^N (cyan), T_B^B (orange), T_N^B (yellow), R_B (magenta), R_N (blue).

3.2.4.4. Effect of loss rate

Figures 3.14 and 3.15 cover the evaluation of varying the loss rate on the ability of each plasmid to compete in a two-species assemblage. In Figure 3.14 the results for the scenario where the cost for both plasmids is zero and the transfer rate is fixed at $1.13 \times 10^{-8} \text{ mL cell}^{-1} \text{ h}^{-1}$ for both plasmids, are shown. Thus, the effects on their frequency can be attributed to the variation in the loss rates for the given set of parameters. The BHR plasmid frequency decreases with the rise in its loss rate. These observations can be explained by an increase in the availability of plasmid-free recipients of species *N* for higher loss rates of the BHR plasmid, which can then become re-infected by the NHR plasmid. The costless NHR plasmid only persists when its loss rate is strictly lower than the one of the BHR plasmid. As expected the frequencies of R_N and R_B hosts go up for higher loss rates of both plasmids, whilst the shortage in plasmid-free recipients for lower loss rates can be explained by the combined effect of low loss rates and the high transfer rate (considering that the cost is zero) assumed for this set of simulations.

Effect of loss rate: $\alpha_{\text{NHR}} = \alpha_{\text{BHR}} = 0\%$

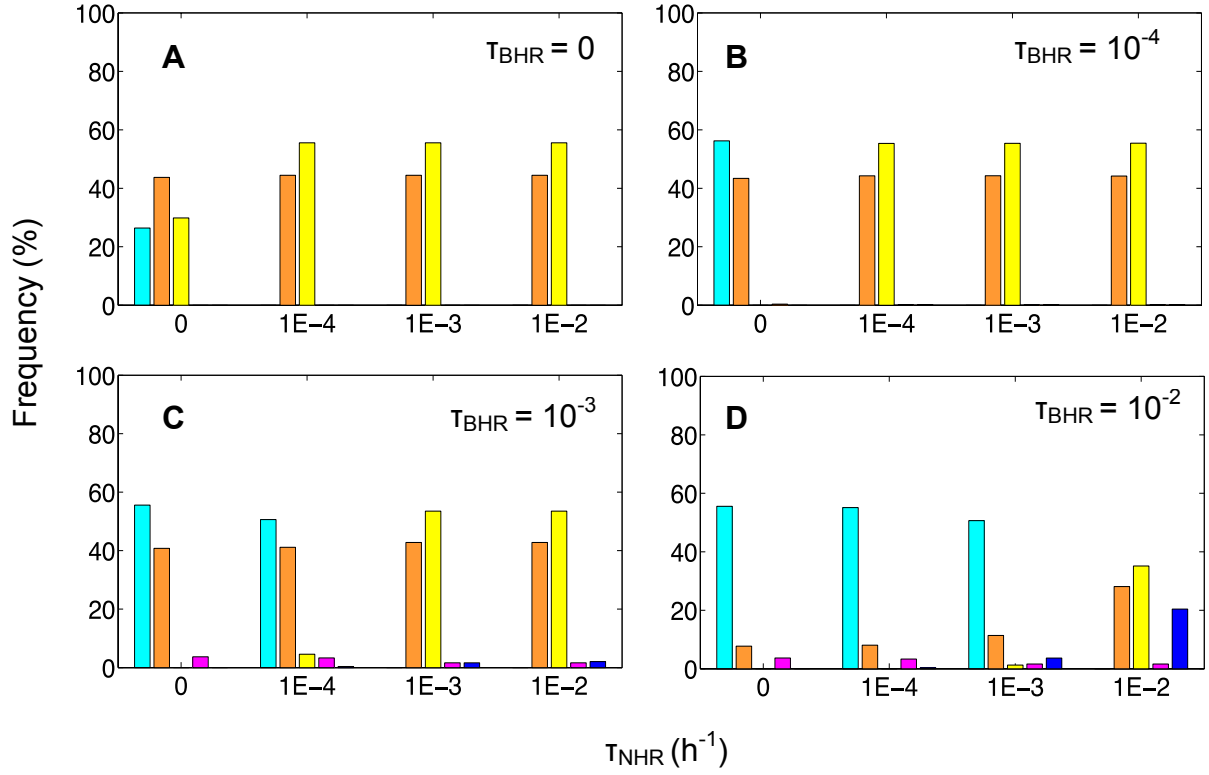


Figure 3.14: Effect of varying the loss rate of incompatible NHR and BHR plasmids competing in a two-species assemblage, on their frequency in steady state (numerical results obtained after > 300 days simulated time). The loss rate for the NHR plasmid is represented on the x-axis whereas the loss rate for the BHR was kept constant in each panel. Parameters are $\alpha_{\text{NHR}} = \alpha_{\text{BHR}} = 0\%$ and $\gamma_{\text{NHR}} = \gamma_{\text{BHR}} = 1.13 \times 10^{-8} \text{ mL cell}^{-1} \text{ h}^{-1}$. Legend: T_N^N T_B^B T_N^B R_B R_N

Given the difference in results obtained for a scenario where plasmids confer different fitness costs, the same analysis for the variation of loss rate was carried out as before, but now the NHR and BHR confer a burden in growth rate of 6% and 12%, respectively. The results in Figure 3.15 show that the qualitative outcomes are quite different from the previous scenario where costs were set to zero.

In this case, there is no strong dependence of the NHR plasmid on the loss rate of the BHR, unless it is very high, where the NHR plasmid becomes extinct even if its loss rate is zero. The high BHR loss rate combined with a higher cost of the BHR ensures that there will be a pool of plasmid-free recipients, which can be infected by the less costly NHR plasmid. Yet, for very high BHR loss rates, the costly NHR plasmid is outcompeted by the faster growing plasmid-free recipients of species B , R_B , which it cannot infect, thus being washed out from the assemblage, further highlighting the dependence of the NHR plasmid on the BHR plasmid. The resulting low frequency of T_N^B and R_N species in the assemblage at steady-state can be explained by the rapid infection of R_N hosts by the NHR plasmid at the beginning of plasmid invasion. In what regards the BHR, high loss rates do not change its frequency in the assemblage except when the NHR loss rate reaches 10^{-2} h^{-1} and the BHR plasmid bearing hosts (in particular T_N^B) can increase in frequency taking advantage of the plasmid-free hosts of species N , R_N .

Thus, for a given combination of costs and loss rates, a large pool of plasmid-free recipients can be maintained in the system, which can be exploited by one or the other plasmid to propagate in the two-species assemblage.

Effect of loss rate: $\alpha_{\text{NHR}} = 6\%$, $\alpha_{\text{BHR}} = 12\%$

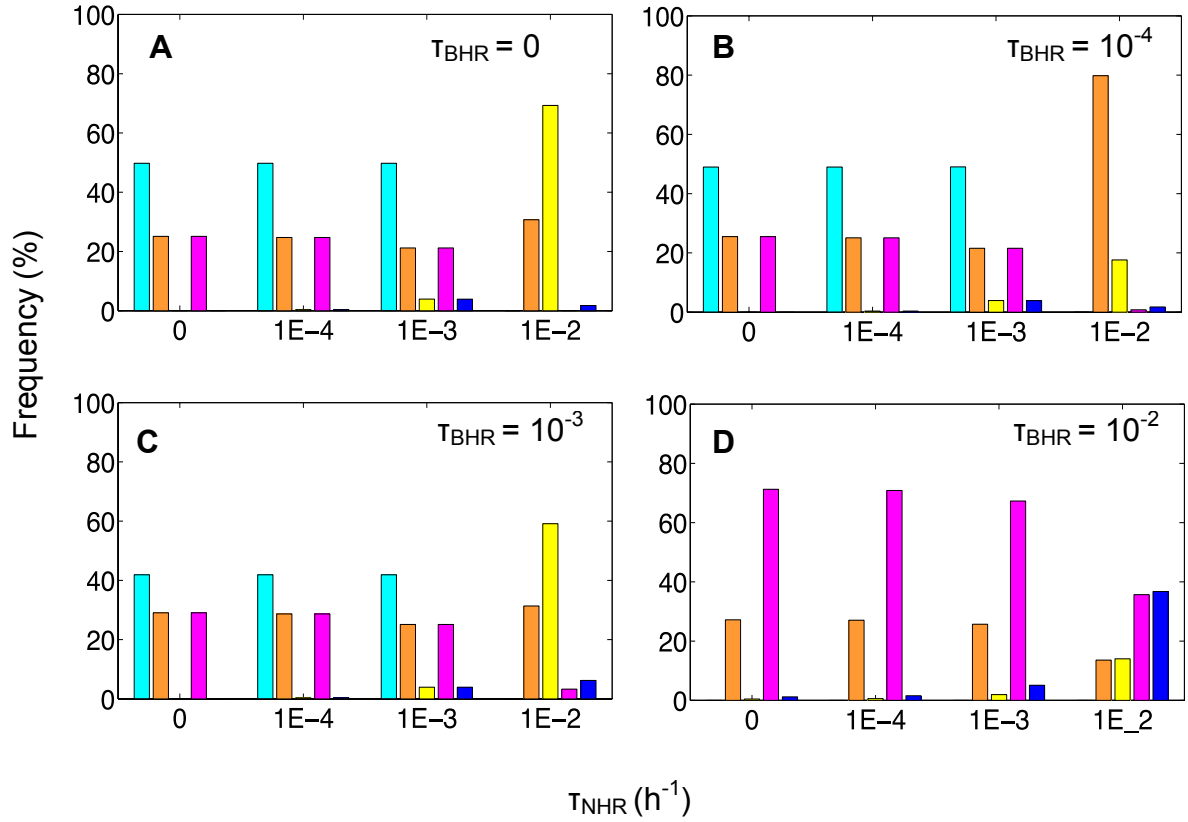


Figure 3.15: Effect of varying the loss rate of incompatible NHR and BHR plasmids competing in a two-species assemblage, on their frequency in steady state (numerical results obtained after > 300 days simulated time). The loss rate for the NHR plasmid is represented on the X-axis whereas the loss rate for the BHR was kept constant in each panel. Parameters are $\alpha_{\text{NHR}} = 6\%$, $\alpha_{\text{BHR}} = 12\%$ and $\gamma_{\text{NHR}} = \gamma_{\text{BHR}} = 1.13 \times 10^{-8} \text{ mL cell}^{-1} \text{ h}^{-1}$. Legend: T_{N}^{N} T_{B}^{B} T_{N}^{B} R_{B} R_{N}

The effect of fitness cost on the coexistence of NHR and BHR plasmids in a two-species assemblage is more complex than the effect of transfer rate, as illustrated in Figure 3.16.

For a given combination of costs, the frequency at steady state of each plasmid in the two-species assemblage will depend solely on the transfer rate of the BHR plasmid, since plasmid frequencies are the same for any transfer rate of the NHR plasmid (recall Figure 3.13). There is a positive relationship between the transfer rate of the BHR plasmid and the frequency of the NHR plasmid (Figure 3.16, panel A). Regarding the effect of fitness cost, for a given transfer rate, the outcome of the competition will depend on the ratio between α_{NHR} and α_{BHR} since different frequencies of each plasmid are obtained depending on the combination of costs of each plasmid (recall Figure 3.12). Nevertheless, Figure 3.16, panel B shows that there is an optimum combination of fitness costs that allows the NHR plasmid to be the most abundant plasmid in the two-species assemblage, if transfer rates for both plasmids are the same. Furthermore, it confirms that the NHR plasmid cannot survive for $\alpha_{\text{NHR}} \geq \alpha_{\text{BHR}}$.

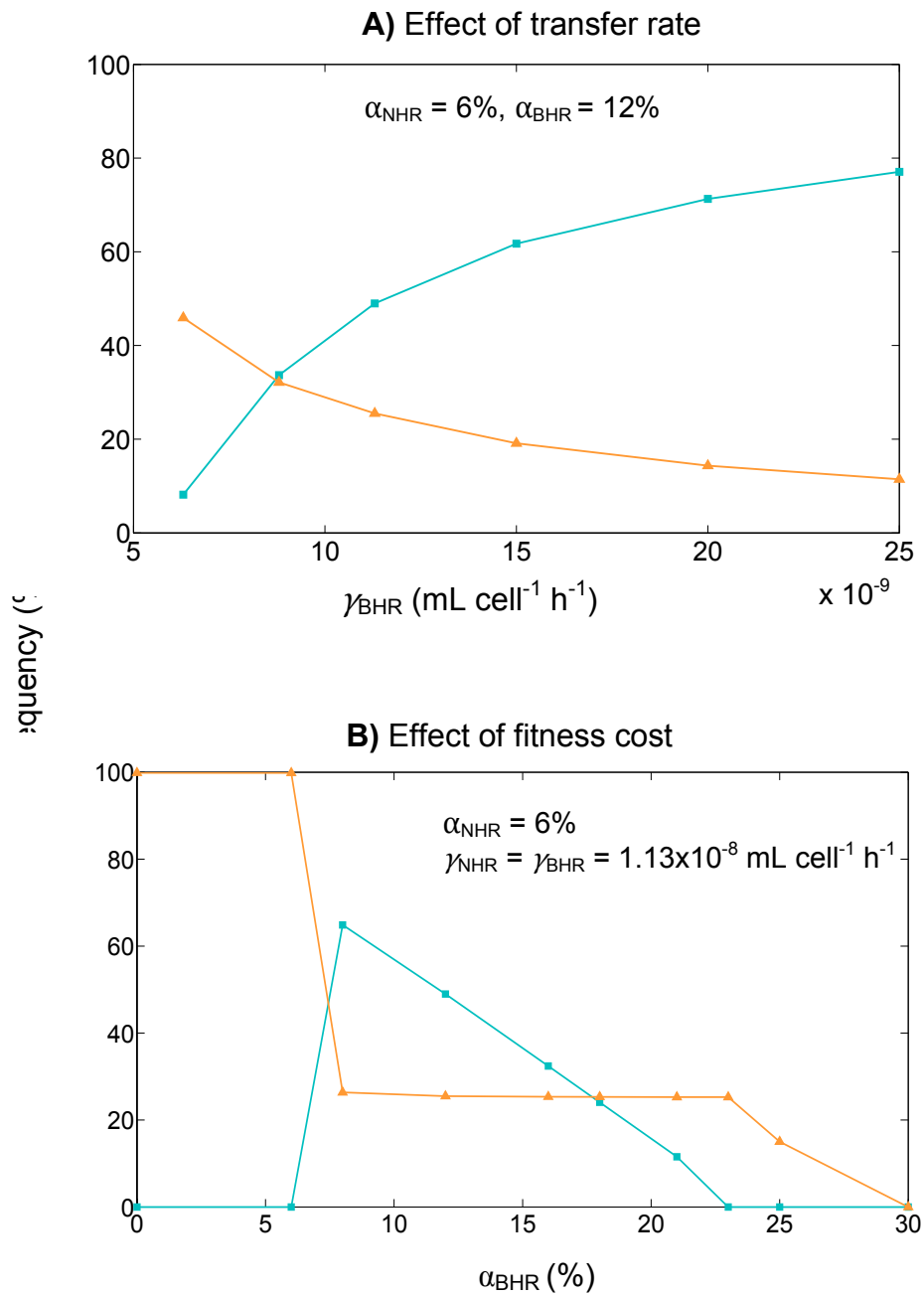


Figure 3.16 Effect of transfer rate of the BHR plasmid (panel A) and fitness cost of the BHR plasmid (panel B) on the frequency at steady-state of BHR and NHR plasmids in a two-species assemblage. Legend: T_N^N (cyan line) $T_{N,B}^B$ (orange line)

Summary for *Incompatible Plasmids*

- NHR can only survive in a two-species assemblage if it confers a smaller burden to the host than its direct competitor, a BHR incompatible plasmid;
- In a single species population, coexistence of two incompatible plasmids requires that plasmids follow opposite strategies: one with high transfer and high fitness costs, and the other with low transfer rate and lower fitness cost;
- In two-species assemblages, a broader host-range allows the costly BHR plasmid to outcompete the less costly and faster transferrable NHR plasmid;
- Coexistence in two-species assemblages requires that $\alpha_{\text{NHR}} < \alpha_{\text{BHR}}$ and a γ_{BHR} that is high enough, but regardless of the γ_{NHR} ;
- Fitness cost and high transfer rates generate damped oscillations in the various species in the system;
- The frequency of the NHR plasmid in the two-species assemblage increases for higher transfer rates of the BHR plasmid;
- The NHR plasmid can persist in the two-species assemblage as long as the pool of plasmid-free recipients R_B is not big enough to outcompete the costly NHR plasmid;
- When the NHR plasmid has a fitness cost advantage over the BHR plasmid, the range of parameters under which they can co-exist is larger

3.2.5. *The role of stochasticity*

In the lbM of the chemostat, the processes of plasmid transfer, plasmid loss and dilution are modeled by probabilities, and thus there is always a chance that the plasmid is not transferred or lost, or that a cell is not washed out. On average, after many simulations, if results from the lbM approach the ones obtained with the deterministic model, the stochasticity does not give rise to different dynamics as in the case of e.g. positive feedbacks that amplify deviations. This is indeed what we observe for the simplest scenario of one plasmid transferring in a single species population, where most of the lbM runs follow the qualitative trend of the ODE model (higher transfer rates lead to higher frequencies of the plasmid in the population). However, in the more complex system of two plasmids with different host-ranges spreading in two-species assemblages we often find differences in the competition outcome between the stochastic and the deterministic model.

For example, for the scenario of two compatible plasmids in a two-species assemblage, using the ODE model, a parameter combination that allowed the NHR plasmid to survive was never found (Figure 3.5), except when its cost is 0. In contrast, in the lbM of the chemostat some simulations showed that both plasmids could co-exist temporarily even when the NHR confers a cost to its host, but this was only observed for low transfer rate values (i.e., low compared to the value required for each individual plasmid to survive alone in a single species population). This is exemplified in Figure 3.17 where time-courses results of one replicate from the lbM model are plotted for four different combinations of transfer rates for both plasmids, while keeping constant their loss rate and fitness cost. Notice how the two plasmids

with different fitness costs can co-exist over a period of 200 days, with transfer rates close to their minimum survival rate (panel B and C).

An increase in BHR transfer rate, results in an oscillatory behaviour of the different species in the system, which can maintain both plasmids for at least 200 days. Yet, when the transfer rate of the NHR plasmid is higher than the BHR transfer rate, the NHR plasmid, which is mostly found in $T_N^{B,N}$ hosts, cannot compete with the faster growing BHR single plasmid-bearing hosts. Because costs of both plasmids add up $T_N^{B,N}$ hosts will grow slower and since the NHR cannot infect hosts of species B , it will be washed out of the two-species assemblage. The higher the transfer rates, the higher the chances of finding both plasmids in the same host and thus the higher the frequency of the less fit $T_N^{B,N}$ hosts.

In the incompatible scenario the qualitative results of the IbM and the ODE model agreed well. This is illustrated in Figure 3.18 where time-courses results obtained with the IbM and the ODE models for three different transfer rates of the BHR plasmid are plotted. An increase in the transfer rate of the BHR plasmid promotes the survival of the NHR plasmid. Furthermore, notice how high transfer rates of the BHR plasmid increase the amplitude of oscillations and over the time, allow the NHR plasmid to obtain a higher frequency.

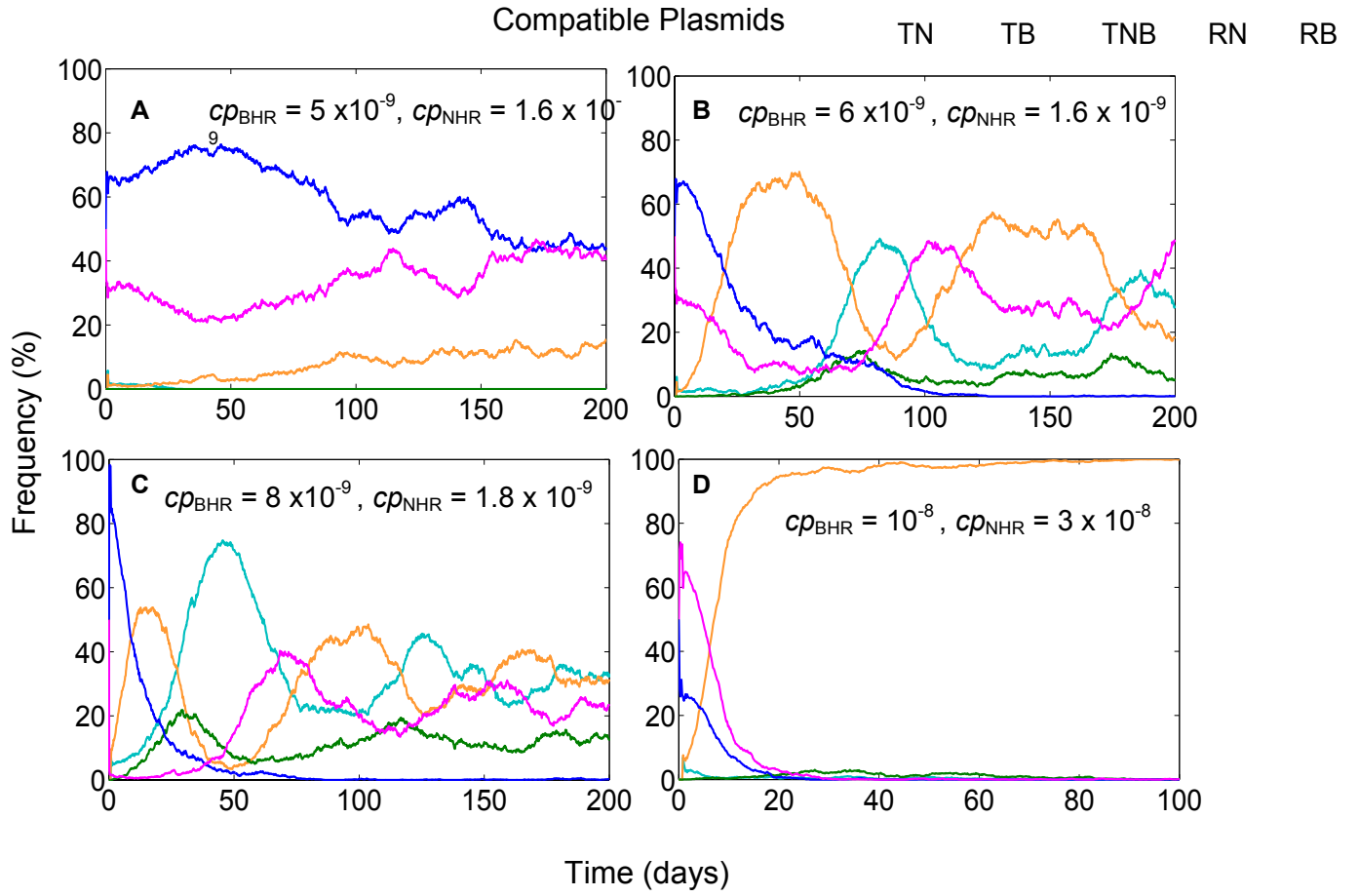


Figure 3.17 Effect of varying the transfer of NHR and BHR compatible plasmids on their transfer dynamics in a two-species assemblage. Results obtained with the lbM: one replicate for each set of parameters is shown. Parameters are $\alpha_{NHR} = 6\%$, $\alpha_{BHR} = 21\%$ and $\tau_{NHR} = \tau_{BHR} = 10^{-4} \text{ h}^{-1}$. Legend: R_N (blue), R_B (magenta), T_N^N (cyan), $T_{N,B}^B$ (orange), $T_N^{B,N}$ (green)

Nevertheless, interesting differences between the two models were found. In Figure 3.19 four different replicates obtained with the lbM model for the same set of parameters are plotted. Because in the individual-based chemostat model each individual cell has the same chance of being washed out, bottlenecks are observed, where a population consisting of only few cells can lead to extinction of either one (see Figure 3.19 R2 and R3) or both plasmids (see Figure 3.19 R4). This type of event is more frequent for higher amplitudes in the oscillations of plasmid-bearing species, which in turn are more common for higher transfer rates of both plasmids. This is particularly the case for replicate 2 and 4 (see Figure 3.19 R2 and R4), where the BHR-bearing hosts reach very low numbers and eventually the last cell carrying a BHR plasmid is washed out and thus re-invasion of the two-species assemblage by the BHR plasmid fails. Similarly, what prevents survival of the NHR plasmid after the BHR is washed out is the abundance of plasmid-free hosts of species *B* (see Figure 3.19 R2 and R4), which grow faster than the T_N^N hosts and cannot be infected by the NHR plasmid. In contrast, if the NHR plasmid is not able to invade the two-species assemblage the BHR takes over the population of plasmid-free hosts benefitting from its broader host-range (see Figure 3.19 R3).

Incompatible Plasmids

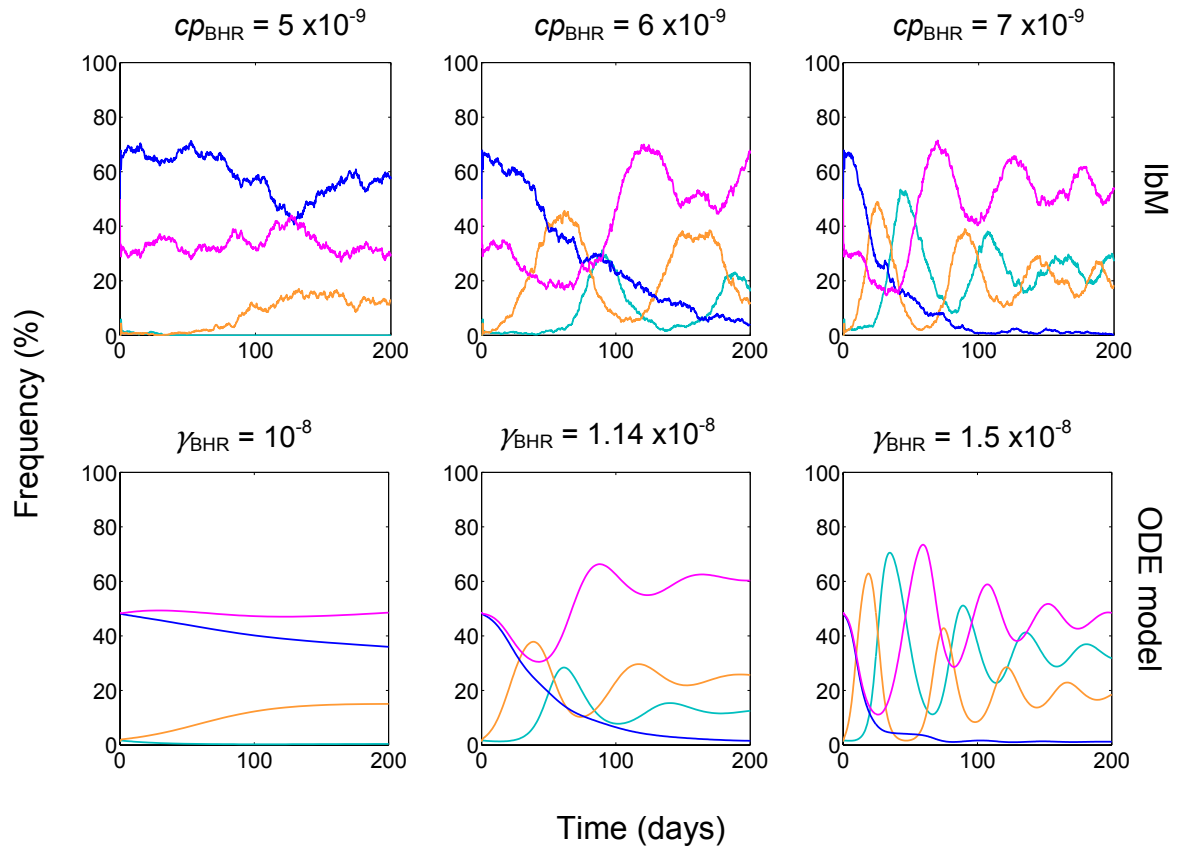


Figure 3.18 Effect of different transfer rates for the BHR plasmid on the dynamics of two incompatible plasmids invading a two-species assemblage. Parameters: $\alpha_{NHR} = 6\%$, $\alpha_{BHR} = 21\%$ and $\tau_{NHR} = \tau_{BHR} = 10^{-4} \text{ h}^{-1}$. IbM: $cp_{NHR} = 1.6 \times 10^{-9} \text{ mL cell}^{-1} \text{ h}^{-1}$, ODE model: $\gamma_{NHR} = 3.75 \times 10^{-9} \text{ mL cell}^{-1} \text{ h}^{-1}$. Legend: — R_N — R_B — T_N^N — $T_{N,B}^B$

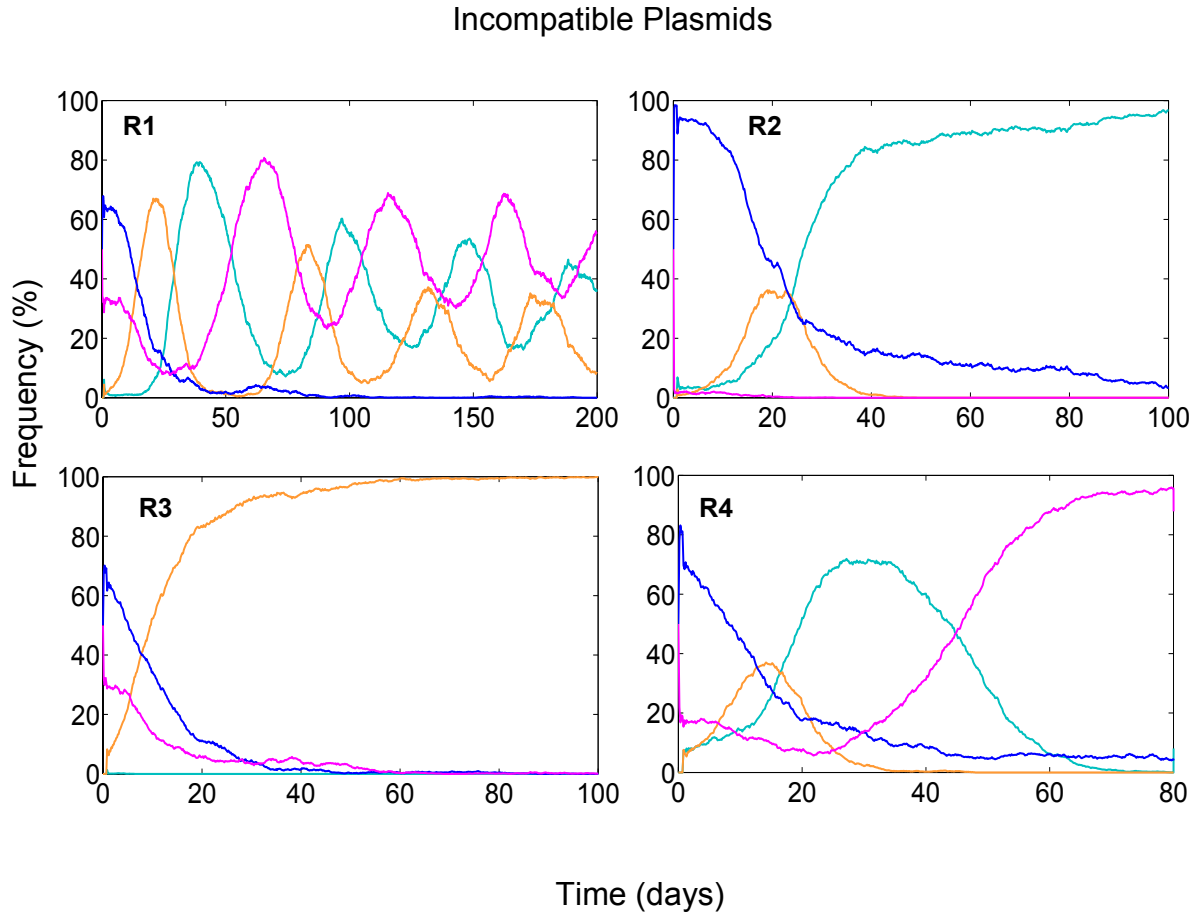


Figure 3.19 Effect of stochasticity on the dynamics of two incompatible plasmids invading a two-species assemblage. Each plot represents a different replicate obtained with the lbM model for the following set of parameters: $\alpha_{NHR} = 6\%$, $\alpha_{BHR} = 21\%$, $\gamma_{NHR} = 1.8 \times 10^{-9}$, $\gamma_{BHR} = 8 \times 10^{-9} \text{ mL cell}^{-1} \text{ h}^{-1}$ and $\tau_{NHR} = \tau_{BHR} = 10^{-4} \text{ h}^{-1}$.

Legend: — R_N — R_B — T_N^N — $T_{N,B}^B$

Overall, stochastic events generate a variety of experimental outcomes that are not observed with a deterministic approach. The results obtained with the IbM model challenge the conclusions drawn from the ODE model; they have shown that a costly NHR plasmid can survive in a two-species assemblage in the presence of a costly BHR plasmid for some time, depending on the total number of cells in the system, growth and plasmid parameters, and dilution rate. In the incompatible case, the four different outcomes obtained with the same set of parameters suggest that the high amplitude oscillations generated by high transfer rates, can be hazardous for the local persistence of both plasmids in a single habitat.

3.3. Discussion

The first theoretical approach to studying the population biology of plasmids was put forward by Bruce Levin and his co-workers in 1979. Despite the complexity of the conjugational process, the authors were able to establish a simple mass-action model that could be used to estimate an intrinsic rate constant describing the dynamics of plasmid transfer in bacterial populations. In the present work, the simplest scenario of one plasmid transferring in one-species population is revisited to point out some undervalued features. A plasmid with a higher transfer rate takes less time to achieve steady state, which would increase its chances of successfully invading and persisting in a population of hosts. This feature is more important for a plasmid to survive in the more realistic stochastic IbM than in the deterministic model, where the initial frequency of plasmid-bearing cells is irrelevant for the final frequency in the population. On the other hand, plasmids with a smaller cost require a lesser increase of their transfer rate to quickly invade and achieve higher frequencies in a population.

In 1984, van der Hoeven carried out the mathematical modeling of incompatible conjugative plasmids transferring in a single bacterial population in chemostats. In her work she concluded that two plasmids were able to co-exist if they follow different survival strategies, one with high transfer rate and a high fitness cost, and the other with a low transfer rate and low costs for the host. Here, her model is revisited and extended in order to accommodate two plasmids with different host-ranges and to investigate under which conditions coexistence is possible. In Figure 3.10, in the single species scenario, the two incompatible plasmids can now coexist by following different survival strategies, one with a higher transfer rate and

high fitness cost (BHR) and the other with a lower transfer rate and a smaller cost (NHR), as predicted by van der Hoeven in 1984.

The conditions under which two conjugative plasmids with different host-ranges can co-exist in a two-species assemblage in the absence of any positive selection favouring their carriage were investigated. It was found that there is a range of plasmid-related parameters under which coexistence is expected. In fact, a costly NHR plasmid, which cannot survive alone in a two-species assemblage, could do so in the presence of an incompatible BHR. Depending on the relationship between the two plasmids, compatible or incompatible, plasmid-related parameters had a different impact on the competitiveness of each plasmid. The biggest difference was due to fitness cost. For compatible plasmids, a costly NHR plasmid was not able to compete against a BHR plasmid. Yet, evidence from the stochastic model shows that it is possible for a costly NHR plasmid to invade and maintain itself in the assemblage at low transfer rates for some time depending on a number of other parameters, total assemblage size and chance. In contrast, for the incompatible case coexistence was possible if the NHR plasmid had a fitness cost advantage over the BHR plasmid and if transfer rate of the BHR plasmid was sufficiently high.

Regarding the transfer rate, the compatible plasmids could coexist under a wide range of transfer rate values as long as the NHR plasmid did not confer a burden. Under these conditions, the NHR plasmid was mostly found in dual-plasmid bearing hosts, $T_N^{B,N}$, while survival of the BHR plasmid in the two-species assemblage only required sufficient transfer activity offsetting the combined factors of loss by segregation and reduction in growth rate. Conditions favoring coexistence of

compatible plasmids in the same host could, in theory, explain the emergence of recombined plasmids carrying multiple replicons, such as those found in plasmids from the IncF and IncHI incompatibility groups (Thomas, 2000). For incompatible plasmids, there is a dependency of the NHR plasmid on the BHR plasmid transfer rate: higher transfer rates of the BHR plasmid enhance the propagation of the NHR plasmid in the two-species assemblage, while having the opposite effect on the BHR plasmid itself. Even more interestingly, the costly NHR is able to maintain itself in the two-species assemblage even if its transfer rate is zero, as long as a costlier BHR competitor is present. Furthermore, a region of coexistence where the transfer rates of both plasmids are lower than their respective minimum transfer rate necessary for their survival in a single species population was identified (see Figure 3.13). This finding challenges the conclusions drawn by Bergstrom and co-workers (2000) in their work on the existence conditions for bacterial plasmids. Specifically, these authors assumed throughout their analysis that plasmids transfer at a rate too low to overcome the joint effects of segregation and selection, and thus plasmids would not be able to persist in the long-term in bacterial populations even if they carry genes that are beneficial to their hosts because these would ultimately be incorporated into the host's chromosome. In contrast, a parameter combination was found where two costly incompatible plasmids transferring at a rate that would otherwise not be enough to overcome the effects of segregational loss and fitness burden (in single species populations), were able to maintain themselves in steady state (see Figure 3.13 A, where $\gamma_{\text{BHR}} = 0.63 \times 10^{-8}$ and $\gamma_{\text{NHR}} = 0 \text{ mL cell}^{-1} \text{ h}^{-1}$).

The loss rate does not seem to have a strong effect on the equilibrium between the two plasmids when these are incompatible, except for very high loss

rates of the BHR plasmid where the NHR plasmid is outcompeted by the faster growing plasmid-free recipients of species *B*. In the compatible scenario an increase in the loss rate of each of the individual plasmids has the expected effect: a reduction in their individual frequency in the two-species assemblage. As a consequence, a combined increase in BHR and NHR loss rates promotes the appearance of more single-plasmid bearing hosts, such as T_N^N and T_N^B or T_B^B . A phenomenon that could also contribute to an increase in single plasmid-bearing hosts is the reciprocal and non-reciprocal fertility inhibition observed among compatible plasmids (Olsen and Shipley, 1975). Fertility inhibition is an interaction among compatible plasmids whereby the transfer frequency of one or both plasmids is diminished. Unilateral transfer inhibition between plasmids was first observed in *E. coli* where F plasmid transfer was inhibited by various types of f_i^+ R plasmids (Watanabe et al., 1964). Subsequently these types of interactions were reported among plasmids belonging to the P, N, W or X incompatibility groups (Pinney and Smith, 1974; Olsen and Shipley, 1975) in *E. coli* strains. Inhibition, but also facilitation of transfer among co-existing plasmids from clinical isolates of *P. aeruginosa* has also been reported (Sagai et al., 1977). Thus, fertility inhibition seems to be a widespread characteristic that could help compatible plasmids gain an unwanted advantage in direct competition for plasmid-free hosts. Moreover, a decrease in dual plasmid-bearing species, would prevent the NHR plasmid from being trapped in the least fit plasmid-bearing $T_N^{B,N}$ hosts and being washed out from the two-species assemblage.

The results obtained with the stochastic model highlight the importance of random events for fate of competing plasmids in complex two-species assemblages. More specifically, the prospect of a costly NHR being able to invade and persist for

long periods of time in two-species assemblages in the presence of a BHR plasmid should be investigated further with *in vitro* and *in situ* experiments. The observation that high transfer rates combined with high fitness costs generate oscillations in the frequency of plasmid-bearing species in the incompatible scenario that can lead to the extinction of one or both plasmids, suggests that under these circumstances plasmids may experience a selective pressure to reduce their transfer rates which avoid oscillations and therefore could make survival in natural bacterial communities more likely. Experimental verification of model observations would be valuable to determine if under similar experimental conditions, different qualitative results would be obtained regarding the fate of each plasmid simply due to drift. Also, one should question if the conclusions drawn from steady states of mathematical models that can take several years to be reached, are biologically relevant in making long-term predictions about the persistence of plasmids in bacterial populations. Given the examples from evolution experiments where plasmid fitness costs are ameliorated (Dahlberg and Chao, 2003; Dionisio et al., 2005), horizontal transfer rates can increase or decrease (Turner et al., 1998) and shifts in the host-range of plasmids can take place (De Gelder et al., 2008; Sota et al., 2010), it is clear that plasmid-related parameters will not remain constant in the long-term. Moreover, since most of the modeling research has not been based on experimentally measured values, only qualitative results should be taken into consideration until further experimental evidence is available. Nevertheless, parameter exploration allowed to test under which conditions a plasmid would be favoured over the other, or which plasmid-related parameter would be expected to be optimized over evolutionary time in order for the plasmid to successfully invade and persist in two-species assemblages. In

the compatible case, over time the NHR plasmid would be expected to minimize its burden down to zero as well as its transfer rate in order to compete with a BHR plasmid. In turn, a compatible BHR plasmid with high enough transfer rate to overcome its fitness cost and rate of segregational loss, is expected to be selected. In fact, generally BHR plasmids belonging to IncP, IncN and IncW groups have their pilus synthesis derepressed suggesting higher transfer rates than their counterpart NHR plasmids from IncI, IncK or IncH groups for which pilus synthesis is repressed resulting in much lower transfer rates (Levin et al., 1979; Bradley, 1980). For incompatible plasmids, coexistence requires a lower fitness cost for the NHR plasmid. From an evolutionary perspective, the results obtained for the compatible and incompatible scenario suggest that a BHR plasmid benefits from interspecific competition. In two-species assemblages carrying compatible plasmids, the BHR plasmid would be able to outcompete its direct NHR competitors due to its broader host-range. If a lineage of the BHR plasmids would evolve towards specialization, hence becoming a NHR plasmid, both still incompatible plasmids, the one evolved to be a NHR plasmid and the ancestor BHR plasmid, would be able to co-exist under a wide range of conditions. This way, incompatibility among plasmids, in particular due to entry exclusion systems, would facilitate the evolution of new incompatibility groups, while compatibility would stimulate recombination events between genetic modules carried by different plasmids co-existing in the same cell. Incompatibility is particularly advantageous for the NHR plasmid since it benefits from an increase in the transfer rate of the BHR plasmid without having to increase its own transfer rate, which could lead to increased fitness costs.

Much attention has been given to finding conditions that allow the persistence of parasitic plasmids in single species populations. Although these studies have facilitated the development of simple mass-action models with which the dynamics of plasmid-bearing and plasmid-free bacteria in *in vitro* and *in situ* systems (Levin et al., 1979; Freter et al., 1982; Lundquist and Levin, 1986) can be understood in the light of a few plasmid-related parameters such as transfer rate, fitness cost and loss rate, their results cannot be generalized to the persistence of parasitic plasmids in two-species assemblages. As demonstrated by the present work, compatibility relationships between plasmids and differences in their host-range can lead to unexpected results that could not be anticipated by a simple one plasmid one species model.

In summary, it was determined that plasmids with different host-ranges can coexist in two-species assemblages under a variety of parameter combinations in the absence of any form of direct selection, with the BHR plasmid being more successful for the majority of the scenarios tested despite its higher fitness cost. Coexistence for compatible plasmids is not possible unless the NHR plasmid confers a zero fitness cost (which in reality is not possible). The NHR plasmid can only survive in if competing with an incompatible BHR plasmid, so incompatibility is an advantage for the NHR plasmid.

Chapter 4

Modeling plasmid dynamics in a biofilm

MODELING PLASMID DYNAMICS IN A BIOFILM

4.1. Introduction

Although most of what has been learned about bacterial physiology and microbial kinetics has been derived from studies of pure and planktonic bacterial populations, in most ecosystems microorganisms can be found predominantly in biofilm communities (Characklis and Marshall, 1990). A biofilm is a film made up of living material, i.e., microorganisms attaching and growing on surfaces such as solid substratum in contact with moisture, soft tissue surfaces in living organisms and at liquid-air interfaces. A mature biofilm is a complex aggregation of microorganisms embedded in an adhesive matrix synthesized by the microbes, which may be composed of exopolysaccharide, proteins and DNA (Wanner et al., 2006).

The spatial organization of a biofilm community provides plentiful opportunities for local cell-to-cell interactions, such as those involved in conjugational transfer of plasmids. A recent report on the gene transfer between *Bacillus subtilis* cells showed how the conjugative DNA rapidly spread through bacterial cell chains in a series of sequential conjugation events (Babic et al., 2011). Also, conjugal plasmid transfer has been shown to induce bacterial biofilm development by expressing factors that induce planktonic bacteria to form or enter biofilm communities and facilitating the spread of biofilm determinants (Ghigo, 2001; Ong et al., 2009). The widespread occurrence of microbial biofilms in hospital environment associated with chronic and acute infections combined with the role of conjugative genetic elements in spreading antibiotic resistance in bacterial communities, represents an imminent

threat to human and animal health. Thus, a better understanding of the factors regulating plasmid invasion and persistence in biofilms is of utmost importance.

Research on plasmid spread in microbial populations has been preferentially carried out in liquid cultures in either chemostats or batch cultures for the past decades. The current knowledge about plasmid spread in surface-associated communities is still limited, although it has been recognized that the dynamics of transfer on surfaces can be very different from that in suspended cultures (Simonsen, 1990; Angles et al., 1993; Licht et al., 1999; Sorensen et al., 2005). In particular, the dependency of plasmid transfer efficiency on the initial donor to recipient ratio (Simonsen, 1990) and the dependency of final transconjugant densities on initial densities of donors and recipients (Pinedo and Smets, 2005) has been observed for transfer on surfaces but not in unstructured liquid environments.

Modeling of conjugal plasmid transfer in mixed environments was started in the 1970's by Levin and his co-workers (Stewart and Levin, 1977; Levin et al., 1979). Their approach consisted of mass-action models that successfully described the dynamics of transfer in chemostat reactors using few parameters describing the rates of transfer and loss of the plasmid (Levin et al., 1979; Knudsen et al., 1988; Clewlow et al., 1990; Simonsen et al., 1990; Smets et al., 1994). To gain insight about transfer dynamics in surface-attached communities, Lagido et al. (2003) modeled bacterial colonies of either recipients or donors growing exponentially until nutrient exhaustion but incorporating the principle that when donor and recipient colonies meet the recipient colony (or presumably the bacteria on the outer edges of the colony) instantly becomes transconjugants. The authors tested the predictions of the model using strains of *P. fluorescens* transferring the RK2 plasmid on filter mating

systems and found that accounting for time of conjugative transfer considerably improved the model predictions. Massoudieh et al. (2007) also included the physiological lag periods observed between rounds of conjugation (Andrup et al., 1998) and found better experimental fit of the model to experiments. Both of these studies considered entire bacterial colonies as the players involved in plasmid transfer without explicitly modeling the behaviour of individual cells. Krone et al. (2007) further developed a stochastic cellular automaton lattice model where individual bacteria are modeled although they are constrained to lie in a lattice and can only divide if there is space in the neighbourhood. Nevertheless, they could reproduce macroscopic patterns of transfer observed in colonies growing on agar plates and their work has also contributed to understanding the dependence of IncP-1 plasmid propagation on spatial structure and nutrient availability (Fox et al., 2008). Individual-based models (IbM) follow a bottom-up approach in which the collective behaviour of a population emerges from the diversity of individual cells. They were first applied to the study of microbes by Kreft et al. (1998) in order to incorporate a physiological characterization of individual cells and have since been used to study biofilm properties for wastewater treatment (Picioreanu et al., 2005; Xavier et al., 2007) and to study various microbial interactions (Kreft et al., 1998; Kreft and Wimpenny, 2001; Kreft, 2004; Xavier and Foster, 2007; Nadell et al., 2008).

More recently an individual-based framework for simulating biofilm growth and individual-based modeling of chemostat environments has been introduced, the iDynoMiCS software (Lardon et al., 2011). This IbM has also been used to explicitly model conjugation in bacterial assemblages with individual bacteria represented by spherical particles located in a continuous space (Merkey et al., 2011). In their work

the authors investigated whether limited plasmid invasion of a biofilm could be explained by a dependence of conjugation on the growth rate of the donor cells and found this to be the case. They also conducted a sensitivity analysis of various factors on the transfer dynamics of a plasmid and found that timing (such as lag times, transfer proficiency and scan speed) and spatial reach (EPS yield, pilus length) parameters are more important for successful plasmid invasion than the recipient's growth rate or the probability of a plasmid being lost upon cell division.

In the present work, the iDynoMiCS framework has been developed further to include more than one type of plasmid transferring in biofilm communities, and additional plasmid features, such as host-range and compatibility relationships between the plasmids, have been introduced. The main goal of this work is to explore the effect of plasmid burden and transfer proficiency on the outcome of competition between two plasmids with different host-ranges (a NHR and a BHR) in two-species spatially structured assemblages, such as biofilms. To this end, two biofilm structures differing in the degree of patchiness, determined by the spatial organization of two microbial species, are used to investigate the role of community structure on the competitiveness of each plasmid. The relationship between the two plasmids, compatible or incompatible, is also considered when analysing their fate in microbial biofilms. The hypothesis being tested is that BHR plasmids are more competitive than NHR plasmids in spatially structured bacterial assemblages, such as biofilms. Albeit, relatively simple, the model reveals that initial localization of donors can control plasmid invasion patterns and that plasmid burden does not affect plasmid survival in mature biofilms.

4.2. Results

Throughout the following sections, we evaluate the effect of fitness cost, transfer probability and host-range parameters on the competitiveness of two plasmids, with different host-ranges, competing for bacterial hosts in two-species biofilms. Although the computational model has the capability to carry out three-dimensional simulations (3D), the results presented here are the outcome of two-dimensional (2D) simulations of biofilm growth due to computational simplicity and because the two dimensions parallel to the surface are equivalent in the absence of strong gradients of flow and shear. In such cases, biofilm growth in 2D or 3D has been shown to be equivalent, see for example Picioreanu et al. (2004).

For the biofilm simulations we took the experimentally measured fitness costs conferred by two plasmids with different host-ranges, the narrow host-range R1 ($\alpha = 6\%$) and the broad host-range RK2 ($\alpha = 21\%$) plasmids (Dahlberg and Chao, 2003), as the starting point as the default values. The fitness cost was varied from 0% to 50% decrease in maximum specific growth rate, while the transfer probability (p) was varied between 1 and 10^{-3} . The probability of losing the plasmid upon cell division was set at 10^{-4} for all the simulations, since segregational loss had been previously identified as one of the least important parameters affecting plasmid spread (Merkey et al., 2011). Each individual parameter was varied while keeping all the others constant. The results come from invasion experiments in which one plasmid-bearing cell was initially located at the bottom of a mature biofilm composed of roughly 9000 agents distributed in the computational domain of size $264\ \mu\text{m}$ length by $54\ \mu\text{m}$ height. All the simulations were carried out for at least 100 days.

Frequencies of the different species in the two-species assemblage represent the average of 3 replicate simulations. The coefficient of variation was always very small ($< 5\%$) and was thus omitted from results presentation for simplicity. The abbreviations T_N^N , $T_{N,B}^B$, $T_N^{B,N}$, R_N , R_B , stand for NHR-bearing hosts, BHR-bearing hosts, NHR and BHR-bearing hosts, plasmid-free recipients of species N and plasmid-free recipients of species B , respectively.

4.2.1. *Biofilm structures*

In order to study the effect of spatial organization of two bacterial species growing as a biofilm on the competition between plasmids with different host-ranges, two biofilm structures were generated: a mixed biofilm and a patchy biofilm. As described in section 2.2.1 of Chapter Two, these biofilm structures do not contain any extracellular polymeric substance (EPS) and thus the bacterial agents take up all the available space in the simulated domain. Glucose was the solute chosen due to the available kinetic information on this substrate and is the sole carbon and energy source limiting bacterial growth. The mixed biofilm structure was obtained by randomly positioning 4500 agents of each species within the computational domain during initialization. The patchy biofilm was obtained by random initial placement of 50 agents of each species throughout the length of the computational domain and left to grow into a mature biofilm. In Figure 4.1 the solute concentration gradient is depicted for both biofilm structures after both biofilms have been growing for 8 days. The gradients are similar in both structures; except that the naturally grown, patchy biofilm has a

more irregular surface giving rise to a less regular solute concentration gradient that follows the contour of the biofilm surface. This gradient extends from the boundary layer (the interface between the bulk liquid and the biofilm compartment) to the biofilm domain and through which the solute can diffuse into or out of the biofilm. As the solute concentration is higher at the top of the biofilm, bacterial growth rate is higher in the outer layers of the biofilm, which results in cell divisions leading to protruding bacterial cells that are removed by erosion keeping the biofilm thickness close to 54 μm at steady state. In the inner layers of the biofilm, cell division becomes a rare event due to the low solute concentrations and thus slower growth. Note, that growth kinetics are identical for both species (N and B).

Figures 4.2 and 4.3 show how plasmid dynamics proceeds in the two different two-species biofilm structures: mixed and patchy. Initially, two plasmid-bearing cells are located at the bottom of the biofilm in separate positions, each carrying a different plasmid. The parameters controlling the number of recipients screened per hour ($v_s = 5$) and the pilus length (2 μm) allow the plasmid bearing-cell to attempt to transfer the plasmid to 5 neighbours in a 2 μm radius every hour. Given that on average a growing cell has a 0.6 μm radius, the plasmid-bearing agent can reach a cell that is not a direct neighbour, approximately reaching cells in the layer around the layer of direct neighbours. This assumes that cells can be reached despite obstacles due to some flexibility of the pilus and lateral diffusion of the pilus along the cell surface combined with variation in pilus length. In the scenarios represented in Figures 4.2 and 4.3 both plasmids transfer at their maximum probability, 1, and do not confer any cost to the host carrying them. As the wave of transfer proceeds, we observe that the spatial organization of the different species in

the biofilm does not affect the BHR plasmid dissemination, as it can infect both species equally well. In contrast, the NHR plasmid spread undergoes a bottleneck as it has to overcome a barrier of recipients of species *B* in the patchy biofilm (see Figure 4.3, $t = 4h$). When the waves of the two spreading compatible plasmids meet, the waves continue spreading with the constraint that the NHR plasmid can only infect recipients of species *N*. Hence, both plasmids can be found together in the same host (represented by the green spheres), but only in species *N*.

In the following sections the effect of varying the transfer probability and the fitness cost of each plasmid on their ability to invade and compete with another plasmid in the two different biofilm structures is analysed.

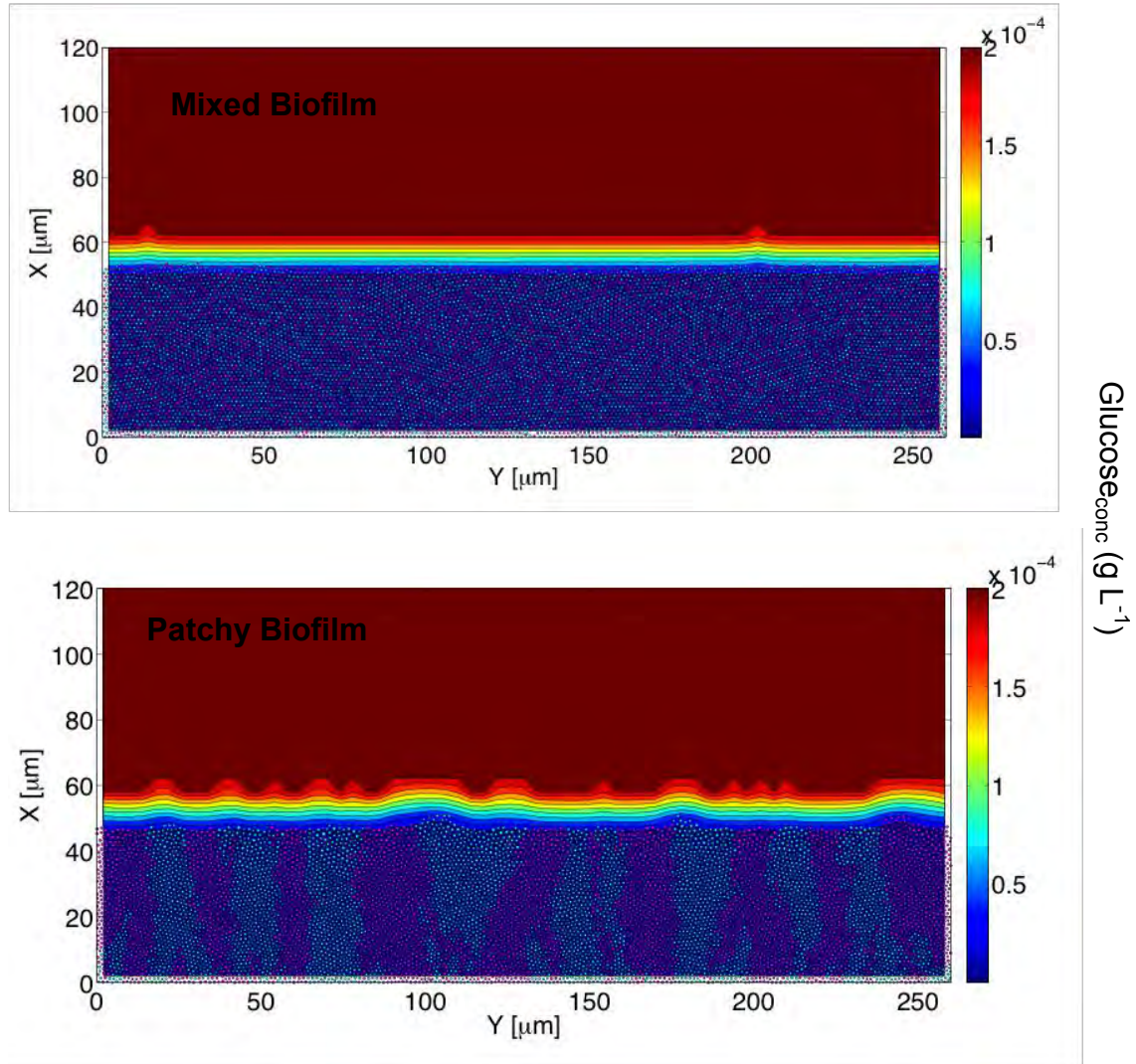


Figure 4.1: 2D representation of biofilm thickness (X) and solute concentration gradient (g L⁻¹) over the length of the biofilm (Y) at steady state after 8 days of growth. Legend: R_B R_N

Transfer in a mixed biofilm

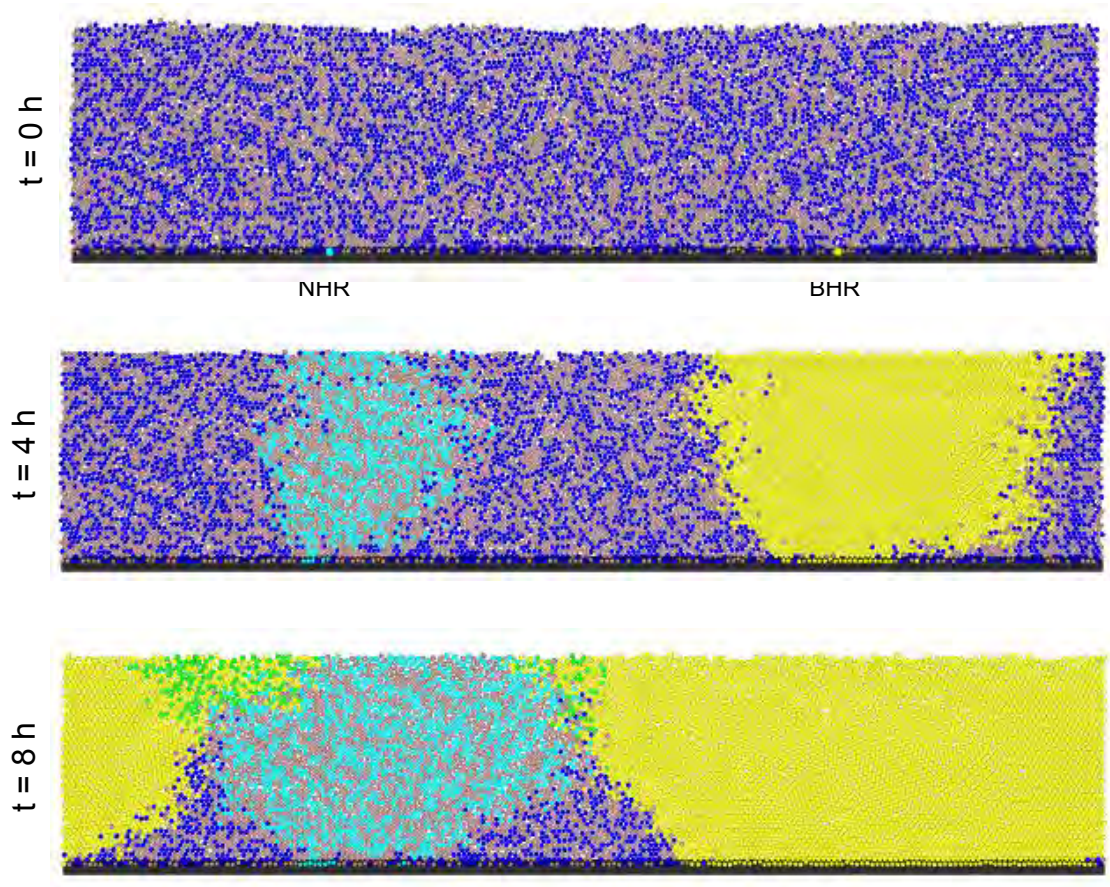


Figure 4.2: Dynamics of transfer of a NHR plasmid and a BHR plasmid in a two-species mixed biofilm illustrated for different time-points. Parameters are $p_{\text{NHR}} = p_{\text{BHR}} = 1$, $\alpha_{\text{NHR}} = \alpha_{\text{BHR}} = 0\%$.

Legend: R_B R_N T_N^N $T_{N,B}^B$ $T_N^{B,N}$

Transfer in a patchy biofilm

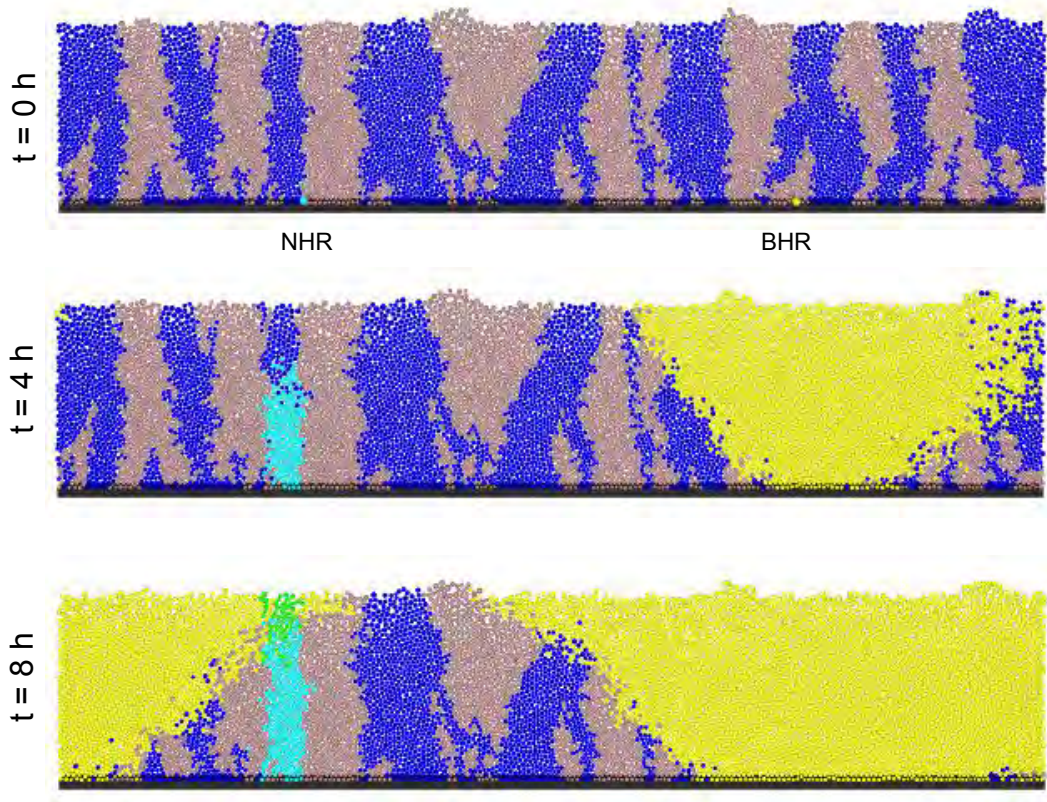


Figure 4.3: Dynamics of transfer of a NHR plasmid and a BHR plasmid in a two-species patchy biofilm illustrated for different time-points. Parameters are $p_{\text{NHR}} = p_{\text{BHR}} = 1$, $\alpha_{\text{NHR}} = \alpha_{\text{BHR}} = 0\%$. Legend: R_B R_N T_N^N $T_{N,B}^B$ $T_N^{B,N}$

4.2.2. *Transfer of a NHR in a two-species assemblage*

In this scenario, a NHR plasmid-bearing cell was introduced at the bottom of the mature biofilm and the transfer of the plasmid was monitored for 100 days. In Figure 4.4 the effect of decreasing the transfer probability on the rate of spread of the NHR plasmid in the mixed biofilm and in the patchy biofilm is compared. In both biofilm structures, the spread of the NHR into suitable recipients of species *N* becomes slower for lower values of the transfer probability. A noticeable difference between the dynamics of spread of the plasmid in the two biofilm structures is the incomplete invasion of hosts of species *N* in the patchy biofilm compared with the complete invasion in the mixed biofilm. Another feature in the transfer dynamics in the patchy biofilm is stepwise progression. By looking at how the transfer of the NHR plasmid progresses in the patchy biofilm as illustrated in Figure 4.5, it becomes clear that the steps in the graph correspond to bottlenecks in free recipients of species *N* due to an adjacent section of biofilm being composed mostly of recipients of species *B*. The existence of large clusters of cells from an unsuitable species can obstruct the spreading of a NHR plasmid, which becomes trapped between clusters of recipients it cannot infect. Thus, delaying the dissemination of the plasmid and decreasing its total frequency in the two-species assemblage to half of the frequency observed for the mixed biofilm.

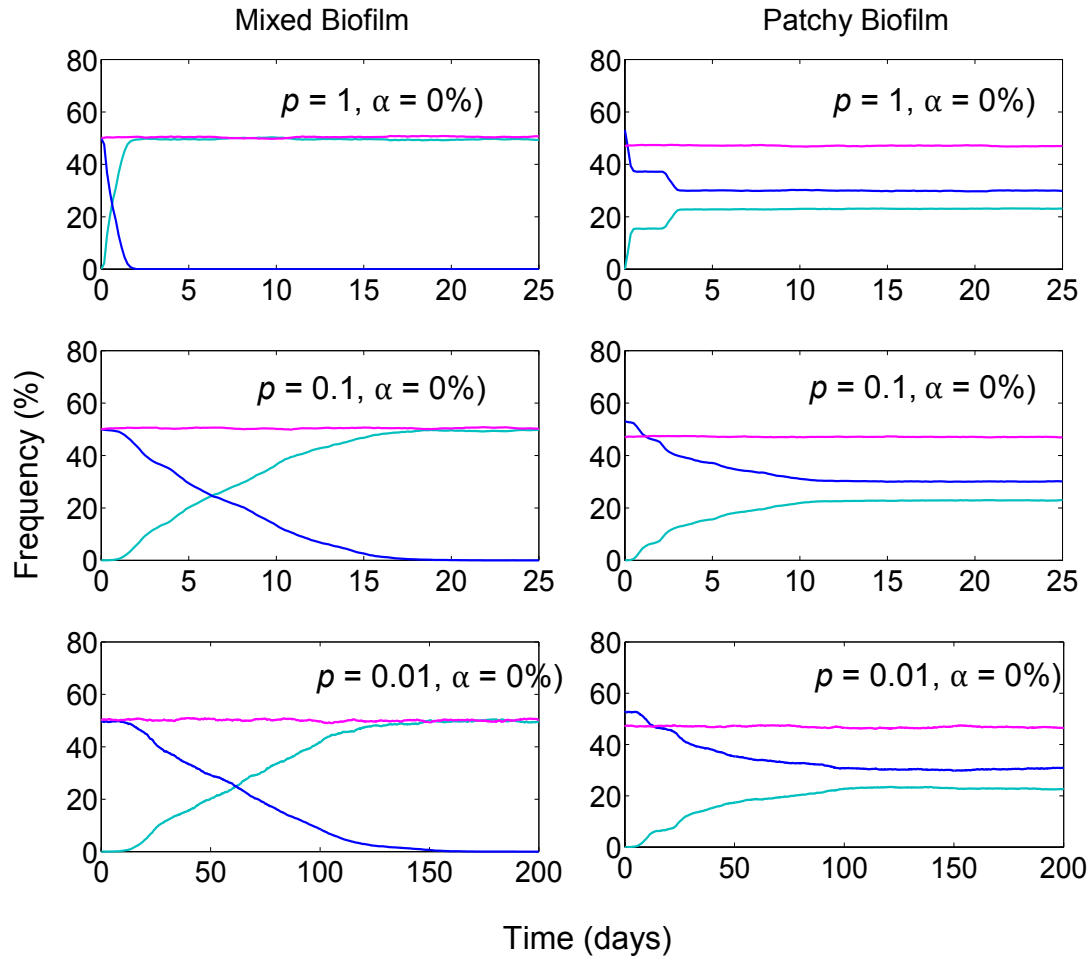


Figure 4.4: Effect of varying the transfer probability on the dynamics of plasmid invasion of a NHR plasmid in a two-species biofilm for the different biofilm structures.

Legend: R_N R_B T_N^N

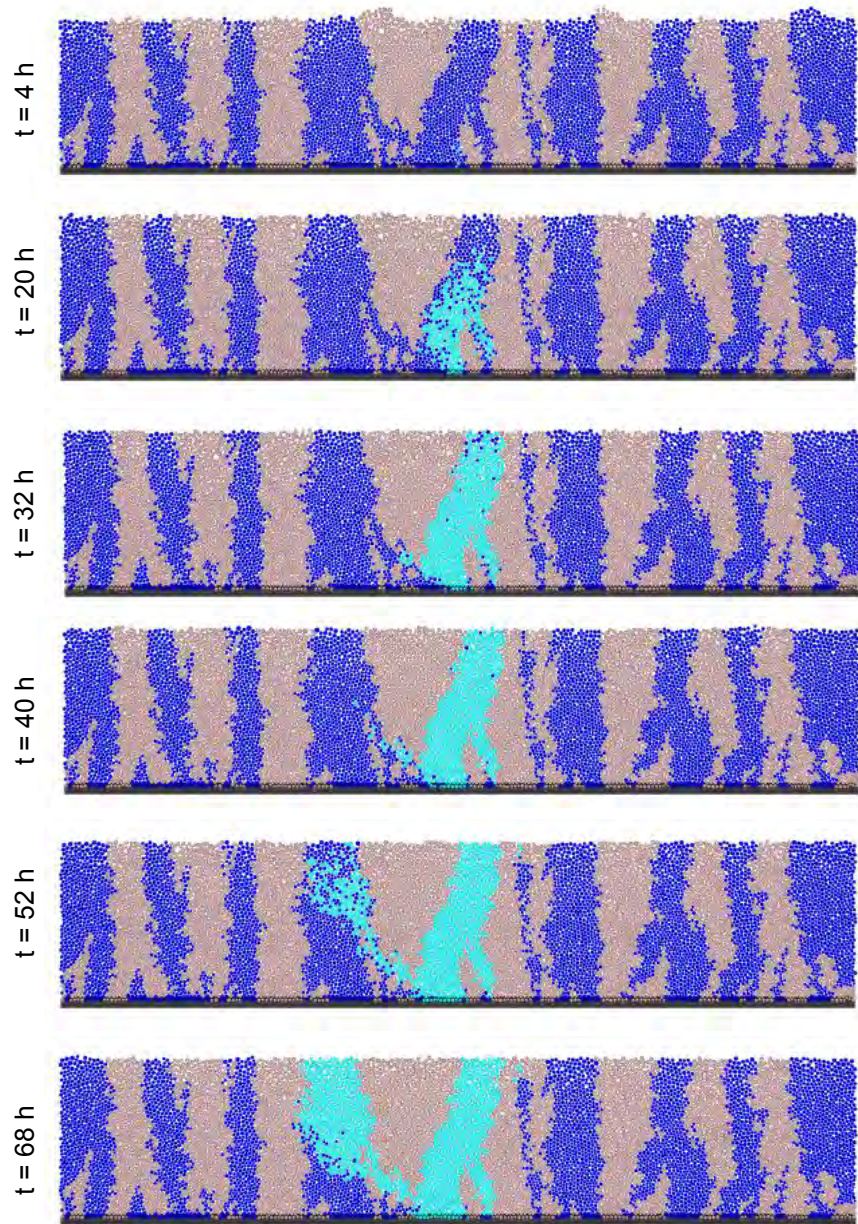


Figure 4.5: Dynamics of transfer of a NHR plasmid in a two-species patchy biofilm illustrated for different time-points. Parameters are $p = 1$, $\alpha = 0\%$. Legend: $\bullet R_B$

$\bullet R_N$ $\bullet T_N^N$

In Table 4.1 the frequency of the NHR plasmid in the total assemblage for different fitness costs and transfer probabilities in the two biofilm structures, is presented. An increase in the fitness cost does not seem to have a large impact on the total frequency of the NHR plasmid, although the trend is a reduction in the number of hosts carrying the plasmid. Reducing the transfer probability will decrease the frequency of the plasmid in the two-species assemblage after 100 days, but this seems to be more pronounced in the patchy biofilm (for $p = 0.001$) than in the mixed structure when compared to the values obtained for the control scenario. Since the spreading of the NHR plasmid is naturally hampered by the patchy structure of the biofilm, decreasing the transfer probability in this scenario has little effect on the total amount of NHR carrying hosts because the scope of suitable recipients available for infection is limited by the clustered-type structure.

Table 4.1: Effect of varying the transfer probability (p) or the fitness cost (α) on the frequency of the NHR plasmid transferring in two-species biofilms after 100 days. The results are the average of three replicates.

Parameter	Mixed	Patchy
Control ($p = 1, \alpha = 0\%$)	49.8 %	23.2 %
Scenario A: $p = 1$		
$\alpha = 0.06$	48.7 %	22.3 %
$\alpha = 0.21$	45.8 %	20.8 %
$\alpha = 0.50$	40.7 %	19.0 %
Scenario B: $\alpha = 0\%$		
$p = 0.1$	49.6 %	23.1 %
$p = 0.01$	38.2 %	22.8 %
$p = 0.001$	37.2%	2.0%

4.2.3. *Compatible plasmids*

In this section two compatible plasmids, NHR and BHR, transfer and compete for bacterial hosts in two species biofilms. The analysis is divided in four parts; the first three address the effect of a different competitiveness factor in mixed biofilms and in the last one the effect of patchiness on the outcome of biofilm invasion by both plasmids is investigated.

4.2.3.1. Effect of host-range

In order to assess the effect of a broader host-range on the ability of a plasmid to compete with another plasmid in biofilm structures the transfer dynamics of two competing plasmids in a single species and two-species mixed biofilms were compared. Figure 4.6 shows the effect of decreasing the transfer probability of the BHR plasmid when competing with a highly transferrable NHR plasmid ($p_{\text{NHR}} = 1$), whilst keeping the fitness costs of both plasmids zero. In the single species biofilm, the decrease in BHR transfer probability allows a peak in NHR-bearing hosts, but ultimately the BHR plasmid spreads throughout the population converting it into a double plasmid-carrying population of hosts. In the two-species mixed and patchy biofilm the broader host-range allows the BHR plasmid to successfully invade the whole assemblage and thus become the most abundant plasmid in the two-species assemblage. Notice that decreasing the transfer probability by 10 fold or 100 fold increases the time needed for the BHR to completely invade the two-species assemblage in both scenarios by about 10 fold or 100 fold, respectively, but not its

final frequency in the two-species assemblage. The main difference between the mixed and patchy biofilm is the way transfer dynamics proceeds, which will be further investigated in section 4.2.3.3.

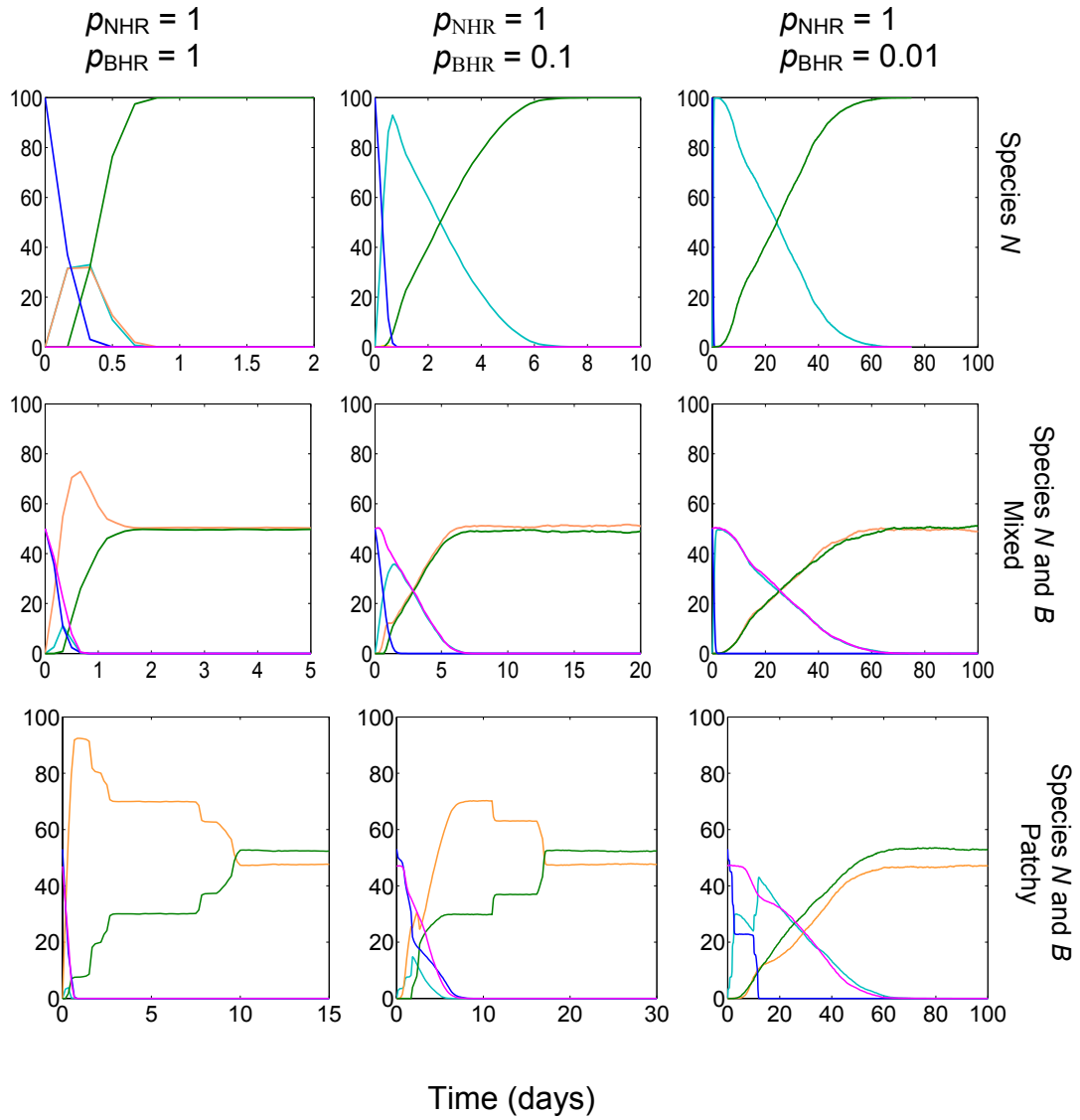


Figure 4.6: Effect of host-range for decreasing values of the transfer probability for the BHR plasmid on the dynamics of two compatible plasmids invasion in single and two-species mixed and patchy biofilms. The costs were zero for both plasmids.

Legend: R_N R_B T_N^N $T_{N,B}^B$ $T_N^{B,N}$

4.2.3.2. Effect of fitness cost and transfer probability in mixed biofilms

In order to evaluate the impact of an increased burden on plasmid-bearing hosts on the competitiveness of the plasmid, the fitness cost of each plasmid was varied, while keeping the cost of its competitor zero. The total frequency of each plasmid after 100 days of simulation is depicted in Figure 4.7. The BHR plasmid is not affected by high fitness costs and is able to successfully invade and persist for at least 100 days in the mixed biofilm, while the NHR frequency in the two-species assemblage declines only a few percent as its fitness cost is increased (first row, first panel). Figure 4.8 shows an example of a time series of the frequencies for a fitness cost of 50% for one replicate. Notice how the frequency of the NHR plasmid is high in the beginning of biofilm invasion boosted by the high transfer probability, but the number of NHR-bearing hosts tends to decline with time due to the growth disadvantage and the shortage in plasmid-free recipients of species *N*.

The transfer probability was varied from 1 to 10^{-3} for each plasmid, while keeping the fitness cost of both plasmids null and the corresponding transfer probability for the competitor plasmid at its maximum, 1. Figure 4.7 summarizes the impact of reducing the transfer rate on the ability of each plasmid to invade and persist in a two-species mixed biofilm for 100 days. The NHR plasmid starts to undergo a decline in its frequency for values of the transfer probability of 10^{-2} and becomes very rare when its transfer proficiency is further reduced to 10^{-3} (first row, second column). A similar trend is observed for the BHR plasmid, which drops in frequency from 100% to less than 10% following a 10-fold reduction in its transfer probability. In Figure 4.9 the transfer dynamics of one replicate for each scenario is

depicted. When the transfer proficiency is reduced, both plasmids face the same challenge: to counteract the growth of free recipients by horizontally transferring into them. Because invasion takes place in a mature biofilm where bacterial growth in the inner layers is reduced due to solute gradients, transfer proceeds at a slower pace but it will eventually lead to a full plasmid invasion. Due to its broader host-range, this process is faster for the BHR plasmid, which after an initial delay rapidly takes over the population of free hosts. The nonexistence of a species barrier for the BHR plasmid means that every neighbour is a potential recipient, and as the wave of transfer propagates through the biofilm it generates a positive feedback turning infection into an exponential process.

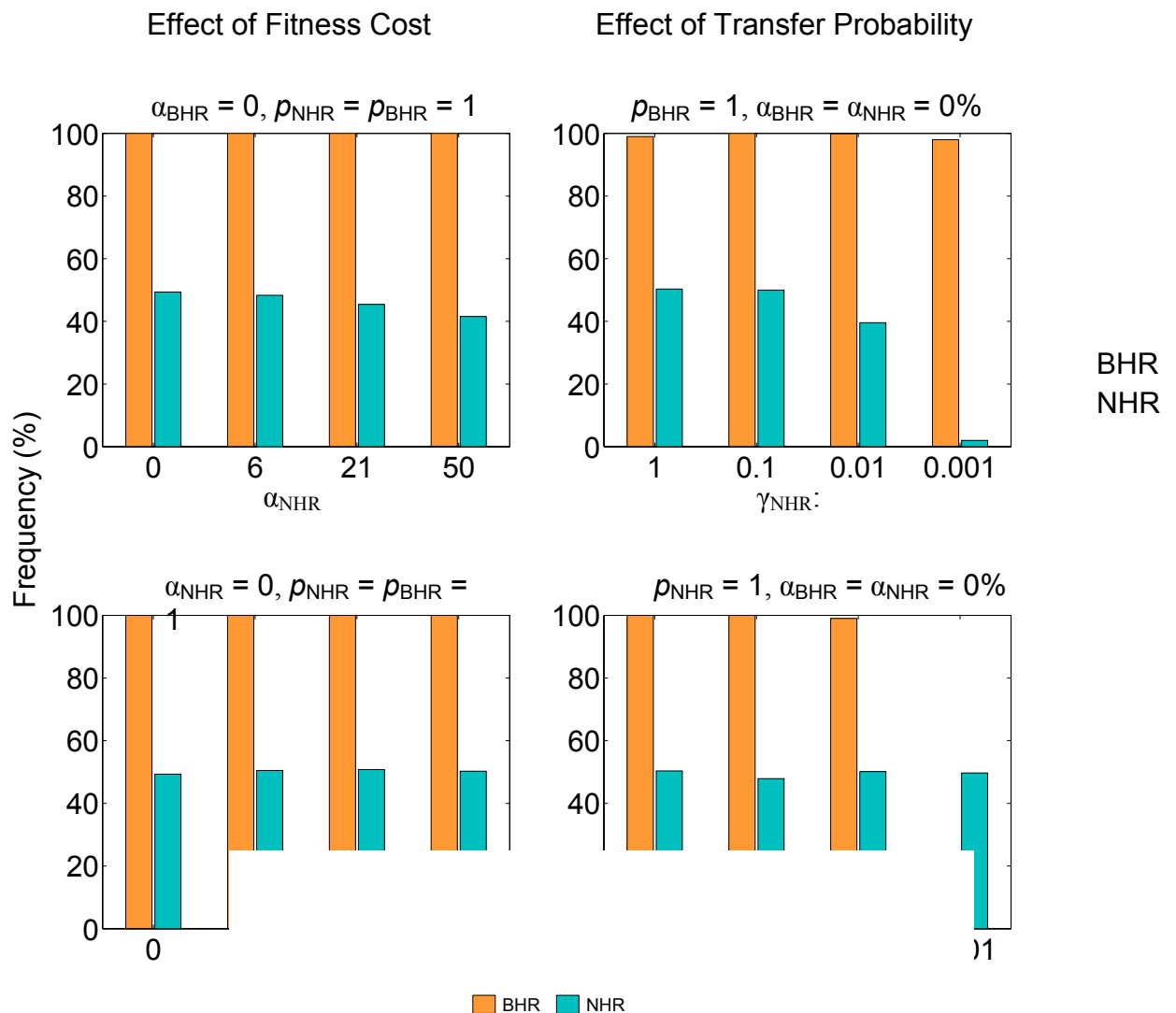


Figure 4.7: Effect of fitness cost and transfer probability on the frequency of compatible BHR and NHR plasmids in a population of one competitor and one film for 100 days. In each panel, the fitness cost of one plasmid is varied, while the fitness cost of the other plasmid is fixed as indicated. Each bar represents the mean of three replicates for which the standard deviation was < 5% (not shown).

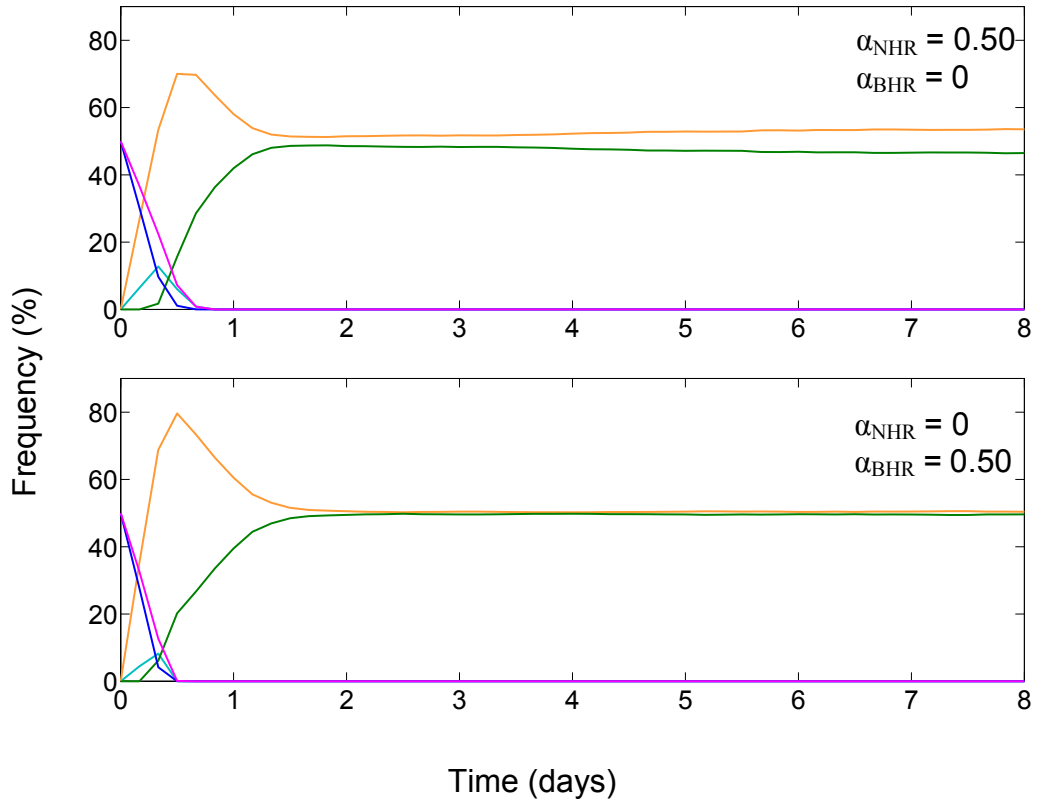


Figure 4.8: Effect of an increased fitness cost on the frequency of plasmids with different host-ranges when competing with each other. A typical replicate simulation of the dynamics of transfer of two compatible plasmids in a two-species mixed biofilm. Legend: — R_N — R_B — T_N^N — $T_{N,B}^B$ — $T_N^{B,N}$

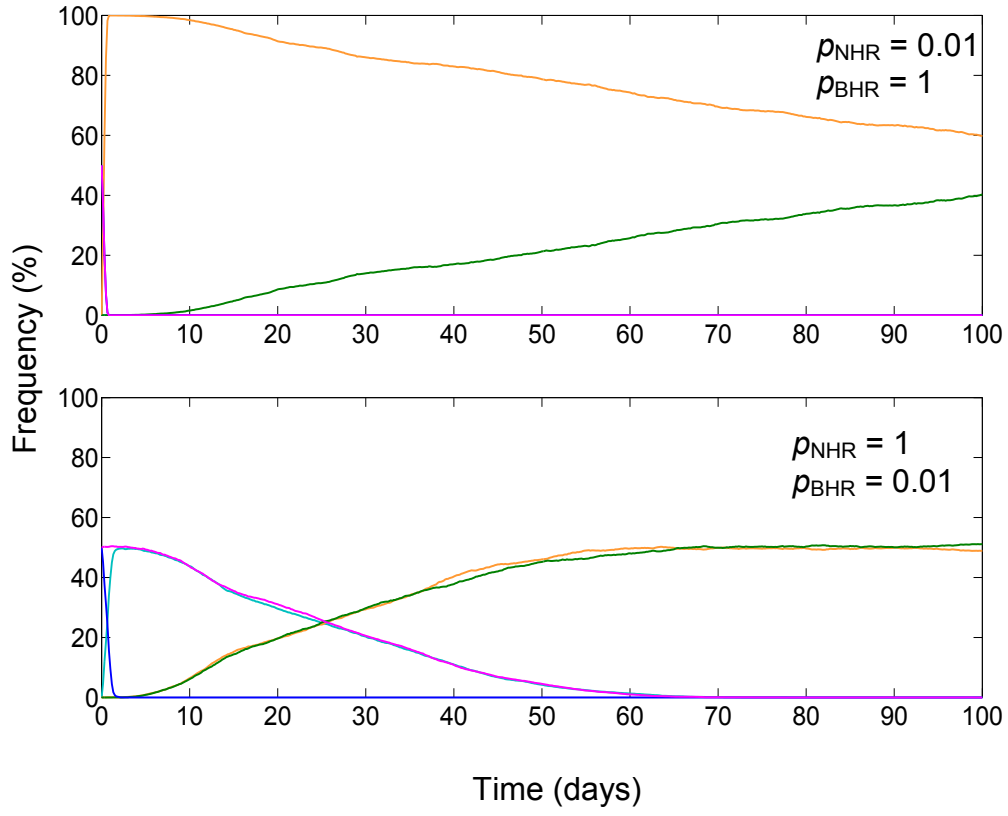


Figure 4.9: Effect of decreasing the transfer probability on the frequency of plasmids with different host-ranges when competing with each other. A typical replicate simulation of the dynamics of transfer of two compatible plasmids in a two-species mixed biofilm. The fitness cost for both plasmids was zero. Legend: — R_N — R_B

— T_N^N — $T_{N,B}^B$ — $T_N^{B,N}$

4.2.3.3. Effect of patchiness

Assessment of the effect of biofilm patchiness on the competitiveness of plasmids with different host-ranges was performed by taking experimentally determined fitness costs of a NHR plasmid ($\alpha_{\text{NHR}} = 6\%$) and a BHR plasmid ($\alpha_{\text{BHR}} = 21\%$) as the default case (Dahlberg and Chao, 2003). Subsequently, either the fitness cost of the competing plasmid was varied between 0% and 50% or its transfer probability was decreased from 1 to 10^{-3} . The total frequency of each plasmid in the biofilm assemblage was calculated by averaging 3 replicates and results can be found in Figure 4.11. An example of the time dynamics is shown in Figure 4.10.

When the fitness costs were varied including various combinations of costs for either NHR or BHR plasmid, the frequencies of the plasmids did not differ from those already presented in Figure 4.7, between the mixed and the patchy biofilm. This is understandable because for the BHR plasmid there are no species obstacles to its propagation as it can transfer in both species *N* and *B*. The frequency of the NHR plasmid after 100 days is similar and a slow decrease in its frequency over time is a common trend in both biofilm structures (Figure 4.10). However, a closer look into the transfer dynamics plotted in Figure 4.10 reveals the differences in horizontal dissemination experienced by the NHR plasmid. After a rapid invasion of the mixed biofilm by the BHR plasmid, the NHR plasmid slowly starts to invade the two-species assemblage by infecting hosts of species *N*, which mostly carry BHR plasmids already. In the patchy biofilm, this process occurs in steps due to the presence of clusters of non-suitable recipients for the NHR to infect, making the invasion by the NHR slower and more dependent on rare opportunities to cross into another patch of

suitable hosts than in the mixed biofilm. Yet, after 6 days an increase in $T_N^{B,N}$ species is observed, indicating that the NHR plasmid is successfully spreading through the previously inaccessible sections of recipients from species N . Recall that during invasion of the patchy biofilm by a single NHR plasmid (see Figure 4.4) the initial donor cell was located in the middle at the bottom of the biofilm, and we observed that the total frequency of the plasmid even after 200 days remained at 23% even after 200 days. In the present scenario, the initial donor cells of the two competing plasmids are placed in a different location, at the bottom, halfway the length of the biofilm (see Figure 4.3). The different initial donor location affected, in particular, the NHR plasmid transfer dynamics. Because the biofilm boundaries are periodic, the new location of the NHR plasmid donor in the patchy biofilm enables the dissemination of the plasmid into all the biofilm clusters of species N by $t = 7$ days. Periodic boundaries were used to avoid edge effects by assuming the borders are wrapped around, allowing one to model a biofilm section as part of a larger system (Lardon et al., 2011). Consequently, in the long term (100 days) no significant differences in plasmid dynamics between the mixed and the patchy biofilm are detectable (Figure 4.10). Regarding the effect of decreasing the transfer probability up to 1000 fold, the frequency of the plasmids is severely affected for a $p = 0.001$ in both biofilm structures (see Figure 4.11). Nevertheless, the NHR plasmid seems to be more sensitive to a drop in the transfer probability when transferring in a patchy biofilm, where already at a $p = 0.01$ its frequency in the two-species assemblage is less than 10% as compared to 38% in the mixed biofilm. The BHR transfer dynamics pattern, when competing with a compatible NHR plasmid, is not affected by the biofilm structure. Moreover, using experimentally measured fitness costs in this set

of simulations while varying the parameters of the other competing plasmid, did not yield any changes in the final frequency of each plasmid when compared with the results obtained in the previous sections where each parameter was varied while keeping the costs null (mixed biofilm scenarios). Hence, an interaction between fitness cost and transfer probability factors on final frequencies was not found.

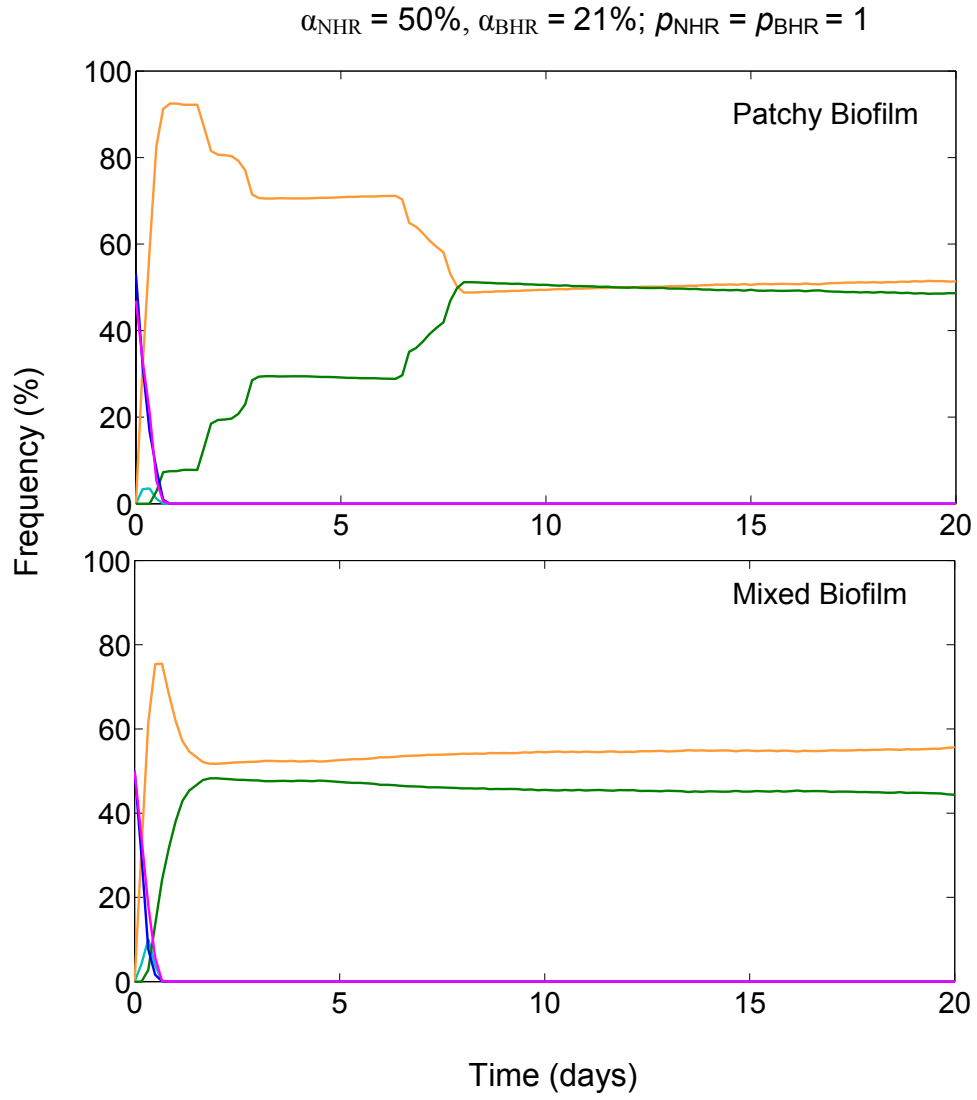


Figure 4.10: A typical replicate simulation of the dynamics of transfer of two compatible NHR and BHR plasmids in two-species biofilms. Effect of fitness cost on the frequency of each plasmid in different biofilm structures. Legend: — R_N — R_B —

T_N^N — $T_{N,B}^B$ — $T_N^{B,N}$

Effect of Patchiness and Transfer Probability

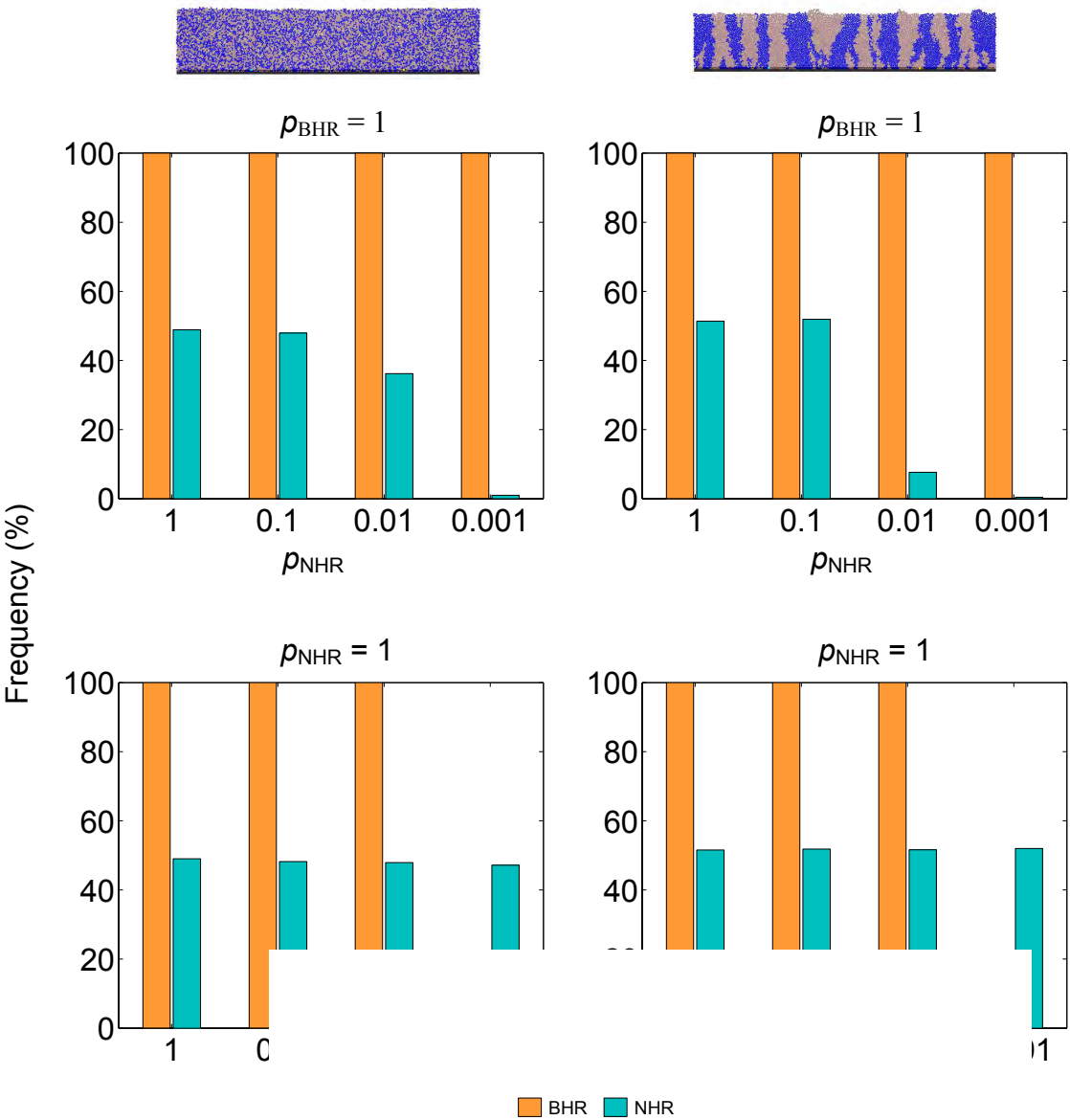


Figure 4.11: Effect of patchiness and NHR plasmids transfer probability on the frequency of BHR and NHR plasmids. For each panel the transfer probability of the NHR plasmid was 1. The fitness costs were 0.1 for BHR and 0.01 for NHR. The results are the mean of three replicates for which the standard deviation was < 5% (not shown).

Summary for Compatible Plasmids

- BHR plasmid transfer dynamics is not significantly affected by increased fitness costs in either mixed or patchy biofilms;
- Higher fitness costs for the NHR plasmid lead to a slow decline in frequency over time, suggesting that in the long-term the NHR could be extinct;
- A decrease of 1000 fold in the probability of transfer considerably reduces the frequency of a plasmid in the biofilm after 100 days, but the slow increasing in frequency of plasmid-bearing hosts indicates that full invasion of the biofilm would occur in the long-term;
- The initial localization of the donor cell can be determinant for invasion of a patchy biofilm by the NHR plasmid;
- Patchy biofilm structures interfere with NHR plasmid horizontal transfer, by blocking or delaying its propagation into species *N* hosts.

4.2.4. *Incompatible Plasmids*

In this section the transfer dynamics of two incompatible NHR and BHR plasmids, i.e., plasmids that cannot co-exist in the same host, under a variety of scenarios was investigated.

4.2.4.1. Effect of host-range

The advantages of possessing a broader-host range were assessed by comparing the transfer of two competing plasmids in a single species population and two-species mixed and patchy biofilms. The results plotted in Figure 4.12 encompass the effect of decreasing the transfer probability of the BHR plasmid when competing with a fully transfer proficient NHR plasmid, whilst keeping the fitness cost of both plasmids zero. As transfer proficiency decreases, the BHR plasmid becomes less competitive and unable to invade and successfully compete with another plasmid in the single species biofilm. But the broader host-range can overcome the deficient transfer and enable the BHR plasmid to successfully invade and propagate in a two-species mixed biofilm. Yet, in the patchy biofilm, a 100 fold drop in BHR transfer proficiency leads to very low frequencies of the BHR-plasmid bearing hosts which is not overcome over time because the plasmid becomes trapped between clusters of NHR-plasmid bearing hosts. This effect is further investigated in section 4.2.4.3. On the other hand, the NHR plasmid benefits from lower p_{BHR} , as more recipients of species N become available for infection allowing the NHR plasmid to spread in the mixed biofilms.

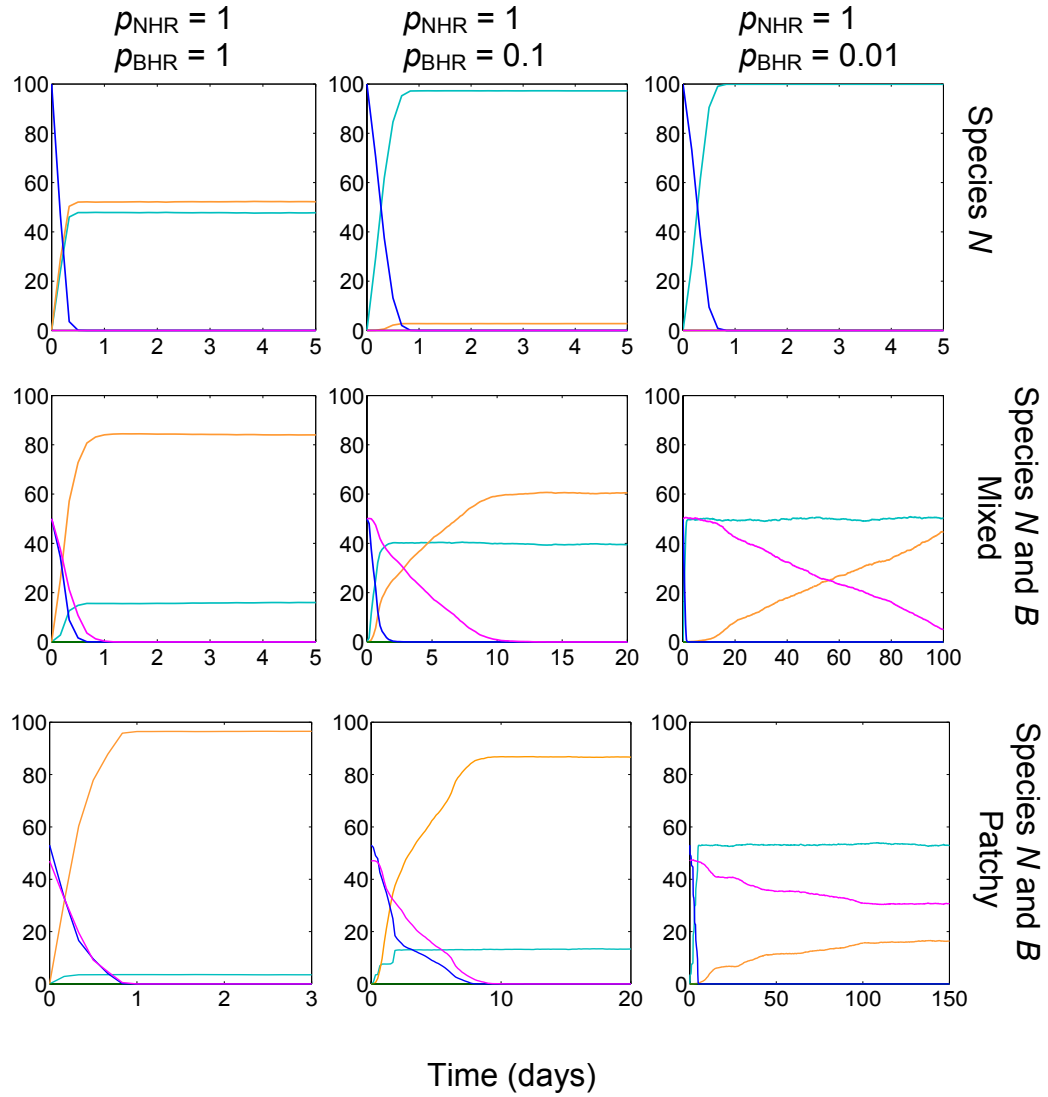


Figure 4.12: Effect of host-range for decreasing values of the transfer probability for the BHR plasmid on the dynamics of invasion of two incompatible plasmids in single and two-species mixed and patchy biofilms. The fitness costs for both plasmids were zero. Legend: R_N R_B T_N^N T_N^B

4.2.4.2. Effect of fitness cost and transfer probability in mixed biofilms

A mixed biofilm was used to evaluate the effect of increasing the fitness cost of a plasmid on its competitiveness. Figure 4.13 shows the plasmid frequencies after 100 days of simulation for different fitness costs. A clear difference regarding the compatible scenario is the much lower amount of NHR-carrying hosts in the mixed biofilm when plasmids are incompatible. The nonexistence of a species barrier for the BHR plasmid combined with the effect of mutual exclusion, leads to a quick invasion of the biofilm by the BHR plasmid which is then blocking the spread of the NHR plasmid. In contrast, even in a mixed biofilm, the NHR plasmid needs to find suitable recipients of species *N* in between small cluster of hosts of species *B*, with the aggravating factor of not being able to infect hosts from species *N* that already contain the competing plasmid. Increased fitness cost has only a marginal effect on the frequency of the plasmids, only noticeable for $\alpha_{\text{BHR}} = 50\%$.

A decrease in the transfer probability severely affects the survival of the NHR plasmid as demonstrated in Scenario A of Figure 4.13. Indeed, a 10-fold reduction in the transfer probability can abolish the chances of the NHR plasmid to invade and persist in the mixed biofilm. Consequently, the BHR plasmid can take over the two-species assemblage. When the transfer probability of the BHR plasmid is decreased, the impact on its frequency is less drastic although it significantly reduces the amount of BHR-bearing hosts in the biofilm. In turn, the frequency of the NHR plasmid rises taking advantage of the available recipients of species *N*.

An important aspect of the incompatible plasmid dynamics in biofilms is that the final plasmid frequencies may depend on the initial distance between the donor

cells carrying the NHR and the BHR plasmid. This is because the closer they are the quicker the plasmids will meet and thus interfere with each other's dissemination. Incompatibility itself can constitute a barrier to plasmid expansion in structured bacterial assemblages, such as biofilms, which can be attenuated by a broader host-range.

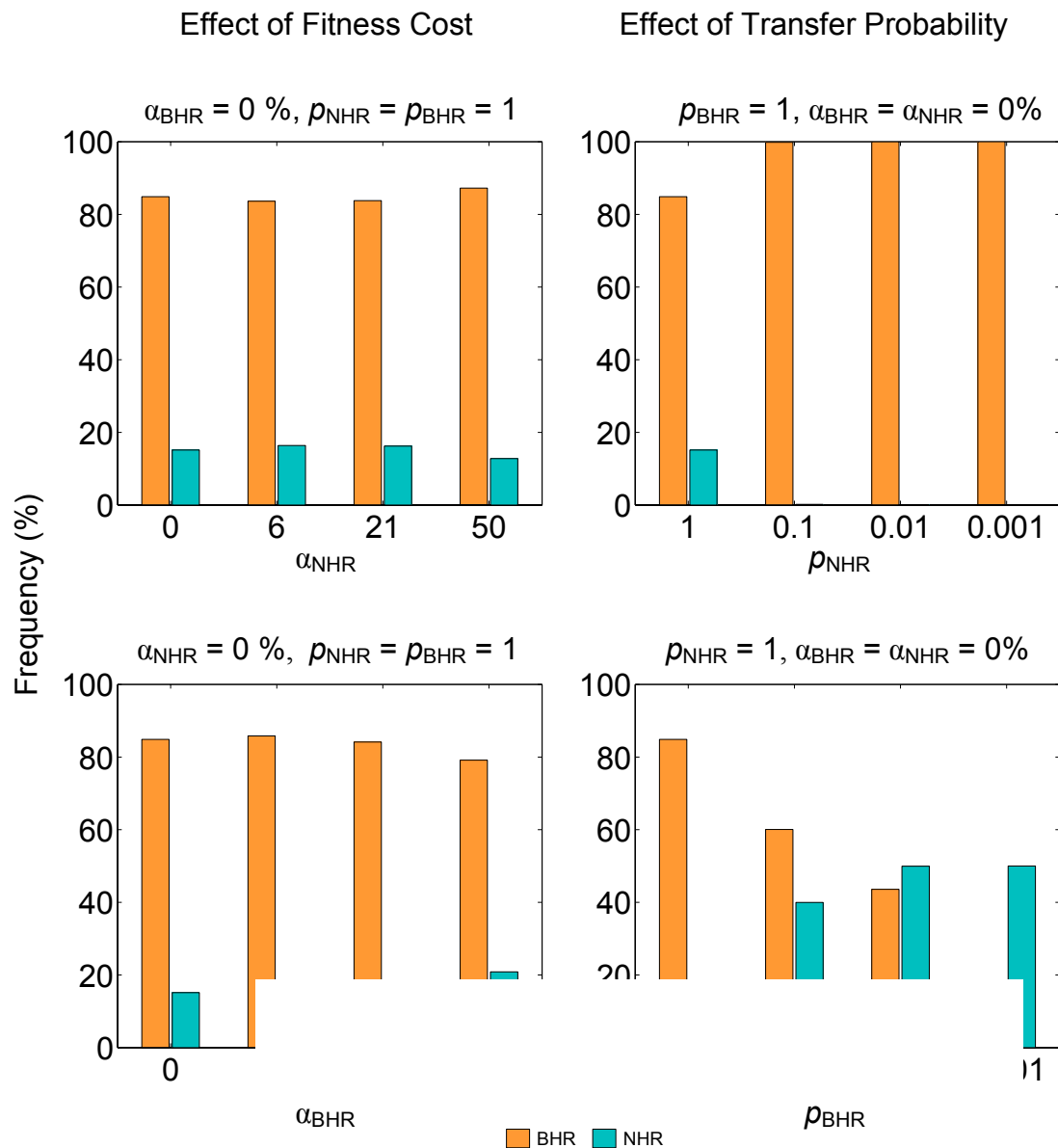


Figure 4.13: Effect of incompatible BHR and NHR plasmids on the frequency of one competitor after 100 days. In each simulation, the fitness cost of one plasmid is varied, while the transfer probability of the other plasmid is fixed as indicated. The standard deviation was < 5% (not shown).

frequency of
film for
of one
competitor
ates for

4.2.4.3. Effect of patchiness

The dissemination of the two incompatible plasmids in mixed and patchy biofilms was compared whilst using the default fitness costs measured experimentally (Dahlberg and Chao, 2003), i.e., the NHR plasmid confers a burden of 6% and the BHR 21%. The results are summarized in Figures 4.14 and 4.15.

When the fitness cost is increased minor changes occur in the frequency of each plasmid (see Figure 4.14), indicating a negligible contribution of this factor to the success of the plasmid. However, for the NHR plasmid, survival is much more affected in the patchy biofilm than in the mixed biofilm because the patchy structure of the biofilm poses an obstruction to the transfer of the NHR plasmid, which becomes trapped in between clusters of unsuitable recipients of species *B* (recall Figure 4.3). As a consequence, the BHR benefits from the delay in NHR propagation and is able to infect more hosts in the patchy biofilm.

In contrast, varying the transfer probability affects the survival of both plasmids, the effect being more severe in the patchy biofilm. For the NHR plasmid even a 10-fold reduction in transfer probability can lead to its extinction in either the mixed or the patchy biofilm (see Figure 4.15, $p < 10^{-1}$). The amount of BHR-bearing hosts in the two-species assemblage is also affected by a drop in the transfer probability, which can lead to frequencies below 10% in both biofilm structures for a transfer probability below 10^{-2} . The reduction in transfer probability of either plasmid results in a positive effect on the frequency of the competitor plasmid. This apparent regulation of plasmid frequency by its competitor's transfer proficiency is a consequence of interspecific competition experienced among incompatible plasmids.

In Figure 4.16 the transfer dynamics of incompatible NHR and BHR plasmids in mixed and patchy biofilms is compared. Despite its broader host-range, the BHR plasmid can not propagate through the two-species assemblage if its transfer probability is very low, due to the presence of the faster spreading NHR incompatible plasmid in large clusters of recipients of species *N*.

Effect of Patchiness and Fitness Cost

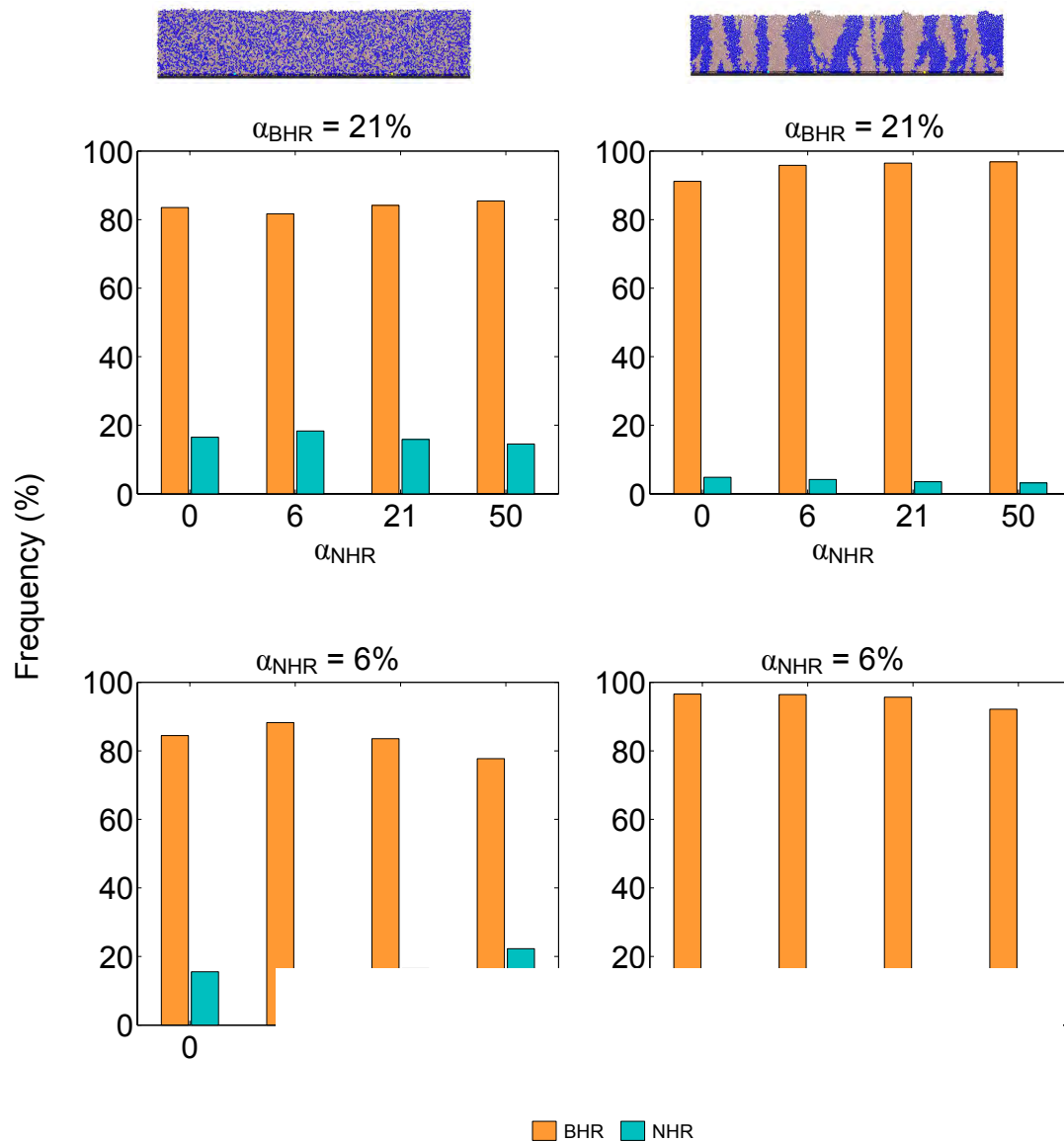
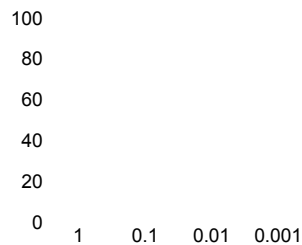
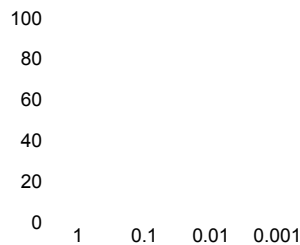


Figure 4.14: Effect of NHR plasmids transfer subplot the fitness cost competitor plasmid fixed plasmids was 1. Each standard deviation was < 5% (not shown).



and each of the r both in the



NHR

∴ For

ig the

varios

mean of

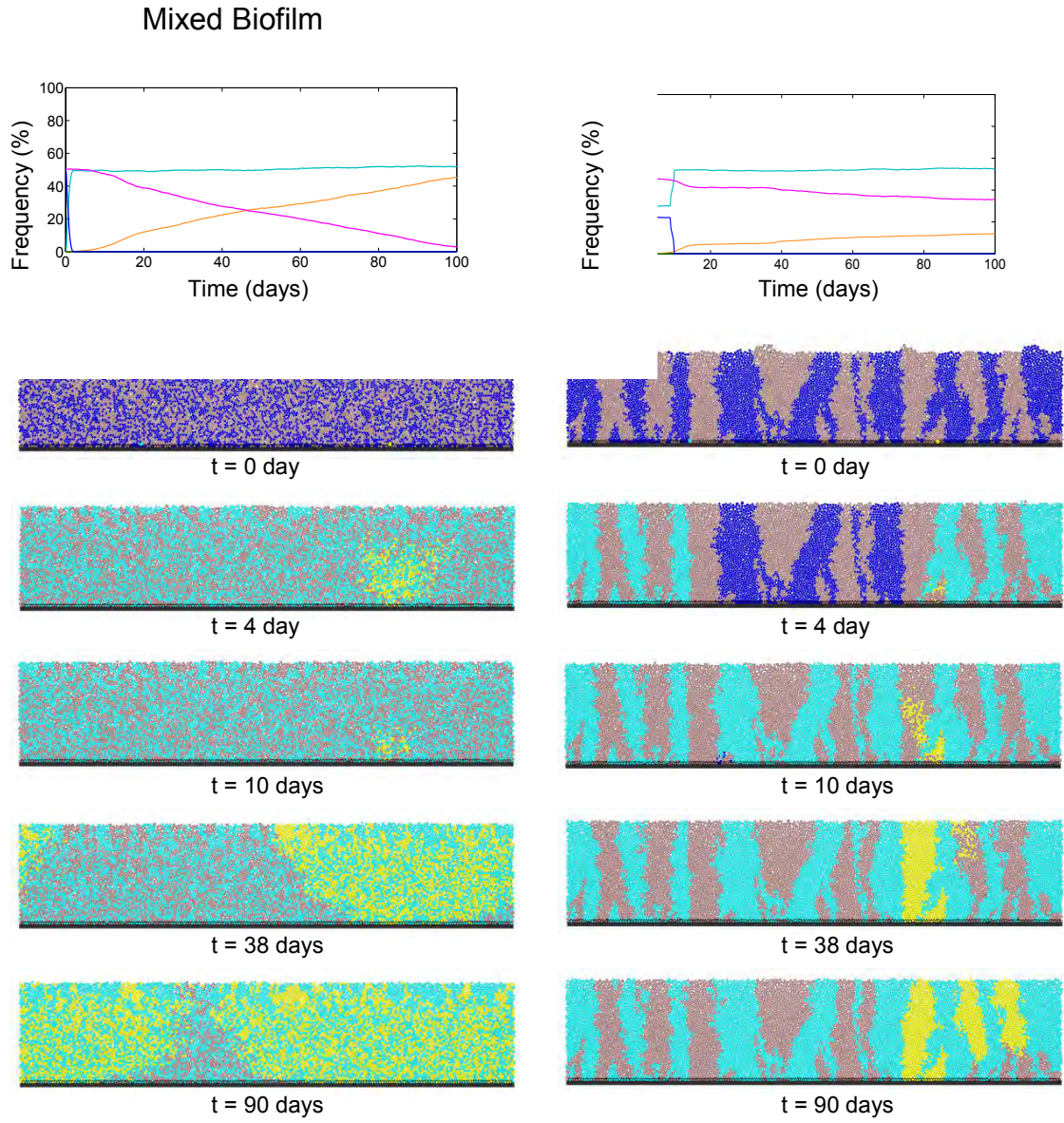


Figure 4.16. Transfer of incompatible NHR and BHR plasmids in mixed and patchy biofilms over time. Parameters are $p_{\text{NHR}}=1$, $p_{\text{BHR}}=0.01$, $\alpha_{\text{NHR}}=6\%$, $\alpha_{\text{BHR}}=21\%$.

Legend: ● R_B ● R_N ● T_N^N ● $T_{N,B}^B$

Summary for Incompatible Plasmids

- The presence of a BHR incompatible plasmid in two-species biofilms significantly reduces the frequency of the NHR plasmid;
- Increased fitness costs have no substantial effect (up to 100 days) on the competitiveness of neither the BHR or the NHR plasmid;
- A reduction in transfer probability has a significant impact on the ability of a plasmid to compete with a faster transferrable competitor plasmid;
- Incompatibility results in mutual exclusion which in itself constitutes a barrier to plasmid dissemination, only attenuated by a broad host-range;
- Patchiness increases the difficulties of spreading of a plasmid in two-species assemblages when competing against another incompatible plasmid.

4.3. Discussion

The role of fitness cost and transfer proficiency on the competition between compatible and incompatible plasmids with different host-ranges in mature biofilms was investigated using iDynoMiCS, an individual-based framework that can simulate biofilm growth as well as chemostats. It was found that fitness cost is not a determinant factor for the spread of the BHR plasmid into the biofilm, but could affect long-term persistence of the NHR plasmid, which cannot infect all competing species and lead to its extinction. The fact that the spreading of two competing plasmids takes place in spatially structured mature biofilms can also explain why increasing fitness costs do not considerably affect the spread of the BHR plasmid. The initial location of the donor cells at the bottom of the biofilm where growth is very limited due to low substrate concentrations ensures that the plasmid transfer front moves faster than the growth front. Thus, BHR plasmid invasion by horizontal transmission can proceed, despite high fitness costs, throughout the whole biofilm until the pool of free recipients is depleted, and persistence of the plasmid in the outer layers of the biofilm where bacterial growth and biomass turnover are greater can be sustained by vertical transmission. Any plasmid loss would be transient as reinfection from neighbouring transconjugants would be fast. Merkey et al. (2011) also observed that deeper inoculation of donor cells leads to highest plasmid spread in old biofilms where old transconjugants dominate over newly infected recipients, as opposed to young biofilms where invasion is faster for shallow inoculations and horizontal transmission is the principal factor driving plasmid persistence (Merkey et al., 2011). Plasmid burden and low transfer rates of naturally occurring plasmids have been the

central argument to justify theoretically the impossibility for a plasmid to persist parasitically (Bergstrom et al., 2000), but the combination of slow growth with faster plasmid invasion can lead to persistence despite the fitness cost, as found in the present work and in Merkey et al. (2011). This points to the possibility for the existence of natural environments where costly but conjugatively proficient plasmids can thrive, specifically in soil and mature biofilms where bacterial growth is slow.

In contrast, reduced transfer proficiency can delay the process of plasmid invasion and control plasmid survival when combined with a narrower host-range and incompatibility among the competing plasmids. Yet, the role of the pilus length on BHR and NHR plasmid invasion and persistence remains to be evaluated. The role of high transfer proficiency in the success of the BHR plasmid, is in line with the observation that broad host-range plasmids from IncP, IncW and IncN (Datta and Hedges, 1972; Mazodier and Davies, 1991) produce very short pili (1 μm) (Eisenbrandt et al., 2000; Kalkum et al., 2004), presumably for efficient mating on spatially structured communities where cells are packed together with very little free space between them. Samuels et al. (2000) have shown the existence of conjugative junctions between *E. coli* carrying the RK2 plasmid and a recipient cell, where no distinguishable pili structures are observed, suggesting that the transfer channel is small or that such channel is only formed transiently. Thus, the assumption that a donor cell can transfer the plasmid to neighbours other than the ones with which there is direct contact may not be a reasonable assumption when modeling plasmids with short and rigid pili. In contrast, the narrow host-range F plasmid expresses long and flexible tube-like structures that can measure between 2 and 20 μm in length (Lawley et al., 2003). Depending on the fluidity of the biofilm

structure, such long pili could reach recipient cells in the vicinity other than the immediate neighbours of the donor cell, and transfer the plasmid. There is evidence for DNA transfer between cells expressing F pili, that were not in surface contact (Harrington and Rogerson, 1990; Ou and Anderson, 1972) but also direct evidence that conjugating cells are typically aggregated in close wall-wall association (Ou and Anderson, 1970; Achtman, 1975; Durrenberger et al., 1991). These tube-like structures are thought to function as attachment devices for inducing aggregation between the two cells following pilus depolymerization (Kalkum et al., 2004). Hence, a long pilus might not be advantageous for conjugational transfer of plasmids in biofilms, if the distant recipient and donor cell cannot come close enough due to obstacles (such as other cells or EPS particles) in their way. In contrast, in planktonic cultures, long pili might be advantageous to search and anchor a donor cell to a recipient cell.

The results presented here reveal that host-range can be advantageous when competing against faster-growing NHR plasmid-bearing hosts, since BHR plasmid frequency in either mixed or patchy biofilms was always higher than its competitor and was not affected by an increased burden on the host (see Figures 4.7 and 4.13). In contrast, due to its narrower host-range, the ability of the NHR plasmid to invade a biofilm can be severely reduced by biofilm patchiness (see Figure 4.10) and mutual exclusion due to the presence of an incompatible BHR plasmid (see Figure 4.14). The combined effect of having a narrow host-range and a lower transfer probability than the incompatible BHR competitor abolishes the chances for survival of the NHR plasmid. BHR plasmid invasion is also severely penalized by a drop in transfer probability in the presence of a faster transferrable incompatible NHR

plasmid and this is even harsher in a patchy biofilm structure, where clusters of NHR-plasmid bearing cells effectively block the wave of transfer of the BHR plasmid (see Figures 4.15 and 4.16). Nevertheless, expansion of host-range would be advantageous under all the scenarios analysed herein and may explain why BHR plasmids are so ubiquitous in natural environments (Heuer et al., 2002; Smalla et al., 2006; Bahl et al., 2009).

The spatial organization of different species in a biofilm was found to be an important factor modulating the pattern of transfer dynamics of a plasmid. Patchy biofilms are, presumably, the predominant form of two-species biofilms in the natural environment, as these emerge naturally following colonization of a surface with few hosts of each species (Banks and Bryers, 1991; Amann et al., 1992). As shown by the results presented herein, the initial localization of donor cells in patchy biofilms can affect the rate at which propagation of a plasmid in the two-species assemblage occurs, as observed for the NHR plasmid spreading in two-species patchy biofilms (compare Figures 4.4 and 4.5 with Figures 4.3 and 4.7). Biofilm patchiness and incompatibility combined with low transfer proficiency can have a strong impact on the fate of the two competing plasmids, and even a broader host-range may not be sufficient to compete against a faster transferrable NHR incompatible plasmid (see Figure 4.15). Under these circumstances, one would expect incompatible plasmids with high transfer proficiency to be selected, even if plasmid burden increased as a consequence of that. The results show that both compatible plasmids can coexist at considerable frequencies in either mixed or patchy two-species biofilms for the parameter range explored, for at least 100 days. Regarding the incompatible

plasmids, due to mutual exclusion, the conditions for co-existence were stricter, in particular for very low transfer proficiencies and patchy biofilms.

Although the present work constitutes a virtual exercise, it exemplifies how interactions between plasmids in biofilms can be explored and competitiveness of a plasmid can be modulated by factors that have not been previously identified, such as biofilm patchiness and incompatibility among competing plasmids. These observations constitute new hypotheses that could be further addressed experimentally in order to better understand the mechanisms underlying the success of some plasmids in invading and persisting in spatially structured bacterial assemblages in the absence of positive selection determinants that may be carried by the plasmid backbone.

Chapter 5

Fitness cost and transfer frequency
of RK2 and R387 in *E. coli*,
P. aeruginosa and *P. putida*

FITNESS COST and TRANSFER FREQUENCY of RK2 and R387 in *E. coli*, *P. aeruginosa* and *P. putida*

5.1. Introduction

Conjugative transfer greatly contributes to the ability of a plasmid to spread and invade new bacterial niches. The successful establishment of a plasmid in a community will depend on numerous factors among which are the genetic background of the bacterial hosts and recipients (De Gelder et al., 2007; Sota and Top, 2008), the physiological state of the donor (Smets et al., 1993; Muela et al., 1994) and the selective pressure (Subbiah et al., 2011). Although many studies have investigated the conditions for persistence of a single type of plasmid in a bacterial population much fewer have addressed the question concerning the dissemination of plasmid(s) in multispecies assemblages. In particular, the importance of the host-range of a plasmid to its ability to compete with other plasmids and to persist among faster-growing plasmid-free hosts has not been investigated. Nonetheless, various reports have revealed that acquired antibiotic resistance can remain for extensive periods of time after the antibiotic treatment has been halted (Andersson and Hughes, 2011; Scott, 2002; Feld et al., 2008; Jakobsson et al., 2010). Thus, it is important to design studies that will allow a thorough understanding of how multiresistant plasmids can persist in multispecies assemblages in the absence of selection for its antibiotic-resistant encoded traits.

In this chapter, the goal was to explore an experimental framework that would allow study of the transfer dynamics of plasmids with different host-ranges in a microbial assemblage composed of two different species growing on nitrocellulose filters on top of agar plates. Specifically, the effect of patchiness on the dissemination of a plasmid and how transfer efficiency of a narrow host-range plasmid is affected by the presence of a non-suitable host (i.e., a host it cannot infect) was investigated. The experiments also address the hypothesis put forward by previous modeling results, that BHR plasmids are more competitive than NHR plasmids in spatially structured assemblages, such as colonies or biofilms, largely due to their broader host-range.

Two plasmids from different incompatibility groups, RK2 from IncP α and R387 from IncK, which have a different host-range (Bradley, 1980; Tschape and Tietze, 1980), were used in the present study. RK2 plasmid is a promiscuous plasmid capable of conjugal transfer and stable maintenance in almost all Gram-negative bacterial species (Schmidhauser and Helinski, 1985), whereas R387 has only been found among members of the Enterobacteriaceae family (Shaw et al., 1972). Each plasmid confers a distinct set of antibiotic resistances to their hosts, which can be used to track their dissemination in two-species assemblages. However, the pair RK2/R387 is not ideal since their transfer functions are inversely regulated, pilus synthesis in RK2 plasmid is tightly regulated leading to a continuous production of pili, whereas in R387 plasmid it is repressed (Bradley, 1980). This could give an advantage to RK2 plasmid when invading a population of plasmid-free hosts. The burden and transfer frequency of the two plasmids, RK2 and R387, in *E. coli*, *P. aeruginosa* and *P. putida* strains was also characterized. Subsequently, the

competitiveness of RK2 and R387 in two-species assemblages composed of *E. coli* and *P. putida* under different temperatures and using different initial ratio between the two recipients was investigated. A strong dependence of transfer frequency and fitness burden of the plasmids on the host species or strain was found. Surprisingly, the majority of the lab strains tested either grew faster in presence of the plasmid or their growth rate was only marginally affected. Preliminary results of mating experiments on filters support the model predictions of a reduced plasmid spread of the NHR plasmid in the presence of non-participating background species.

5.2. Materials and methods

5.2.1. Strains and plasmids

Strains from *Escherichia* and *Pseudomonas* genera were chosen to evaluate the effect of plasmid carriage and rate of transfer at the intra- and inter-species level. The different strains and plasmids used throughout the work are listed in Table 5.1. The RK2 plasmid is known for its ability to transfer among distantly related species, whereas R387 is believed to have its host-range restricted to the Enterobacteriaceae family (Shaw et al., 1972).

Table 5.1: List of plasmids and strains used in the present work.

Strain	Relevant characteristics ^a	Source
<i>E. coli</i> K12 MV10nal	Nal ^R F- thr ⁻¹ thi ⁻¹ leuB6 lacYI tonA21 supE44 rfbD1 ΔtrpE5 λ-	<i>b</i>
<i>E. coli</i> K12 DH5α	F- endA glnV44 thi-1 recA1 relA1 gyrA96 deoR nupG φ80d/lacZΔM15 Δ(lacZYA-argF)U169 hsdR17(r _K ⁻ m _K ⁺) λ-	<i>b</i>
<i>E. coli</i> J53	F- met pro	
<i>P. aeruginosa</i> PAO 1161	Km ^R , Tc ^R , Amp ^R , Str ^R leu-38, rmo ⁻	<i>b</i>
<i>P. putida</i> KT2440	Gent ^R	<i>b</i>
Plasmid		
RK2	IncP-1, 60 Kb Km ^R , Amp ^R , Tc ^R , Crb ^R	<i>b</i> , 1
R387	IncK, 80 Kb Cm ^R , Str ^R	<i>b</i> , 2

^a Nal, Nalidixic acid; Km, Kanamycin; Amp, Ampicillin; Tc, Tetracycline; Crb, Carbenicillin; Cm, Chloramphenicol; Str, Streptomycin; Gent, Gentamycin.

^b Chris Thomas" lab strain and plasmids collection

¹ Thomas and Smith, 1987; Datta et al., 1971; Pansegrau et al., 1994

²

5.2.2. *Growth curves*

Growth curves of the different bacterial species with and without a plasmid were carried out in Luria Broth or minimal medium M9. Optical density was measured at 600 nm at room temperature. Overnight cultures were set up by inoculating 10 mL of medium with a single colony, and grown at the target temperature of 30 or 37°C. On the next day, the ON cultures were diluted 100 fold into 50 mL fresh medium (250 mL Erlenmeyer flasks) at room temperature and then incubated at the chosen temperature. For each growth curve, a total of three replicates were monitored. Time points were taken at suitable intervals to capture the doubling in population density.

Determination of growth rates and doubling times

The data were plotted on a logarithmic scale and the growth rates (μ) derived from an exponential fit using at least 5 points chosen from the exponential growth phase. Doubling times were calculated according to $t_d = \ln(2)/\mu$. Values presented are the mean of three replicates \pm SD.

5.2.3. Membrane filter matings

Conjugative transfer

Matings between different strains and species were carried out as follows. Overnight cultures of donors and recipients were set up by inoculating a single colony in LB supplemented with the appropriate antibiotics and incubated at the target temperature of mating (26, 30 or 37°C).

On the next day the ON cultures were diluted 100 fold in LB supplemented with the appropriate antibiotics and grown to exponential phase (OD~ 0.6-0.7). From this, donors were diluted to an OD of 0.1 with PBS while the recipients were used at an OD between 0.6 and 0.7. Approximately 10^8 donor cells (J53, DH5 α or PAO111 carrying appropriate plasmids) were mixed with an approximately 10-fold excess of exponential phase recipient cells (MV10NaI^R, PAO1161 or *P. putida*).

The final mixture was composed of 100 μ L of recipients, 100 μ L of donors and 800 μ L of PBS, which was then filtered onto sterile nitrocellulose 0.22 μ m filters (Millipore, ref GSWP02400) and further placed on an agar plate pre-warmed for 30 minutes at the target temperature (26, 30 or 37°C).

Selective media and enumeration

Cells were washed from the filter with sterile PBS, diluted into sterile PBS to give countable number of colonies, and plated onto agar plates selective for donors or selective for transconjugants. The antibiotic combination used for selection of donors, transconjugants and recipients for each mating pair are listed in Table 5.2.

Table 5.2 Summary of the antibiotics used to select for donors, transconjugants and recipients in the mating experiments performed between the different strains.

Mating pair			Selected resistance ^a (µg mL ⁻¹)		
Donor	Recipient	Plasmid	Donors + Transconjugants	Transconjugants	Recipients
DH5α	MV10	RK2	Km (50)	Km (50) + Nal (50)	Nal (50)
J53		R387	Str (50)	Str (50) + Nal (50)	
MV10	<i>P. putida</i> KT2440	RK2	Crb (150)	Crb (150) + Gent (20)	Gent (20)
MV10	PAO1161	RK2	Crb (150)	Crb (150) + Str (50)	Str (50)
PAO1161	<i>P. putida</i> KT2440	RK2	Crb (150)	Crb (150) + Gent (20)	Gent (20)

^a Nal, Nalidixic acid; Km, Kanamycin; Crb, Carbenicillin; Str, Streptomycin; Gent, Gentamycin.

Transfer frequency

Transfer frequency was calculated as the number of transconjugants divided by the number of donors. Transfer frequency values presented are means from at least two replicate matings ± standard deviations.

Statistical methods

The two-sample t-test was used when comparing the means of two growth rates. Non-parametric Kruskal-Wallis test was applied to non-normal group data in order to

test the significance of different explanatory factors on the observed population medians. Statistical significance was set at ≤ 0.05 . All the statistical analyses were carried out in R, version 2.14.1 GUI.

5.2.4. Plasmid propagation in two-species assemblages

In these experiments we adopted the same mating protocol as described in section 5.2.3, except that the plasmids were left to propagate in two-species assemblages composed of *E. coli* and *P. putida* strains on nitrocellulose filters on LB agar plates at either 26 or 37°C for at least 24 hours. The choice of antibiotics used for selecting donors, transconjugants and recipients in the two-species scenario was dependent on the plasmid and strain combination as depicted in Table 5.3.

Table 5.3 List of antibiotics used for selecting donors, transconjugants and recipients in the two-species scenario for R387 and RK2 plasmids.

Plasmid	Selected resistance ^a (µg mL ⁻¹)			
	Donors + Transconjugants	Recipients	Transconjugants	
			<i>E. coli</i> MV10	<i>P. putida</i> KT2440
R387	Str (100)	Gent (20) (<i>P. putida</i> KT2440)	Str (100) + Nal (100)	Str (100) + Gent (20)
RK2	Crb (150)	-	Crb (150) + Nal (100)	Crb (150) + Gent (20)

^a Nal, Nalidixic acid; Crb, Carbenicillin; Str, Streptomycin; Gent, Gentamycin.

5.2.5. Materials

The antibiotics used throughout this work are listed in Table 5.4. The filters used in the mating experiments were from Millipore (0.22 μm pores, 24 mm diameter).

Table 5.4 List of antibiotics and suppliers

Antibiotic	Supplier
Ampicillin	Fisher bioreagents
Kanamycin	Fisher bioreagents
Rifampicin	Apollo scientific
Carbenicillin disodium	Melford
Chloramphenicol	Sigma
Streptomycin sulfate	Calbiochem
Tetracycline HCl	Calbiochem
Nalidixic acid	Fluka

5.3. Results

The results presented here are divided into four sections: the relative fitness of the host when it harbours a plasmid, the transfer frequency of the plasmid between different bacterial species or strains and preliminary experiments on the propagation dynamics of a plasmid in a two-species assemblage.

5.3.1. *Relative Fitness*

In order to assess the effect of a plasmid on the growth rate of a bacterial host, a series of batch growth curves for different bacterial strains and species carrying either RK2 or R387 plasmids, in different temperatures and growth media were performed. A summary of growth rates and doubling times for the different strains carrying either R387 or RK2 plasmids is shown in Table 5.5. The values presented are the mean of three replicates and the corresponding standard deviation, for statistical analysis see Table 5.6 and Table 5.7.

The effect of a plasmid on host fitness is very dependent on the strain and plasmid combination as well as on temperature and medium. Nonetheless, as expected, growth rates are lower at 30°C particularly in the case of *E. coli* strains. In minimal medium we observe the same trend, i.e., slower growth due to the absence of ready-made aminoacids in the medium (except for leucine and tryptophan which the *E. coli* MV10 cannot produce).

Various factors could explain the differences between the mean growth rates, namely the growth medium, the temperature, the bacterial strain and the presence or

absence of a plasmid. In order to assess the importance of each factor, a Kruskal-Wallis test was carried out to determine which factor was statistically significant in explaining the measured growth rates. The results of this analysis can be found in Table 5.6. The differences found in growth rate are most likely due to differences in the strain, temperature and medium as suggested by the low p -values obtained ($p < 0.05$). The presence and type of plasmid does not seem to be a determinant factor in explaining the observed differences in growth rate (Table 5.6, p -value > 0.05).

The growth rates were then used to calculate the fitness of the bacterial host carrying the plasmid relative to the host without the plasmid. To assess whether the difference in fitness between the plasmid-bearing host and the plasmid-free host was significant, a t -test was carried out to calculate the p -values for those pair-wise comparisons. The results are shown in Table 5.7. Both plasmids conferred a significant fitness advantage to *E. coli* MV10 at 37°C but not at 30°C. At 30°C for the same strain, R387 did not significantly affect fitness and RK2 conferred a significant fitness cost. In *E. coli* DH5 α at 37°C RK2 did not affect the hosts' growth, but at 30°C it conferred a fitness advantage. In *Pseudomonas* species, RK2 significantly improved the growth rate of *P. aeruginosa* PAO1161 at both temperatures in LB.

Table 5.5 Summary of growth rates and doubling time for the bacterial strains chosen for this study, carrying either RK2 or R387 plasmid or no plasmid, under different growth conditions. Three replicates were used to calculate the mean and the corresponding standard deviation.

Strain	Plasmid	Temp (°C)	Medium	Growth Rate ± SD (h ⁻¹)			Doubling time ± SD (min)
<i>E. coli</i> MV10	-	37	LB	1.09	±	0.01	38.16 ± 0.32
	RK2			1.63	±	0.06	25.48 ± 0.99
	R387			1.61	±	0.02	25.83 ± 0.24
	-	30		1.03	±	0.02	40.31 ± 0.80
	RK2			0.78	±	0.02	53.49 ± 1.66
	R387			0.99	±	0.01	42.10 ± 0.29
	-	37	M9	0.77	±	0.02	54.03 ± 1.06
	RK2			0.73	±	0.01	56.66 ± 0.54
	R387			0.87	±	0.03	48.06 ± 1.69
<i>E. coli</i> DH5α	-	37	LB	1.01	±	0.01	41.26 ± 0.25
	RK2			1.07	±	0.09	39.13 ± 3.28
	-	30		0.56	±	0.01	74.01 ± 0.91
	RK2			0.64	±	0.09	64.66 ± 2.85
<i>P. aeruginosa</i> PAO1161	-	37		1.04	±	0.02	40.15 ± 0.59
	RK2			1.46	±	0.04	28.58 ± 0.84
	-	30		0.67	±	0.04	62.03 ± 3.69
	RK2			1.07	±	0.03	39.03 ± 1.03
<i>P. putida</i> KT2440	-	37	1.16	±	0.06	35.78 ± 1.72	
	RK2		1.03	±	0.03	40.32 ± 1.01	

Table 5.6 Summary of Kruskal-Wallis test results for the effect of each main factor on the observed growth rates.

Main Effect	H (d.F., N=57)	p-value
Strain	H (3) = 8.13	0.0433
Plasmid	H (2) = 1.34	0.511
Temperature	H (1) = 13.9	1.97×10^{-4}
Medium	H (1) = 7.19	7.33×10^{-3}

Table 5.7 Summary of t-test results for the relative fitness of strains carrying either RK2 or R387 plasmids.

Host	Temp (°C)	Medium	Plasmid	Relative fitness* (μ _p ⁺ /μ _p ⁻)	<i>t</i> [<i>d.F.</i>]	<i>p</i> -value (t-test)	
<i>E.coli</i> MV10	37	LB	RK2	1.50	t[2.08]= 14.5	3.99 x 10 ⁻³	
			R387	1.48	t[3.23]= 51.0	6.82 x 10 ⁻⁶	
	30		RK2	0.76	t[3.91] = 13.8	1.86 x 10 ⁻⁴	
			R387	0.96	t[2.43]= 3.48	0.055	
	37	M9	RK2	0.95	t[2.8]= 3.8	3.7 x 10 ⁻²	
			R387	1.13	t[2.94]= - 4.92	1.68 x 10 ⁻²	
<i>E.coli</i> DH5α	37	LB	RK2	1.06	t[2.02]= -1.14	0.370	
	30			1.14	t[3.73]= -5.37	7.03 x 10 ⁻³	
<i>P. aeruginosa</i> PAO1161	37			1.40	t[2.48]= -15.8	1.50 x 10 ⁻³	
	30			1.60	t[2.63]= -14.9	1.28 x 10 ⁻³	
<i>P. putida</i> KT2440	37				0.89	t[3.9]= 3.2	3.4 x 10 ⁻²

* μ_p^+ growth rate of the plasmid-bearing host, μ_p^- growth rate of the plasmid-free host

5.2.2. Transfer frequency

In order to evaluate the transfer proficiency of the two conjugative plasmids, RK2 and R387, a series of mating experiments combining different donor and recipient strains were performed. The effect of temperature on the transfer frequency was also investigated for specific mating pairs. The results are summarized in Table 5.8. The transfer frequency values presented are means from 2 replicate experiments \pm standard deviations.

Table 5.8 Summary of the transfer frequency (T/D) for RK2 and R387 plasmids in different hosts.

Mating pair		Plasmid	Temp (°C)	Transfer Frequency (T/D) \pm SD
Donor	Recipient			
DH5 α	MV10	RK2	26	0.020 \pm 0.008
			30	0.079 \pm 0.002
			37	0.008 \pm 0.001
J53		R387	37	0.00014 \pm 0.00002
MV10	PAO1161	RK2	37	0.001 \pm 0.000
	KT2440			0.008 \pm 0.004
PAO1161	KT2440	RK2	26	0.173 \pm 0.004
			30	0.014 \pm 0.007
			37	0.012 \pm 0.001

From this set of results (Table 5.8) it can be observed that the transfer frequency (T/D) of R387 plasmid is nearly 60 times lower than that of RK2 when transferring into MV10 strain at 37°C. A difference in the transfer frequency (T/D) of RK2

between *P. aeruginosa* and *P. putida* at different temperatures is also noticeable, with transfer frequencies (T/D) at 26°C 10 times higher than at 30 or 37 °C.

In order to evaluate the statistical significance of each factor (temperature, recipient and donor strain) on the observed differences, a Kruskal-Wallis test was carried out. The results are presented in Table 5.9. This analysis yielded no significant difference between the medians in transfer rate due to recipient strain effect (p-value > 0.05), but both the donor strain and the temperature seem to have a significant role (p-value < 0.05).

Table 5.9 Summary of Kruskal-Wallis test results for the effect of each main factor on the observed transfer frequencies.

Main Effect	H (d.F., N=18)	p-value
Temperature	H (2) = 11.2	3.78×10^{-3}
Recipient strain	H (2) = 3.55	0.170
Donor strain	H (3) = 10.4	0.0158

In Figure 5.1 it can be seen that RK2 transfer between *Pseudomonas* species at 26°C is higher than at 30 or 37°C. Transfer among *Escherichia* strains is higher at 30°C. Thus, RK2 seems to transfer quicker in *Pseudomonas* species at a lower temperature (26°C) than in *Escherichia* species. In both cases, there seems to be an optimum temperature at which RK2 plasmid transfer is fastest.

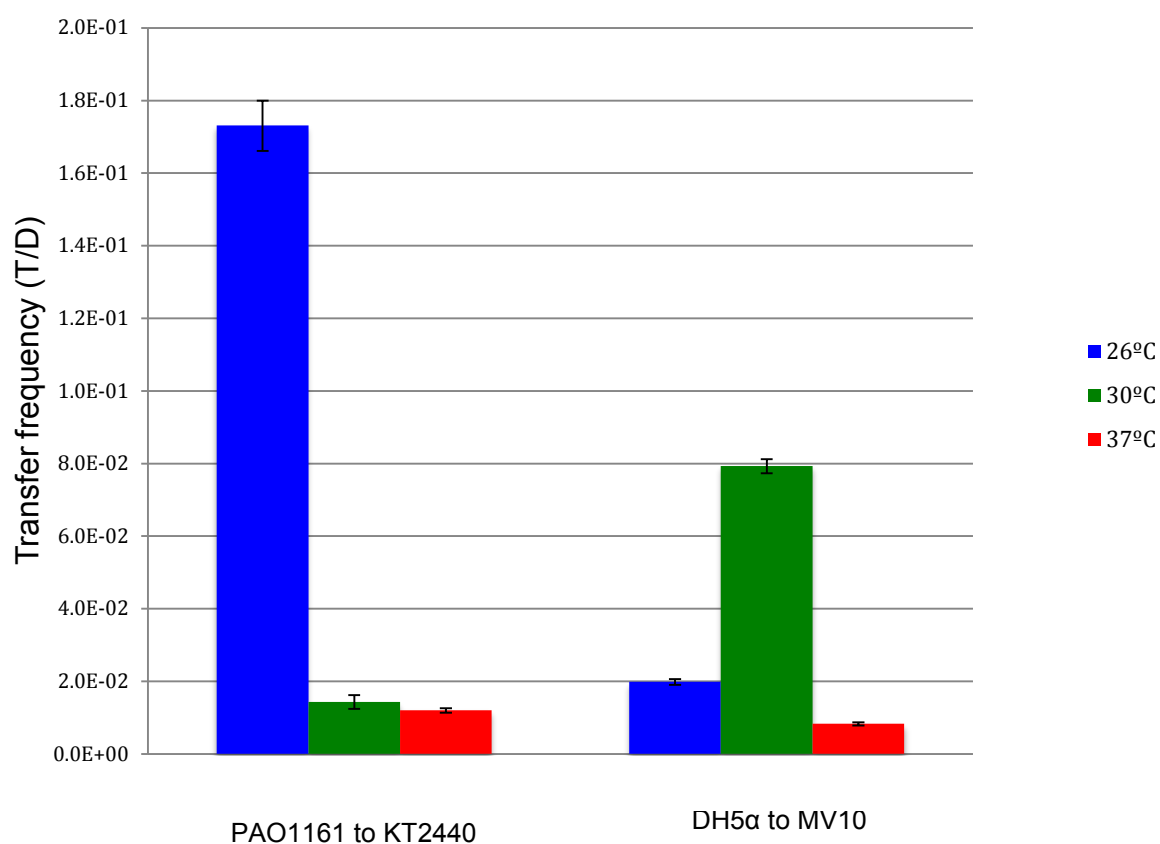
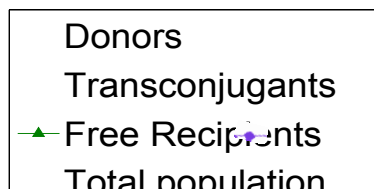
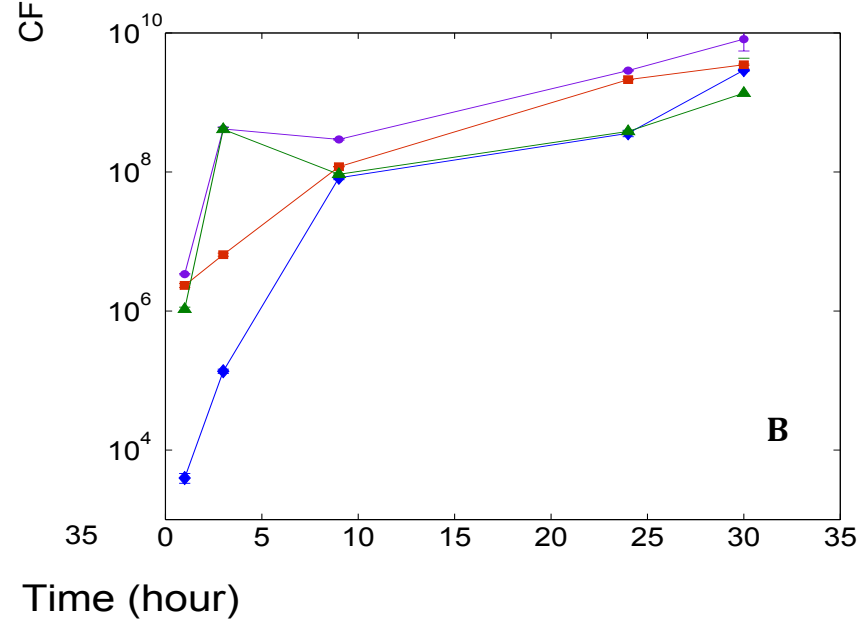
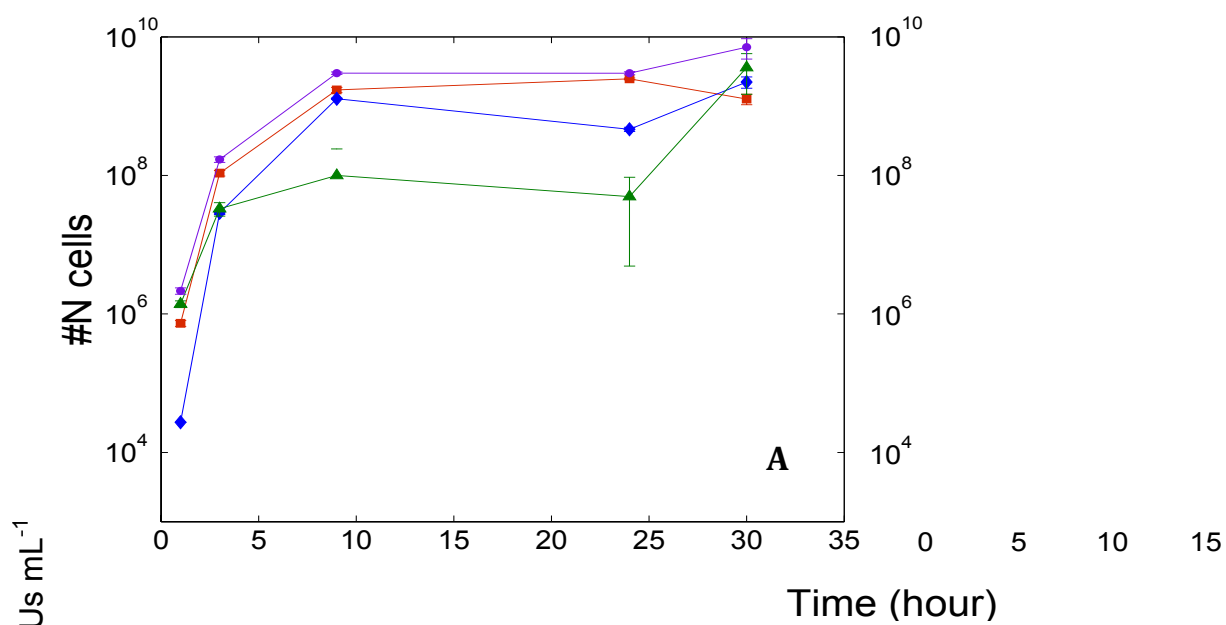


Figure 5.1 Transfer rate of RK2 among *Pseudomonas* and *Escherichia* species during 30 minutes on nitrocellulose filters on LB agar plates at three different temperatures. For each experimental condition data presented corresponds to the average of three replicates. Error bars represent the standard deviation.

Transfer dynamics of RK2 plasmid in E. coli

Next, a time series of the transfer dynamics of RK2 in *E. coli* on nitrocellulose filters on LB agar plates at two different temperatures, 26 and 37°C, was conducted. In Figure 5.2 the number of colony forming units (CFU) per mL is plotted on a log scale as a function of time. Donors and transconjugants were counted directly using appropriate antibiotic selection, whereas recipient numbers were calculated from the difference between total counts and sum of donors and transconjugants. Each time point is the mean of two replicate filters and their respective standard deviation. In both scenarios an increase in the number of transconjugants that culminates with a complete invasion of the recipient population is observed, despite the initially low frequency of RK2 plasmid donors. The difference between the two temperatures lies in the rate at which transconjugants appear. This seems to be faster at 37°C than at 26°C, even though the transfer frequencies measured before were higher at 26°C. Nevertheless, after 8 hours the number of transconjugants is high and keeps increasing. Overall two growth phases, exponential and stationary, are observed and at the same time the quick propagation and maintenance (after 24 hours) of RK2 in *E. coli* populations in the absence of any selection for its antibiotic resistance markers is observed.



5.2.3. Transfer dynamics in two-species assemblages

In these experiments the plasmids were left to propagate in two different recipients, *E. coli* and *P. putida* on filters on LB agar plates at 37°C. The underlying hypothesis is that the spread of the narrow-host plasmid R387 in a two-species assemblage would be limited in the presence of a non-suitable host and this effect would be stronger as the initial frequency of the non-suitable host in the two-species assemblage is increased. For the broad-host range RK2 plasmid the presence of two recipient species into which it can transfer should not have an effect in its ability to propagate in the two-species assemblage.

In order to test these hypotheses, the effect of different recipient ratios on the propagation proficiency of each plasmid, i.e. their ability to infect their suitable recipients in the shortest period of time, was investigated. In scenario A, both recipients were at a ratio ~ 1:1 at the start of the experiment, whereas in scenario B an excess of *E. coli* recipients was used (roughly 4 times more *E. coli* than *P. putida*). Donors were inoculated at a ratio of approximately 1:10 in respect of total number of recipients. The results are shown in Figure 5.3, where the total CFU's mL⁻¹ obtained for the donors (DH5α with RK2 or J53 with R387), transconjugants in *E. coli* MV10 (labelled as Tecoli), transconjugants in *P. putida* KT2440 (labelled as Tputida for the RK2 plasmid) and plasmid-free *P. putida* KT2440 hosts (only in the R387 case) is plotted as a function of time. Each time point is the result of one single experiment.

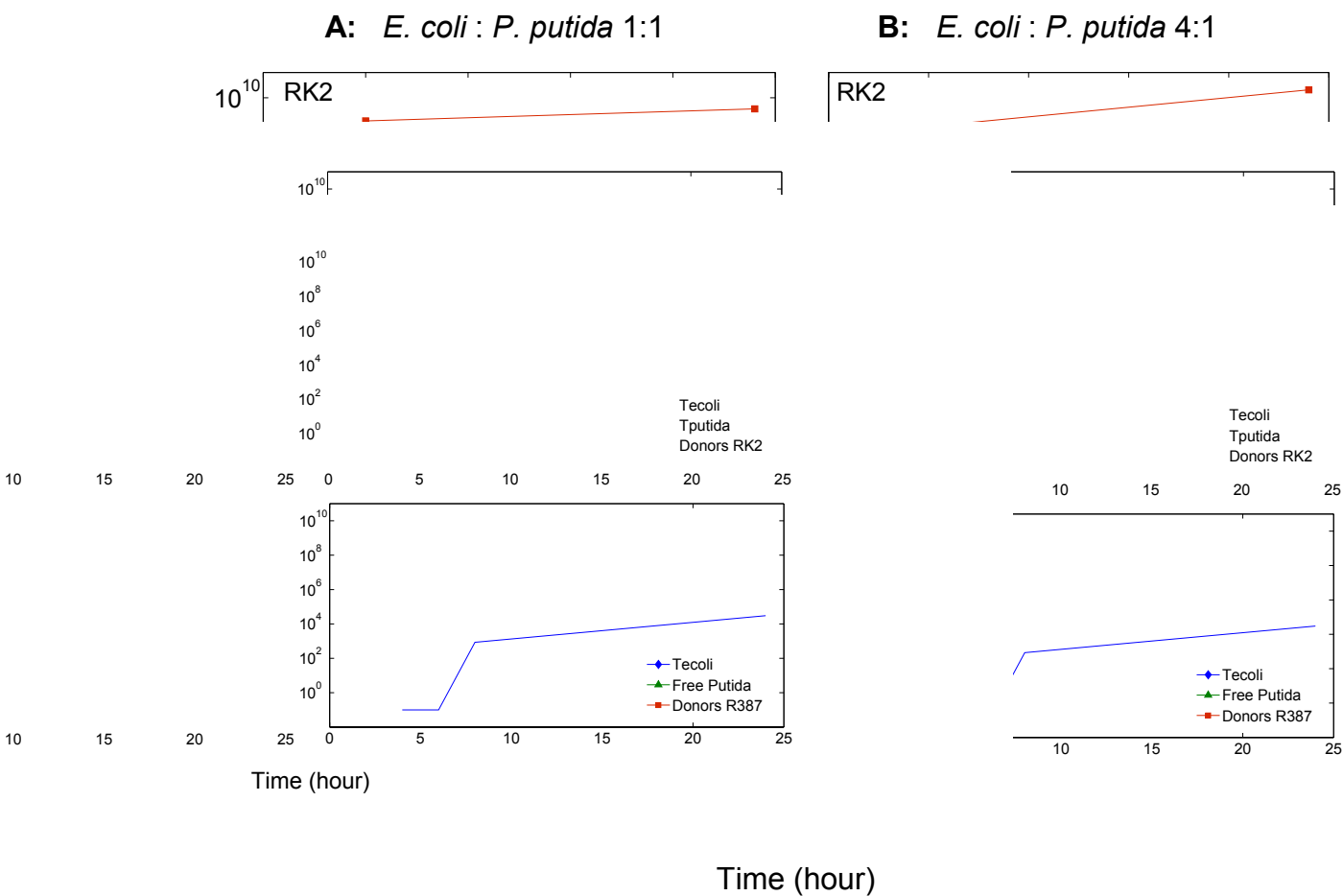


Figure 5.3 Transfer dynamics of RK2 or R387 in a two-species assemblage in LB agar plates at 37°C for 24 hours. Donors are *E. coli* DH5 α with RK2 or R387; recipients are *E. coli* MV10 and *P. putida* KT2440. On the left panel *E. coli* MV10/ *P. putida* KT2440 initial ratio \sim 1:1, and on the right *E. coli* MV10/ *P. putida* KT2440 initial ratio \sim 4:1. The data presented is the result of one experiment. Legend: Tecoli - transconjugants in *E. coli* MV10 (either RK2 or R387), Tputida - transconjugants of RK2 in *P. putida* KT2440, Donors RK2 represent *E. coli* DH5 α with RK2, Donors R387 represent *E. coli* J53 with R387.

The preliminary data suggests that RK2 transconjugants in both *E. coli* MV10 and *P. putida* KT2440 do occur, but there seems to be a preference for the *Pseudomonas* host (Figure 5.3, left panel). Nonetheless, an increase in *E. coli* recipients has a positive effect on the amount of *E. coli* MV10 transconjugants (Figure 5.3, right upper panel). The difference in growth rates between the different strains is unlikely to be the explanation for the discrepancy in the number of transconjugants of RK2 in *E. coli* and *P. putida* (from the growth rates *P. putida* with RK2 grows at 1.03 h^{-1} and MV10 with RK2 grows at 1.63 h^{-1} ; the difference in growth rate between the DH5 α with RK2, MV10 and *P. putida* is not significant). Instead, a higher transfer frequency of RK2 between hosts from *P. putida* at 37°C as recorded in Table 5.7, could be a more plausible reason but not all transfer rates have been measured yet. Unfortunately there is not enough data on transfer rates (namely between *E. coli* MV10 strains, and *P. putida* KT2440 strains) to establish if this is the determinant factor leading to the observed outcome. For R387 virtually no transconjugants were observed for the period of 24 hours when the starting ratio between the two recipient species was roughly 1:1 (Figure 5.3, bottom left panel). Increasing the initial amount of suitable recipients, i.e. *E. coli* MV10, allowed the emergence of R387 transconjugants (Figure 5.3, bottom right panel) although at low frequencies, which could be explained by the low transfer rate of R387 among *E. coli* strains.

Overall, these preliminary experiments set the basis for future experimental design aiming at a better understanding of the factors that determine the ubiquity of narrow-host range plasmids and the success of promiscuous plasmids in a two-species world, as sketched in the discussion.

5.3. Discussion

Fitness cost

The general idea that plasmids confer a burden on their host has been challenged by the results obtained here. The majority of the lab strains tested either grew faster or their growth rate was only marginally affected by the presence of the plasmid. The only exceptions were *E. coli* MV10 in LB at 30°C and *P. putida* KT2440 at 37°C in LB, both of which showed a significant decrease in growth rate when RK2 was present. Despite the differences in host-range, size and pili expression between the two plasmids, their effect on *E. coli* MV10 growth was not significantly different. Both increased the fitness of this host when growing in rich medium, LB, at 37°C. However, other factors related to growth requirements and the complex medium composition could have contributed to the great improvement in fitness seen in *E. coli* MV10 carrying either RK2 or R387 plasmids. Previous studies using *E. coli* J53-1 showed that RK2 imposes a burden of 21% reduction in growth rate in Davis minimal medium at 37°C (Dahlberg and Chao, 2003). Yet, our results show that in M9 minimal medium, at 37°C, the growth rate of *E. coli* MV10 without a plasmid was identical to the plasmid-bearing host regardless of the plasmid. The absence of a clear trend in the effect of a plasmid on its host, even within the same bacterial species further underlines the complexity of the interactions between each plasmid-host pair and the environmental factors and how these contribute to the overall fitness of the host. More recently, Humphrey et al. (2012) investigated the fitness impact of IncP1 and IncN BHR plasmids on *E. coli* strains from the four phylogenetic groups. They found that even small differences in the host or in the plasmid, such as

the silencing of an antibiotic resistant gene or the loss of the Tn1 transposon, can have considerable effects on fitness. Thus, evidence argues for a more thorough analysis on the real impact of plasmid carriage among different hosts and the molecular host-plasmid interactions that are on the basis of the observed discrepancies.

The positive effect of RK2 on *P. aeruginosa* PAO1161 growth under the conditions tested may be the result of long-term co-evolution of RK2 with this *P. aeruginosa* in the natural environment setting (recall that RK2 was first isolated from a *P. aeruginosa* strain at Birmingham's hospital, Ingram et al., 1973). The opposite effect is observed when the other *Pseudomonas* species, *P. putida* KT2440, is carrying RK2, indicating that the host's genetic background is also an important factor.

It has always been assumed that the energy required for plasmid replication and transfer would come at a cost for the host. But perhaps this assumption does not hold for all environmental conditions as exemplified by this work, and other factors related to the interaction between the hosts' genetic background and the plasmid become more important. Further studies on the competition between plasmid-free and plasmid-bearing hosts using a range of different and well-defined culture media and temperatures are needed to assess the actual impact of various plasmids on the growth of the bacterial species carrying them.

Transfer frequency

The transfer frequency (T/D) of RK2 and R387 on LB nitrocellulose filters was characterized for different temperatures and donor/recipient combinations. Although the donor strain used for each plasmid was different, their transfer frequency into *E. coli* MV10 recipient at 37°C was significantly different, with the transfer frequency for R387 (1.4×10^{-4}) being approximately 60-fold lower than RK2 (8×10^{-3}). R387 plasmid has been classified as being repressed for pilus synthesis (Bradley, 1980), which could be an explanation for the observed low frequency. In contrast, RK2 is known to continuously produce its pilus units. Attempts to transfer R387 into PAO1161 or KT2440 were not successful, since no transconjugants were ever recovered. On the contrary, RK2 was able to transfer from *E. coli* MV10 to both PAO1161 and KT2440 at 37°C at similar frequencies (1×10^{-3} and 8×10^{-3} , respectively). Comparison between the transfer rate of RK2 in *Escherichia* species and *Pseudomonas* species revealed differences that were temperature dependent. Transfer occurred at a higher frequency between PAO1161 and KT2440 at 26°C (0.173), whereas between DH5 α and MV10 the maximum was obtained at 30°C (0.079). Even so, transfer was higher among *Pseudomonas* species. A previous study using *P. aeruginosa* as donors of RK2 at 37°C in minimal media, reported transfer frequencies in the range of 1×10^{-2} and 2.1×10^{-3} after 30 minutes of mating, whereas in *E. coli* they were nearly 10-fold lower in the range of 1.5×10^{-3} and 6.3×10^{-5} (Stanisich and Ortiz, 1976). Despite the difference in media and strains these values are somewhat in line with the ones obtained in this report for RK2 transfer in *Pseudomonas* species (1.2×10^{-2}) and in *Escherichia* species (8×10^{-3}) at 37°C in LB. It is worth mentioning that there are very few reports from literature where the authors have taken short periods of time (ideally shorter than one generation) to

measure the number of transconjugants formed per donor cell. Prolonged incubation periods lead to an increase in transconjugants due to growth and not necessarily due to transfer, making the final result on transfer frequency unreliable. The different environmental conditions used by each researcher makes it impossible to make a direct comparison with each other's results. In another study by Venables et al., (1995), two-gradient plates that cover a range of temperature and pH conditions were used to determine the optimal conditions for conjugation for RK2 among *P. putida* and *E. coli* strains. They followed the dynamics of transfer for 24 hours, after which their results showed a higher number of transconjugants at 25°C for matings between *E. coli* strains and at 30°C for matings between *P. putida* strains. Thus, there seems to be an optimum temperature for transfer, which depends on the donor/recipient combination, and is possibly correlated with the environmental conditions where the host is usually found.

The dependency of transfer frequency on different temperatures could influence the chances of a plasmid successfully invading a population of plasmid-free hosts. For example, a population of *E. coli* that grows at half of its growth rate at 30°C could be more easily invaded by the RK2 plasmid whose transfer frequency is 10-fold higher at 30°C than at 37°C. Hence, at a lower temperature the horizontal propagation of the plasmid could become a relevant mechanism for the establishment of RK2 in the population. From the experiments on transfer dynamics of RK2 at 26°C and at 37°C in *E. coli* it was found that, even though the number of transconjugants was lower at 26°C for the first 9 hours, by the end of the experiment the majority of the recipients had been infected by the plasmid in both scenarios. Thus, no significant difference in the transfer dynamics at the two different

temperatures tested could be detected, possibly because RK2 transfer rate in these strains of *E. coli* is not significantly different at 26°C and at 37°C (0.02 and 0.008, respectively).

Transfer in two-species assemblages

The preliminary experiments on the dynamics of plasmids spreading in two-species assemblages suggest a role for the assemblage structure in the success of plasmid invasion. The hypothesis is that propagation of narrow-host range plasmids would be limited in structured two-species assemblages due to physical barrier between colonies of suitable and non-suitable recipients. As more individuals of the non-suitable recipient are introduced the more difficult it is for the NHR plasmid to spread. Indeed, preliminary results point towards this expectation. When the number of R387 transconjugants formed in *E. coli* MV10 in two-species assemblages composed by *P. putida* and *E. coli* were measured, only an increase of transconjugants over time in the scenario where the initial ratio between the two types of recipients favoured *E. coli* species (Figure 5.4) was found. In the case of the broad-host range plasmid RK2, even though it can transfer and replicate in both *E. coli* and *P. putida*, fewer transconjugants were obtained in MV10 than KT2440 when starting at 1:1 for the two types of recipients. When the initially available amount of *E. coli* MV10 recipients was increased, an increase of RK2 transconjugants in this host followed. Differential preference for hosts could shift the direction of propagation of this plasmid, as exemplified here. Nevertheless, these preliminary experiments have shown that a better experimental framework is needed. Namely, a higher number of replicate experiments and shorter times for data acquisition. It seems that most of the

changes in the number of transconjugants, donors and recipients takes place in the first few hours. Therefore, the time course during which each plasmid is monitored should be adapted on a case-by-case basis, in order to better capture its transfer dynamics in the two-species assemblage. It would also be useful if one could measure all types of hosts, namely donors, transconjugants, recipients and total population for each time point in order to have a clear picture of what are the most important players changing the course of transfer dynamics.

Amongst the best-studied groups of plasmids are the IncF and the IncP groups. The representative plasmid of IncF group, the F plasmid is classified as having a narrow-host range (Guiney, 1982; Zhong et al., 2005) and a low transfer rate (Cullum et al., 1978a; Levin et al., 1979) whereas RK2 the prototype of IncP- α group, is known to be readily transferrable to a wide variety of bacterial species and is highly infectious (Thomas and Smith, 1987). A survey on pilus morphology and synthesis by David Bradley in 1980 revealed that most of the plasmids belonging to the IncN, IncP or IncW groups of broad-host range plasmids showed continuously pilus production, indicating that they are ready to be transferred at all times. In contrast, the narrow-host range plasmids from IncK, IncI or IncF groups generally have their pilus expression functions repressed. In the present work the transfer rate of a narrow host-range plasmid from IncK group, R387 was compared with that of the broad host-range RK2 plasmid and found that R387 plasmid transferred at a much lower rate in *E. coli* strains. Given these observations, the hypothesis that plasmids with higher transfer rates have a higher probability of expanding their host-range becomes pertinent. Since conjugative transfer is a replicative process there is an inherent rate of mutation associated with each transfer event (Christensen et al.,

1985; Kunz and Glickman, 1983). Hence, the more a plasmid attempts to transfer into a new host the higher the probability a mutation will arise and allow its replication in the new host (Sota et al., 2010).

A combination of *P. aeruginosa* and *P. putida*, and a narrow-host range form of RK2 with different transfer efficiencies could be used to test this hypothesis. Replication of RK2 in *P. aeruginosa* requires the complete sequence of the initiation replication protein TrfA, but in *P. putida* both short (33 KDa) and long (44 KDa) forms of TrfA are active (Caspi et al., 2001). A reduced transfer frequency in RK2 has been achieved by introducing a point mutation (G to A transition) in the *trbB* promoter, which regulates the *trb* operon (responsible for production of the matting pair formation apparatus) and is the target for the global regulator TrbA involved in the regulation of conjugative transfer (Bingle et al., 2003). These constructs could be employed in competition experiments in two-species assemblages to follow the fate of each plasmid by flow cytometry as exemplified in the recent work by Irene del Campo (2012), where the authors employed the cytometric method to estimate conjugation rates adapted to surface-based conjugation environments. Thus, the necessary genetic modifications to create a RK2 with a restricted host-range among *Pseudomonas* species with different degrees of transfer frequency have been established by earlier studies, and they could be used to investigate if an increased transfer rate leads to the rapid expansion of a plasmid's host-range.

Chapter 6

General discussion

GENERAL DISCUSSION

Horizontal gene transfer is a major mechanism of bacterial evolution that facilitates rapid adaptation to environmental changes. Self-transmissible plasmids are key players in the generalized spreading of antibiotic resistance genes, which have been shown to remain in the natural microbial communities such as the gut for extensive periods of time even in the absence of antibiotic selective pressure (Andersson and Hughes, 2011). Important to the success of plasmids as gene shuttles can be their ability to transfer and replicate in distantly related hosts (such as BHR plasmids). However, the cost of replicating and transferring the extra piece of DNA and expression of plasmid genes, can render the plasmid-bearing cells less competitive than their plasmid-free counterparts. Extended plasmid host-ranges and periodic selection of antibiotic resistance genes carried by plasmids could increase the risk of spread and persistence of these genetic determinants among distantly related bacteria.

In the present work, mathematical models of two plasmids with different host-ranges transferring in two-species assemblages were developed to investigate the conditions that support coexistence of parasitic plasmids in chemostats and biofilms. Transfer in a chemostat was modelled with a set of deterministic ODE equations, but a stochastic version of this model was also implemented in the iDynoMiCS platform, which can simulate both the growth of biofilms on inert surfaces and microbial growth in chemostats. Conjugative plasmids can persist in the two-species assemblages by two mechanisms: infection of new hosts (horizontal transfer) and vertical transmission to daughter cells. The plasmid can be lost upon cellular division, a

process known as segregational loss. These three mechanisms constituted the basis for the development of mass-action models of plasmid transfer in bacterial populations growing in chemostats in the late 1970's, in which the processes underlying plasmid dissemination and loss are described by three parameters: transfer rate, fitness cost and loss rate.

However, plasmid transfer dynamics in a chemostat and in a biofilm are very different. In chemostats, random encounters between any two cells, where one is a donor and the other a recipient cell, can lead to a transfer event. In biofilms, the spatial organization of the cells restricts cell-to-cell contact to neighbouring cells. Although mathematical modeling of the parameter controlling transfer activity in chemostats (transfer rate) and in biofilms (transfer probability) is different, a qualitative comparison between the results obtained with the chemostat and biofilm simulations can yield important insights about the factors controlling competition between NHR and BHR plasmids in spatially unstructured and structured environments. In chemostats a costly NHR plasmid, which cannot survive alone in a two-species assemblage, could do so in the presence of a costlier BHR incompatible plasmid because now the recipients of species *B* (which the NHR plasmid cannot infect) become infected by the BHR plasmid and thus becoming less fit than the NHR-plasmid-bearing hosts, allowing the fitter NHR-bearing hosts to survive. In contrast, when competing against a compatible BHR plasmid, the NHR plasmid can only survive if its cost is zero, otherwise T_N^N hosts become infected with the BHR plasmid forming $T_N^{B,N}$ hosts, which are less fit (costs add up) than all the other single plasmid-bearing hosts or recipients, and the NHR plasmid is outcompeted by fitter hosts and washed out from the chemostat. Since, in natural environments it is

unlikely that a plasmid has no effect on the overall fitness of its host, the probability that a NHR plasmid is able to survive in two-species assemblage in the presence of a compatible BHR plasmid may depend on a fitness advantage conferred by the NHR plasmid to its host. In a biofilm, the frequency of a costly NHR plasmid in a two-species assemblage declines over time because it is outcompeted by faster growing hosts in the biofilm (e.g., BHR-plasmid bearing hosts with lower cost or plasmid-free hosts), which can eventually lead to its extinction in the long-term. Yet, an increase in fitness cost of the BHR plasmid has no effect on the ability of the BHR plasmid to invade and persist in the mature biofilm. This is because the BHR plasmid can transfer into both species, but also because the cells in a mature biofilm are not growing at their maximum rate, and thus the burdened BHR-plasmid bearing hosts can successfully compete with plasmid-free hosts and infect them, which is in line with the observation made by Merkey et. al (2011). Thus, a broader-host range is an advantageous feature when competing with other compatible plasmids in two-species assemblage in both chemostats and biofilms.

A reduction in the transfer probability of a NHR plasmid competing with an incompatible BHR plasmid in a patchy biofilm can lead to the extinction of the NHR plasmid. Dissemination of NHR plasmids in patchy biofilm structures is hindered by both the presence of clusters of recipients it cannot infect (R_B) and hosts carrying an incompatible BHR plasmid. Spreading of a BHR plasmid is also diminished, although to a less extent, by a lower transfer proficiency and biofilm patchiness when competing against a faster transferrable incompatible NHR plasmid. Thus, incompatibility among plasmids spreading in biofilms is detrimental for the NHR plasmid. In contrast, in the chemostat, higher transfer rates for the BHR plasmid

have a negative effect on the frequency of BHR plasmid-bearing hosts, whilst enhancing the propagation of the incompatible NHR plasmid and thus promoting the survival of the NHR plasmid in the two-species assemblage. The transfer rate of the NHR plasmid can be zero without affecting its survival, provided that the NHR plasmid has a cost advantage over the BHR plasmid and that the BHR plasmid transfers at sufficiently high rate to infect faster growing recipients of species *B* which would otherwise outcompete NHR plasmid-bearing hosts. Yet, simulations performed with the stochastic individual-based chemostat model indicate that high transfer rates can generate damped oscillations with an initially high amplitude in the number of plasmid-bearing hosts, which can lead to bottlenecks in the population of plasmid-bearing hosts and failure to re-invade the assemblage of hosts and the quick extinction of one or both plasmids. Hence, one would expect incompatible plasmids with high transfer rates to be selected for in biofilms but not in chemostats. In biofilms both compatible and incompatible costly plasmids could thrive, but in chemostats higher fitness costs demand higher transfer rates, which could be disadvantageous in the case of incompatible plasmids as explained before. Generally, model simulations showed that coexistence of plasmids with different host-ranges is possible under a range of plasmid-related parameters, but conditions for this are more stringent for compatible plasmids transferring in chemostats, where only a costless NHR plasmid can survive, and for incompatible plasmids spreading in patchy biofilms where high transfer proficiency is determinant for survival of a NHR plasmid.

The observation that non-transmissible (transfer rate is zero) NHR plasmids could persist in bacterial assemblages growing in chemostats in the presence of BHR

incompatible plasmids raises questions about the fate of cloning vectors that frequently carry more than one antibiotic resistance genes on their backbone, in natural environments such as rivers or wastewater treatment stations. In fact, observations that multiple antibiotic resistance plasmids remain in microbial communities in the absence of selective pressure have been reported (Merlin et al., 2011; Poole et al., 2011). Thus, absence of selection for antibiotic resistance may not be sufficient to prevent persistence of plasmids due to unforeseen interactions between competing plasmids (compatibility and host-range differences), as demonstrated throughout the present work. Moreover, the assumption that conjugative plasmids impose a burden on their hosts (rendering competition against plasmid-free hosts ineffective) is likely to not hold for many plasmid-host pairs in the natural environment, as exemplified by the observation that RK2 confers a higher fitness to *P. aeruginosa*, a major nosocomial pathogen (Mesaros et al., 2007). Also, in natural environments attack by phages may represent a higher cost for plasmid-bearing bacteria and would favour a reduction in pili expression and thus conjugational transfer, which could result in a decrease in the burden imposed by a plasmid on host's growth. In 2005 Dionisio built a mathematical model to investigate the role of pili diversity and male-specific phages on the survival of conjugative plasmids in chemostats. He found that plasmids with low expression of pili (and thus low transfer rate) and plasmids with high expression of pili (high transfer rate) constitute two sink habitats that help maintain both phages and conjugative plasmids in the same population (Dionisio, 2005). Hence, diversity in pili expression and thus differences at the level of transfer rate for different plasmids can also contribute to their survival.

The main goal in Chapter Five was to conduct preliminary attempts to studying the transfer dynamics of plasmids with different host-ranges in an assemblage composed of two bacterial species growing on nitrocellulose filters on top of agar plates. The two plasmids used in the experiments belong to different incompatibility groups: the BHR plasmid RK2 from IncP-1 and the NHR plasmid R387 from IncK group. Filter mating and growth curve experiments in batch cultures in *E. coli*, *P. aeruginosa* and *P. putida* showed that plasmid's transfer frequency and fitness cost are very dependent on the species background. Yet, surprisingly the majority of the lab strains tested either grew faster or marginally slower as the result of carrying the plasmid, for which no obvious explanation could be found. In filter matings, RK2 exhibited higher transfer frequencies than R387 in *E. coli* strains, which is in accordance with the view that R387 pili expression is repressed and RK2 continuously produces its pili units (Bradley, 1980). When plasmids were left to propagate in two-species assemblages composed by *E. coli* and *P. putida*, the spreading of R387 plasmid, which cannot infect *P. putida*, was severely affected when higher numbers of *P. putida* hosts were present. This observation is in line with the model predictions of NHR plasmid dissemination being halted by biofilm patchiness, where patches of recipients of species *B*, which the NHR plasmid cannot infect, effectively block its spread to other patches of recipients of species *N*. This work sets the basis for further development of an experimental framework where competition of plasmids with different host-ranges transferring in defined and spatially structured two-species assemblages can be investigated.

Chapter 7

Conclusions and future prospects

CONCLUSIONS AND FUTURE PROSPECTS

The present work represents the first attempt to model the transfer dynamics of two plasmids with different host ranges in two-species assemblages. It is clear that competition between plasmids spreading in two-species assemblages can yield very different outcomes regarding plasmid persistence that could have not been anticipated by simple one plasmid one species models. The main conclusions from this investigation are:

- (i) A costly NHR plasmid that cannot survive alone in a two-species assemblage growing in a chemostat can do so in the presence of a BHR incompatible plasmid;
- (ii) In chemostats, high transfer rates can lead to the extinction of two incompatible plasmids;
- (iii) In biofilms, fitness cost is not a determinant factor for the persistence of a BHR plasmid in mature two-species biofilms, but can affect survival of a NHR plasmid in the long-term.
- (iv) In biofilms, reduced transfer proficiency and incompatibility among plasmids can lead to the extinction of NHR plasmids in patchy biofilms and considerably reduce the dissemination of BHR plasmids;
- (v) In chemostats, costly incompatible plasmids competing for plasmid-free hosts should reduce their transfer rate to increase chances of survival; whereas in biofilms, high transfer rates among incompatible plasmids would favour their survival and co-existence;

- (vi) The BHR is a better strategy for compatible plasmids transferring in both biofilms and chemostats, but in biofilms if the two plasmids are incompatible a faster transferrable NHR plasmid can outcompete a transfer deficient BHR plasmid;
- (vii) Transfer frequency and burden imposed on the host by a plasmid are very dependent on species background and temperature;
- (viii) Dissemination of the narrow host-range R387 plasmid in bacterial assemblages is hindered by increasing numbers of *P. putida*, a host in which this plasmid cannot be maintained.

The individual-based model iDynoMiCS is a suitable platform to explore the effect of individual variability on the overall performance of a group (e.g., plasmid type or bacterial species). In particular, in the plasmid biology field it could be used to test evolutionary hypothesis related to the evolution of plasmids, surface exclusion incompatibility and broadening of host-range. For example, the monotonic function (Eq 2.3, Chapter Two) that describes the cost amelioration experienced by a plasmid over a bacterial lineage, could be used to track the coevolution between host and plasmid and test the hypothesis that plasmids with a lower cost are more likely to be selected over time, i.e., that in the long term plasmids that confer a lower burden to their hosts represent the majority of plasmids in the two-species assemblage. Furthermore, implementation of a parameter describing the dependency of host-range expansion on transfer rate could be employed to address the hypothesis that plasmids that transfer frequently are more likely to expand their host-range. Yet, the analysis presented in this work exploits the relationships between plasmids transferring in two-species assemblages under no positive selection for the carriage

of a plasmid, but selection favouring the carriage of either plasmid is likely to change its ability to invade and persist in two-species bacterial assemblages.

On the experimental side, further development of experimental setups using defined microbial assemblages are needed to assess the impact of patchiness and competition on the fate of plasmids.

REFERENCES

- Acebo, P, Alda, M, Espinosa, M, and Del Solar, G. (1996) Isolation and characterization of pLS1 plasmid mutants with increased copy numbers. **FEMS Microbiol Lett**, 140: 85-91.
- Achtman, M. (1975) Mating aggregates in *Escherichia coli* conjugation. **J Bacteriol**, 123: 505-15.
- Adamczyk, M and Jagura-Burdzy, G. (2003) Spread and survival of promiscuous IncP-1 plasmids. **Acta biochimica Polonica**, 50: 425–53.
- Amann, R, Stromley, J, Devereux, R, Key, R, and Stahl, D. (1992) Molecular and microscopic identification of sulfate-reducing bacteria in multispecies biofilms. **Appl Environ Microbiol**, 58: 614-23.
- Andersson, D and Hughes, D. (2011) Persistence of antibiotic resistance in bacterial populations. **FEMS Microbiol Rev**, 35: 901-11.
- Andrup, L, Smidt, L, Andersen, K, and Boe, L. (1998) Kinetics of conjugative transfer: A study of the plasmid pXO16 from *Bacillus thuringiensis* subsp. *Israelensis*. **Plasmid**, 40: 30-43.
- Andrup, L and Andersen, K. (1999) A comparison of the kinetics of plasmid transfer in the conjugation systems encoded by the F plasmid from *Escherichia coli* and plasmid pCF10 from *Enterococcus faecalis*. **Microbiology**, 145: 2001-09.
- Angles, M, Marshall, K, and Goodman, A. (1993) Plasmid transfer between marine bacteria in the aqueous phase and biofilms in reactor microcosms. **Appl Environ Microbiol**, 59: 843-50.
- Babic, A, Lindner, AB, Vulic, M, Stewart, EJ, and Radman, M. (2008) Direct visualization of horizontal gene transfer. **Science**, 319: 1533–36.
- Babic, A, Berkmen, M, Lee, C, and Grossman, A. (2011) Efficient gene transfer in bacterial cell chains. **mBio**, 2: e00027-11.
- Bahl, M, Sorensen, S, and Hestbjerg Hansen, L. (2004) Quantification of plasmid loss in *Escherichia coli* cells by use of flow cytometry. **FEMS Microbiol Lett**, 232: 45-49.

- Bahl, M, Burmolle, M, Meisner, A, Hansen, L, and Sorensen, S. (2009) All IncP-1 plasmid subgroups, including the novel epsilon subgroup, are prevalent in the influent of a Danish wastewater treatment plant. **Plasmid**, 62: 134-39.
- Banks, M and Bryers, J. (1991) Bacterial species dominance within a binary culture biofilm. **Appl Environ Microbiol**, 57: 1974-79.
- Beaudoin, D, Bryers, J, Cunningham, A, and Peretti, S. (1998) Mobilization of broad host range plasmid from *Pseudomonas putida* to established biofilm of *Bacillus azotoformans*. I. Experiments. **Biotechnol Bioeng**, 57: 272-79.
- Bergquist, P, Saadi, S, and Maas, W. (1986) Distribution of basic replicons having homology with RepFla, RepFlb, and RepFlc among IncF group plasmids. **Plasmid**, 15: 19-34.
- Bergstrom, CT, Lipsitch, M, and Levin, BR. (2000) Natural selection, infectious transfer and the existence conditions for bacterial plasmids. **Genetics**, 155: 1505–19.
- Bingle, L, Zatyka, M, Manzoor, S, and Thomas, C. (2003) Co-operative interactions control conjugative transfer of broad host-range plasmid RK2: Full effect of minor changes in TrbA operator depends on KorB. **Mol Microbiol**, 49: 1095–108.
- Bradley, D. (1980) Morphological and serological relationships of conjugative pili. **Plasmid**, 4: 155-69.
- Brendler, T, Reaves, L, and Austin, S. (2004) Interplay between plasmid partition and postsegregational killing systems. **J Bacteriol**, 186: 2504-07.
- Bucci, V, Bradde, S, Biroli, G, and Xavier, J. (2012) Social interaction, noise and antibiotic-mediated switches in the intestinal microbiota. **PLoS Comput Biol**, 8: e1002497.
- Burmolle, M, Thomsen, T, Fazli, M, Dige, I, Christensen, L, Homoe, P, Tvede, M, Nyvad, B, Tolker-Nielsen, T, Givskov, M, Moser, C, Kirketerp-Moller, K, Johansen, H, Hoiby, N, Jensen, P, Sorensen, S, and Bjarnsholt, T. (2010) Biofilms in chronic infections - a matter of opportunity - monospecies biofilms in multispecies infections. **FEMS Immunol Med Microbiol**, 59: 324-36.
- Campbell, A, Mrazek, J, and Karlin, S. (1999) Genome signature comparisons among prokaryote, plasmid, and mitochondrial DNA. **PNAS**, 96: 9184-89.

- Campo, I, Ruiz, R, Cuevas, A, Revilla, C, Vielva, L, and De La Cruz, F. (2012) Determination of conjugation rates on solid surfaces **Plasmid**, 67: 174-82.
- Caspi, R, Pacek, M, Consiglieri, G, Helinski, DR, Toukdarian, a, and Konieczny, I. (2001) A broad host range replicon with different requirements for replication initiation in three bacterial species. **EMBO J** , 20: 3262-71.
- Casse, F, Boucher, C, Julliot, JS, Michel, M, and Dénarié, J. (1979) Identification and characterization of large plasmids in *Rhizobium meliloti* using agarose gel electrophoresis **J Gen Microb**, 113: 229-42.
- Chao, L, Levin, B, and Stewart, F. (1977) A complex community in a simple habitat: An experimental study with bacteria and phage. **Ecology**, 58: 369-78.
- Characklis, W and Marshall, K. (1990) Biofilms New York, USA: John Wiley & Sons.
- Christensen, RB, Christensen, JR, and Lawrence, CW. (1985) Conjugation-dependent enhancement of induced and spontaneous mutation in the LacI gene of *E. coli*. **Mol Gen Genet**, 201: 35-37.
- Clarke, M, Maddera, L, Harris, R, and Silverman, P. (2008) F-pili dynamics by live-cell imaging. **PNAS**, 105: 17978–81.
- Clewlow, L, Cresswell, N, and Wellington, E. (1990) Mathematical model of plasmid transfer between strains of streptomycetes in soil microcosms. **Appl Environ Microbiol**, 56: 3139-45.
- Cooper, T and Heinemann, J. (2000) Postsegregational killing does not increase plasmid stability but acts to mediate the exclusion of competing plasmids. **PNAS**, 97: 12643-48.
- Corchero, J and Villaverde, A. (1998) Plasmid maintenance in *Escherichia coli* recombinant cultures is dramatically, steadily, and specifically influenced by features of the encoded proteins. **Biotechnol Bioeng**, 58: 625-32.
- Costerton, J, Geesey, G, and Cheng, K. (1978) How bacteria stick **Sci American**, 238: 86-95.
- Costerton, J, Lewandowski, Z, Caldwell, D, Korber, D, and Lappin-Scott, HM. (1995) Microbial biofilms. **Annu Rev Microbiol**, 49: 711-45.

- Cullum, J, Collins, J, and Broda, P. (1978a) The spread of plasmids in model populations of *Escherichia coli* K12. **Plasmid**, 1: 545-56.
- Cullum, J, Collins, J, and Broda, P. (1978b) Factors affecting the kinetics of progeny formation with F'lac in *Escherichia coli* K12. **Plasmid**, 1: 536-44.
- Da Silva-Tatley, FM and Steyn, L. (1993) Characterization of a replicon of the moderately promiscuous plasmid, pGSH5000, with features of both the mini-replicon of pCU1 and the ori-2 of F. **Mol Microbiol**, 7: 805-23.
- Dahlberg, C and Chao, L. (2003) Amelioration of the cost of conjugative plasmid carriage in *Escherichia coli* K12. **Genetics**, 165: 1641-49.
- Datta, N and Hedges, R. (1972) R factors identified in paris, some conferring gentamicin resistance, constitute a new compatibility group. **Ann Inst Pasteur (Paris)**, 123: 849-52.
- Datta, N (1979), 'Plasmid classification: Incompatibility grouping', Plasmids of medical, environmental and commercial importance 3-12.
- Datta, N and Hedges, R. (1972) Host ranges of r factors. **J Gen Microbiol**, 70: 453-60.
- Datta, N, Hedges, RW, Shaw, EJ, Sykes, RB, and Richmond, MH. (1971) Properties of an r factor from *Pseudomonas aeruginosa* **Journal of Bacteriology**, 108: 1244-49.
- Davison, J. (1999) Genetic exchange between bacteria in the environment. **Plasmid**, 42: 73-91.
- De Gelder, L, Williams, J, Ponciano, J, Sota, M, and Top, E. (2008) Adaptive plasmid evolution results in host-range expansion of a broad-host-range plasmid **Genetics**, 178: 2179–90.
- De Gelder, L, Ponciano, JM, Joyce, P, and Top, EM. (2007) Stability of a promiscuous plasmid in different hosts: No guarantee for a long-term relationship. **Microbiology**, 153: 452-63.
- Del Solar, G, Alonso, J, Espinosa, M, and Diaz-Orejas, R. (1996) Broad-host-range plasmid replication: An open question. **Mol Microbiol**, 21: 661-66.

- Del Solar, G, Giraldo, R, Ruiz-Echevarria, MJ, Espinosa, M, and Diaz-Orejas, R. (1998) Replication and control of circular bacterial plasmids. **Microbiol Molec Bio Rev**, 62: 434–64.
- Dionisio, F. (2005) Plasmids survive despite their cost and male-specific phages due to heterogeneity of bacterial populations. **Evol Ecolo Res**, 7: 1089-107.
- Dionisio, F, Conceicao, I, Marques, A, Fernandes, L, and Gordo, I. (2005) The evolution of a conjugative plasmid and its ability to increase bacterial fitness. **Biol Lett**, 1: 250-52.
- Durrenberger, M, Villiger, W, and Bachi, T. (1991) Conjugational junctions: Morphology of specific contacts in conjugating *Escherichia coli* bacteria. **J Struct Biol**, 107: 146-56.
- Durrett, R and Levin, S. (1994) The importance of being discrete (and spatial) **Theor Popul Biol**, 46: 363-94.
- Eberl, H, Parker, D, and Van Loosdrecht, M. (2001) A new deterministic spatio-temporal continuum model for biofilm development **J Theor Med**, 3: 161-75.
- Ehlers, LJ and Bouwer, EJ. (1999) RP4 plasmid transfer among species of *Pseudomonas* in a biofilm reactor **Water Sci Technol**, 39: 163-71.
- Eisenbrandt, R, Kalkum, M, Lurz, R, and Lanka, E. (2000) Maturation of IncP pilin precursors resembles the catalytic dyad-like mechanism of leader peptidases. **J Bacteriol**, 182: 6751-61.
- Ermentrout, GB and Edelstein-Keshet, L. (1993) Cellular automata approaches to biological modeling **J Theor Bio**, 160: 97-133.
- Elsas, JD and Bailey, MJ. (2002) The ecology of transfer of mobile genetic elements. **FEMS Microbiol Ecolo**, 42: 187–97.
- Feld, L, Schjorring, S, Hammer, K, Licht, TR, Danielsen, M, Krogfelt, K, and Wilcks, A. (2008) Selective pressure affects transfer and establishment of a *Lactobacillus plantarum* resistance plasmid in the gastrointestinal environment. **J Antimicrob Chemother**, 61: 845–52.
- Foster, K and Xavier, J. (2007) Cooperation: bridging ecology and sociobiology. **Curr Biol**, 17: R319-21.

- Fox, RE, Zhong, X, Krone, SM, and Top, EM. (2008) Spatial structure and nutrients promote invasion of IncP-1 plasmids in bacterial populations. **ISME J**, 2: 1024–39.
- Freter, R, Freter, R, and Brickner, H. (1983) Experimental and mathematical models of *Escherichia coli* plasmid transfer in vitro and in vivo. **Infect Immun**, 39: 60–84.
- Garcillan-Barcia, M and De La Cruz, F. (2008) Why is entry exclusion an essential feature of conjugative plasmids? **Plasmid**, 60: 1–18.
- Gear CW. (1971) Numerical initial value problems in ordinary differential equations. Upper Saddle River, NJ, USA: Prentice Hall.
- Gelder, LD, Vandecasteele, FPJ, Brown, CJ, Forney, LJ, and Top, EM. (2005) Plasmid donor affects host range of promiscuous IncP-1 β plasmid pB10 in an activated-sludge microbial community **App Env Microbiol**, 71: 5309–17.
- Ghigo, J. (2001) Natural conjugative plasmids induce bacterial biofilm development. **Nature**, 412: 442–45.
- Gordon, D. (1992) Rate of plasmid transfer among *Escherichia coli* strains isolated from natural populations. **J Gen Microbiol**, 138: 17–21.
- Gregory, R, Saunders, J, and Saunders, V. (2008) Rule-based modelling of conjugative plasmid transfer and incompatibility. **Bio Systems**, 91: 201–15.
- Grimm, V. (1999) Ten years of individual-based modelling in ecology: What have we learned and what can we learn in the future? **Ecological Modelling**, 115: 129–48.
- Grimm, V, Berger, U, Bastiansen, F, Eliassen, S, Ginot, V, Giske, J, Custard-Goss, J, Grand, T, Heinz, S, Huse, G, Huth, A, Jepsen, J, Jorgensen, C, Mooij, W, Muller, B, Pe'Er, G, Piou, C, Railsback, S, Robbins, A, Robbins, A, Rossmanith, E, Ruger, N, Strand, E, Souissi, S, Stillman, R, Vabo, R, Visser, E, and Deangelis, D. (2006) A standard protocol for describing individual-based and agent-based models **Ecol Model**, 198: 115–26.
- Guiney, D. (1982) Host range of conjugation and replication functions of the *Escherichia coli* sex plasmid flac. Comparison with the broad host-range plasmid RK2. **J Mol Biol**, 162: 699–703.

- Guiney, D, Hasegawa, P, and Davis, C. (1984) Plasmid transfer from *Escherichia coli* to *Bacteroides fragilis*: Differential expression of antibiotic resistance phenotypes. **PNAS** 81: 7203-06.
- Haagensen, J, Hansen, S, Johansen, T, and Molin, S. (2002) In situ detection of horizontal transfer of mobile genetic elements. **FEMS Microbiol Ecol**, 42: 261-68.
- Haft, R, Mittler, J, and Traxler, B. (2009) Competition favours reduced cost of plasmids to host bacteria. **ISME J**, 3: 761-69.
- Harrington, L and Rogerson, A. (1990) The f pilus of *Escherichia coli* appears to support stable DNA transfer in the absence of wall-to-wall contact between cells. **J Bacteriol**, 172: 7263-64.
- Hausner, M and Wuertz, S. (1999) High rates of conjugation in bacterial biofilms as determined by quantitative in situ analysis. **Appl Environ Microbiol**, 65: 3710-13.
- Hellweger, FL and Bucci, V. (2009) A bunch of tiny individual: individual-based modeling for microbes **Ecological Modelling**, 220: 8-22.
- Heuer, H, Krogerrecklenfort, E, Wellington, E, Egan, S, Van Elsas, JD, Van Overbeek, L, Collard, J, Guillaume, G, Karagouni, A, Nikolakopoulou, T, and Smalla, K. (2002) Gentamicin resistance genes in environmental bacteria: Prevalence and transfer. **FEMS Microbiol Ecol**, 42: 289-302.
- Heuer, H, Binh, CTT, Jechalke, S, Kopmann, C, Zimmerling, U, Krogerrecklenfort, E, Ledger, T, Gonzalez, B, Top, E, and Smalla, K. (2012a) IncP-1 α plasmids are important vectors of antibiotic resistance genes in agricultural systems: Diversification driven by class 1 integron gene cassettes **Front Microbiol**, 3: 2 .
- Heuer, H, Smalla, K, and Gonzalez, B. (2012b) Plasmids foster diversification and adaptation of bacterial populations in soil **FEMS Microbiol Rev**, DOI: 10.1111/j.1574-6976.2012.00337.x
- Hoffmann, A, Thimm, T, Droge, M, Moore, E, Munch, J, and Tebbe, C. (1998) Intergeneric transfer of conjugative and mobilizable plasmids harbored by *Escherichia coli* in the gut of the soil *Microarthropod folsomia candida* (collembola). **Appl Environ Microbiol**, 64: 2652-59.

- Humphrey, B, Thomson, N, Thomas, C, Brooks, K, Sanders, M, Delsol, A, Roe, J, Bennett, P, and Enne, V. (2012) Fitness of *Escherichia coli* strains carrying expressed and partially silent IncN and IncP1 plasmids. **BMC Microbiol**, 12: 53.
- Ingram, L, Richmond, M, and Sykes, R. (1973) Molecular characterization of the r factors implicated in the carbenicillin resistance of a sequence of *Pseudomonas aeruginosa* strains isolated from burns. **Antimicrob Agents Chemother**, 3: 279-88.
- Jain, R, Rivera, M, Moore, J, and Lake, J. (2003) Horizontal gene transfer accelerates genome innovation and evolution. **Mol Biol Evol**, 20: 1598-602.
- Jakobsson, H, Jernberg, C, Andersson, A, Sjolund-Karlsson, M, Jansson, J, and Engstrand, L. (2010) Short-term antibiotic treatment has differing long-term impacts on the human throat and gut microbiome. **PLoS One**, 5: e9836.
- Kalkum, M, Eisenbrandt, R, and Lanka, E. (2004) Protein circlets as sex pilus subunits. **Curr Protein Pept Sci**, 5: 417-24.
- Kissel, J, Mccarty, P, and Street, R. (1984) Numerical simulations of mixed culture biofilms **Environ Eng**, 110: 393-411.
- Knudsen, G, Walter, M, Porteous, L, Prince, V, Armstrong, J, and Seidler, R. (1988) Predictive model of conjugative plasmid transfer in the rhizosphere and phyllosphere. **Appl Environ Microbiol**, 54: 343-47.
- Koonin, E, Makarova, K, and Aravind, L. (2001) Horizontal gene transfer in prokaryotes: Quantification and classification. **Annu Rev Microbiol**, 55: 709-42.
- Kreft, J.U. (2009), 'Mathematical modeling of microbial ecology: Spatial dynamics of interactions in biofilms and guts', *Food microbiology*, Food-born microbes: Shaping the host ecosystem 347-77.
- Kreft, J, Booth, G, and Wimpenny, J. (1998) Bacsim, a simulator for individual-based modelling of bacterial colony growth. **Microbiology**, 144: 3275-87.
- Kreft, J and Wimpenny, J. (2001) Effect of EPS on biofilm structure and function as revealed by an individual-based model of biofilm growth. **Water Sci Technol**, 43: 135-41.
- Kreft, J, Picioreanu, C, Wimpenny, J, and Van Loosdrecht, MC. (2001) Individual-based modelling of biofilms. **Microbiology**, 147: 2897-912.

- Kreft, J. (2004) Biofilms promote altruism. **Microbiology**, 150: 2751-60.
- Krone, SM, Lu, R, Fox, R, Suzuki, H, and Top, EM. (2007) Modelling the spatial dynamics of plasmid transfer and persistence. **Microbiology**, 153: 2803–16.
- Kunz, B and Glickman, B. (1983) The infidelity of conjugal DNA transfer in *Escherichia coli*. **Genetics**, 105: 489-500.
- Lagido, C, Wilson, I, Glover, L, and Prosser, J. (2003) A model for bacterial conjugal gene transfer on solid surfaces. **FEMS Microbiol Ecol**, 44: 67-78.
- Lale, R, Brautaset, T, and Valla, S. (2011) Broad-host-range plasmid vectors for gene expression in bacteria. **Methods Mol Biol**, 765: 327-43.
- Lanka, E and Wilkins, B. (1995) DNA processing reactions in bacterial conjugation. **Annu Rev Biochem**, 64: 141-69.
- Lardon, LA, Merkey, BV, Martins, S, Dotsch, A, Picioreanu, C, Kreft, J-U, and Smets, BF. (2011) iDynoMiCS: Next-generation individual-based modelling of biofilms. **Environ Microbiol**, 13: 2416-34.
- Larrainzar, E, O'Gara, F, and Morrissey, J. (2005) Applications of autofluorescent proteins for in situ studies in microbial ecology. **Annu Rev Microbiol**, 59: 257-77.
- Laspidou, C and Rittmann, B. (2004) Modeling the development of biofilm density including active bacteria, inert biomass, and extracellular polymeric substances **Wat Res**, 38: 3349-61.
- Lawley, T, Klimke, W, Gubbins, M, and Frost, L. (2003) F factor conjugation is a true type iv secretion system. **FEMS Microbiol Lett**, 224: 1-15.
- Lawrence, J, Korber, D, Hoyle, B, Costerton, J, and Caldwell, D. (1991) Optical sectioning of microbial biofilms. **J Bacteriol**, 173: 6558-67.
- Lederberg, J and Tatum, E. (1946a) Gene recombination in *Escherichia coli*. **Nature**, 158: 558.
- Lederberg, J and Tatum, E. (1946b) Detection of biochemical mutants of microorganisms. **J Biol Chem**, 165: 381.

- Levin, B, Stewart, F, and Chao, L. (1977) Resource-limited growth, competition and predation: A model and experimental studies with bacteria and bacteriophage. **American Naturalist**, 111: 3-24.
- Levin, B, Stewart, F, and Rice, V. (1979) The kinetics of conjugative plasmid transmission: Fit of a simple mass action model. **Plasmid**, 2: 247-60.
- Levin, B and Stewart, F. (1980) The population biology of bacterial plasmids: A priori conditions for the existence of mobilizable nonconjugative factors. **Genetics**, 94: 425-43.
- Levy, S and Marshall, B. (2004) Antibacterial resistance worldwide: Causes, challenges and responses. **Nat Med**, 10: S122-9.
- Licht, TR, Christensen, BB, Krogfelt, KA, and Molin, S. (1999) Plasmid transfer in animal intestine and other dynamic bacterial populations: The role of community structure and environment **Environ Microbiol**, 145: 2615-22.
- Lotka, A. (1920) Analytical note on certain rhythmic relations in organic systems. **PNAS**, 6: 410-15.
- Lundquist, P and Levin, B. (1986) Transitory derepression and the maintenance of conjugative plasmids. **Genetics**, 113: 483-97.
- Markowitz, S, Macrina, F, and Phibbs, PJ. (1978) R-factor inheritance and plasmid content in mucoid *Pseudomonas aeruginosa*. **Infect Immun**, 22: 530-39.
- Marshall, K. (1976) Interfaces in microbial ecology **Harvard University Press**, Cambridge, Massachusetts, USA.
- Massoudieh, A, Mathew, A, Lambertini, E, Nelson, KE, Ginn, TR, and Ection, SPS. (2007) Horizontal gene transfer on surfaces in natural porous media : Conjugation and kinetics **Soil Science**, 6: 306–15.
- MATLAB version 7.12.0.635. Natick, Massachusetts: **The MathWorks Inc.**, 2011.
- May, T and Okabe, S. (2008) *Escherichia coli* harboring a natural IncF conjugative F plasmid develops complex mature biofilms by stimulating synthesis of colanic acid and curli. **J Bacteriol**, 190: 7479-90.
- Mazodier, P and Davies, J. (1991) Gene transfer between distantly related bacteria. **Annu Rev Genet**, 25: 147-71.

- Mc Mahon, MA, Blair, I, Moore, J, and Mc Dowell, DA. (2007) The rate of horizontal transmission of antibiotic resistance plasmids is increased in food preservation-stressed bacteria. **J Appl Microbiol**, 103: 1883-88.
- Merkey, BV, Lardon, LA, Seoane, J, Kreft, JU, and Smets, BF. (2011) Growth dependence of conjugation explains limited plasmid invasion in biofilms: An individual-based modelling study. **Environ Microbiol**, 13: 2435-52.
- Merlin, C, Bonot, S, Courtois, S, and Block, J-C. (2011) Persistence and dissemination of the multiple-antibiotic-resistance plasmid pB10 in the microbial communities of wastewater sludge microcosms. **Water Res**, 45: 2897-905.
- Mesaros, N, Nordmann, P, Plesiat, P, Roussel-Delvallez, M, Van Eldere, J, Glupczynski, Y, Van Laethem, Y, Jacobs, F, Lebecque, P, Malfroot, A, Tulkens, P, and Van Bambeke, F. (2007) *Pseudomonas aeruginosa*: Resistance and therapeutic options at the turn of the new millennium. **Clin Microbiol Infect**, 13: 560-78.
- Meyer, R. (2009) Replication and conjugative mobilization of broad host-range IncQ plasmids. **Plasmid**, 62: 57-70.
- Mitri, S, Xavier, J, and Foster, K. (2011) Social evolution in multispecies biofilms. **PNAS**, 108 Suppl 2: 10839-46.
- Molin, S and Tolker-Nielsen, T. (2003) Gene transfer occurs with enhanced efficiency in biofilms and induces enhanced stabilisation of the biofilm structure **Curr Opin Biotechnol**, 14: 255–61.
- Mongold, JA. (1992) Theoretical implications for the evolution of postsegregational killing by bacterial plasmids **The American Naturalist**, 139: 677-89.
- Moura, A, Henriques, I, Smalla, K, and Correia, A. (2010) Wastewater bacterial communities bring together broad-host range plasmids, integrons and a wide diversity of uncharacterized gene cassettes. **Res Microbiol**, 161: 58–66.
- Muela, A, Pocino, M, Arana, I, Justo, J, Iriberrri, J, and Barcina, I. (1994) Effect of growth phase and parental cell survival in river water on plasmid transfer between *Escherichia coli* strains. **Appl Environ Microbiol**, 60: 4273-78.
- Nadell, C, Xavier, J, Levin, S, and Foster, K. (2008) The evolution of quorum sensing in bacterial biofilms. **PLoS Biol**, 6: e14.

- Nadell, C, Xavier, J, and Foster, K. (2009) The sociobiology of biofilms. **FEMS Microbiol Rev**, 33: 206-24.
- Nicolella, C, Van Loosdrecht, MC, and Heijnen, J. (2000) Wastewater treatment with particulate biofilm reactors. **J Biotechnol**, 80: 1-33.
- Nolling, J, Van Eeden, FJ, Eggen, R, and De Vos, WM. (1992) Modular organization of related archaeal plasmids encoding different restriction-modification systems in *Methanobacterium thermoformicum*. **Nucleic Acids Res**, 20: 6501-07.
- Novais, A, Canton, R, Valverde, A, Machado, E, Galan, J, Peixe, L, Carattoli, A, Baquero, F, and Coque, T. (2006) Dissemination and persistence of blaCTX-M-9 are linked to class 1 integrons containing CR1 associated with defective transposon derivatives from Tn402 located in early antibiotic resistance plasmids of IncHI2, IncP1-alpha, and IncFI groups. **Antimicrob Agents Chemother**, 50: 2741-50.
- Novick, R. (1969) Extrachromosomal inheritance in bacteria. **Bacteriol Rev**, 33: 210-63.
- Novick, R. (1989) *Staphylococcal* plasmids and their replication. **Annu Rev Microbiol**, 43: 537-65.
- Ochman, H, Lawrence, J, and Groisman, E. (2000) Lateral gene transfer and the nature of bacterial innovation. **Nature**, 405: 299-304.
- Olsen, RH and Shipley, PL. (1975) Rp1 properties and fertility inhibition among P, N, W, and X incompatibility group plasmids. **J Bacteriology**, 123: 28–35.
- Ong, CLY, Scott, AB, Mcewan, AG, and Schembri, MA. (2009) Conjugative plasmid transfer and adhesion dynamics in an *Escherichia coli* biofilm **App Env Microb**, 75: 6783-91.
- Ou, J and Anderson, T. (1970) Role of pili in bacterial conjugation. **J Bacteriol**, 102: 648-54.
- Ou, J and Anderson, T. (1972) Effect of Zn²⁺ on bacterial conjugation: Inhibition of mating pair formation. **J Bacteriol**, 111: 177-85.
- Pamp, S, Gjermansen, M, Johansen, H, and Tolker-Nielsen, T. (2008) Tolerance to the antimicrobial peptide colistin in *Pseudomonas aeruginosa* biofilms is linked

- to metabolically active cells, and depends on the *pmr* and *mexAB-oprM* genes. **Mol Microbiol**, 68: 223-40.
- Pamp, S, Sternberg, C, and Tolker-Nielsen, T. (2009) Insight into the microbial multicellular lifestyle via flow-cell technology and confocal microscopy. **Cytometry A**, 75: 90-103.
- Pansegrau, W, Lanka, E, Barth, P, Figurski, D, Guiney, D, Haas, D, Helinski, D, Schwab, H, Stanisich, V, and Thomas, C. (1994) Complete nucleotide sequence of Birmingham IncP- α plasmids. Compilation and comparative analysis. **J Mol Biol**, 239: 623-63.
- Parsek, MR and Tolker-Nielsen, T. (2008) Pattern formation in *Pseudomonas aeruginosa* biofilms. **Curr Opin Microbio**, 11: 560–66.
- Peters, J, Bartoszyk, I, Dheer, S, and Benson, S. (1996) Redundant homosexual f transfer facilitates selection-induced reversion of plasmid mutations. **J Bacteriol**, 178: 3037-43.
- Picioreanu, C, Van Loosdrecht, M, and Heijnen, J. (1998a) A new combined differential-discrete cellular automaton approach for biofilm modelling: Application for growth in gel beads **Biotechnol Bioeng**, 57: 718-31.
- Picioreanu, C, Van Loosdrecht, M, and Heijnen, J. (2001) Two-dimensional model of biofilm detachment caused by internal stress from liquid flow **Biotechnol Bioeng**, 72: 205-18.
- Picioreanu, C, Batstone, D, and Van Loosdrecht, MC. (2005) Multidimensional modelling of anaerobic granules. **Water Sci Technol**, 52: 501-07.
- Picioreanu, C, Van, L, MCM, and Heijnen, J. (1998b) Mathematical modeling of biofilm structure with a hybrid differential-discrete cellular automaton approach. **Biotechnol Bioeng**, 58: 101–16.
- Picioreanu, C, Kreft, J-U, and Loosdrecht, MCMV. (2004) Particle-based multidimensional multispecies biofilm model **App Environ Microbiol**, 70: 3024–40.
- Pinedo, CA and Smets, BF. (2005) Conjugal transfer from *Pseudomonas putida* to *Pseudomonas aeruginosa*: Effects of restriction proficiency, toxicant exposure, cell density ratios, and conjugation detection method on observed transfer efficiencies **App Environ Microbiol**, 71: 51-57.

- Pinney, R and Smith, J. (1974) Fertility inhibition of an N group R factor by a group X R factor, R6K **Journal of General Microbiology**, 82: 415-18.
- Pizarro, G, Griffeth, D, and Noguera, D. (2001) Quantitative cellular automaton model for biofilms **J Environ Eng**, 127: 782-89.
- Ponciano, JM, De, G, Leen, Top, EM, and Joyce, P. (2007) The population biology of bacterial plasmids: A hidden markov model approach **Genetics**, 176: 957-68.
- Poole, T, Brichta-Harhay, DM, Callaway, T, Beier, R, Bischoff, K, Loneragan, G, Anderson, R, and Nisbet, D. (2011) Persistence of resistance plasmids carried by beta-hemolytic *Escherichia coli* when maintained in a continuous-flow fermentation system without antimicrobial selection pressure. **Foodborne Pathog Dis**, 8: 535-40.
- Projan, S and Novick, R. (1984) Reciprocal intrapool variation in plasmid copy numbers: A characteristic of segregational incompatibility. **Plasmid**, 12: 52–60.
- Projan, S, Monod, M, Narayanan, C, and Dubnau, D. (1987) Replication properties of pLM13, a naturally occurring plasmid found in *Bacillus subtilis*, and of its close relative pE5, a plasmid native to *Staphylococcus aureus*. **J Bacteriol**, 169: 5131-39.
- Reisner, A, Holler B M, Molin S, and Zechner, EL. (2006) Synergistic effects in mixed *Escherichia coli* biofilms: conjugative plasmid transfer drives biofilm expansion. **J Bacteriol**, 188: 3582-88.
- Rittmann, B and Mccarty, P. (1980) Model of steady-stat-biofilm kinetics **Biotechnol Bioeng**, 22: 2343-57.
- Rittmann, B and Mccarty, P. (1981) Substrate flux into biofilms of any thickness **J Environ Eng**, 108: 831-49.
- Rittmann, B and Manem, J. (1992) Development and experimental evaluation of a steady-state, multi-species biofilm **Biotechnol bioeng**, 39: 914-22.
- Roberts, R, Spangler, C, and Helinski, D. (1993) Characteristics and significance of DNA binding activity of plasmid stabilization protein ParD from the broad host-range plasmid RK2. **J Biol Chem**, 268: 27109-17.

- Sagai, H, Shizuko, I, and Susumu, M. (1977) Inhibition and facilitation of transfer among *Pseudomonas aeruginosa* R plasmids **Journal of Bacteriology**, 131: 765-69.
- Samuels, A, Lanka, E, and Davies, J. (2000) Conjugative junctions in RP4-mediated mating of *Escherichia coli*. **J Bacteriol**, 182: 2709-15.
- Schmidhauser, T and Helinski, D. (1985) Regions of broad-host-range plasmid RK2 involved in replication and stable maintenance in nine species of Gram-negative bacteria. **J Bacteriol**, 164: 446-55.
- Scott, K. (2002) The role of conjugative transposons in spreading antibiotic resistance between bacteria that inhabit the gastrointestinal tract. **Cell Mol Life Sci**, 59: 2071-82.
- Shampine LF. (1982) Implementation of Rosenbrock methods. **ACM Trans. Math. Software**, 8: 93-113.
- Shampine LF, Reichelt MW. (1997) The Matlab ODE Suite. **SIAM J. Sci. Computing**, 18: 1-22.
- Shaw, W, Sands, L, and Datta, N. (1972) Hybridization of variants of chloramphenicol acetyltransferase specified by f_i^+ and f_i^- R Factors. **PNAS**, 69: 3049-53.
- Simonsen, L. (1990) Dynamics of plasmid transfer on surfaces. **J Gen Microb**, 136: 1001-07.
- Simonsen, L. (1991) The existence conditions for bacterial plasmids: Theory and reality **Microbiol Ecol**, 22: 187-205.
- Simonsen, L, Gordon, D, Stewart, F, and Levin, B. (1990) Estimating the rate of plasmid transfer: An end-point method. **J Gen Microbiol**, 136: 2319-25.
- Smalla, K and Sobecky, P. (2002) The prevalence and diversity of mobile genetic elements in bacterial communities of different environmental habitats: Insights gained from different methodological approaches. **FEMS Microbiol Ecol**, 42: 165-75.
- Smalla, K, Haines, AS, Jones, K, Krogerrecklenfort, E, Heuer, H, Schlöter, M, and Thomas, CM. (2006) Increased abundance of IncP-1 β plasmids and mercury resistance genes in mercury-polluted river sediments: First discovery of IncP-1 β plasmids with a complex *mer* transposon as the sole accessory element. **App Environ Microbiol**, 72: 7253–59.

- Smets, BF, Rittmann, BE, and Stahl, D. (1994) Stability and conjugal transfer kinetics of a TOL plasmid in *Pseudomonas aeruginosa* PAO 1162 **FEMS Microbiol Ecolo**, 15: 337–50.
- Smets, B, Rittmann, B, and Stahl, D. (1993) The specific growth rate of *Pseudomonas putida* PAW1 influences the conjugal transfer rate of the TOL plasmid. **Appl Environ Microbiol**, 59: 3430-37.
- Smillie, C, Garcillan-Barcia, MP, Francia, M, Rocha, E, and De La Cruz, F. (2010) Mobility of plasmids. **Microbiol Mol Biol Rev**, 74: 434-52.
- Smith, M and Bidochka, M. (1998) Bacterial fitness and plasmid loss: The importance of culture conditions and plasmid size. **Can J Microbiol**, 44: 351-55.
- Smith, D, Lus, R, Rubio Calvo, MC, Datta, N, Jacob, A, and Hedges, R. (1975) Third type of plasmid conferring gentamicin resistance in *Pseudomonas aeruginosa*. **Antimicrob Agents Chemother**, 8: 227-30.
- Smorawska, M, Szuplewska, M, Zaleski, P, Wawrzyniak, P, Maj, A, Plucienniczak, A, and Bartosik, D. (2012) Mobilizable narrow host range plasmids as natural suicide vectors enabling horizontal gene transfer among distantly related bacterial species **FEMS Microbiol Lett**, 326: 76-82.
- Soler, N, Marguet, E, Cortez, D, Desnoues, N, Keller, J, Van Tilbeurgh, H, Sezonov, G, and Forterre, P. (2010) Two novel families of plasmids from hyperthermophilic archaea encoding new families of replication proteins. **Nucleic Acids Res**, 38: 5088-104.
- Sorensen, S, Bailey, M, Hansen, L, Kroer, N, and Wuertz, S. (2005) Studying plasmid horizontal transfer in situ: A critical review. **Nat Rev Microbiol**, 3: 700-10.
- Sota, M and Top, E. (2008) Host-specific factors determine the persistence of IncP-1 plasmids **World Journal of Microbiology and Biotechnology**, 24: 1951-54.
- Sota, M, Yano, H, Hughes, J, Daughdrill, G, Abdo, Z, Forney, L, and Top, E. (2010) Shifts in the host range of a promiscuous plasmid through parallel evolution of its replication initiation protein. **ISME J**, 4: 1568-80.
- Stanisich, V and Ortiz, JM. (1976) Similarities between plasmids of the p-incompatibility group derived from different bacterial genera. **J Gen Microbiol**, 94: 281-89.

- Stewart, F and Levin, B. (1977) The population biology of bacterial plasmids: A priori conditions for the existence of conjugationally transmitted factors. **Genetics**, 87: 209-28.
- Subbiah, M, Top, E, Shah, D, and Call, D. (2011) Selection pressure required for long-term persistence of blaCMY-2-positive IncA/C plasmids. **Appl Environ Microbiol**, 77: 4486-93.
- Suzuki, H, Sota, M, Brown, C, and Top, E. (2008) Using mahalanobis distance to compare genomic signatures between bacterial plasmids and chromosomes. **Nucleic Acids Res**, 36: e147.
- Suzuki, H, Yano, H, Brown, C, and Top, E. (2010) Predicting plasmid promiscuity based on genomic signature. **J Bacteriol**, 192: 6045-55.
- Szipirer, C, Top, E, Couturier, M, and Mergeay, M. (1999) Retrotransfer or gene capture: A feature of conjugative plasmids, with ecological and evolutionary significance. **Microbiology**, 145: 3321-29.
- Tamminen, M, Virta, M, Fani, R, and Fondi, M. (2012) Large-scale analysis of plasmid relationships through gene-sharing networks **Mol Biol Evol Full**, DOI: 10.1093/molbev/msr292.
- Thisted, T, Sorensen, N, and Gerdes, K. (1995) Mechanism of post-segregational killing: Secondary structure analysis of the entire hok mRNA from plasmid R1 suggests a fold-back structure that prevents translation and antisense RNA binding. **J Molec Biol**, 247: 859-73.
- Thomas, CM and Smith, CA. (1987) Incompatibility group p plasmids: Genetics, evolution, and use in genetic manipulation **Annu Rev Microbiol**, 41: 77-101.
- Thomas, CM and Summers, D. (2008) Bacterial plasmids **eLS**, DOI: 10.1002/9780470015902.a0000468.pub2.
- Thomas, C and Nielsen, K. (2005) Mechanisms of, and barriers to, horizontal gene transfer between bacteria. **Nat Rev Microbiol**, 3: 711-21.
- Timmerly, S, Modrie, P, Minet, O, and Mahillon, J. (2009) Plasmid capture by the *Bacillus thuringiensis* conjugative plasmid pXO16. **J Bacteriol**, 191: 2197-205.

- Tolker-Nielsen, T and Molin, S. (2000) Spatial organization of microbial biofilm communities. **Microb Ecol**, 40: 75-84.
- Tschape, H and Tietze, E. (1980) Genetic and molecular characterization of R plasmids incompatible with R387 (IncK). **J Gen Microbiol**, 118: 515-21.
- Turner, P, Cooper, V, and Lenski, R. (1998) Tradeoff between horizontal and vertical modes of transmission in bacterial plasmids **Evolution**, 52: 315-29.
- van der Hoeven, N. (1984) A mathematical model for the co-existence of incompatible, conjugative plasmids in individual bacteria of a bacterial population. **J Theor Biol**, 110: 411-23.
- Velmurugan, S, Mehta, S, Uzri, D, and Jayaram, M. (2003) Stable propagation of 'selfish' genetic elements. **J Biosci**, 28: 623-36.
- Venables, W, Wimpenny, J, Ayres, A, Cook, S, and Thomas, L. (1995) The use of two-dimensional gradient plates to investigate the range of conditions under which conjugal plasmid transfer occurs. **Microbiology**, 141: 2713-18.
- Volterra, V. (1926) Variazioni e fluttuazioni del numero d'individui in specie animali conviventi **Mem Acad Lincei Roma**, 2: 31-113.
- Wanner, O and Gujer, W. (1984) Competition in biofilms **Wat Sci Technol**, 17: 27-44.
- Wanner, O, Eberl, H, Morgenroth, E, Noguera, D, Picioreanu, C, Rittmann, B, and Van Loosdrecht, M. (2006) Mathematical modeling of biofilms **IWA Scientific**, Technical report No.18: ISBN 1843390876.
- Watanabe, T. (1963) Infective heredity of multiple drug resistance in bacteria. **Bacteriol Rev**, 27: 87-115.
- Watanabe, T, Nishid, H, Ogata, C, Arai, T, and Sato, S. (1964) Episome-mediated transfer of drug resistance in Enterobacteriaceae **J Bacteriol**, 88: 716-26.
- Watanabe, T. (1967) Evolutionary relationships of r factors with other episomes and plasmids. **Fed Proc**, 26: 23-28.
- Watve, M, Dahanukar, N, and Watve, M. (2010) Sociobiological control of plasmid copy number in bacteria. **PLoS One**, 5: e9328.

- Wei, W and Krone, SM. (2005) Spatial invasion by a mutant pathogen. **J Theor Bio**, 236: 335–48.
- Williamson, K and PI, M. (1976) A model of substrate utilization by bacterial films **J Water Pollut Control Fed**, 48: 9-24.
- Wimpenny, J and Colasanti, R. (1997) A unifying hypothesis for the structure of microbial biofilms based on cellular automaton models **FEMS Microbiol Ecol**, 22: 1-16.
- Xavier, JB, Picioreanu, C, and Van Loosdrecht, M. (2005a) A general description of detachment for multidimensional modelling of biofilms. **Biotechnol Bioeng**, 91: 651-69.
- Xavier, J, Picioreanu, C, and Van Loosdrecht, MC. (2004) Assessment of three-dimensional biofilm models through direct comparison with confocal microscopy imaging. **Water Sci Technol**, 49: 177-85.
- Xavier, J, Picioreanu, C, and Van Loosdrecht, M. (2005b) A framework for multidimensional modelling of activity and structure of multispecies biofilms. **Environ Microbiol**, 7: 1085-103.
- Xavier, J and Foster, K. (2007) Cooperation and conflict in microbial biofilms. **PNAS**, 104: 876-81.
- Xavier, J, De Kreuk, MK, Picioreanu, C, and Van Loosdrecht, MC. (2007) Multi-scale individual-based model of microbial and bioconversion dynamics in aerobic granular sludge. **Environ Sci Technol**, 41: 6410-17.
- Yamaichi, Y and Niki, H. (2000) Active segregation by the *Bacillus subtilis* partitioning system in *Escherichia coli*. **PNAS**, 97: 14656-61.
- Zatyka, M and Thomas, CM. (1998) Control of genes for conjugative transfer of plasmids and other mobile elements **FEMS Microbiol Rev**, 21: 291-319.
- Zhong, X, Krol, J, Top, E, and Krone, S. (2010) Accounting for mating pair formation in plasmid population dynamics. **J Theor Biol**, 262: 711-19.
- Zhong, Z, Helinski, D, and Toukdarian, A. (2005) Plasmid host-range: Restrictions to F replication in *Pseudomonas*. **Plasmid**, 54: 48-56.

Zobell, C and Anderson, D. (1936) Observations on the multiplication of bacteria in different volumes of stored seawater and the influence of oxygen tension and solid surfaces. **Biol Bull Woods Hole**, 71: 324-42.

APPENDIX

Lardon, LA, Merkey, BV, **Martins, S**, Dotsch, A, Picioreanu, C, Kreft, J-U, and Smets, BF. (2011) iDynoMiCS: Next-Generation Individual-Based Modelling of Biofilms. **Environ Microbiol**, 13: 2416-34.